

ENHANCED VEHICLE COLLISION COMPATIBILITY – PROGRESS REPORT OF US TECHNICAL WORKGROUP FOR FRONT-TO-FRONT COMPATIBILITY

Mukul K. Verma

EVC Technical Workgroup for Front-to-Front Compatibility

USA

Paper number 07-0291

ABSTRACT

This paper presents estimates of benefits resulting from the voluntary agreement by the motor vehicle manufacturers in the USA for enhancing compatibility in front-to-front collisions between light truck based vehicles and passenger cars. Two studies of accident data and one study based on crash tests are reported herein.

In addition, the members of the technical workgroup are researching methods to measure and predict the structural interaction of vehicles in crashes and to quantify their relative structural strength levels. Ongoing work on three parallel paths of research for improving vehicle compatibility is described in this paper - (a) full-width fixed deformable barrier with load cell wall approach; (b) CAE-based evaluations of vehicle to vehicle impacts; and (c) development of car surrogate mobile deformable barrier as a test device.

INTRODUCTION

The Enhanced Vehicle Compatibility (EVC) technical workgroup was created in order to develop solutions for improving crash compatibility between passenger cars and light truck based vehicles (LTVs). Organized initially by the Alliance of Automobile Manufacturers, this workgroup now has members from automakers (BMW Group, DaimlerChrysler Corporation, Ford Motor Company, General Motors, Honda, Hyundai Motor, Isuzu Motors, Kia Motors, Mazda, Mitsubishi Motors, Nissan, Subaru, Suzuki, Toyota and Volkswagen) as well as from the Insurance Institute for Highway Safety, Transport Canada, and Transport Research Laboratory (UK). Studies conducted by members of this workgroup have led to recommendations for primary and secondary energy absorbing structures for LTVs to improve collision compatibility in frontal crashes with cars [1]. These recommendations include criteria for increased geometric overlap of these structures with the zone specified for passenger car energy absorbing structures as well as criteria for minimum structural strength of secondary energy absorbing

structures. These have been voluntarily accepted as performance criteria by almost all manufacturers for LTVs sold in the USA. This paper presents estimates of potential benefits in collision compatibility that may result from the workgroup's recommendations and summarizes the status of research activities of this workgroup.

ESTIMATED BENEFITS FROM WORKGROUP RECOMMENDATIONS

Three studies have been completed for estimating the effect of the previous recommendations made by this workgroup regarding light truck vehicles (LTV).

IIHS Study

A study was conducted [2] to estimate the benefits that may occur from SUVs and pickup trucks conforming to this workgroup's recommendations. This was done by looking at passenger car driver deaths in two-vehicle collisions where the car was struck by a pickup truck or an SUV. FARS data from years 2001 to 2004 for car-to-SUV and car-to-pickup truck collisions were studied and comparisons were made between SUVs and pickups that conform to the recommendations to those that did not conform to these guidelines. Only SUVs and pickup trucks of model years 2000 through 2003 were included in the study for both front-to-front as well as front-to-side collisions (where the front end of a light truck strikes the driver side of a passenger car).

The vehicles were divided into 500 lb groups. The fatality rate for each group was obtained by dividing the number of car driver fatalities by the number of vehicle registrations reported by R. L. Polk for SUVs and pickup trucks in that specific group. The resulting rate is the number of fatalities in the struck car per million striking vehicle registered-vehicle-years. These weight group rates are then combined to calculate overall estimated benefits for SUVs and for pickup trucks in each of the two collision configurations.

In front-to-front collisions with SUVs, conforming vehicles had a 16% reduction in estimated risk of fatalities whereas conforming pickups had a 20%

Overall Estimated Fatality Risk Reduction		
Crash type	Vehicle type	Risk Reduction
Front-to-front	SUVs	16%
	Pickups	20%
Front-to-driver side	SUVs	30%
	Pickups	10%

Table 1: Estimated Benefits in Compatibility

reduction. In front-to-side impacts, a 30% risk reduction for SUVs and a 10% risk reduction for pickups were observed.

Ford Study

The effect of adding SEAS to LTVs (one of the recommendations of this workgroup) was evaluated by comparing collision data for LTVs with SEAS to that for similar vehicles without SEAS and is presented separately [5].

GM Study

In this study, the effect of adding a secondary energy absorbing structure to an LTV was measured in controlled, full-overlap frontal crash tests with a passenger car (Figure 1). In each case, a stationary LTV was impacted by a passenger car moving at 58 mph to obtain the intended ΔV of 35 mph in the struck car. In these tests, SEAS designed in accordance with the ‘option 2’ criteria was added to a baseline LTV whose PEAS structure did not have the amount of overlap with Part 581 zone necessary for conformance with the ‘option 1’ criteria [1].



Figure 1: Pre-Impact Setup for Car versus LTV Tests

Some of the results from these tests are shown in Figures 2 and 3. Figure 2 shows the measured passenger car intrusions from impact with the baseline LTV compared to those from impact with the modified LTV. It is observed that the effect of added SEAS is a significant decrease in almost all the intrusion values measured in the car.

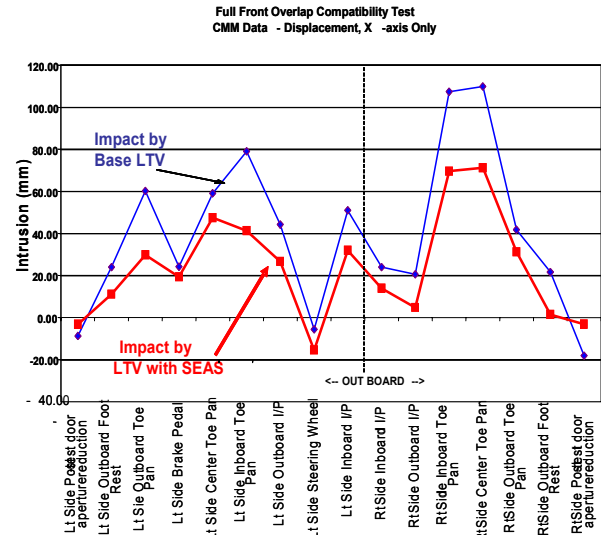


Figure 2: Measured Intrusions in Car-to-LTV Impacts – Effect of SEAS

Figure 3 below shows the response of a 50th percentile Hybrid III anthropomorphic test device (ATD) in the car driver seat in impact with the baseline and modified LTVs. Again, the effect of the added SEAS is observed to be an improvement in the car occupant protection as measured by ATD response.

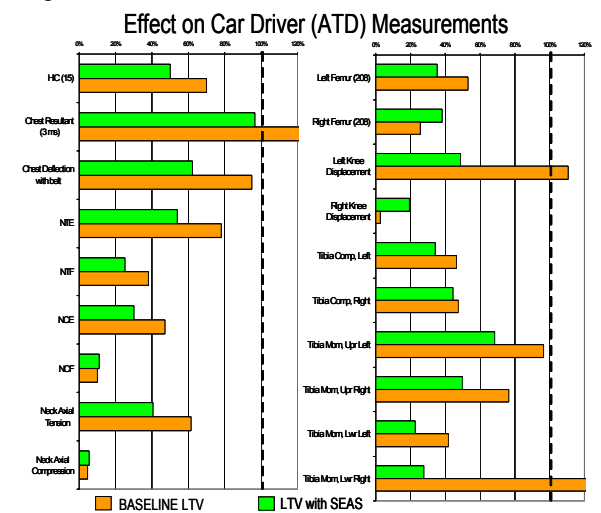


Figure 3: Measured Response of Car Driver ATD in Car-to-LTV Impacts – Effect of SEAS in LTV

CURRENT RESEARCH ACTIVITIES OF WORKGROUP

From the above studies, it is evident that the workgroup’s recommendations will provide significant benefits in collision compatibility as they are implemented in the design of LTVs. However, research continues by the workgroup members for developing additional recommendations leading to further improvements in collision compatibility in front-to-front impacts [3].

This workgroup’s charter is to develop compatibility improvement proposals for LTVs that do not cause significant reductions in the self-protection in these vehicles. Currently, there are three distinct research paths being pursued by this workgroup and these are described below.

1. Fixed Barrier Load Cell Wall (LCW) Approach

The aim of this research path is to develop a dynamic test procedure using a full-width deformable barrier (FWDB) load cell wall (LCW) and load-based metrics to quantitatively evaluate the collision compatibility of LTVs.

Three series of studies (Figure 4) have been performed.

Research Goal	Bullet Vehicle	vs Target	Diagram
TEST			
1 Understand the effect of ride height in V-t-V collision and evaluate ability of FWDB and various metrics to detect this change.	Mid-sized PU at normal ride height [Option 1 compliant]	vs Mid-sized PC1	
	Mid-sized PU raised by 10 cm [Option 1 non-compliant]	vs Mid-sized PC1	
	Mid-sized PU at normal ride height [Option 1 compliant]	vs FWDB-LCW	
	Mid-sized PU raised by 10 cm [Option 1 non-compliant]	vs FWDB-LCW	
2 Understand the effect of BlockerBeam®-type SEAS in V-t-V collision and evaluate ability of FWDB and various metrics to detect this type of SEAS.	HD-PU with standard BlockerBeam® SEAS [Option 2 compliant]	vs Mid-sized PC2	
	HD-PU with BlockerBeam® SEAS removed [Option 2 non-compliant]	vs Mid-sized PC2	
	HD-PU with standard BlockerBeam® SEAS [Option 2 compliant]	vs FWDB-LCW	
	HD-PU with BlockerBeam® SEAS removed [Option 2 non-compliant]	vs FWDB-LCW	
SIMULATION	SUV with standard subframe raised by 12.5 cm [Option 2 non-compliant]	vs Mid-size PC3	
	SUV with elongated subframe raised by 12.5 cm [Option 2 compliant]	vs Mid-size PC3	
	SUV with standard subframe raised by 12.5 cm [Option 2 non-compliant]	vs FWDB-LCW	
	SUV with elongated subframe raised by 12.5 cm [Option 2 compliant]	vs FWDB-LCW	
	SUV with standard subframe [Option 1 compliant]	vs Mid-size PC3	
	SUV with elongated subframe [Option 1 over-compliant]	vs Mid-size PC3	
	SUV with standard subframe [Option 1 compliant]	vs FWDB-LCW	
	SUV with elongated subframe [Option 1 over-compliant]	vs FWDB-LCW	

Figure 4: FWDB related test and simulation series.

Test Series 1 – Height of PEAS

The baseline pickup truck has PEAS whose height conforms to ‘option 1’ criteria [1] and the modified truck’s ride height was increased from this by 10 cm. In the truck versus car tests (Figure 5), it was

observed that the PEAS of the baseline truck overlapped that of the car by a significant amount but there was no overlap when the truck was raised. Also,



Figure 5: Pre-test alignment of baseline (left) and raised pickup (right) with car.

the raised truck’s PEAS height did not conform to the ‘option 1’ [1]. Shown in Figure 6 are the interactions between the vehicles in each case.

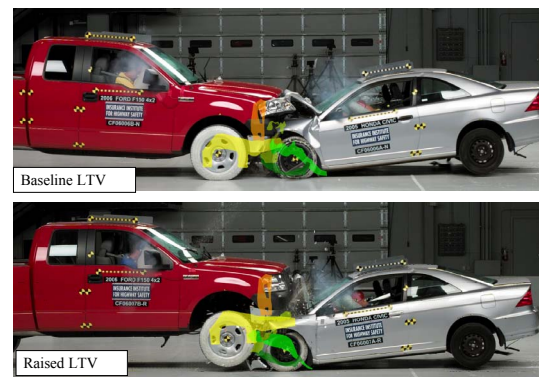


Figure 6: LTV vs Car tests for baseline LTV (top) and for raised LTV

Examination of the test film showed structural engagement between the truck and the car in the test with the baseline truck whereas in the test with the raised truck, it was observed that the truck’s wheels lifted off ground during the test.

Figure 7 shows measured intrusions in the passenger car in each test. The intrusions in the car were low in both the cases even though the structural engagement

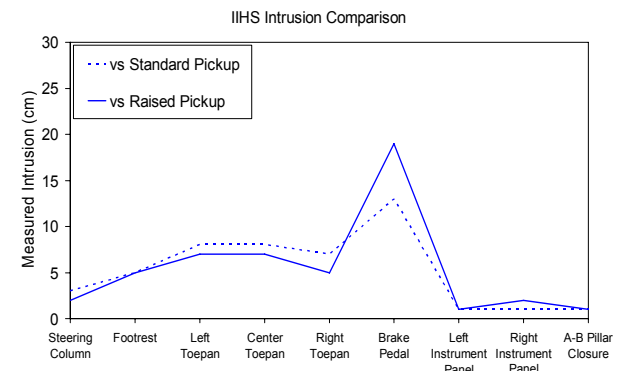


Figure 7: Car Compartment Intrusion

with the truck was different in the two tests. Raising the height of the truck appears to have the effect of reduced intrusions at all points except at the brake pedal which showed an increase.

Figure 8 shows the measured decelerations in the car in impacts with the baseline truck and with the raised truck. The effect of raising the truck is observed to be lower deceleration in the car earlier in the impact but an increase in the peak value later in the impact.

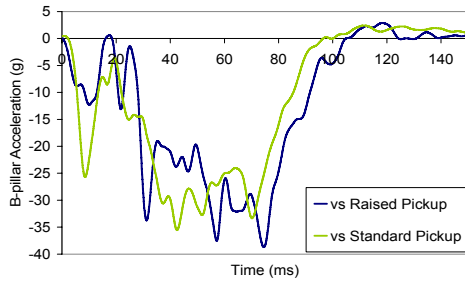


Figure 8: Car Deceleration vs Time Results

The resulting response of the 50th percentile Hybrid III ATD on the driver side in the car is shown in Figure 9. Relatively lower deceleration levels earlier in the event with the raised LTV caused delayed front airbag deployment in the car and this may be a factor in the observed ATD response. The ATD injury criteria were all below the standard regulatory limits (except for the tibia index) although the values were generally higher for the test against the raised truck.

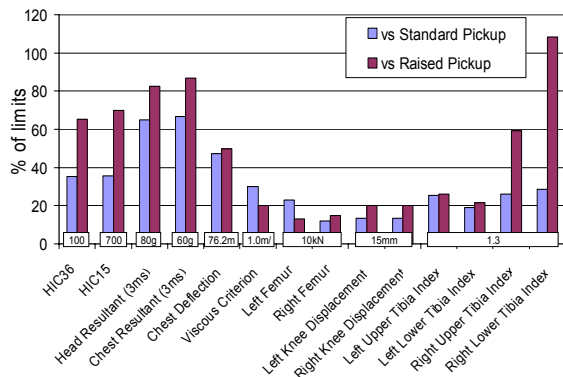


Figure 9: ATD Responses in Car to LTV Impact

Results from FWDB impact of the baseline truck and the raised truck indicate that the raised truck applies lower load in row 3 and higher load in row 4 than the baseline truck (rows 3 and 4 are the rows in alignment with the top and bottom of the CFR49 Part 581 zone, respectively). The sum of the peak cell loads is shown in Table 2 where ‘metric 1’ is the summation of peak values of measured loads

independent of time and ‘metric 2’ is the value when the results are truncated to 40 milliseconds.

Truck	Metric 1 Sum peak cell loads (kN)		Metric 2 Sum peak cell loads up to 40 ms (kN)	
	Row 3	Row 4	Row 3	Row 4
Baseline	279	328	205	321
Raised	94	447	45	397

Table 2: Comparison of Peak Cell Loads on Rows 3 & 4 for Baseline Truck and Raised Truck

These values should be compared to an example value of 100 kN.

A comparison of the AHOF (Figure 10) shows that AHOF does not define the location of the PEAS of the vehicle but may be able to show the change in height although with a significant (20%) error.

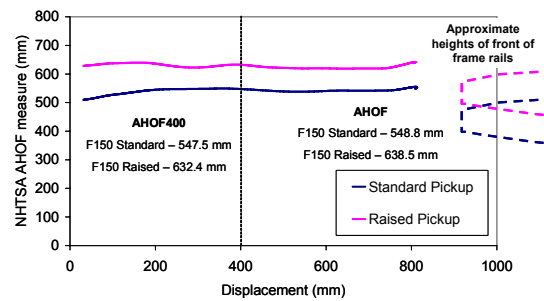


Figure 10: Comparison of AHOF versus B-pillar Displacement for Baseline and Raised Trucks.

In conclusion, the results of this test series show that the alignment of this LTV's PEAS with the CFR49 Part 581 zone increased its structural interaction with the test car and reduced most of the injury measures on ATD in the car. Also, FWDB results show that metrics based on peak cell loads on rows 3 and 4 can detect a large (> 10 cm) change in height of PEAS of the LTV. AHOF also appears to provide this discrimination but it is not an indicator of the position of the vehicle structure.

Test Series 2 – BlockerBeam[®] type SEAS

The capability of FWDB metrics to detect removal of SEAS in a full size pickup truck was investigated and detailed results from this test series are reported in a separate publication [5].

Simulation Series – Sub-frame type SEAS

Finite element models of an LTV and a car were used to study the effect of adding sub-frame type SEAS to the LTV. Two simulations were conducted with

raised SUVs - one being an SUV with a sub-frame type SEAS and the other one without SEAS. Both the vehicles were raised in the simulation by 125 mm over the standard height so that the vehicle with SEAS conformed to the ‘option 2’ criteria [1] and the vehicle without SEAS did not conform. In the SUV-versus-car simulations, the front end structure of the car (Figure 11, 12) shows significant overlap with the

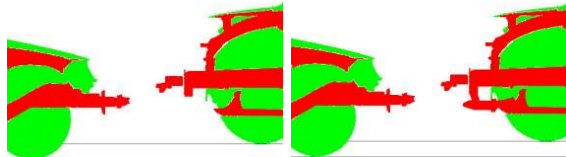


Figure 11: Alignment of Raised (left) SUV and Raised SUV with sub-frame SEAS versus Car.

with that of the sub-frame SEAS, but not so for the SUV without the added SEAS.

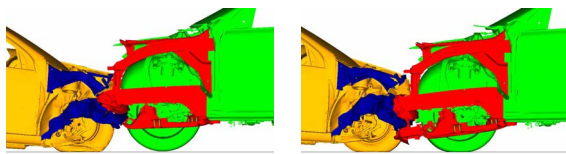


Figure 12: SUV vs Car Simulation at 75 msec – Increased structural interaction for Raised SUV with sub-frame SEAS (right)

The cars’ compartment intrusions in the simulated impact (Figure 13) were very low (all but one <50 mm) in both studies, the raised SUV with sub-frame SEAS causing approximately 14% less intrusion in the car than the raised SUV without the SEAS.

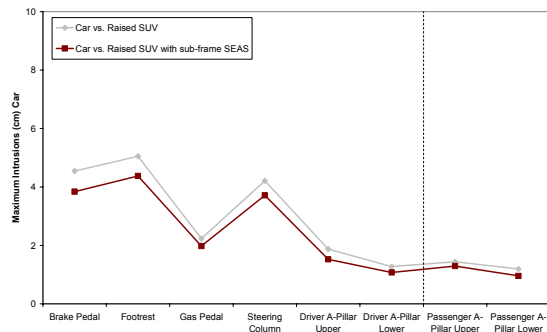


Figure 13: Car compartment intrusion in LTV Impacts

The Load Cell Wall (LCW) results for both SUVs are shown in Table 3. The addition of the sub-frame SEAS adds significantly to the loading of row 3 and row 4. In both cases, row 4 loads exceeded 100 kN.

Vehicle	Metric 1		Metric 2	
	Sum peak cell loads (kN)		Sum peak cell loads up to 40 ms (kN)	
	Row 3	Row 4	Row 3	Row 4
Raised SUV	75	154	38	130
Raised SUV with sub-frame SEAS	237	248	135	150

Table 3: Loads on rows 3 and 4 for Raised SUV with and without sub-frame SEAS.

A plot of the average height of force (AHOF) against B-pillar displacement (Figure 14) shows a change in AHOF between two vehicles. Similar simulation studies were also conducted for SUVs at the standard

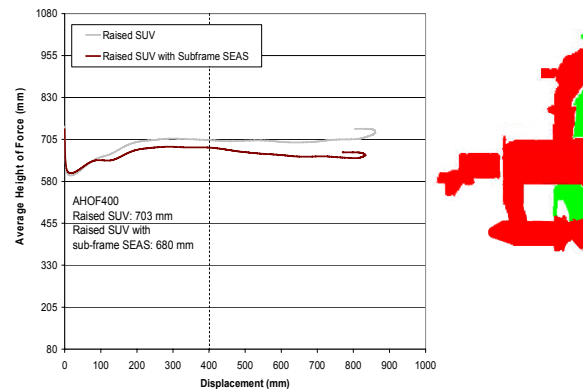


Figure 14: AHOF versus B-pillar Displacement for Raised SUV with and without sub-frame SEAS

ride height. In these studies, intrusions in car were low in impact by either SUV; however the addition of the sub-frame increased the intrusions by an average of 51%. Similar results were also seen in the car’s peak and average decelerations where the SUV with sub-frame SEAS causes higher values. A comparison of the metric 1 and 2 row loads shows that both configurations of the standard SUVs meet the 100kN requirement for both row 3 and row 4. Hence these metrics would not encourage the addition of SEAS to the baseline SUV. The AHOF value was lowered by the addition of the SEAS.

In summary, the results of the FWDB simulations show that metrics 1 and 2 can detect the presence of sub-frame type SEAS for this case of raised SUVs, although the minimum row load of 100 kN was met with or without SEAS. The AHOF value shows that addition of SEAS lowers the calculated AHOF in this case. Another observation from this study is that the addition of SEAS to the raised SUV resulted in lower intrusions in the car but for the standard height SUV, addition of SEAS indicated increased intrusions

which may indicate the need for integrating SEAS design with the overall front end design.

2. CAE- Based Approach

This research path is intended to develop a procedure for using finite element models of vehicles for compatibility evaluations. The planned tasks are

- Evaluation of LTVs in simulated impacts with finite element model of a 'representative car';
- Results to be synthesized into 'compatibility metric';

With this approach, it may be possible to evaluate collision compatibility in multiple impact configurations. The availability of appropriate finite element models of vehicles and the protocol for sharing such data is being currently discussed in the workgroup.

3. Development of Car Surrogate MDB for LTV Impacts

This approach is based on the assumption that 'improved collision compatibility' between a large vehicle and a smaller one implies 'improved protection of occupants in the smaller vehicle'. This of course needs to be achieved without any significant degradation in self-protection of either vehicle. Thus, an objective measure of improvement of occupants' safety in the smaller vehicles (when impacted by a larger vehicle) is a suitable measure of improved compatibility of the larger vehicle.

The intent of this research is to develop a moveable deformable barrier (MDB) that is a surrogate of a representative car for the purpose above. Thus, one of the challenges of the study was to select the 'US fleet representative' car in a 'field-representative' impact configuration [5]. The values selected for this are as follows [6]:

- Car mass of 1600-1700 kg,
- Full frontal impact with LTV as first priority,
- ΔV of 35 mph in struck car, representing 97th percentile in LTV to car crashes.

The car-surrogate MDB is developed to be representative of the car in front crush and in deceleration levels. In order to evaluate the degree of surrogacy achieved, it is necessary to compare these crush and deceleration levels in the reference car to those obtained using the MDB in impacts with LTVs. Since test results are subject to variations, it was necessary to determine the range of responses that may be achieved in nominally identical (but subject to test variations and build variations) LTV to car impacts and to define the MDB to represent this

range. The range of responses in the vehicles selected is shown in Figure 15.

Response Corridor measured in car in LTV Frontal Impact at 35 MPH

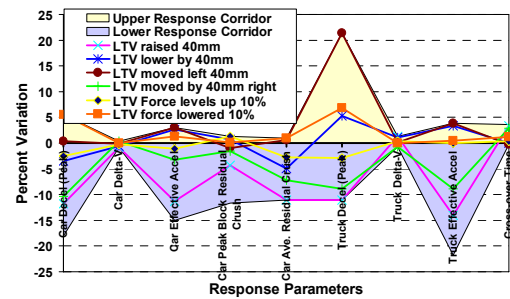


Figure 15: Response Corridor of Car in Impacts with LTV

An MDB configuration has been developed [6] using finite element simulations of the car and the LTVs. This MDB (Figure 16) consists of aluminum plates and blocks of honeycomb material of various densities and strengths to approximate the components in the front end of the vehicle.

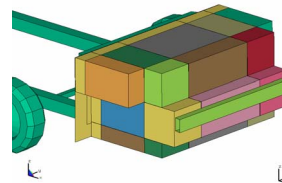


Figure 16 - Schematic of Car-surrogate MDB

The response of the proposed MDB as compared to the response corridor of car is shown in Figure 17.

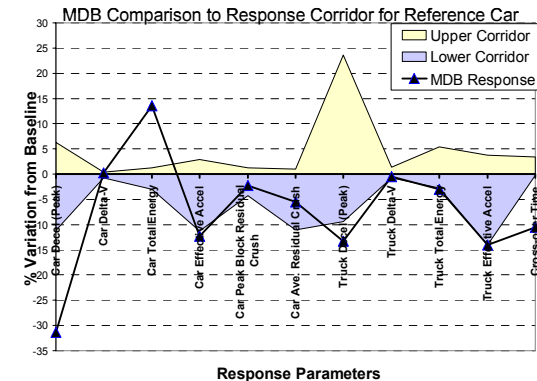


Figure 17: Comparison of MDB to Car Response Corridor

Physical prototypes of the MDB have been built and the MDB has been evaluated in component level tests (Figure 18). Based on the results from such

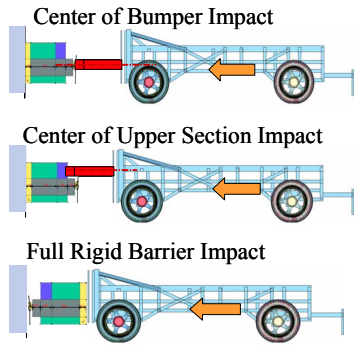


Figure 18: Component Test Configurations for Car Surrogate MDB Evaluation

tests (e.g. deformations in one test shown in Figure 19), several modifications have been made in the original configuration. The modified MDB is being fabricated and MDB-to-LTV tests and comparative evaluations with car-to-LTV tests have been planned.

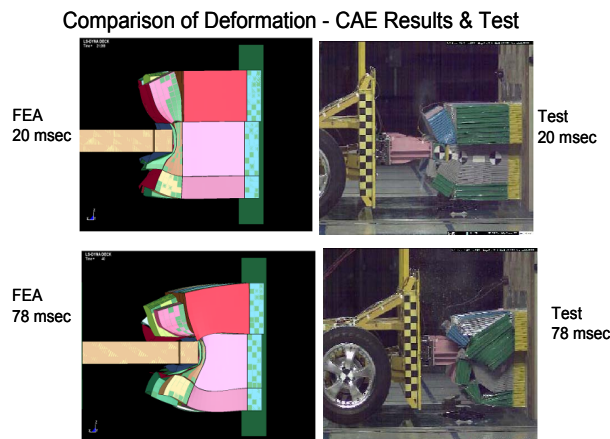


Figure 19: Comparison of Test Results from Centre of Bumper Impact to CAE results

ACKNOWLEDGEMENTS

This paper is a summary of contributions by many members of the workgroup. Special thanks are due to Mervyn Edwards of Transportation Research Laboratory, Sean O’Brian of Volkswagen and Alex Genetos of the Insurance Institute for Highway Safety for providing much of the written material.

REFERENCES

1. Barbat, S., (2005). ‘Status of Enhanced Front-To-Front Vehicle Compatibility Technical Working Group Research and Commitments’, 19th ESV, Washington, DC 2005, Paper No 05-463.

2. Baker, B., Nolan, J., O’Neill, B., Genetos, A., ‘Crash Compatibility between Cars and Light Trucks: Benefits of Lowering Front-End Energy-Absorbing Structure in SUVs and Pickups’, Insurance Institute for Highway Safety, Arlington, VA, 2007.
3. Verma, M., ‘Progress in Vehicle Collision Compatibility Improvements – A Report from EVC Technical Group’, Presented at Final Workshop VC-COMPAT Project, Eindhoven, October 2006. <http://vc-compat.rtdproject.net/>.
4. Edwards et al. (2007). ‘Current Status of the Full Width Deformable Barrier Test’, Paper No. 07-0088, 20th ESV Conference, Lyon, France 2007.
5. Barbat, S., ‘Vehicle Compatibility Assessment Using Test Data of Full Frontal Vehicle-to-Vehicle and Vehicle-to-Full Width Deformable Barrier Impacts’, Paper number 07-0348, 20th ESV Conference, Lyon, France 2007.
6. Peddi, S., Subramaniam K., Sharma V., Verma M., Schuyten H., ‘Development of a Mobile Deformable Barrier as Car Surrogate’, Paper no. 2007-01-1179, SAE Annual Congress, 2007.

OPPORTUNITIES FOR A WORLDWIDE COMPATIBILITY EVALUATION

- GERMAN MANUFACTURER'S POSITION PAPER ON CRASH COMPATIBILITY

Willibald Ablaßmeier

Audi AG

Thomas Slaba

BMW AG

Stefan Walner

BMW AG

Markus Hartlieb

DaimlerChrysler AG

Steffen Böning

FordWerke GmbH

Bert Wrobel

Adam Opel GmbH

Martin Kamm

Dr.Ing.h.c. F. Porsche AG

Sean O'Brien

Volkswagen AG and RMIT University Melbourne

Thomas Schwarz

Volkswagen AG

Robert Zobel

Volkswagen AG

Hans-Thomas Ebner

VDA

Paper Number 07-0323

ABSTRACT:

The passenger car manufacturers within VDA (German Association of the Automotive Industry) provide a position statement that has the potential to combine research by the American Alliance of Automobile Manufacturers with that of IIHS as well as the efforts of EEVC to constitute a feasible and realistic step for a worldwide compatibility evaluation. This paper provides the technical background of the suggestion. It discusses the relationship between self and partner protection in the current European accident scene and discusses benefits and drawbacks of alternatives currently being discussed in the various groups involved in compatibility research.

Compatibility offers the opportunity to increase safety in a limited manner. However, if it reduces the self-protection of passenger cars, there is the risk that it significantly compromises the currently very positive development of the national road safety figures in Europe.

INTRODUCTION

The main goal of this paper is to provide a first and feasible step towards better compatibility between

passenger cars. There are also a couple of drawbacks to be taken into account. But the main message is a positive one: There is a possibility for a feasible first step, and before we create new problems by attempting to solve everything, we should take feasible steps. The first section provides the common position in the VDA, the German Association of the Automotive Industry. In the sections following that, background information is provided.

THE VDA-POSITION ON COMPATIBILITY

- Increased self protection of passenger cars is the main reason for the continuous trend of reduced number of fatalities.
- Potential compatibility improvements must not compromise self protection. Current self protection level shall not be reduced.
- Geometrical alignment provides additional potential to further increase safety in car-to-car collisions, creating load paths between the colliding vehicles. This shall be the primary step for assessing compatibility.
- The geometrical alignment requirement may be based on geometrical measurement as long as no final

applicable dynamic evaluation method is defined. The evaluation of geometrical alignment shall assure that structural engagement and sufficient support is created in the common interaction zone as specified in sections below.

- A dynamic evaluation method may be based on full-width restraint test with load cells assessing forces and/or deformations. The applicable evaluation criteria shall have a strong correlation with improved partner protection without degrading self-protection.
 - The interaction area should be the common zone for structural interaction as specified below.
 - The evaluation should assure that sufficient support is created.
 - In case of force measurement, an upper limitation of force should be avoided due to the draw backs in self protection.
- However, for individual secondary structures (e.g. blocker beams, sub frames), which may not be identified by the full-width restraint test, an optional test or assessment method may be applied.
- If, in the future, new test or assessment procedures are provided, they shall be considered under the objectives of this statement, especially regarding self and partner protection.

Common Zone for Structural Interaction:

- 1) The presence of structures within a common zone for structural interaction (between 330 and 580 mm of ground clearance) needs to be confirmed for all vehicles including trucks, SUVs/LTVs, Sports Cars and Sedans).
- 2) Structures above the zone should not be penalised, providing sufficient support is present within the interaction zone.
- 3) Structures below the zone should be credited, providing sufficient support is present within the interaction zone.

Assessment methods should be defined in accordance to points 1, 2, 3.

This is the original wording of the VDA-position on compatibility.

THE DEVELOPMENT OF VEHICLE SAFETY IN GERMANY AND EUROPE

The comment made in the VDA-Position above – that there is a positive trend in German accident figures – can be easily proven using the data of the German Statistics Office.

Figure 1 shows a clear trend, which has remained fundamentally stable since 1970. Following the oil crises it was initially very pronounced and then, after an increase, it remained relatively stable until re-unification. With the exception of the increase caused by German re-unification, the number of people killed in traffic accidents has decreased by an average of 370 persons every year since 1983. This is a very encouraging development and may result in Germany achieving its goal of reducing the number of traffic fatalities by one half between the years 2000 and 2010.

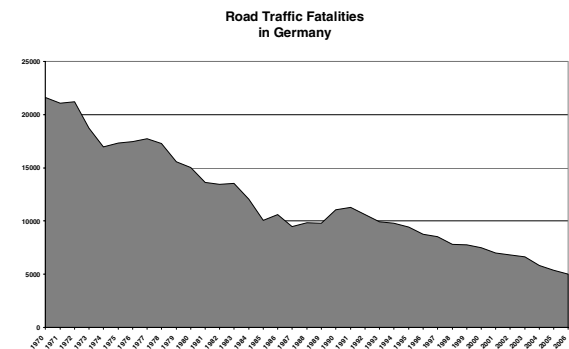


Figure 1. Time history of the number of fatalities in Germany since 1970. The 2006-figure was estimated by BASt in November 2006. (Source IRTAD)

Figure 2 shows that this positive trend affects all road users. Figure 3 presents the same data with a reference year of 1980. This makes the reduction achieved in the individual groups of road users more visible.

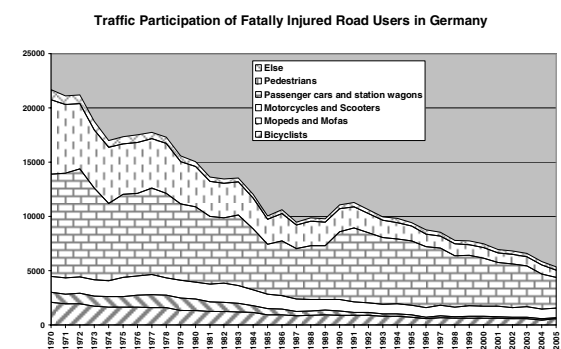


Figure 2. Time history of the number of fatalities in Germany since 1970 for individual groups of road users. (Source IRTAD)

In Figure 3, the results for mopeds and motor-assisted bicycles are especially positive. Due to the unknown total travel distances of mopeds and motor-assisted bicycles, it cannot be directly concluded that there has been an increase in the safety of these vehicles. Nevertheless, the enforcement of helmet use and the low speeds of

these vehicles have a special significance. In 2005, fatalities of moped and motor-assisted bicycle riders had dropped to only 10.1% of the 1980 figure.

The pedestrian category also shows a considerable reduction to 18.4% of the 1980 figure. This trend has continued uninterrupted since 1970.

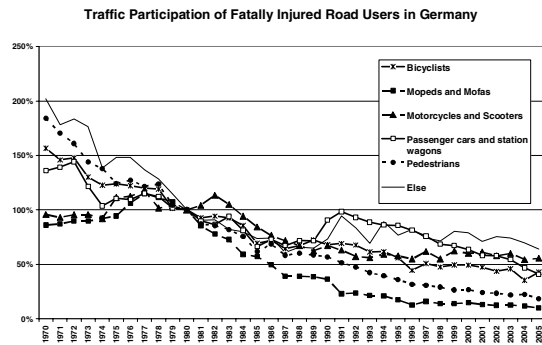


Figure 3. Time history of the number of fatalities in Germany since 1970 for individual groups of road users. 1980 was used as the reference year to enable comparison between the groups. (Source IRTAD)

Passenger car occupants follow as the third group, with a reduction to 41% of the value from 1980. Here, it must be taken into account that the number of fatally injured car occupants in 1991, immediately following re-unification, rose to equal the value from 1980. A very low level had been achieved in 1987. Thus, a more relevant observation is that the car occupant group has in fact achieved a 59% reduction in the period from 1991 until the present.

Bicycles and motorcycles show a less pronounced reduction during the last 15 years.

Nevertheless, it can be summarised that a marked increase in the level of traffic safety, which affects all road users, can be observed in Germany.

Looking at the other EU member states shown in Figure 4, a similar trend may be observed. It would be too complicated to discuss each member country individually, but it is readily apparent that many member countries display a similarly positive trend. The exceptions are Greece and the new European member states.

The effects of the trend can be better observed looking at the reduction expected between the years 2000 and 2010. Figure 5 shows a linear regression of the last 10 years for each country until the year 2010. The expected reduction in traffic deaths compared to the year 2000 is indicated. Only Germany can expect a reduction of more than 50%.

Some countries – namely Portugal, Austria and Hungary – are expected to reach over 40%. In total, the 18 EU members for whom IRTAD (International Road Traffic Accident Database) provides data should achieve a reduction of 23%. This is an encouraging number, even if the ambitious goals set by the EU are unlikely to be achieved.

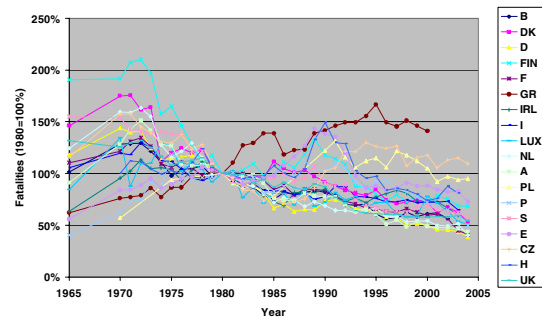


Figure 4. European trend with regard to the number of fatalities in 18 member states of the EU. 1980 was used as the reference year in order to achieve comparable data.

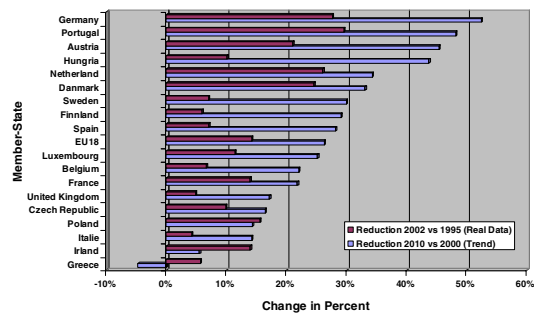


Figure 5. Current change and expected trend seen in 18 major member states of the EU.

Overall, these numbers show that considerable progress has been made in Europe. Steady progress in almost all the member states is especially visible in the last ten years.

This means that caution must be exercised with regard to the modification of safety-relevant regulations. We should do whatever possible to ensure that the positive trend continues.

THE SIGNIFICANCE OF THE COLLISION TYPES FOR BELTED PASSENGER VEHICLE OCCUPANTS

Figure 6 provides an overview of how the collision types are distributed for the various injury classes. The categories are divided as follows:

MAIS 0+ includes all injured and uninjured car occupants involved in GIDAS accidents, and

demonstrates the distribution of collision modes in accidents with injured persons,

MAIS 1+ includes all injured car occupants,

MAIS 2+ to MAIS 4+ include injured car occupants with progressively increasing seriousness of injury,

MAIS 5+ includes car occupants with critical injuries and a low chance of survival,

and finally MAIS 6 includes only the maximally injured car occupants with very little chance of surviving.

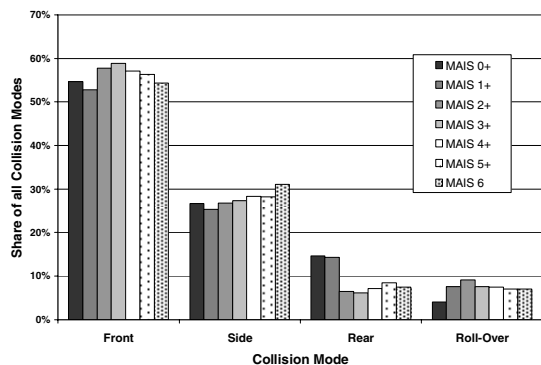


Figure 6. Collision mode distribution for belted occupants of passenger cars, according to GIDAS database. The distribution is shown for all injury severity classes. The relative number of occupants of a particular injury severity is shown in percentage terms for each of the collision modes.

Figure 6 shows that the percentage of frontal collisions, regardless of the severity of injury, is always approximately 55%. Only belted occupants are taken into account. Side collisions follow with 30% and a slightly rising trend. Rear collisions are down to 7 to 8%. Rollovers have also stayed in the same range of about 7 to 8%. They are somewhat under-represented for MAIS 0+ occupants, but no special relevance for rollovers can be deduced from this data.

The effects of previous safety measures cannot be seen in Figure 6, so in the following two figures, the collision mode and injury distributions are considered for older and newer passenger vehicles.

If the MAIS 0+ percentages in Figure 7 and Figure 8 are compared, it can be seen that side collisions have always been less frequent than frontal collisions. However, in vehicles built before 1980, 42% of the MAIS 6 injuries to car occupants resulted from frontal collisions, and 42% resulted from side collisions. This was because the

significance of side collisions increased with increasing injury severity. Frontal and side collisions were thus equally represented among the most serious injuries.

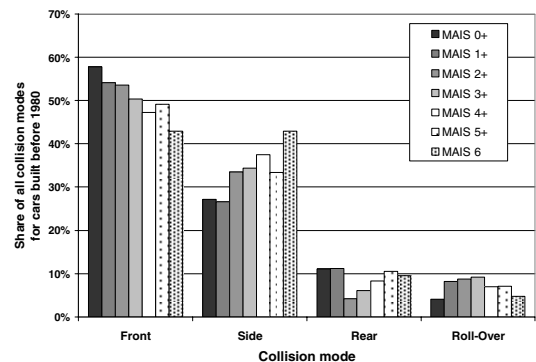


Figure 7. Collision mode distribution for passenger cars built before 1980, according to GIDAS database. The distribution is shown for all injury severity classes. The relative number of occupants of a particular injury severity is shown in percentage terms for each of the collision modes.

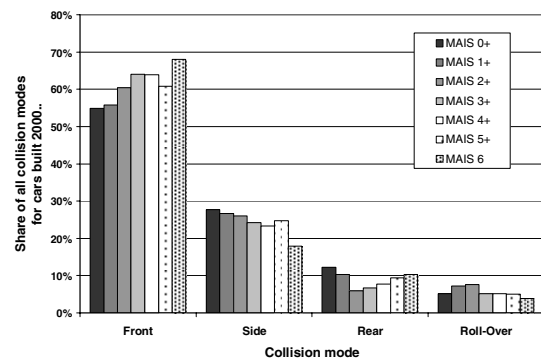


Figure 8. Collision mode distribution for passenger cars built after 2000, according to GIDAS database. The distribution is shown for all injury severity classes. The relative number of occupants of a particular injury severity is shown in percentage terms for each of the collision modes.

For vehicles built after 2000 (Figure 8), the opposite effect is apparent. Today a frontal collision represents a greater danger than a side collision. At higher levels of injury severity, a greater proportion of occupants are involved in frontal collisions.

This illustrates that the measures which were adopted for side protection were more effective than the measures used to address frontal collisions. The distribution of collision types shows that the incidence of severe side collisions has been reduced more than that of frontal collisions. Frontal

collisions must therefore be given a higher priority than they were in the past. The previous section clearly illustrated that the total number of fatal injuries has gone down.

In addition it should be considered that high speed side collisions against narrow objects (e.g. trees or utility poles) with the correspondingly higher injury risk have been significantly reduced due to the introduction of ESC (Electronic Stability Control). This further reduces the number of serious side collisions and points to the fact that it makes sense to prioritise frontal collisions.

THE RELEVANCE OF SELF-PROTECTION AND PARTNER PROTECTION

Europe has a tradition of paying special attention to car-to-car collisions. The high speed frontal offset test described in ECE Regulation R94 (Uniform provisions concerning the approval of vehicles with regard to the protection of the occupants in the event of a frontal collision) was originally developed to mimic car-to-car collisions with a partial overlapping of the fronts of the vehicles. As the above analysis of the European statistics shows, the test has been effective. Considering the current emphasis being placed on developing a regulation to improve compatibility, it could be presumed that car-to-car collisions represent the greatest risk to car occupants. This is not the case, as studies from many different countries demonstrate. Good examples are the situation in Germany, Italy and France, shown in Figures 9 to 11. For Italy the data for seriously injured persons is lacking, so only two categories can be taken into account.

The message is clear, single vehicle accidents account for a considerable share of injuries and become dominant with regard to fatalities. Therefore self protection is the major key to save lives and protect occupants, while the combination of self and partner protection only decides the outcome of car-to-car accidents.

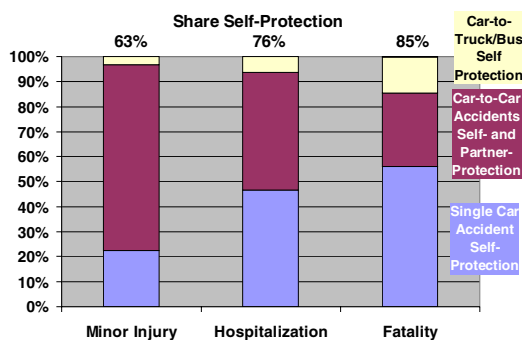


Figure 9. Relevance of self- and partner protection in Germany for different injury severity classes.

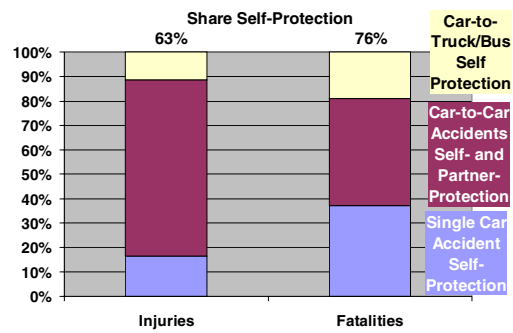


Figure 10. Relevance of self- and partner protection in Italy for different injury severity classes.

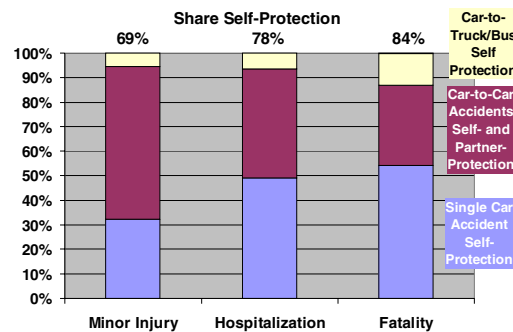


Figure 11. Relevance of self- and partner protection in France for different injury severity classes.

THE DEVELOPMENT OF SELF-PROTECTION AND PARTNER PROTECTION IN GERMANY

Many accident researchers expected that the significant increase in self-protection would have a negative effect on partner protection. This was supported by a spectacular crash test performed by a German test institution, in which a very old vehicle was crashed against a new version of the same vehicle. However, it can easily be seen that, statistically speaking, such an extreme combination is relatively rare. Older vehicles are rapidly disappearing from the vehicle fleet and being replaced by modern cars. It also makes no sense to avoid safety improvements for the future by looking at outdated vehicles that are about to be phased out of the vehicle fleet.

Therefore, the GIDAS database was examined to see how deformation behaviour and the severity of injuries have developed with respect to vehicle build year. During this process, it was consciously taken into account that a new vehicle involved in a collision in 2005 collides with a different fleet to a vehicle built in 1985 involved in a collision in 1990. In other words, the vehicles built in different years were analysed with regard to vehicles that they actually crashed into. A car occupant is only

interested in the level of risk he is subjecting himself to when he buys a car and drives in current traffic conditions. The results are as clear as those shown in the IRTAD data for all of Europe and Germany in particular.

Figure 12 shows that modern vehicles undergo large deformations much more seldom than older vehicles. Assuming that impact speed has not decreased for current vehicles compared to older vehicles, the stiffness of the vehicle fleet must have increased.

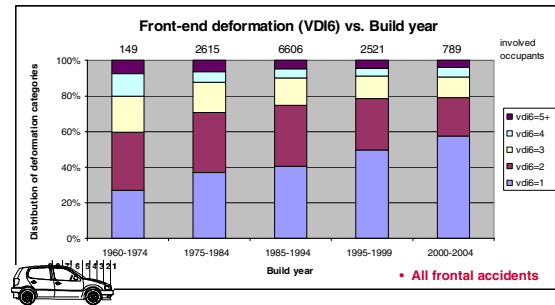


Figure 12. Front end deformation in frontal accidents described by Vehicle Deformation Index VDI6 versus build year. This implicitly describes the effect of structural measures that have been implemented into the vehicle fleet in recent decades.

Figure 13 examines the injuries that people in these vehicles have suffered and it is evident that injuries have been reduced to a similar extent. Figure 14 includes only the upper 20% from Figure 13 to more clearly show that the number of seriously injured occupants has been reduced by half. Especially impressive are the improvements for occupants who suffered MAIS 2 or higher. In vehicles built before 1975 their share was over 20%. In contrast to this, for vehicles built in the current decade it is only 6%. The same also applies to critically injured car occupants.

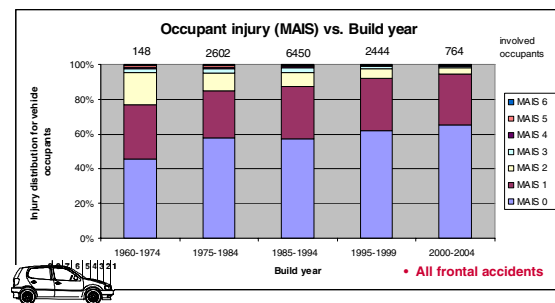


Figure 13. Decrease of injury severity versus build year for belted occupants in frontal collisions.

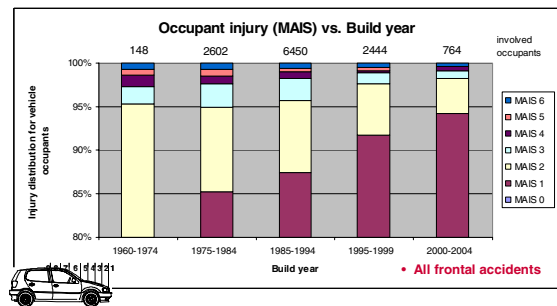


Figure 14. Same graph as Figure 13, but with y-axis limited to 80..100% to show the effect on the most severely injured occupants.

Only belted occupants were taken into account throughout the study, so the higher belt-wearing rate in recent years has no influence on the result.

So far these results are not surprising and fit into the overall pattern which was developed from observing European countries using the IRTAD database.

The following figures evaluate the crash events from the partner protection perspective by looking at the collision partner. This way, it can be investigated how a vehicle of a particular build year affects other vehicles in a collision.

Figure 15 shows the crush depth in the opposing (target) vehicle over the build years of the impacting (bullet) vehicle. This demonstrates that, on average, the depth of intrusions in the collision partner of a newer car is less than those caused by an older bullet vehicle. Or in other words, partner protection with regard to structural deformation has improved. Keeping in mind that the average front end stiffness of the vehicle fleet has increased, the reduction of crush depth in the opponent vehicles can be attributed to the fact that the share of modern cars in the vehicle fleet has over-compensated for the increase of front end stiffness.

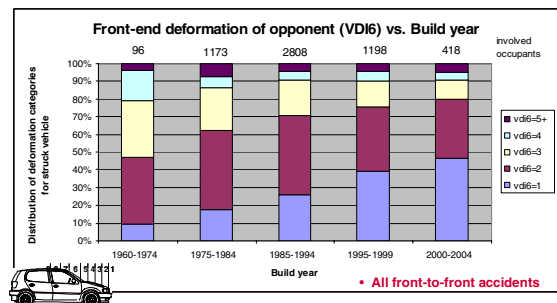


Figure 15. Like Figure 12: Front end deformation in frontal accidents described by Vehicle Deformation Index VDI6 versus build year. But now the deformation of the opponent of the car under consideration is analysed.

Figure 16 and Figure 17 look at the injuries caused in the opponent vehicle with respect to the build year of the impacting vehicle. Here the same pattern is apparent. The injuries in the opponent vehicle have not increased; modern vehicles cause fewer and lesser injuries in the vehicles that they collide with. If the vehicles from 1995 to 1999 are compared with the vehicles from 2000 to 2004 in Figure 16, a slight increase can be seen. Due to the low number of cases, this should not be given too much significance. Therefore, in Figure 17 these two groups are combined. A clear improvement can be seen for the enlarged group. The slight deviation from this trend visible in Figure 16 will be the object of further investigation in the future.

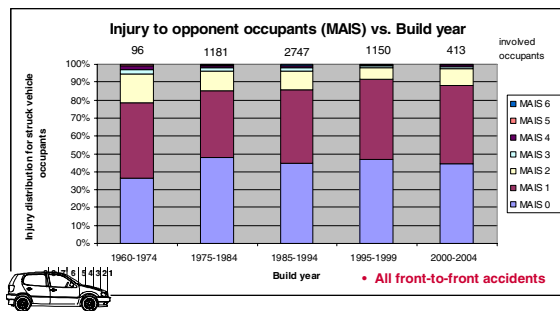


Figure 16. Decrease of injury severity versus build year in frontal accidents for belted occupants of opponent car. This is the partner protection view point, analysing the degree of compatibility in vehicle fleet versus time.

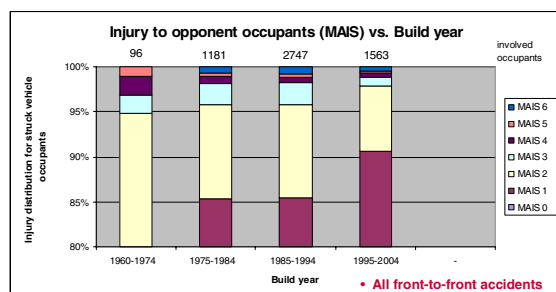


Figure 17. Same graph as Figure 16, but with y-axis limited to 80..100% to show the effect on the most severely injured occupants. To achieve sufficient sample sizes, the latest cars were put in one group.

Overall, it is clear that vehicle development in the past decade has gone in the right direction with regard to both self-protection and partner protection. So far the current regulations have had a positive effect on both self and partner protection.

However, the path of self-protection cannot be stretched out indefinitely by continually increasing test speeds. In this way the results for vehicles from 2000 to 2004 can also be understood as a warning signal. At present, the authors are not in a position

to prove the plausibility and statistical tenability of the results for vehicles from 2000 to 2004 using the available numbers.

In any case, it may be concluded that proposals for new test procedures or even for the replacement of Regulation ECE R94 must first demonstrate that the modified procedures will continue the positive trend which have been achieved under the conditions of ECE R94.

FRONTAL COLLISIONS: A BRIEF REVIEW OF THE DEVELOPMENT OF TEST BARRIERS

Test barriers can be considered to come in three relatively discreet forms: rigid barriers, barriers with limited deformation and barriers with unlimited deformation. Naturally, no barrier can be truly unlimited, but if enough depth is provided to prevent bottoming out, the barrier can be considered from the car's point of view to be unlimited. This section will consider the development of these barriers for European offset crash tests.

EEVC developed a limited deformation barrier in the 1980s, which consisted of a relatively small deformation element in front of a rigid wall (Figure 18). This barrier, with a 40 % offset and 56 km/h collision velocity, was a compromise solution representing partly a rigid object collision and partly a 50 km/h, 50 % offset car-to-car collision. Although not completely representative of either collision type, this barrier creates a realistic acceleration pulse and deformation pattern, and ensures significant deformation of the vehicle structures through bottoming out. It entered into regulation in the mid 1990s and is also used in EuroNCAP testing.

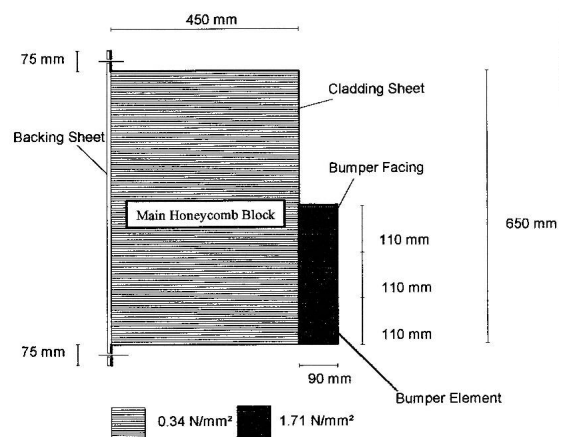


Figure 18. ECE-R94-barrier.

During this time, auto motor und sport, an auto magazine based in Stuttgart, performed tests with a rigid offset barrier. Although these tests

mercilessly revealed the deformation potential of the vehicle front end, the pulse was unrepresentative of many collisions and all vehicle front-end components were equally deformed.

At the beginning of the 1990s, Dr. Klanner from ADAC developed a barrier which was deep enough to provide effectively unlimited deformation (Figure 19). In a collision with the ADAC barrier, the reaction forces exerted on the car structures are controlled by the stiffness of the barrier, and the high forces of a rigid object collision are never reached. Furthermore, the deformation potential of the barrier is very large, meaning that rather than forcing deformation of the vehicle structure, as is the case in a collision with a rigid object, the barrier itself absorbs a large part of the kinetic energy. EEVC considered this barrier and rejected it, choosing to adopt the limited deformation barrier described above.

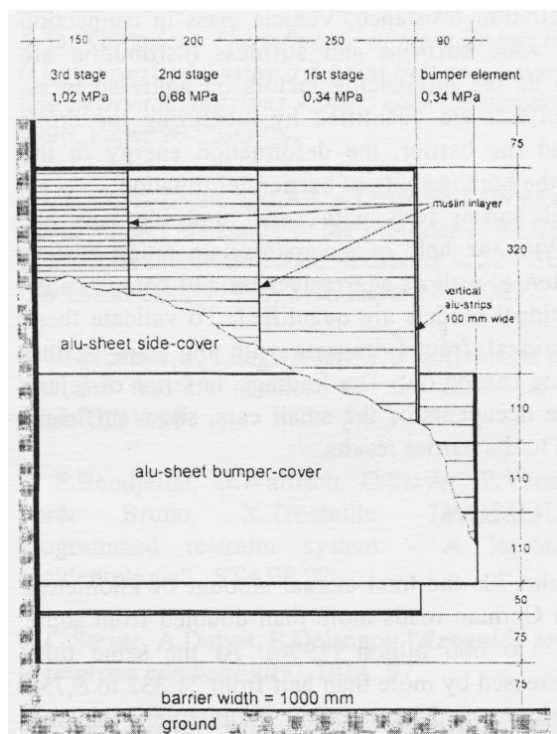


Figure 19. ADAC-barrier.

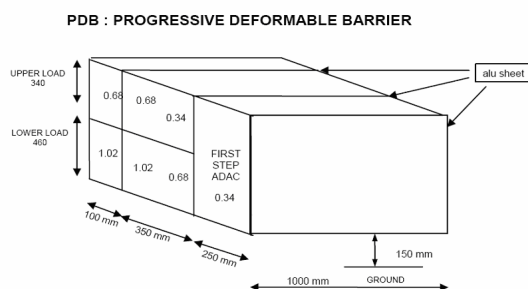


Figure 20. Progressive Deformable Barrier (PDB).

French Industry saw merit in Klanner's idea, and further developed it into an alternative barrier with effectively unlimited deformation, the PDB (Figure 20). Like the ADAC barrier, the forces exerted on the vehicle structure are limited by the barrier stiffness, and the barrier itself is able to absorb a large amount of energy.

The fact remains that discussion of further developments in frontal crash testing is currently very difficult. For Europe, two main alternatives are under consideration: a combination of the PDB with a rigid full width test, and a continuation of the existing R94 with an additional full width test with a deformable element and load cell wall.

In considering such barriers for the assessment of vehicle safety and compatibility, it is essential that the specific test procedures and analyses are assessed according to strict scientific criteria which, together with relevant accident analysis, answer the following questions:

What are the advantages of the proposed compatibility test procedures and assessments for real world safety?

What are the disadvantages or foreseeable drawbacks of the proposed test procedures and assessments?

What is the potential of the proposed test procedures and assessments regarding world-wide harmonisation?

The following attempts to discuss some of the possibilities which accident research and FEM simulation offer us to predict developments through modified test conditions.

FRONTAL COLLISIONS: OPPORTUNITIES AND RISKS OF A BARRIER WHICH PREVENTS BOTTOMING OUT

Klanner's idea, when he defined the ADAC barrier, was to prevent bottoming out of the barrier. A longitudinal member should not impact with a rigid and ideally smooth wall but, as in real life, should interact with an obstacle with a defined stiffness. This is closer to the reality of a car-to-car accident. The aluminium honeycomb structure punishes penetrating skewers, such as longitudinal members which are not supported by a stable cross member. It offers only limited resistance to these elements. The aluminium honeycomb creates pressure and the level of force is determined by the surface pressure. A small surface means the longitudinal member receives only a small amount of support force in the barrier, and is thus not deformed.

Sometimes effects such as these are seen in car-to-car collisions. The goal of structural interaction is to provide sufficient support between two colliding vehicles so that deformation of the front ends of the vehicles will dissipate as much energy as possible; thereby ensuring that the survival space in both cars remains intact.

However, other vehicles are not the only opponents in car crashes. For example, the opponent could also be a tree. Let us assume that a manufacturer has built a vehicle with a longitudinal member that is too rigid and is now testing the vehicle with a PDB. The longitudinal member will penetrate deep into the barrier, but with only moderate force. The manufacturer would therefore only find a moderate deceleration in the vehicle during the test and would consider the vehicle to be safe. But if this vehicle crashes into a tree, the tree will exert resistance against the longitudinal member. The longitudinal member will be deformed, not the tree, but now at a high level of force and with high decelerations. The seemingly safe vehicle with the moderate compartment deceleration suddenly shows itself to be highly dangerous. Possible results are increased intrusions into the compartment and/or occupant decelerations for which the restraint system is not designed.

This situation was simulated in FEM. In Figure 21 to Figure 23, the effect of a "normally" designed longitudinal member is compared with that of a very rigid longitudinal member.

Figure 21 shows that the ECE-R94 test at 56 km/h identifies the differences; increased deformations can be seen in the compartment of the rigid vehicle. This effect becomes even more apparent when the vehicle impacts the ECE-R94 barrier at 64 km/h (Figure 22). The behaviour of the vehicle in both tests is very similar to the expected result. Since the rigid longitudinal member creates a bridge of force from the front of the vehicle to the compartment and thus prevents most parts of the front of the car from being deformed, less deformation work is done in the front of the car. But since kinetic energy must be absorbed, the deformation takes place in the passenger compartment. This is similar to what would occur in a collision with a tree. In a vehicle-vehicle accident, the vehicle would still have the chance to receive the lacking deformation energy from the other vehicle. This is not desirable, however. At a sufficient speed it would only shift the intrusion to the compartment of the opposing vehicle.

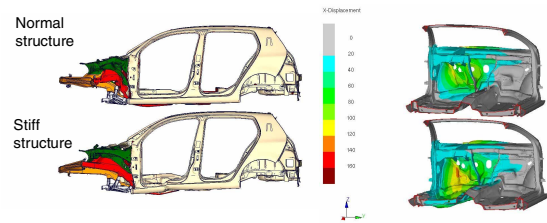


Figure 21. ECE-R94-test of a normal car and a car with a very stiff longitudinal. The increased stiffness can be detected by the higher level of intrusion into the compartment.

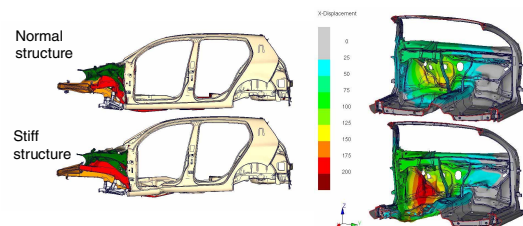


Figure 22. ECE-R94-barrier-test with impact velocity of 64km/h (EuroNCAP) of a normal car and a car with a very stiff longitudinal (same as Figure 21). The increased stiffness can be even better detected by the higher level of intrusion into the compartment.

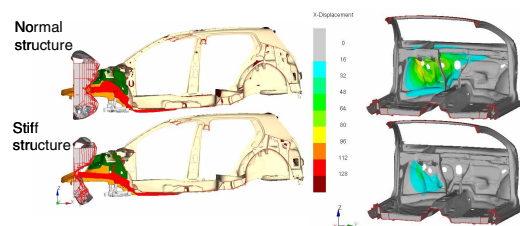


Figure 23. PDB-test of a normal car and a car with a very stiff longitudinal (same as Figure 21). The increased stiffness is compensated by greater deformation of the barrier and identified as a positive measure providing more safety, because intrusion into the compartment is significantly reduced.

The PDB conceals this effect (Figure 23). If the compartment deformation of the vehicle with the rigid longitudinal member is examined, it can be seen that the intrusions are reduced in comparison to the vehicle with the normal longitudinal member. This is very problematic. In this example, the designer would be tempted to adopt a measure which would actually decrease the safety level of the vehicle. He or she would be faced with the moral conflict of whether to objectively improve the vehicle or to develop it in such a way that it would perform well in the test. Such a situation should not arise.

A further aspect is the large amount of deformation energy which the PDB provides. This is illustrated for the individual elements of the barrier in Figure 24. The total available deformation energy is 302 kJ, and with 700 mm of impact area 212 kJ are still available. The volume of deformation energy in the barrier is critical because it conceals how much energy a vehicle itself has to dissipate during the impact. 212 kJ is the amount of kinetic energy a 1524 kg vehicle possesses when travelling 60 km/h. Therefore, such a vehicle does not need to contribute any of its own deformation energy in a test against the PDB. As such, there are broadly different structural designs, with broadly different degrees of available deformation energy, which could be used in a small vehicle to pass a test against the PDB. Details about this were published at the ESV conference (Zobel, 2005 [6]). However, since the volume of deformation energy which is built into the deformable structures in the front of the car is responsible for a vehicle's self-protection level, this means that the PDB test can be passed even if the level of self-protection is low.

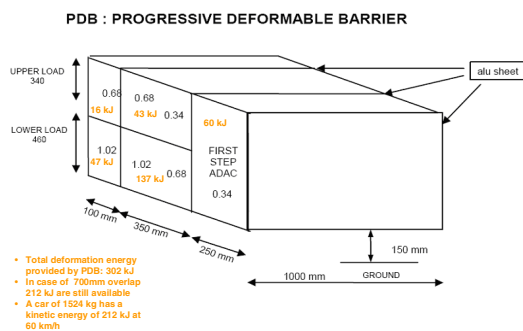


Figure 24. Deformation energy, provided by the different segments of PDB.

The German Federal Highway Research Institute (BASt) tried in one publication (Pastor, 2005 [7]) to determine the influence of the available deformation energy on the accident. This can only be done very roughly, but is representative with regard to the scale. If 28% more deformation energy were available, according to the calculations of the BASt, we would have 8% fewer fatalities. Even if the absolute accuracy of these numbers is disputed, the tendency they show is correct. This implies, conversely, that reducing the deformation by 28% would increase the number of fatalities accordingly. The introduction of a barrier such as the PDB would therefore have the potential to increase the number of fatalities, since it is possible to reduce the available deformation energy in the vehicle and thereby lower the level of self-protection.

FRONTAL COLLISIONS: OUTLINE OF A CONTRIBUTION TOWARD THE IMPROVEMENT OF STRUCTURAL INTERACTION

Influenced by these ideas, the German manufacturers represented in the VDA have jointly investigated ways in which compatibility in Europe could be improved. It is clear from the accident research that the dynamic which forms the basis of the positive European trend should be treated with caution. Therefore, radical changes have been deemed undesirable. The ECE-R94, which had obviously proven effective, was not questioned. Instead, methods were found by which to improve the structural interaction of vehicles, in order to make better use of the deformation energy available in car-to-car collisions. It is undisputed that the central goal of vehicle safety is that vehicles need deformation energy (for self-protection) and that their structures must be designed in such a way that the kinetic energy present in car-to-car crashes is dissipated in the crumple zone. It is for this reason that structural interaction is important. At the beginning of the compatibility debate it was observed that two vehicles which both have sufficient deformation energy for a collision with the wall at speed x , also have sufficient deformation energy in a car-to-car accident for a collision at the closing speed $2x$. This applies regardless of the weight ratio (Zobel, 1997 [8]) and (Zobel, 1998 [9]). The significance of structural interaction is very well described by IIHS with reference to the problems posed by Sport Utility Vehicles (SUV) in America. (Farmer, Lund, 2006 [10]). The German manufacturers are following this accident-oriented path. They see a geometrical alignment of the structures as their first priority.

The VDA-position on compatibility promotes steps for a regulation, oriented towards compatibility, based on accident statistics. The position is open for new scientific enhancements, as long as these will have additional positive effect in real world accidents. We see this as a basis which can be used to bring diverging interests together. Measures which offer the most help to the affected persons should be taken into consideration. They should take into account injury mitigation as well as accident prevention measures, which have proven to be even more effective than injury mitigation today.

SUMMARY AND OUTLOOK

The following provides a generally positive outlook:

Europe has made significant progress in the area of vehicle safety. Germany has taken a leading role in this transformation.

Europe is unlikely to achieve its ambitious goal of reducing the number of persons killed in traffic accidents by half in the first decade of the new millennium. Nevertheless, with a reduction of approximately 25%, considerable progress will have been made.

Infrastructure measures could raise the EU-wide improvement up to 35%. This would happen if, in all EU-member-states, 50% of rural traffic was on motorways.

Germany is expected to be one of the few countries to achieve the EU goal. This shows that the traffic safety concepts developed in Germany are very effective. The German automotive industry demonstrably has an important stake in this.

Frontal collisions make up a greater percentage of severe accidents than they did in the past. This indicates that the safety level in the area of side collisions has improved disproportionately.

Self-protection is a primary factor in vehicle safety and should therefore be given top priority in the future.

Vehicle compartments have become more stable. This has led to an increase in the protection of vehicle occupants.

Nevertheless, partner protection has also improved in the European fleet.

When developing a barrier, care must be taken not to stop or reverse the extremely positive trends described above.

A further improvement in vehicle safety is possible with careful steps within the limitations of the existing regulations. German manufacturers are prepared to support such an approach and have outlined it in a position statement (see first section).

The foreseeable future developments for accidents should also to be taken into consideration in the further development of the side impact barrier.

Fundamentally, a greater integration of accident research into the development of vehicle safety regulations is absolutely necessary. It is not enough

to identify the target population of a measure, but before a proposed measure is put forward for regulation, research should be conducted to establish the benefit of this specific proposal in a future fleet.

No positive trend is so stable that it cannot be significantly damaged or even reversed.

REFERENCES:

- [1]: Klanner, W., Felsch, B. und van West, F. (1998) "Evaluation of Occupant Protection and Compatibility out of Frontal Crash Tests against the Deformable Barrier" 16th ESV Conference, Windsor.
- [2]: Dellanoy, P. (2000) "EUCAR Summary" EEEV Document Number 111, 15th Meeting of EEEV Working Group 15, Crawthorne, UK.
- [3]: Martin, T. und Dellanoy, P. (2006) "Validation of PDB approach" VC-Compat Final Workshop, Eindhoven, NL.
- [4]: UTAC (2004) "Self and partner protection test and assessment protocol based on current regulation R94 and PDB Barrier" Version 2.2.
- [5]: Schwarz, T., Strube, C., Zobel, R. und O'Brien, S. (2005) "Aspekte zur Entwicklung eine weltweit harmonisierten Kompatibilitäts-Bewertungsverfahrens" VDI Tagung Innovativer Kfz-Insassen- und Partnerschutz, Berlin.
- [6]: Zobel, R., Thomas, G., Schwarz, T. (2005) "Towards beneficial, scientifically meaningful and applicable compatibility testing" 19th International Technical Conference on the Enhanced Safety of Vehicles, Washington.
- [7]: Pastor, Claus. (2005) "Potential benefit of improved vehicle compatibility" Conference proceedings: Kompatibilität im Straßenverkehr, Dresden
- [8]: Zobel, Robert. (1997) "Barrier Impact Tests and Demands for Compatibility of Passenger Vehicles" Conference proceedings: Innovativer Insassenschutz, Berlin
- [9]: Zobel, Robert. (1998) "DEMANDS FOR COMPATIBILITY OF PASSENGER VEHICLES" 16th International Technical Conference on the Enhanced Safety of Vehicles, Windsor, Canada
- [10]: Farmer, C.M. and Lund, A.K. (2006) "Trends over time in the risk of driver death: What if vehicle designs had not improved?" *Traffic Injury Prevention* 7:335-42.
- [11]: Rieger, G., Scheef, J., Becker, H., Stanzel, M., Zobel, R. (2005) "ACTIVE SAFETY SYSTEMS CHANGE ACCIDENT ENVIRONMENT OF VEHICLES SIGNIFICANTLY - A CHALLENGE FOR VEHICLE DESIGN" 19th International Technical Conference on the Enhanced Safety of Vehicles, Washington.

THE DEVELOPMENT OF A MOBILE DEFORMABLE BARRIER TEST PROCEDURE

Richard Schram

Ton Versmissen

TNO Integrated Safety

The Netherlands

Paper Number 07-0327

ABSTRACT

Frontal compatibility assessment, including self and partner protection, is a major topic in crash safety testing today. Currently none of the regulatory and consumer test procedures is able to assess the vehicle on vehicle frontal compatibility on the three main aspects; structural interaction, frontal stiffness and compartment strength. It is hypothesized that a test procedure using a Mobile Deformable Barrier (MDB) could be able to assess compatibility on the aspects mentioned above. This paper presents the development of a MDB test trolley for frontal offset testing and its full scale test results.

First, a load sensing trolley was developed. The specifications of the trolley, mass, CoG and inertia properties are based on EU and US vehicle geometry databases. The trolley mass was made adjustable between 1300 kg and 1800 kg, with tunable inertia properties. The trolley was designed to be equipped with the progressive deformable barrier (PDB) as deformable element. The PDB was chosen based on the available test-data and for its stability and its ability to allow a barrier face deformation measurement to evaluate partner protection. Based on the current PDB test protocol, a test protocol has been developed for the MDB, called MPDB test procedure. A number of vehicles, ranging from small to large, were tested according the MPDB protocol. The closing speed was selected such that comparable initial kinetic energy is involved as in a static PDB test for a mid sized car with mass of 1500 kg. The test results with the full scale MPDB tests were analyzed and compared to test results of static PDB tests with the same vehicle. It was concluded that for small vehicles the severity of the MPDB tests is relatively higher than for larger vehicles. The MPDB test procedure was shown to be feasible and repeatable. Further investigations into test parameters like trolley mass and test velocity are recommended.

INTRODUCTION

Frontal compatibility assessment is a major topic in crash safety research world-wide. With the changing

fleet composition, the differences between cars are increasing in terms of mass, front end stiffness and geometry. Research in the field of compatibility is ongoing world-wide and a general objective of the compatibility research is to ensure that future vehicle developments are more balanced in terms of occupant protection of both striking and struck vehicle, in case of a vehicle-to-vehicle collision.

Methods to assess frontal compatibility should take into account three aspects:

- Structural interaction to ensure an optimal force transfer between the colliding vehicles
- Compartment strength to prevent compartment collapse
- Frontal stiffness to match deformation force levels between the colliding vehicles

Moreover, the occupant's self-protection should not be compromised by increasing the level of partner protection.

Currently none of the regulatory and consumer test procedures is able to assess vehicle to vehicle compatibility on these main aspects. The current procedures are for self-protection assessment and restraint system optimization only, which is not necessarily beneficial for partner protection. Furthermore there is a lack of world-wide harmonization in the current protocols.

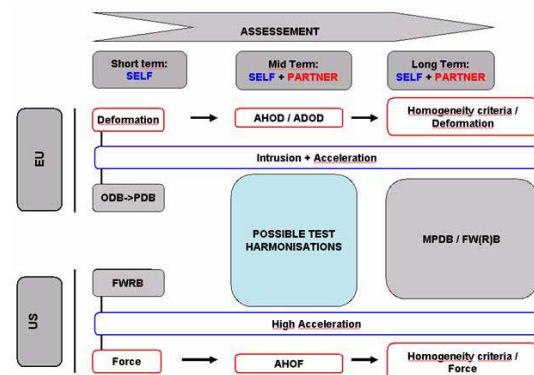


Figure 1. Future outlook for compatibility assessment. AHOD: average height of deformation. ADOD: average depth of deformation. AHOF: average height of fore

A short, mid, and long term view on compatibility assessment, taking also into account the desire for world-wide harmonization acknowledging fleet differences across the world, are presented in Figure 1. For the short term assessment of compatibility two test procedures are under development within EEVC WG15; the FWDB and PDB approaches.

For the long term, a mobile deformable barrier test procedure for compatibility testing is generally seen as the best achievable compromise by both Europe and US, and therefore opens the possibility for harmonization. To support the foreseen long term direction of compatibility assessment, TNO Automotive decided to develop the required load sensing MDB for frontal offset testing. A clear demand has emerged for advanced assessment of car compatibility, based on a more innovative approach. By combining smart measurement technology, in-depth knowledge on compatibility and crash test experience, this projects aims to develop an advanced compatibility test method for assessing frontal compatibility. Partners in this project are TNO, initiator and project-management, UTAC, GME, PSA, Renault, AFL and FTSS.

OBJECTIVES

The goal of this project is to develop a future step in compatibility testing for the long term. This step should take self as well as partner protection into account. The partner protection assessment will be based on the barrier deformation as well as on loadcell wall recordings.

The first objective to achieve this goal is to design and develop a trolley equipped with a high resolution loadcell wall. Second the feasibility and merits of a Moving Deformable Barrier (MDB) in a frontal offset test procedure are assessed.

APPROACH

The initial step in the project was to develop a trolley equipped with a High Resolution Loadcell Wall (HR-LCW) and with mass and inertia properties that are representative for an average European car. The long term approach of a mobile test procedure is based on the hypothesis that the striking vehicle is an average car. Therefore, the trolley with deformable barrier should be representative for a vehicle class in Europe or US. The main specifications of the trolley, such as mass, CoG location and inertia properties are based on European and US vehicle geometry databases [1, 2] and current regulations also using a trolley. Secondly, the developed trolley is calibrated and the LCW is evaluated by performing MDB-to-wall tests.

As final step in this project a series of MPDB-to-car tests are performed with vehicles of different mass as shown in Table 1.

Table 1.
Details of the vehicles used in the MPDB-to-car tests

Vehicle brand and model	Vehicle test mass	MPDB mass	Mass ratio vehicle/trolley
Opel Astra	1403	1486	0.94
Opel Astra	1406	1486	0.95
Citroen C2	1250	1486	0.84
Renault Clio	1313	1486	0.88
Renault Laguna	1853	1486	1.25

The first two tests are performed with identical vehicles to check the test repeatability. The MPDB-to-car results are compared with the results of static PDB tests to study the effect of mobilizing the barrier.

TROLLEY DEVELOPMENT

The trolley dimensions are based on specifications of European vehicles which are presented in Table 2.

The inertia properties of the trolley are based on the values given in the NHTSA database for a large range of vehicles [1]. The default mass of the trolley was selected to be 1500±25 kg and the trolley mass was made adjustable between 1300 and 1800 kg for research purposes. All other main dimensions of the trolley were selected to fit in the range found for an average European passenger car.

In addition the MDB trolley mass is in line with the trolley-mass of proposed test procedures for side impact, AE MDB in Europe and the IIHS in the US.

Table 2.
MPDB design specifications (default conditions)

Description	Average EU vehicle [2]	MDB
Total mass [kg]	1200-1700	1500
CG location from front, w.r.t. length [m]	0.43 – 0.47	0.45
Vehicle front to front axle distance H [m]	0.720 – 0.980	0.900
Vehicle front to CG distance I [m]	1.700 – 2.100	1.900
Vehicle front to rear axle distance J [m]	3.200 – 3.700	3.500
Overall length K [m]	3.800 – 4.700	4.250
CG height L [m]	0.560 – 0.640	0.600
Axle height M [m]	0.270 – 0.290	0.280
Wheel base [m]	2.450 – 2.750	2.600
Mass front axle [kg]	710 – 990	900
Mass rear axle [kg]	465 -735	600

Deformable barrier

The trolley was designed to be equipped with a deformable element. In this study the progressive deformable barrier (PDB) was used as a deformable element for its stability and its ability to allow a barrier face deformation measurement in order to evaluate the potential aggressiveness of cars.

Force measurement

For advanced assessment criteria the feasibility and potential of additional force measurements in MDB tests is evaluated in this project. The trolley is equipped with a light weight high resolution strain gauge loadcell wall (HR-LCW) behind the deformable element. In total 48 strain gauge loadcells of 125x125 mm are mounted in 6 rows and 8 columns to the front of the trolley. The HR-LCW, developed by FTSS, is equipped with a built-in data-acquisition system so that the trolley is a stand alone system. In addition it is possible to mount the HR-LCW to the right or left hand side of the trolley to be able to test LHD and RHD vehicles. The final trolley design with HR-LCW and PDB barrier is shown in Figure 2.



Figure 2. Final design of the MPDB with HR-LCW and PDB barrier

CALIBRATION TESTS

After the development of the trolley a calibration test was performed with the PDB as deformable element mounted to the trolley face. The trolley was driven into a rigid wall at a velocity of 45 km/h at perpendicular impact angle shown in Figure 3.



Figure 3. MPDB calibration test result

As a first evaluation of the HR-LCW the total recorded force, the summation of the 48 loadcells, and the trolley mass times acceleration are compared and presented in Figure 4. The trolley acceleration was measured in the trolley CoG.

In general, the curves of the acceleration and force measurements show a good correlation. The summation of the load cell wall force results in a lower total force with a maximum difference smaller than ~8%. The slight difference is most probably caused by yaw and pitch of the trolley during impact, but most important the trolley sustained the test without any problems.

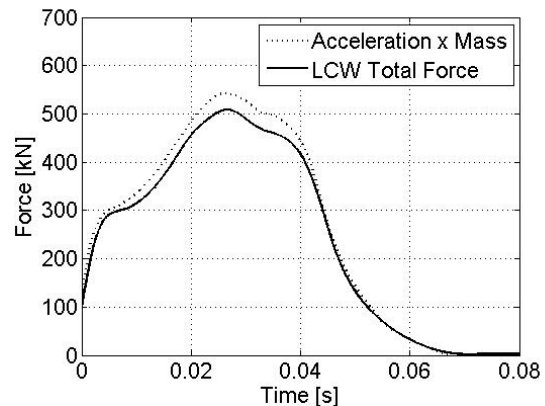


Figure 4. Force vs time of the calibration test

Secondly the LCW of the trolley was further evaluated by running the trolley into a rigid wall twice at 35 km/h. At one of the two tests a rigid block of 250x250x100 mm was mounted on the rigid wall and aligned with the 4 middle loadcells, see Figure 5.



Figure 5. Rigid wall with a square block mounted on it

In these tests the trolley mass was set to 1500 kg and the trolley was equipped with a barrier face of 1000x700x400 mm honeycomb with a constant stiffness between 0.34 and 0.40 MPa. Again the total recorded force by the loadcell wall is compared with the trolley mass times trolley acceleration for both tests, shown in Figure 6 and Figure 7.

The acceleration times mass and the total recorded force again show a good correlation. Although the deformable face was made from material with a constant stiffness, the total force is increasing after reaching the theoretical plateau force between 5 and 10 ms. Air trapped in the barrier causes an increase in stiffness when the barrier deforms. It is noted that air locking or air inclusion is strongly related to the selected test conditions (full overlap, rigid wall).

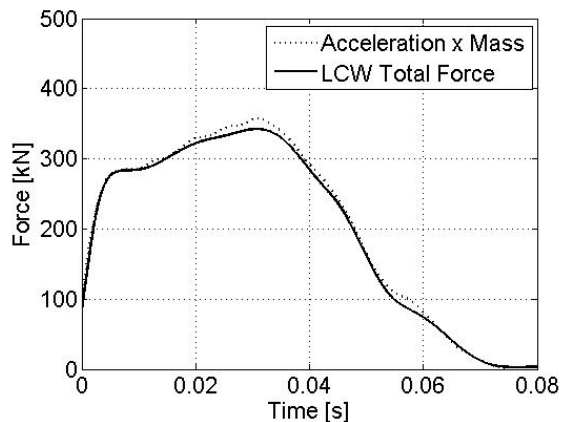


Figure 6. Trolley into the flat rigid wall

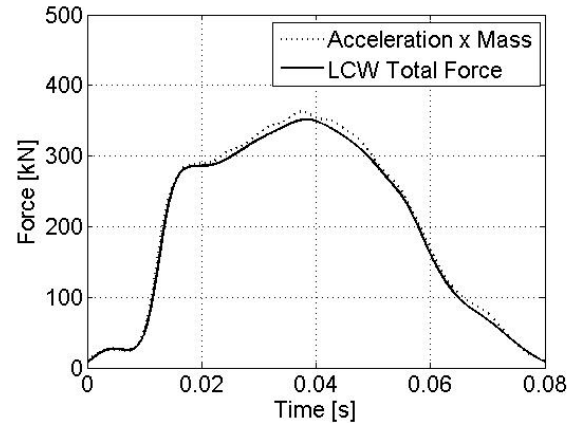


Figure 7. Trolley into flat wall with the rigid block

The force versus time measurements for each individual loadcell for the two tests is given in Figure 8. The rigid block mounted on the wall was aligned with loadcells D3, D4, E3 and E4. These loadcells clearly show a different recording when compared to the surrounding loadcells were for the test with the block the force build up was post-poned. Because of a slight misalignment and some spread of loads due to the back plate at the back of the honeycomb material, the loadcells in the column next to the block also observe some loading at the start of the measurement (e.g. see column F, row 3 and 4). The lowest row of loadcells was not fully covered with deformable material and hence equivalent lower loads are recorded by row 1.

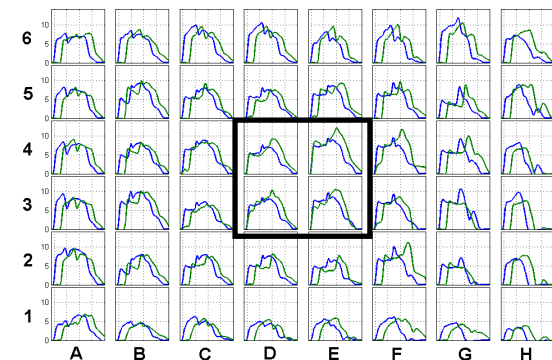
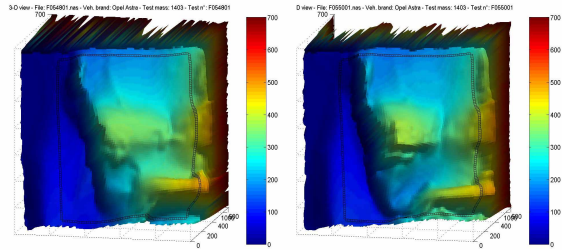
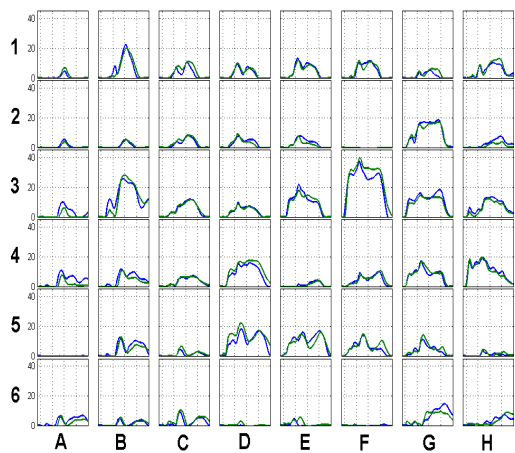


Figure 8. Forces (kN) in time for all loadcells, frame indicates the rigid block at the rigid wall

MPDB-TO-CAR TESTS

Following the good results of the calibration tests the project continued by performing MPDB-to-car tests. The test specifications for the MPDB-to-car tests are chosen in such a way that an equal amount of initial



	Test 1	Test 2
ADOD (X)	242.2 mm	231.8 mm
AHOD (Z)	492 mm	493 mm

Figure 9. Load cell wall recordings and barrier deformations of both Astra-to-MPDB tests

kinetic energy is put into the test compared to a static PDB test for a car of mass ratio 1, using a 1500 kg trolley. This results in a closing speed of 90 km/h (both car and MPDB traveling at 45 km/h). The offset and ground clearance are chosen equally to the static PDB test at respectively 50% and 150mm. Other test specifications like seat position, dummy positioning are according to the PDB protocol as well.

Repeatability

Two MPDB-to-car tests were performed with an Opel Astra to investigate the practicality and repeatability of the draft test procedure. The HR-LCW recordings show a good correlation between the two MPDB-to-Astra tests on individual load cell level as can be seen in Figure 9. Furthermore the barrier deformation, also shown in Figure 9, shows a very good resemblance between the two tests. Based on these results it is concluded that the test method is shown to be feasible and repeatable.

MPDB-to-vehicle test

In addition to the repeatability tests vehicles with different mass ratios compared to the trolley mass of 1500 kg were tested, see Table 1. The effect of mass and car design of the vehicles in terms of acceleration levels is examined. The vehicle accelerations in **Figure 10**, show that the test severity was higher for the smaller vehicles compared to the larger vehicle based on the acceleration levels.

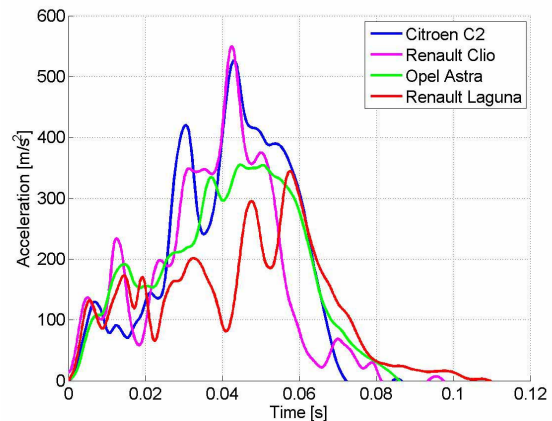


Figure 10. Vehicle accelerations for all tested vehicles

The trolley acceleration profiles in Figure 11 show that all vehicles deform the barrier in a different manner. For instance the Citroen C2 penetrates the barrier at a small contact area in the beginning of the crash resulting in a lower acceleration level at the beginning of the pulse. On the other hand the Renault Laguna and Clio have a homogeneous front end shown as a constantly increasing acceleration signal right from the start of the crash.

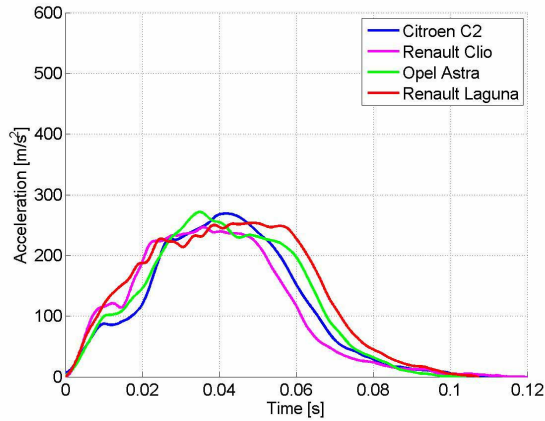


Figure 11. Trolley acceleration for all tested vehicles

When two vehicles collide with a mass ratio other than one there will be a post-crash velocity. This effect is also seen in the post crash velocity of the trolley. For a mass ratio of 1 the post crash velocity will be equal with the rebound vehicle velocity in case of a static PDB tests. Figure 12 shows the velocity profile of the trolley for all tested vehicles. The heaviest vehicle, being the Renault Laguna, forces the trolley in a negative post-crash trolley velocity due to the higher mass of the Laguna compared to the trolley mass. In other words, the higher the mass the larger the ΔV of the trolley. In addition the ΔV increases for vehicles lighter than 1500 kg.

This implies that a moving barrier test is a far more realistic representation of a car-to-car crash than a fixed barrier test.

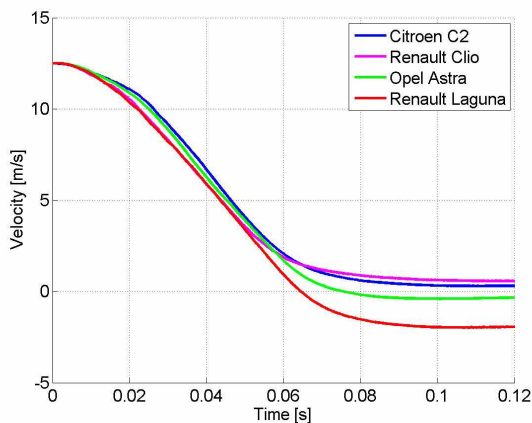


Figure 12. Trolley velocity for all tested vehicles

Moving PDB versus fixed PDB

To get a full understanding of the effect of mobilizing the barrier the energy levels of the MPDB are

compared with fixed PDB tests. As mentioned before, the test velocities of the MPDB tests were chosen in such a way that the level of kinetic energy was equal for both MPDB and PDB tests for the Opel Astra with mass ratio 1. The kinetic energy that is put into each test is illustrated in Figure 13. For the C2 and Clio with a mass ratio smaller than 1 more energy is involved in the MPDB test compared to the PDB test. For the Laguna with a mass ratio over 1 less energy is involved.

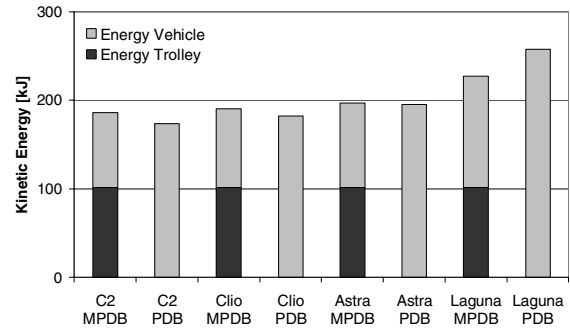


Figure 13. Kinetic energy comparison for all tested vehicles

For both PDB and MPDB the kinetic energy vs. mass is shown in Figure 14. The difference in the slope of the energy-mass curve for the MPDB and the PDB is a result of a partly fixed amount of the initial kinetic energy is by the constant trolley mass and velocity. In other words the severity of the crash in terms of EES is more inline over the mass range than for a fixed barrier test. However, more research is needed to find the most appropriate trolley mass and test velocity so that the test procedure will improve partner protection without decreasing the self-protection, in particular for heavy vehicles.

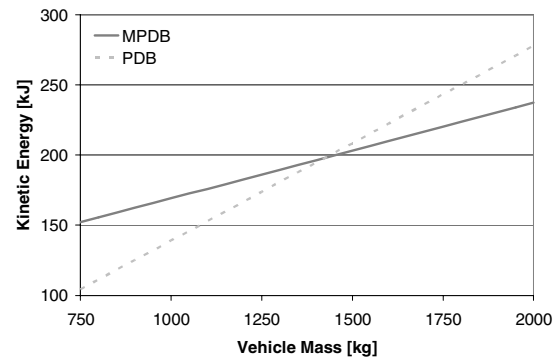


Figure 14. Kinetic energy vs mass for both PDB and MPDB

Finally for all vehicles the barrier average deformations for both MPDB and PDB tests are compared. Again the same effect regarding

mobilization of the barrier is demonstrated inline with the differences in initial kinetic energy and in delta V.

For the Citroen C2 and Renault Clio the deformations are higher in the MPDB tests due to the higher severity and energy level.

Table 3 – Barrier deformations of both the MPDB and PDB tests for the different vehicles

		PDB	MPDB
Citroen C2	<i>ADOD (X) [mm]</i>	204	232
	<i>AHOD (Z) [mm]</i>	458	466
Renault Clio	<i>ADOD (X) [mm]</i>	147	195
	<i>AHOD (Z) [mm]</i>	417	438
Opel Astra	<i>ADOD (X) [mm]</i>	228	232
	<i>AHOD (Z) [mm]</i>	480	493
Renault Laguna	<i>ADOD (X) [mm]</i>	294	273
	<i>AHOD (Z) [mm]</i>	492	510

CONCLUSIONS

Within the project a HR-LCW trolley was successfully developed to be used for frontal offset testing. The trolley mass and inertia properties can be altered to find the optimal set-up for improving partner and self-protection without decreasing the current level of self protection.

The test results show that the severity for small cars is increased due to a higher initial kinetic energy level. This resulted in higher acceleration levels and larger barrier deformations. For the Opel Astra with mass ratio ~1 it was shown that the severity was inline with the fixed PDB procedure. The heavier Renault Laguna showed a decrease in acceleration level and barrier deformation which means that the severity of the crash is less for vehicles with mass ratio > 1.

The MPDB test protocol has shown to be feasible and a far better representation of a car-to-car collision than static barrier tests. More-over the MPDB protocol has the potential of assessing all compatibility issues without decreasing the current level of self-protection.

RECOMMENDATIONS

As a final step in this initial project a MPDB and PDB test using a vehicle with a mass ratio >> 1 is scheduled.

Further work is ongoing to develop an advanced assessment protocol using HR-LCW measurement, barrier deformations and trolley accelerations.

The final test specifications of a MPDB protocol, such as trolley mass and closing speed, must be defined on accidentology studies and the prediction of trends in vehicle design and masses.

REFERENCES

- [1] http://www-nrd.nhtsa.dot.gov/database/nrd-11/veh_db.html
- [2] T. Martin, "Car geometrical/ structural database and analysis of car to car geometric compatibility" UTAC VC-Compat WP1-D9v1.1, June 2004.

EEVC Approach to Develop Test Procedure(s) for the Improvement of Crash Compatibility Between Passenger Cars

Eberhard Faerber
Bundesanstalt für Strassenwesen (BASt)
Federal Highway Research Institute, Germany
on behalf of EEVC WG 15
Paper Number: 06-0331

ABSTRACT

As set out in the *Terms of Reference*, the objective of European Enhanced Vehicle-safety Committee (EEVC) Working Group (WG) 15 *Car Crash Compatibility and Frontal Impact* is to develop a test procedure(s) with associated performance criteria for car frontal impact compatibility. This work should lead to improved car to car frontal compatibility and self protection without decreasing the safety in other impact configuration such as impacts with car sides, trucks, and pedestrians.

Since 2003, EEVC WG 15 served as a steering group for the car-to-car activities in the “Improvement of Vehicle Crash Compatibility through the development of Crash Test Procedures” (VC-COMPAT) project that was finalised at the end of 2006 and partly funded by the European Commission.

This paper presents the research work carried out in the VC-COMPAT project and the results of its assessment by EEVC WG 15. Other additional work presented by the UK and French governments and industry - in particular the European industry - was taken into consideration. It also identifies current issues with candidate testing approaches. The candidate test approaches are:

- an offset barrier test with the progressive deformable barrier (PDB) face in combination with a full width rigid barrier test
- a full width wall test with a deformable aluminium honeycomb face and a high resolution load cell wall supplemented by the forces measured in the offset deformable barrier (ODB) test with the current EEVC barrier.

These candidate test approaches must assess the structural interaction and give information of frontal force levels and compartment strength for passenger vehicles.

Further, this paper presents the planned route map of EEVC WG 15 for the evaluation of the proposed test procedures and assessment criteria.

INTRODUCTION

Since the 2005 ESV-Conference [1] WG 15 continued to focus its research activities on the VC-COMPAT project [2] with unchanged Terms of Reference and Route Map. The VC-COMPAT project was completed in November 2006. It was funded by the European Commission and the contributions of national governments and industry. This paper is a compilation of the latest activities of European Enhanced Vehicle-safety Committee Working Group 15 – Car Crash Compatibility and Frontal Impact (EEVC WG15). Besides the VC-COMPAT project research work the paper comprises information from three main origins: 1) activities of the individual working group members conducted in national or industrial projects; 2) joint research activities involving several working group members; and 3) activities of organisations outside the working group and reported at specific meetings.

Working Group 15 was created in 1996 to develop a better understanding of crash compatibility between passenger cars. This was reported in 2001. The group was then tasked with developing test procedures that would evaluate a vehicle’s frontal crash compatibility. The key characteristics that were deemed to influence compatibility are:

1. Structural interaction (local geometric and stiffness properties that determine how structures will deform)
2. Global force levels (total force / deformation properties that govern how energy dissipation is shared between crash partners)
3. Compartment strength (passenger compartments must be maintain the survival space for the occupants as well as support the deformation processes in the vehicle front).

ACCIDENT AND COST BENEFIT ANALYSIS

General trends in accident data

The historical performance of passenger cars in frontal crashes has been presented to WG15 by VW. The main details were derived from the GIDAS database (Germany). The first important result presented is that the US fatality rate is not improving as quickly as in Europe. This suggests that the reduction in Europe is not part of a global trend, but it is a consequence of the special situation in Europe, as a consequence of European car design and European regulation. Benefits in the European fleet are attributed to increasing levels of self protection.

There are indications that vehicle deformations, in particular compartment intrusions, for both the vehicle and its collision partner are decreasing. The reduced deformations are attributed to increased vehicle stiffness encouraged by recent legislated and consumer test requirements in Europe. Parallel to reduced vehicle deformations are reductions in occupant injury levels (lower proportions of AIS 3+) for both vehicles in the collision. The improvements in occupant safety cannot be solely attributed to post-crash rescue since no improvement in the fatality outcomes were observed for the different MAIS levels over the years of investigation.

Cost benefit analysis

In 2004 there were, according to the Community database on Accidents on the Roads In Europe (CARE), 32,951 traffic accident deaths and 251,203 seriously injured casualties in the 15 member states of the EU-15. EFR (European Union Road Federation) state that 54% of these road fatalities were car passengers or drivers.

The aim of this part of the work was to estimate the costs and benefits for improved frontal impact car to car compatibility for Europe (EU15). For the benefit analysis the approach illustrated in [Figure 1](#) was followed.

A target population was estimated using data from Germany and Great Britain (GB) and scaled to calculate the target population for the EU15 countries. The target population was defined as the number of casualties who might experience some injury risk reduction as a result of the implementation of improved compatibility. As a definite set of test procedures to assess a car's compatibility was defined, the methodologies were based on the assumptions of how a compatible car would perform.

The methodology used for the GB analysis was based on a retrospective review of real-world vehicle crashes that occurred in GB and an in-depth evaluation of what injuries could have been prevented if the vehicle crash performance was enhanced. The methodology only considered the crashes for injury mitigation where it was believed that it would be realistic to predict some benefit, so high speed crashes and under-run impacts were excluded. The methodology used for the German analysis was based on theoretical concepts that evaluated the current risk of car occupant injury following frontal impacts with respect to collision speed; re-assessed the risk functions for an improved compatibility vehicle fleet with better energy management characteristics and subsequently predicted the likely future casualty reductions.

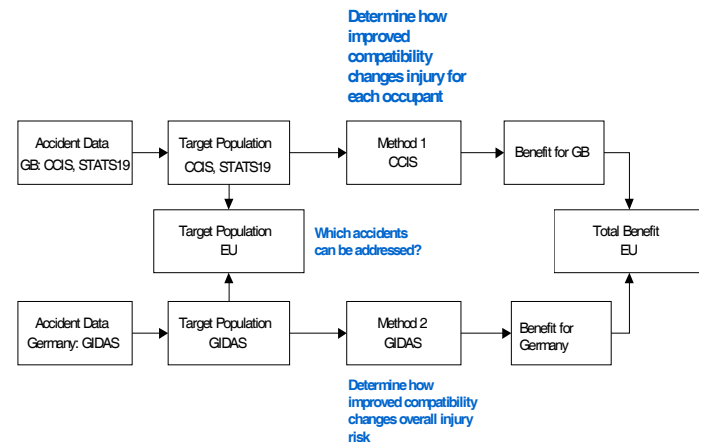


Figure 1: Benefit analysis approach.

The economic analysis was undertaken by Fiat and considered the fixed, variable, and associated design costs. Two cases were chosen, a worst case, modification of a 4 star EuroNCAP car, and a best case, modification of a 5 star EuroNCAP car. The costs for each star rated car were then evaluated with respect to the number of car units that would be modified per year, with the greater the number of units the lower the cost per car.

It should be noted that the cost benefit was calculated for the steady state, when the entire vehicle fleet is compatible. The benefit will be less during the initial years as compatible cars are introduced into the fleet.

The costs for improved compatibility show [Table 1](#) below.

	Cost per car (€)	No. of cars registered p.a.	Total cost p.a. (€)
Best case scenario	102	14,211,367	1,449,559,394
Worst case scenario	282	14,211,367	4,007,605,383

Table 1: Cost of implementing compatibility

To estimate the benefit for the EU15 the benefit estimates for GB and Germany were scaled to give the following results, see [Table 2](#).

	Frontal car casualties	Predicted Reduction in EU-15 Casualties		
		CCIS intrusion model	CCIS contact model	German model
Fatal	16,014	721	1,332	1,281
Serious	122,084	5,982	15,383	5,128

Table 2: Predicted reduction in EU-15 casualties

The financial benefit for the EU15 was calculated by multiplying the benefit in terms of casualties by the value of life saved and serious injury prevented, see [Table 3](#). For the GB estimate the casualty value used was that given in Road Casualties Great Britain 2005 (RCGB 2005), which estimates the average value per prevention of casualty. For the German estimate the casualty value used was that calculated by the BAST (German Federal Highway Research Institute).

	Benefit per person		Predicted Total benefit		
	Fatal	Serious	CCIS: Intrusion	CCIS: Contact	German model
RCGB 2005 (€)	2,136,262	240,043	2,976,180,313	6,538,077,822	-
German (€)	1,161,885	87,269	-	-	1,936,005,641

Table 3: Value of EU15 Benefit

From this and the cost information presented above the cost / benefit ratio of improved frontal impact compatibility for the EU15 was estimated, see [Table 4](#).

	Ratio of financial benefits to implementation costs		
	CCIS intrusion model	CCIS contact model	German model
Best case scenario	2.05	4.51	1.34
Worst case scenario	0.74	1.63	0.48

Table 4: Cost Benefit Ratio of improved compatibility for EU15

As a result of the analysis, the cost benefit ratio appears to be better than 1:1 if all the cost benefit results are considered as a group. These results are independent of any specific crash test procedure for

compatibility and only reflect the total expected benefit of improved compatibility. These estimates should be considered conservative since benefits to other crash configurations (side impact, single vehicle collisions, etc.) have not been included. In addition, the costs for vehicle modifications are likely overestimated, particularly for the worst case conditions.

Further analysis of accident data is needed to observe if other benefits of improved structural interaction can be detected in the current fleet. An improved interaction should provide more predictable crash pulses that facilitate the crash detection and safety system triggering algorithms. It is also expected that improved crash compatibility will lead to better coupling of the occupant and vehicle dynamics during the crash which facilitates the restraint system performance. It is important to use the existing accident data to begin identifying methodologies for analysing these characteristics.

Further accident data analyses are needed to allow the benefit (and cost) analyses to be reported to date updated and improved. In particular, the different analyses conducted with French and GB data identify how small changes to the approach will influence the result and a standardised benefit calculation for improved compatibility is not yet developed. Finally, the cost benefit analysis for a proposed crash test procedure must be recalculated to more accurately reflect the influence of the crash test procedure on vehicle designs. Future activities should be coordinated with EEVC WG21 (Accident Analysis) to ensure the best database and analysis procedures are used.

TEST PROCEDURE STATUS

Overall Development Strategy

To assess a car's frontal impact performance, including its compatibility, an integrated set of test procedures is required. The set of test procedures should assess both the car's partner and self protection. To minimise the burden of change to industry, the set of procedures should contain a minimum number of procedures which are based on current procedures as much as possible. Also, the procedures should be internationally harmonised to reduce the burden further. Above all, the procedures and associated performance limits should ensure that the current self protection levels are not decreased. Good self protection is required for car to car impacts. Also good self protection is required by all vehicles for impacts with road side obstacles.

The set of test procedures should contain both a full overlap test and an offset (partial overlap) test, as both of these tests are required to fully assess a car's frontal impact crash performance. In 2001, the IHRA frontal impact working group recommended the adoption of an offset deformable barrier and full width tests worldwide [3]. A full width test is required to provide a high deceleration pulse to control the occupant's deceleration and check that the car's restraint system provides sufficient protection at high deceleration levels. An offset test is required to load one side of the car to check compartment integrity, i.e. that the car can absorb the impact energy in one side without significant compartment intrusion. The offset test also provides a softer deceleration pulse than the full width test which checks that the restraint system provides good protection for a range of pulses and is not over-optimised to one pulse.

As mentioned previously, compatibility is a complex issue which consists of three major aspects, structural interaction, frontal force matching and compartment strength. To make vehicles more compatible, substantial design changes will be needed which will require some years to implement. Because of this the set of test procedures need to be designed so that compatibility requirements can be introduced in a stepwise manner over a time period of the order of years. This requirement is reflected in the current EEC WG15 route map [1] which proposes that compatibility should be introduced in two steps which are:

Short term

- Improve structural interaction
- Ensure that force mismatch (stiffness) does not increase and compartment strength does not decrease from current levels

Medium term

- Improve compartment strength, especially for light vehicles
- Take first steps to improve frontal force matching
- Further improve structural interaction

In summary the strategy aims for development of the set of procedures is:

- Integrated set of test procedures to assess a car's frontal impact protection
 - o Address partner and self protection without decreasing current self protection levels
 - o Minimum number of procedures
 - o Internationally harmonised procedures
- Both full width and offset tests required

- o Full width test to provide high deceleration pulse to assess the occupant's deceleration and restraint system
- o Offset test to load one side of car for compartment integrity
- Procedures designed so that compatibility can be implemented in a stepwise manner

Based on the route map and the previous activities in WG 15, methods to fully assess frontal impact and compatibility can be divided into the following approaches:

Set 1

- Full Width Deformable Barrier (FWDB) test
 - Structural interaction
 - High deceleration pulse
- ODB test with EEC barrier
 - Frontal force levels
 - Compartment integrity

Set 2

- Full Width Rigid Barrier (FWRB) test
 - High deceleration pulse
- Progressive Deformable Barrier (PDB) test
 - Structural interaction
 - Frontal force matching
 - Compartment integrity

Set 3

- Combination of FWDB and PDB

Sets 1 and 2 have been formally investigated while Set 3 has not been explicitly investigated to date. Further details of the strategies for Sets 1 and 2 and the development of each approach are given in the following sections.

TEST PROCEDURE STATUS, FWDB APPROACH

The Full Deformable Barrier (FWDB) test forms part of an integrated set of two procedures proposed to assess a car's frontal impact crash performance, including its compatibility:

FWDB test:

- (1) To assess structural interaction potential.
- (2) To provide a high deceleration pulse to test the restraint system.

Offset Deformable Barrier (ODB) test with EEC barrier:

- (1) To assess frontal force levels.
- (2) To load one side of the car to check its compartment integrity.
- (3) To provide a softer deceleration pulse than the FWDB test to check the restraint system performs over a range of decelerations.

Originally the approach also included a high speed (80 km/h) ODB test to measure compartment strength using a Load Cell Wall (LCW). This test is not currently included in the approach because it is thought that adequate control of the compartment strength should be possible using a lower speed (e.g. regulatory or EuroNCAP) ODB test or the PDB test.

FWDB Test

The FWDB test is effectively a modification of the US FMVSS208 test, the modifications being the addition of a deformable element and a high resolution Load Cell Wall. The LCW consists of cells of nominal size 125 mm by 125 mm. The load cells are mounted 80 mm above ground level so that the division line between rows 3 and 4 is at a height of 455 mm which is approximately mid-point of the US part 581 bumper beam test zone¹, see [Figure 2](#). The reason that this particular height was chosen was to be able to detect whether vehicles had structures in alignment with the top and bottom halves of the Part 581 zone by examining the loads on rows 3 and 4 of the LCW. The intention is to enable the test procedure to be used to encourage all vehicles to have crashworthy structures in a common interaction zone that spans the part 581 zone. This should ensure structural interaction between high SUV type vehicles and cars as most cars have their main longitudinal structures in the Part 581 zone to meet the US bumper beam requirement.

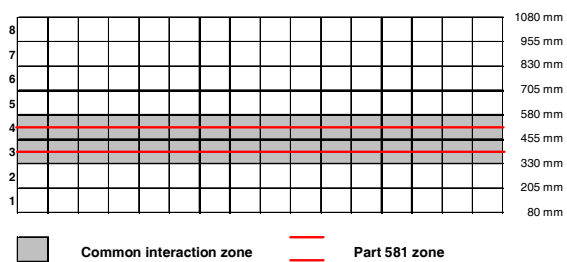


Figure 2: FWDB test LCW configuration showing row number and height above ground level.

¹ Part 581 zone: Zone from 16” to 20” above ground established by NHTSA in its bumper standard (49 CFR 581) for passenger cars.

The purpose of the deformable element has been discussed previously [3]; the main purpose being to improve detection of crossbeam structures which may not be strained in an impact with a rigid wall and to reduce engine dump loading that may otherwise confound the measured force distribution.

The FWDB Test Assessment intention is to control both self and partner protection. For self protection the occupants deceleration and restraint system performance will be assessed using dummy measures in a similar way to the current FMVSS208 test. For partner protection the car’s structural interaction potential will be assessed using the measures from the LCW.

A new criterion, called the Structural Interaction (SI) criterion, has been developed to resolve issues with the previous Homogeneity Criterion [4]. Its details are described in another paper presented at this conference [5], so only a brief description is given here. Its development was based on the following requirements:

- An ability to be applied in a stepwise manner to allow manufacturers to gradually adapt vehicle designs
- To encourage better horizontal force distribution (crossbeams).
- To encourage better vertical force distribution (multi-level load paths).
- To encourage a common interaction area with minimum load requirement.

It is calculated from the peak cell loads recorded in the first 40 ms of the impact. Compared to using peak cell loads recorded throughout the duration of the impact (as with the previous Homogeneity Criterion), this has the advantage of assessing structural interaction at the beginning of the impact when it is more important and minimising the loading applied by structures further back into the vehicle such as the engine. The 40 ms time interval allows detection of structures up to approximately 400 mm from the front of the vehicle, which aligns with a recent NHTSA proposal to assess the Average Height of Force (AHOF) over the initial 400mm vehicle displacement.

The SI criterion consists of two parts which assess the LCW force distribution over two different areas, Area 1 and Area 2. These parts could be applied in two phases to allow manufacturers to gradually adapt vehicle designs to become more compatible. The first part assesses over a common interaction area (Area 1) which is from 330 mm to 580 mm above ground level and consists of LCW rows 3 and 4. The intention of

this part of the assessment is to ensure that all vehicles have adequate structure in alignment with this area to ensure interaction. The second part assesses over a larger area (Area 2) which is from 205 mm to 705 mm above ground level and consists of LCW rows 2, 3, 4 and 5. The intention of this part of the assessment is to encourage cars to distribute their load more homogeneously over a larger area to reduce the likelihood of over/under-ride and the fork effect. However, further work is needed to ensure that the structural changes encouraged by this are not detrimental for side impact collisions. For example, although a strong shotgun type structure that extended to the front of the car should improve frontal impact compatibility performance it could be detrimental in side impact. If this was found to be the case, additional measures that limited the loads applied to specific areas of the LCW early in the impact may be needed to discourage this type of structure.

Some initial validation of the SI criterion has been performed. It has been shown that the SI criterion correctly distinguishes the vehicles which showed better structural interaction performance in car to car tests in the VC-COMPAT project [5, 6]. Also, it has been shown to rank the bumper crossbeam strength correctly for a series of FWDB tests performed by ACEA with a large family car with different strength bumper crossbeams [7].

The FWDB Test Repeatability has been investigated using full scale car crash tests and component sled tests. The results of this work are described in another paper presented at this conference [5]. In summary, from the limited testing performed test repeatability was found to be adequate. However, further work is recommended to check test repeatability with greater impact alignment differences and investigate the greater than expected cell load differences seen in component sled tests with a flat rigid impactor.

ODB Test

A methodology to measure a vehicle's frontal force levels in an ODB test has been developed in the VC-COMPAT project [2]. In summary, the car's frontal force level is estimated by determining the LCW peak 10 msec exceedence force. The reason that an exceedence measure is used is to minimise the effect of unrealistic loads seen in this test which are not seen in car to car crashes such as those caused by the sudden deceleration of the engine when it bottoms out the barrier face, see [Figure 3](#).

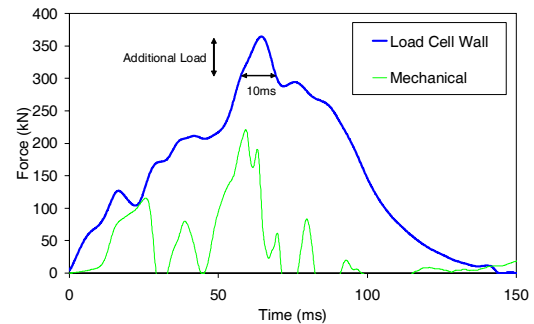


Figure 3: LCW force in ODB test showing additional load caused by 'engine dump'. Note: the mechanical force is the load applied by the powertrain components.

In initial steps to improve compatibility this force could be monitored and in later steps the minimum and / or maximum force could be controlled to encourage some degree of force matching.

Further Work Required

The following work is required to complete the development of the FWDB approach:

FWDB test

Partner protection (LCW based measurements)

- Criteria and performance limits

A new criterion to assess a vehicle's structural interaction potential has been developed and shown to correctly rank different vehicles. Further work is recommended to validate the criterion and set performance limits. This work should include a test series to show that changing the vehicle to meet the performance requirement correlates to better performance in car to car impacts, which could then be used to help perform a benefit analysis for the introduction of this test procedure.

- Test repeatability / reproducibility

A limited number of tests to investigate repeatability have been performed to date, which found no significant problems. Further work is recommended to check the validity of this conclusion with different vehicle types and confirm the appropriateness of the proposed vertical impact alignment tolerance of +/- 10 mm.

In sled component tests using a flat rigid impactor, the load distribution measured on the LCW for cells in alignment with the impactor showed a greater variation than expected. Even though it was shown that this variation should not have a substantial effect on test repeatability it is recommended that further

work is performed to understand why this variation occurred and ideally to minimise it.

Self-protection (Dummy based measures)

- Dummy

Work to determine the most appropriate dummy (THOR or HYBRIDIII), seating positions and size of dummy for inclusion in this test is recommended.

- Criteria and Performance limits

Further work is recommended to determine appropriate criteria and performance limits. However, if the HYBRIDIII dummy is used as in the current FMVSS208 test, then criteria and limits could be based on those in FMVSS 208.

ODB test

- Criterion

Work to complete the development of a criterion to control a vehicle's frontal force levels is recommended.

TEST PROCEDURE STATUS, PDB APPROACH,

Current situation

Car to car accident data shows that fatalities and severe injury are caused by compartment intrusion. It is mainly due to unbalance energy absorption between both cars resulting from a low level of self-protection and a high level of aggressiveness. The first step in compatibility leads to reduce this compartment intrusion by improving car structure.

The present demand on self protection is increasing the local strength and global force deformation of all cars. The design of a large car makes it stiffer than a small one in order to compensate the mass.

Furthermore, the current frontal offset test is more severe for heavy vehicles because of the specific barrier used. Associated to self protection trends, compatibility requirements are unreachable today without changing deformable element.

Due to the current test conditions it is desirable to improve light car compartment strength without increasing the heavy car strength requirements and to limit heavy vehicle front units' aggressiveness. In other words, it is necessary to assess the possibility to check and improve partner protection with regards to self-protection. To achieve this new requirement, an amendment of ECE R94 test procedure is needed.

The current European barrier face was a good compromise in the past but so far, with new compatibility

requirements, these characteristics are creating new problems. Front end car designed changed a lot in the last 10 years with to respect new constraints (repeatability, pedestrian, self protection etc), so the deformable element should be revised. The element weakness causes bottoming out, constant energy absorbed and instability that leads to lack of repeatability and inaccurate FEM simulation, see [Figure 4](#).



Figure 4: Current ODB: instability and bottoming out

To answer the question of improving self protection level of the light car, it is necessary to increase the test speed (56 to 60 km/h) to reach vehicle structural load levels where compartment deformation starts. However, this increasing speed must be accompanied by a barrier change to reach compatibility requirements and to stop heavy vehicles getting stiffer and stiffer.

Checking half of the front end is needed for partner protection assessment in the future. Secondly, overlap tests are closer to real world accident data and car to car test configuration. Finally, combined with a stiffer barrier it generates higher acceleration pulses. This test is also able to generate intrusion and acceleration pulse in the same time, considering that combinations of both are responsible for fatal and serious injuries in real world accident.

Compatibility in car to car crashes depend on correct distribution of energy between the two vehicles. In the case of cars that are ideally compatible impacting each other at a closing speed of 100 km/h, each car must individually sustain deformation corresponding to an impact against a wall at 50 km/h.

The objective is to offer the same survival potential in both vehicles; in other words, any intrusion should be similar to that observed in a barrier impact at half the closing speed. This is equivalent to say that the EES (Equivalent Energy Speed) is identical for both vehicles. As a consequence, the energy absorbed by each vehicle is proportional to its mass.

Accident studies in France show that 60% of cases of people involved (MAIS3+) in the light car would be covered by choosing 100 km/h closing velocity. It is specified that these progress will be also applicable for higher closing speeds.

In order to take advantage of the full energy absorption potential of both cars, their structure must interact correctly. In term of design, one way to achieve good structural interaction is to offer a large front surface which a homogeneous stiffness. Ideal case would be a rigid plane between both cars sustained by multiple load paths. The real solution that satisfies all the requirements involves a multiple number of strongly inter-related load transfer paths and a progressive stiffness increase. The proposed test procedure should be able to detect this front end design, in order to put this item under control.

In order to detect all structural components involved during a car to car impact, the investigation area needs to check, in height, from the subframe to longitudinal, but also, in depth, a sufficient crush distance to check lower load path back from the front end. Structural analysis performed within VC-Compat project shows that to take into account important front structures, the investigation area on a car needs to be included:

- in height : between 180 mm to 650 mm from the ground
- in depth: from the font bumper to 700mm

PDB Strategy

The strategy of the PDB (Progressive Deformable Barrier) approach is to develop a test procedure which takes into account all following items:

- Vehicle: front end design, mass, geometry
- Accident data: structural interaction, compartment strength
- Environmental effects to increased vehicle mass: consumption, emissions, CO₂, etc
- Current frontal test procedures
- Worldwide context: harmonization, different fleets
- Global cost: number of test proposed, number of material needed
- Other constraints: pedestrian, reparability, side impact.

The first priority of the PDB approach is to harmonise the test severity (EES) for all mass range (see

Figure 5: EES evolution with introduction of PDB test procedure

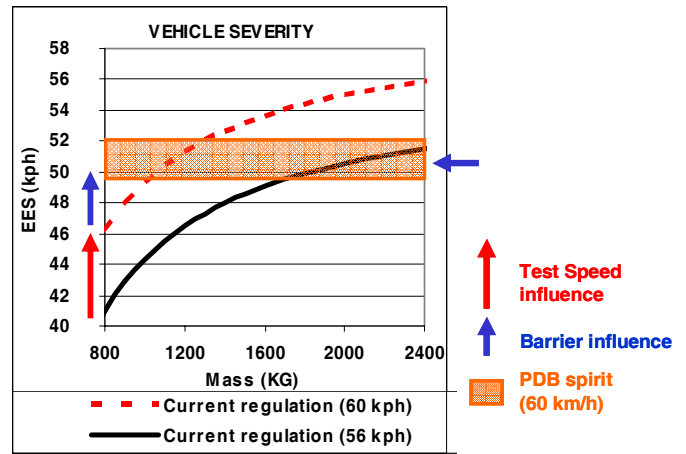


Figure 5: EES evolution with introduction of PDB test procedure

⇒ **The demand of self protection level for light cars is clearly higher than the current regulation without penalising heavy vehicles.**

The combination of deformable element and higher test speed leads to higher severity for light cars without increasing severity for heavy ones. It represents the first step towards force matching.

Due to test severity harmonization, it will allow balancing front end forces even if perfect force matching is unrealistic due to vehicle front end geometry (limited overhang) and same intrusion level requirement, see Figure 6.

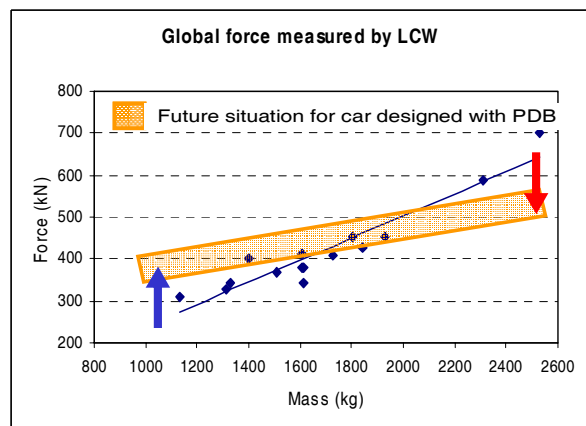


Figure 6: Possible improvement of force matching

PDB approach

The PDB test is a 50% overlap offset test. The barrier stiffness increases with depth and upper and lower load levels to represent an actual car structure, see Figure 7. The dimensions and stiffness of the PDB make the bottoming-out phenomenon very unlikely. The barrier face is capable of generating sufficient differential deformation of the weak and stiff parts of the car's front structure to replicate what happens in most accidents. This will encourage future car designs to incorporate structures which distribute the force on a large surface. Consequently, the stiffness of the barrier face is adapted to check this phenomenon.

Car design for frontal crash must limit passenger compartment intrusion (first cause of fatal injuries) and generate acceptable deceleration from the occupant point of view. Higher acceleration pulse combine with higher intrusion level allows getting closer to real life accident where both parameters are responsible for fatal injuries and injured.

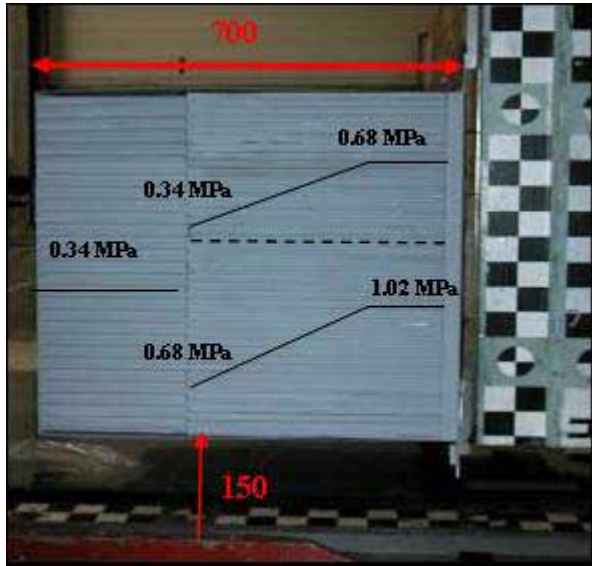


Figure 7: PDB Side view. Dimensions, position and stiffness.

PDB test Procedure

Comparing with current ECE R94 Frontal ODB test, 3 parameters are changed:

- Obstacle : PDB Barrier
- Speed: 60 km/h
- Overlap: 50%

The aim is to answer compatibility requirements:

- Test severity harmonisation
- Structural interaction
- Frontal force level
- Evaluation of compartment strength

PDB Assessment

Three parameters have been identified as important for compatibility. The PDB test protocol proposes tools and measurements to assess them:

- self protection coming from vehicle analysis and dummy criteria
- partner protection coming from barrier deformation

Today, self protection assessment is very well known. According to current ECE R94 and Euro NCAP, the assessment is based on dummies criteria and possible assessment of intrusion measurements such as dashboard, firewall and A-pillar. Deceleration pulse closer to car to car accident is generated with stiffer barrier face and higher overlap.

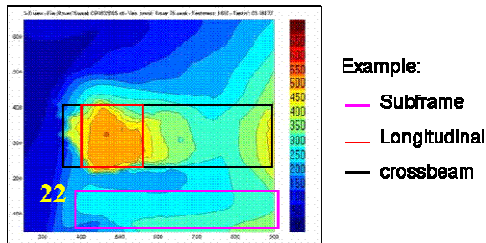
In terms of design, one way to achieve structural interaction is to offer a front surface which is homogeneous in stiffness over a surface which is large enough. In order to take advantage of all the potential for energy absorption of both cars, their structure must interact correctly. To achieve this result, the stiffness on the front block must be distributed along multiple load paths. The PDB deformation already showed its capacity to verify the behaviour of new vehicles in regard to the partner protection targets.

The PDB barrier is able to detect local stiffness but also transversal and horizontal links among load paths. The barrier records front cross member, lower cradle subframe, pendants linking position and stiffness that improve vehicles compatibility, see Figure 8.



Barrier deformation

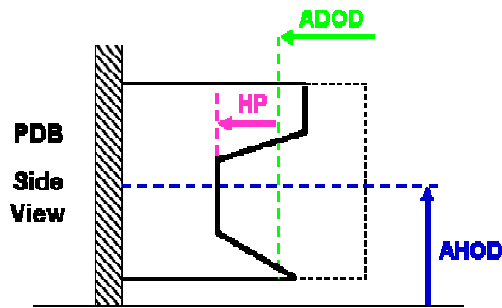
Barrier digitisation (3D)



Investigation area

Figure 8: PDB test - Barrier deformation

The assessment proposed for the future will be based on deformation because information is inside. Laser scanning techniques are used to measure the 3D barrier deformations. Define criteria is under process, only parameters today can be proposed:



- Average Height Of Deformation (AHOD): linked to the geometry and architecture.
- Average Depth Of Deformation (ADOD): linked to the front force of the car
- Homogeneity (HP): supposed to detect local penetration in the front barrier face that indicates bad homogeneity.

However, it is too early to introduce a partner protection assessment because, today, the notion of partner protection is not yet validated by the international communities. An international working group must clearly define what is a good structural interaction, what is an aggressive vehicle and suggests a aggressivity scale among vehicles. Further work is required before proposing a set of criteria.

PDB, possible Route Map for implementation

As a first step, the PDB approach is to replace the current ODB barrier by the PDB one in regulation. The first effect of the progressive barrier is the ability to test all vehicles at a more or less constant severity that lead to better force matching. PDB barrier intro-

duction will be able to improve self protection of light vehicles (overloaded) without increasing heavy ones due to energy capacity absorption. Dummy criteria limits are the same as the current ECE R94 and integrity of the passenger compartment could be assessed with the help of intrusion level in different parts of the front compartment. In this first phase, safety assessment remains focused on self-protection.

This offset test could be combined with a Full Width Rigid Barrier test in order to check the restraint system.

In a second step all criteria and investigations will be based on the barrier deformation. The PDB barrier is able to detect local stiffness but also transversal and horizontal links among load paths. It looks like car to car accident or test analysis, except that in this case, the barrier deformation is investigated instead of the car's. An aggressive vehicle would be identified by large and non homogeneous deformation.

In a long term step, to be closer to real life accident, the PDB could be fixed on a mobile trolley. A quick energy analysis clearly shows that this test due to conservation of momentum associated to different energy absorbed in the barrier allows to progressively switching from a light car overload to a heavy car partner protection test. The test is intended to represent a normal car to car impact.

Work Required to Complete Development of PDB Approach

- Propose criteria and associated performance limits when clear "compatibility definition" will be define by international working groups.
- Confirm that PDB approach leads to stiffer light car and allows force matching concept
- Confirm that Repeatability and reproducibility is achievable.
- Confirm that the PDB barrier will be useful for front end design with FEM simulation.

CONCLUSIONS AND DISCUSSION

Two main testing approaches have been investigated by WG15. These tests have been proposed as complete packages to assess compatibility and self protection for frontal impacts. They can be summarized as tests incorporating:

- 1) Full Width Deformable Barrier test and an Offset Deformable Barrier test
- 2) Progressive Deformable Barrier test and Full Width Rigid Barrier test

- 3) Mixture of the two approaches.

Discussion – WG15

Two testing approaches have been the focus of the WG15 research activities. These two approaches have exhibited desirable performance features but also require further development and validation. Independent of the procedure, some common issues must be resolved before any test procedure can be put into general use. First, any test that assesses vehicle crash performance must be validated for as wide a range of vehicle types as possible. Particularly relevant is the classification of vehicle to be assessed. The original test procedures developed for VC-COMPAT focused on passenger vehicles up to 2.5 tonnes. Any extension of crash test requirements for vehicles up to 3.5 tonnes will require that the test equipment and materials are suitable for this range of vehicle masses.

The working group has identified the following general criteria for compatibility:

- 1) Good structural interaction
- 2) Good compartment strength
- 3) Force matching

The first two criteria have been investigated in the limited crash tests available to the working group and preliminary requirements have been discussed. To further the development of the procedures, a rigorous definition of the global boundary conditions for compatibility must be put forward. These boundary conditions will identify performance limits for vehicle compatibility and requires the translation of the current subjective analyses into fully objective criteria.. There is however no validated, quantitative method to translate these into objective crash test criteria

The following discussion presents the concerns documented by the members of WG15.

FWDB Test Procedure

The approach promoted by the FWDB is to address both self and partner protection of the vehicle. This is accomplished by the two tests as described above – a full width and an offset test. Both tests would be required to properly assess all aspects of compatibility. The primary test method to identify the structural interaction characteristics of the vehicle is the full width test at 56 km/h using a high resolution load cell barrier with a deformable barrier face. To be suitable for implementation in a legislated test program the following must be addressed:

- Understand the relationship between the honeycomb deformation and load cell measurements:

Results from different testing programs indicate that the forces measured behind the honeycomb material are not necessarily distributed as suggested by the honeycomb deformation. This has been initially investigated and further work needs to determine how this variation could influence the assessment criteria.

- Must verify that all important vehicle structures can be detected by the barrier (horizontal structures): Only a limited number of vehicle types have been tested and a range of vehicle types must be tested to determine if all relevant structures are detected. This must be referenced to vehicle-vehicle testing.
- Repeatability: The test method has sensitivity due to the discrete placement of the load cells. The impact accuracy has been investigated but further work is needed to determine requirements for test accuracy (vertical and lateral) to ensure minimal variation in the assessment criteria.

PDB Test procedure

The PDB Test approach contains two test procedures to assess vehicle self and partner protection. The PDB test itself is a 50% offset test at 60 km/h. The honeycomb barrier used in the test has a progressively increasing stiffness designed to represent a car's behaviour. The PDB test is proposed to address compatibility and self protection issues and a full width rigid barrier test complements the PDB test by providing a high pulse for testing interior restraint systems.

The most relevant issues that must be addressed in a PDB test procedure are

- No assessment criteria available for partner protection: The PDB collects force and barrier deformation data to assess partner protection. There is no current assessment criteria that objectively evaluates the partner protection. The available parameters do not have threshold limits.
- Calculation of absorbed barrier energy to find vehicle EES value must be validated: The PDB barrier is scanned and an absorbed energy is calculated using the deformation properties. The dynamic force deflection characteristics are not necessarily identical to the static values used to describe the barrier. Honeycomb barrier is also subject to off axis effects that can lead to lower dynamic stiffnesses and can lead to overestimates of the energy absorbed by the barrier during a crash test.
- Validate the PDB introduces a minimum EES severity for all test vehicles: The PDB barrier properties have been designed to

harmonise the EES of the test vehicle, independent of mass. This harmonisation must ensure that all vehicles are sufficiently loaded to assess self and partner protection. The current range of EES is 45-52 km/h.

General opinion of the group

Working Group 15 has developed a list of assessment criteria presented in the 2005 ESV-Conference [1] that are used to assess the different test criteria against each other on a point-by-point basis. This list uses a numerical rating (0-3) that has been provided by the group members. WG15 does not support the use of this sheet to sum some or all the points as method to select a test method since each point has a different weighting and these weighting factors have not been derived.

To get an overview about the opinion of the different group members on the candidate test procedures to assess compatibility, a rating exercise was carried out in the group.

The following analysis of the ratings of the group members is divided into the four main groupings.

- 1) Structural interaction – The group tends to rank the PDB first and then the FWDB barrier tests as being the most effective at detecting structural interaction properties in cars. The rating of each of these two tests varies from point to point but the variance indicates that the methods' performance are generally agreed to by the group
- 2) Reproduction of collapse modes of load paths - The group generally rates the PDB highest for most of the points in this section. The ODB (ECE R94) also rates high when it comes to compartment strength issues. The FWDB is best at measuring local forces over time. There is less agreement within the group in this section so further analysis of test data is needed create consensus within the group.
- 3) Test Procedure – This section is used to assess the simplicity, accuracy and repeatability of the different procedures. It is clear that the FWRB (full width rigid barrier) is the most reliable test method but also the least applicable according to the previous analysis. The FWDB and ODB tests tend to be higher rated.
- 4) Others – This section includes general issues such as harmonisation issues and availability of assessment criteria. Like Point 1, the FWDB and PDB are essentially similar in ranking within the group.

Conclusions WG15

- 1) Test procedures to control compatibility must assess the structural interaction, frontal force levels, and compartment strength of the vehicle. Current passive safety levels should not be compromised if the global improvements of road safety are to be achieved
- 2) One test procedure alone is not sufficient for assessing frontal impact. Both of the main test approaches combine a full width and offset type test. These two test conditions are needed to fully assess the structures and safety equipment of the vehicle
- 3) Three different candidate sets of procedures are proposed for assessing compatibility in passenger vehicles:

Set 1

- Full Width Deformable Barrier (FWDB) test
 - Structural interaction
 - High deceleration pulse
- ODB test with EEVC barrier
 - Frontal force levels
 - Compartment integrity

Set 2

- Full Width Rigid Barrier (FWRB) test
 - High deceleration pulse
- Progressive Deformable Barrier (PDB) test
 - Structural interaction
 - Frontal force matching
 - Compartment integrity

Set 3

- Combination of FWDB and PDB.

Of the three candidates, only the first two have been explicitly evaluated in Working Group 15.

- 4) The two central test procedures, the PDB and FWDB, are not sufficiently developed to allow test approaches to be compared and select a preferred test procedure. The discussions of WG15 show that all test procedures have issues to be investigated and that each test procedure has specific strengths that are not often found in another.

Recommendations for the Way Forward

This section outlines the recommended work to reach the position to make a proposal for a 1st step to improve compatibility. The work can be classified as global issues which are independent of a testing approach and work specific to a test procedure.

Global Issues:

- Further accident and benefit analysis to update information on changing vehicle fleet
- Finalise the test severity (EES) for regulation test using real world crash requirements.
- Finalise assessment criteria for regulation test.
- Finalise objective assessment procedures to analyse results of car to car tests with respect to:
 - Good structural interaction
 - Good compartment strength
 - Compatible car
 - Importance of width of frontal structures.
- Identify critical injury mechanisms (in particular relevance of thorax injuries in high deceleration pulses).
- Finalise a compatibility scale for a rating system.

These global issues will require research that focuses on car-car testing as well as accident analysis using detailed databases. The work previously reported to WG15 provides an important, but incomplete basis.

Test Procedure Specific issues:

Further development of test approaches to the point where a decision on the most appropriate set of test procedures can be made.

For the FWDB the major work items are:

- Determine if possible assessment criteria of the FWDB are sufficiently insensitive to the load spreading behind the honeycomb barrier seen in the rigid impactor tests and confirm the link between deformation and loads.
- Verify that all important vehicle structures, identified in accident analysis, can be detected by the barrier (for example horizontal structures):
- Determine and control the sensitivity of the test method to the vehicle alignment with the load-cells.

For the PDB test major work items are:

- Propose and validate assessment criteria when fundamental questions have been answered Validate the EES calculation method
- Validate that the PDB test guarantees a minimum EES test severity for all vehicles.

Performance limits for 1st step:

For this a car to car crash testing programme with associated barrier tests will be required to show that cars that meet the performance requirement perform better in car to car tests than those that don't. It is likely that modified cars will be required for this. Some of the tests already performed in the VC-COMPAT project could form a starting point for this programme.

Cost benefit analysis for implementation of 1st step:

The results from the test programme to set the performance limits will be used to make the assumptions to perform this analysis.

Membership of EEVC WG 15

Official Members:

Eberhard Faerber, BAST, Germany, *chairman*
Tiphaine Martin, UTAC, France, *technical secretary*

Giancarlo Della Valle, Elasis, Italy
Dr. Mervyn Edwards, TRL, United Kingdom
Joaquim Huguet, IDIADA, Spain
Dr. Robert Thomson, Chalmers University of Technology, Sweden
Cor van der Zweep, replaced by Richard Schramm TNO, The Netherlands

Industry Advisors:

Domenico Galeazzi, FIAT, Italy
Anders Kling, Volvo Car Corporation, Sweden
Richard Zeitouni, PSA Peugeot Citroen, France
Dr. Robert Zobel, Volkswagen AG, Germany
Martin Harvey, Jaguar, UK

Observers:

Pascal Delannoy, Teuchos-Safran Group, France

ACKNOWLEDGEMENTS:

EEVC WG 15 would like to thank the EEVC Steering Committee and the European Commission for supporting and funding the VC-COMPAT project. The support of the national governments of France, United Kingdom, Germany, Sweden, and the Netherlands also ensures that work continues within the group.

REFERENCES

- 1 Faerber, E., et al, "EEVC Approach to the Improvement of Crash Compatibility between Pas-

- senger Cars”, Proceedings of the 19th ESV Conference Paper 05-0155, Washington, 2005
- 2 VC-COMPAT - Final Technical Report, Title: "Improvement of Vehicle Crash Compatibility through the Development of Crash Test Procedures", Contract N°: GRD2/2001/50083/VC-COMPAT, Project N°: GRD2/2001/50083, Project partly funded by the European Commission, 22.01.2007
 - 3 Lomonaco C and Gianotti E (2001). '5-YEARS STATUS REPORT OF THE ADVANCED OFFSET FRONTAL CRASH PROTECTION' 17th ESV conference, Amsterdam, Netherlands, 2001.
 - 4 Edwards M et al. (2003). 'Development of Test Procedures and Performance Criteria to Improve Compatibility in Car Frontal Collisions', 18th ESV conference, Paper no. 86, Nagoya, 2003.
 - 5 Edwards M et al. (2005). 'Current Status of the Full Width Deformable Barrier Test', 20th ESV conference, Paper No. 07-088, Lyons, France, 2007.
 - 6 Thomson R and Edwards M (2005). 'Passenger Vehicle Test Procedure Developments in the VC-COMPAT project', Paper No. 05-0008, 19th
 - 7 Zobel et al. (2005). 'Towards a Beneficial, Scientifically Meaningful, and Applicable Compatibility Testing', 19th ESV, Paper No. 05-0052, Washington, 2005.

BUMPER BAG FOR SUV TO PASSENGER VEHICLE COMPATIBILITY AND PEDESTRIAN PROTECTION

Bengt Pipkorn
Rikard Fredriksson
Jan Olsson

Autoliv Research
Sweden
Paper Number 07-0056

ABSTRACT

An external airbag (bumper bag) for improved sport utility vehicle (SUV) to passenger vehicle compatibility in side impact and improved pedestrian protection was developed. The bag was developed and evaluated by means of mathematical simulations and mechanical crash tests.

The mounting location of the bumper bag was below the bumper structure of an SUV. The volume of the bag was 134 liters and the peak pressure of the bag when loaded was approximately 7 bars.

In the mechanical crash tests a Ford Explorer with and without a bumper bag was run into the side of a Toyota Corolla. The impact angle was 90 degrees and the impact velocity was 48 kph (30 mph). It was found that the bumper airbag significantly reduced the b-pillar peak intrusion velocities and maximum deformation of the impacted vehicle.

The potential injury reducing benefits for a pedestrian impacted by an SUV equipped with a bumper bag was also evaluated. Using a pedestrian leg form both impact and inadvertent firing tests were carried out. In the impact test the leg form was impacting the front of the Ford Explorer at 40 kph (25 mph) with and without bumper airbag. In the inadvertent firing tests the leg form was positioned in contact with the bumper of the SUV when inflation of the bumper bag was initiated. It was found that the bumper bag reduced the knee bending angle, shear displacement and tibia acceleration significantly. All injury measures but one was below the EuroNCAP injury assessment values for the lower extremity.

The potential reduction in injury measures for an occupant on the impacted side of the passenger car impacted by an SUV with a bumper airbag was evaluated. The evaluation was carried out by means of sled tests. The intrusion velocities at the chest level of the impacted vehicle in the crash tests were used to drive the sled in sled tests. In the sled tests a state of the art occupant protection system was used. The system comprised a seat belt system and

a side airbag. It was found that chest injury measures were significantly reduced when a bumper bag was used in a SUV to passenger vehicle side impact.

Future development of the bumper airbag system will include improved frontal impact compatibility and self protection.

INTRODUCTION

The crashworthiness of passenger cars have been considerably improved during the last decades. From the early 1980's until 2000, the driver death rate per million cars registered decreased 47 percent according to IIHS [1]. However, this improvement was mainly made in frontal crashes for which driver death rate decreased 52 percent, compared to only 24 percent in side impact.

In side impact crashes, on the other hand, IIHS found that side impact crashes accounted for 51 percent of driver deaths during 2000 and 2001 compared to 31 percent during 1980 and 1981. According to information in the FARS database the driver of a struck vehicle involved in a side impact crash is more likely to be killed when the striking vehicle is a large pickup than when it is a passenger car [1] (Figure 1). Out of 40 fatal side impact of pickups into passenger cars, 39 occupants will die in the passenger car while one will die in the LTV (Light Trucks and Vans). Large SUVs such as Ford Explorer are included in the definition of LTV.

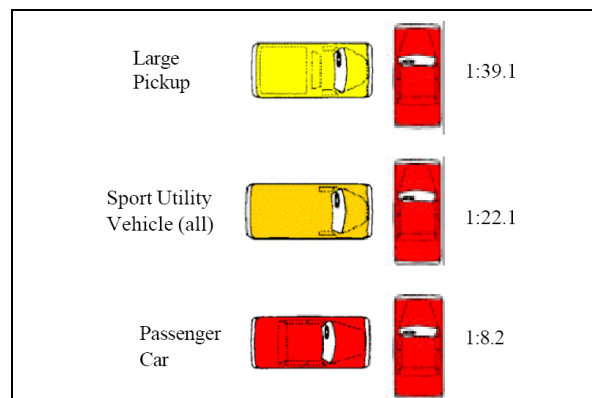


Figure 1
Driver Fatality Ratio of Side Impact Crashes Into Passenger Cars [1]

A study by IIHS confirms the increased risk for an occupant in a passenger vehicle impacted in the side by a SUV. The relative risk of death can be 27-48 times greater for the occupant of a passenger car (Figure 2) [2].

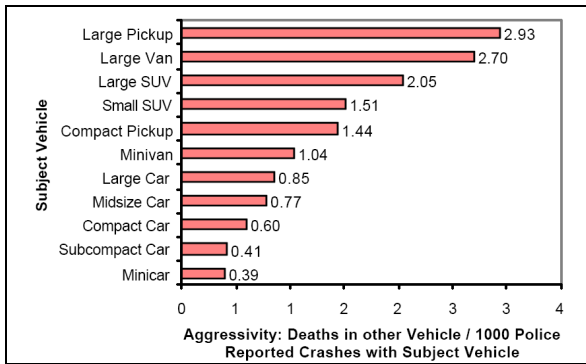


Figure 2
Death in Other Vehicle /1000 Police Reported Crashes with Subject Vehicle [2]

The sales and registration of LTV's in the US have steadily increased as the percentage of the fleet, since 1981 (Figure 3) [1]. In 2004 LTVs represented 45% of the vehicles sold in the US [3]. As the number of LTVs on the roads increases the number of accidents in which a LTV is a part increases.

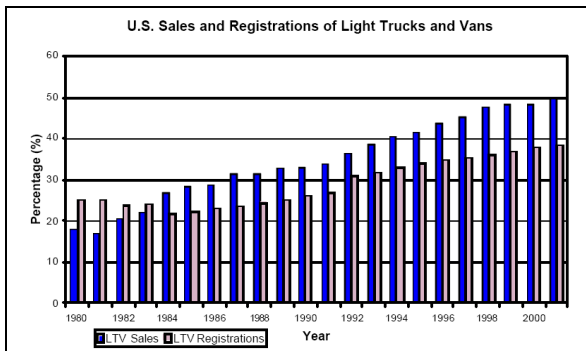


Figure 3
LTV US sales and registrations [1]

The increased number of LTVs relative to the number of passenger cars has led to an increasing number of fatalities for car occupants that are struck by LTV's, while the fatalities have decreased in car to car crashes (Figure 4) [4].

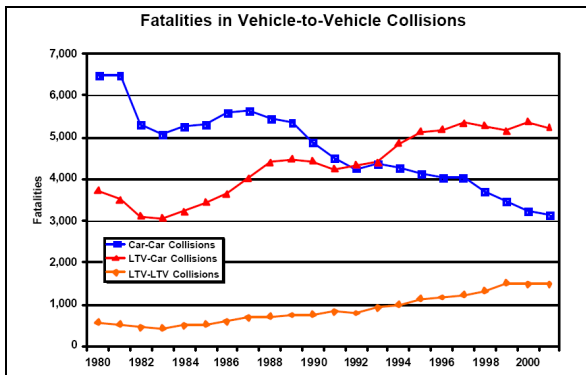


Figure 4
Occupant Fatalities in Vehicle-to-Vehicle Crashes [4]

A reason for the increased risk for an occupant at the impacted side of a passenger car in a SUV to passenger car side impact is that the SUVs are stiffer, heavier than passenger cars. In addition the frame structures of the SUVs are also located higher above the ground. There is a significant height mismatch between a Sport Utility Vehicle (SUV), such as a Ford Explorer, and a passenger car, such as a Honda Accord (Figure 5) [5]. When an SUV impacts a passenger vehicle in the side, the SUV bumper completely mismatches the sill floor of the passenger vehicle. Since the sill and floor is one of the stiffer structures of the car side, there will be a great risk for the SUV to deform the passenger vehicle heavily, thereby increasing the intrusion velocity of the b-pillar and the door. It will result in reduced survival space for the passenger.

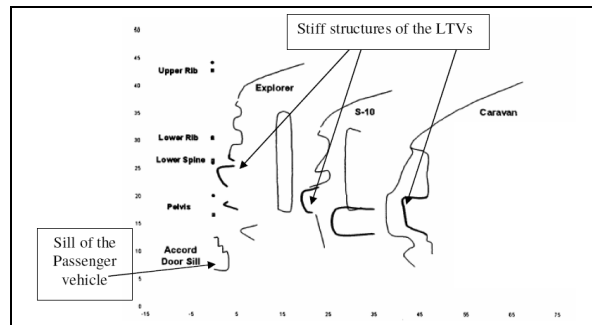


Figure 5
Front Profile of Various Vehicles [5]

Side impacts are the second most frequent type of crashes causing serious injury and death. More than half occur at intersection collisions, and the most serious impacts are those in which the vehicle is struck centrally.

The most common areas for injury include the chest (73%) and the head (53%) (Figure 6) [6].

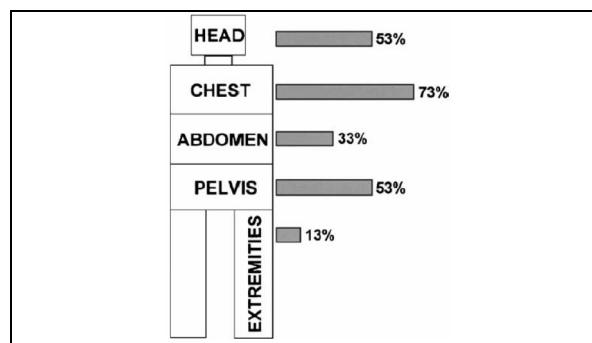


Figure 6
Percent of Patients with Injury AIS ≥ 2 designated body regions [6]

These injuries are related to the intrusion of the door panels and B-pillar, and in some cases direct contact with the impacting vehicle.

The intrusion is related to many factors for example the vehicles weight, stiffness, design and speed. Data used by Acierno [6] shows that the intrusion of a pickup into the driver compartment of a passenger car was in the range of 20 cm to 50 cm. The maximum intrusion often appeared above the mid to lower door reinforcement of the passenger vehicle due to the height of the SUV bumpers. In some cases, the occupant's head had a direct contact with the hood of the SUV. The SUV frame contacted the side of the passenger car in weaker, non-reinforced areas, leading to maximal intrusions into the head and upper thorax of the occupants.

The current regulation does not include the SUV to passenger car load case. The lower edge of the ECE R95 side impact barrier is 300 mm above the ground [7]. The FMVSS 214 side impact barrier lower edge is 280 mm above the ground and the bumper part of the barrier is 330 mm above the ground [8]. That means that the FMVSS 214 barrier begins 127 mm (5 inches) above the bottom of the door and ends no more than 13 mm above the window sill (Figure 7). The average LTV front end is considerably higher, striking above the reinforcement added to the vehicles to pass both the ECE R95 and FMVSS 214 regulation.

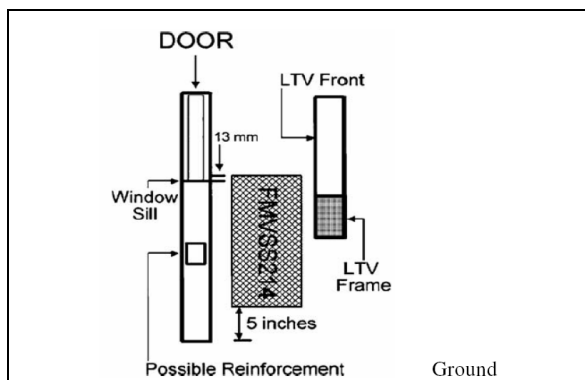


Figure 7
FMVSS 214 Crash Test Barrier Compared to Average LTV Front End [8]

A consumer test procedure that takes the height of the LTV front end above ground into account is a test method developed by IIHS [9]. The moving deformable barrier used in this test was designed to match the front end geometry and ride height of LTVs and SUVs. The bottom of the barrier is 379 mm above ground and the bumper part of the barrier is 430 mm above ground. This is considerably higher than what it is for the ECE R95 and FMVSS 214 barrier.

After analyzing the injury consequences of a side impact an LTV impacting a passenger vehicle, physical criteria had to be found to analyze the severity of simulated side impact since no dummy

model was implemented into the passenger car model used in a mathematical analysis. As Ludo [10] demonstrated, it is appropriate to use the velocity change along the y-axis (perpendicular to the side doors) as a representative parameter for dummy impact severity.

To conclude, the following statements by Ludo [10] were useful for the study:

- The door structure velocity in the same time frame of occupant impact is controlled much more by stiffness ratio of the two vehicles than by the mass ratio.
- The door skin peak velocity is that of the bullet car.
- The mass ratio controls the final velocity of the two vehicles.
- A stiffer door reinforcement structure decreases the velocity with which the occupant is struck.
- The velocity change in y-direction of the b-pillar is appropriate to evaluate occupant injuries.

Many concepts and designs of bumper airbag systems have been proposed and patented [11, 12 and 13]. In one external airbag study, two crash tests were carried out using a Cutlass Sierra four door sedans equipped with bumper airbags. The first test was a frontal crash into a rigid barrier at 48.5 kph using two unventilated bags, one set at a high pressure (2.21 bars) and the other set at a low pressure (0.35 bars). With this test setup, 19% of the crash energy was absorbed by the bags. The second test was a side impact crash in which a rigid barrier impacted the passenger car at 48.5 kph. A pressurized bag (0.6 bars) was placed on the side of the passenger car above the sill, overlapping the side door and centered on the B-pillar. The result of this test was not successful. The bag deformed the weak structures of the panel of the side doors providing little additional protection. Two important conclusions were drawn from this study:

- The bumper airbag must deform with a stopping force up to 300 kN for a frontal airbag and 200 kN for a side airbag.
- The deformation of the bumper airbag will deform weak structures of the panel of the side doors.

An additional application of a bumper airbag system can be to reduce injuries to the lower leg of pedestrians in SUV to pedestrian accidents. In pedestrian accidents with passenger vehicles, knee and lower leg are the most frequently injured area. The most frequent injury producing part of the car is the bumper. Therefore EEVC working group 17 proposed in 1998 a test method for the leg to

bumper impact which was later introduced in the EuroNCAP rating testing [14]. In the EEVC test method bending and shearing requirements were proposed to mitigate knee injuries as well as an acceleration requirement for the upper tibia mitigating the risk for tibia fractures. A bending of 15 degrees and a shearing of 6 mm was proposed as a threshold values for the knee and 150 g for the upper tibia acceleration. To design a passenger car in order to meet these requirements there are basically two features that can be added. First thick and soft foam in the bumper can be introduced and secondly a support for the tibia below the bumper can be added. All EU regulations and proposals are limited to cars with a gross weight of less than 2.5 tons. This means that many LTVs and SUVs will be excluded. Recently there was a proposal by the US to increase the gross weight to 3.5 tons or even 4.5 tons. This would include more or less all SUVs.

For SUVs the occurrence of leg and knee injuries are slightly lower than for passenger cars, when calculating as a percentage of all injuries, not actual risk. Longhitano et al (2005) reported that for SUVs in the US leg and knee injuries place 3rd after head and chest for both AIS 2+ and AIS3+ injuries [15]. However, for AIS2+ injuries the occurrence was very similar to chest injuries. Lefler and Gabler reported that the overall fatality and injury risk increases with SUVs compared to passenger cars [16]. This involved accidents 1995-2000 in the US. Per 1000 reported single vehicle/pedestrian impacts 115 were killed when an SUV was involved compared to 45 when a passenger car was involved. The fatality risk was thereby increased with more than 2.5 times for SUVs compared to passenger cars. Also it was likely that the risk of so called “run-over” accident increases with SUVs compared to passenger cars due to the higher bumper and ground clearance.

There is a need for a system that will improve the LTV and SUV to passenger car side impact compatibility and pedestrian protection.

AIM

The aim of the study was to by means of mathematical simulations and mechanical crash tests evaluate possible side impact compatibility and pedestrian protection benefits from mounting an external airbag (bumper bag) in the front end of an SUV.

MATHEMATICAL MODEL

The initial development of the bumper airbag was carried out by means of mathematical simulations.

The vehicle models used were Chevrolet C250 Pickup Truck model and a Ford Taurus model (Figure 8). The number of elements of the Chevrolet Pickup was 53856 and for the Ford Taurus 65921. The models were developed and initially validated by NCAC [17]. The Ford Taurus model was additionally validated by means of in house crash tests.

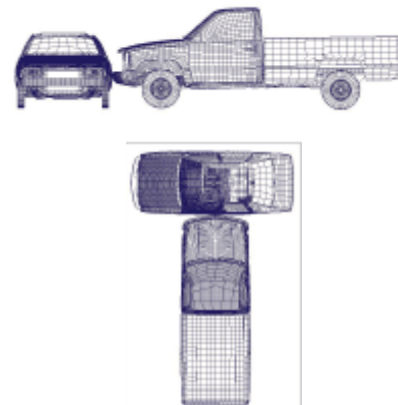


Figure 8
Vehicle Models Used

For evaluation of the potential benefits of using a bumper bag the intrusion velocity and intrusion depth were analyzed for four sensor locations on the b-pillar in the Ford Taurus model (Figure 9). The four locations were sill, pelvis, chest and head level on the b-pillar of the impacted vehicle.

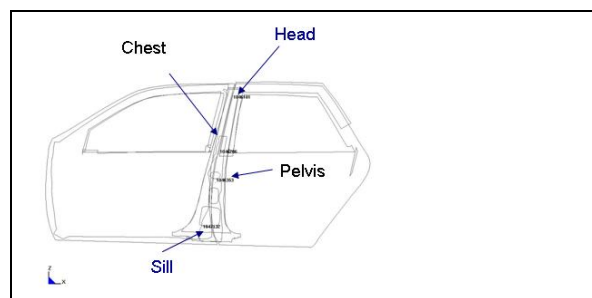


Figure 9
Sensor Locations Used to Record B-Pillar Intrusion Velocity and Intrusion Distance

In the development of the bumper bag the influence of a great number of parameters were evaluated by means of mathematical simulations. The parameters were shape, location, pressure, volume and ventilation of proposed bumper bag. In the shape, ventilation, location and volume evaluation of the bumper bag a pressure of 7 bars was used.

Two different locations for the bumper bag were evaluated. The locations were in front of the bumper and below the bumper (Figure 10).

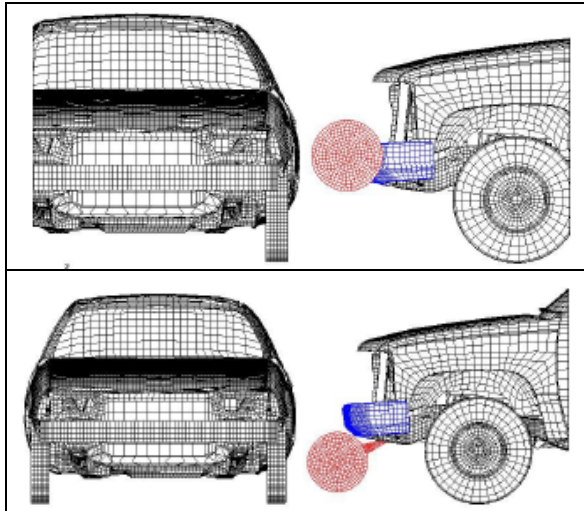


Figure 10
Location of the Bumper Bag

The initial over pressures evaluated were 1, 3, 7 and 10 bars and the volume of the bag evaluated was 47, 102, 147 and 189 liters.

RESULTS MATHEMATICAL MODEL

Some of the most important simulation results from the parameter study are summarized below. The results shown are peak intrusion velocity and peak intrusion distance. The intrusion velocity was the velocity of a point on the b-pillar on the impacted side of the vehicle relative a point on an undeformed location, such as the tunnel, of the impacted vehicle. The intrusion distance was the displacement of a point on the b-pillar on the impacted side of the vehicle relative a point on an undeformed location, such as the tunnel, of the impacted vehicle.

For the evaluation of the location of the bumper bag the lowest intrusion velocity and intrusion distance was obtained for a bumper bag mounted below the bumper (Figure 12). For head, chest and pelvis sensor locations the intrusion velocity was significantly reduced with a bag mounted below the bumper. For the sill sensor location only minor reductions in peak intrusion velocity was obtained. For a bag mounted in front of the bumper only minor reductions were obtained for the head and sill sensor locations. For the chest and pelvis sensor locations no reductions were obtained.

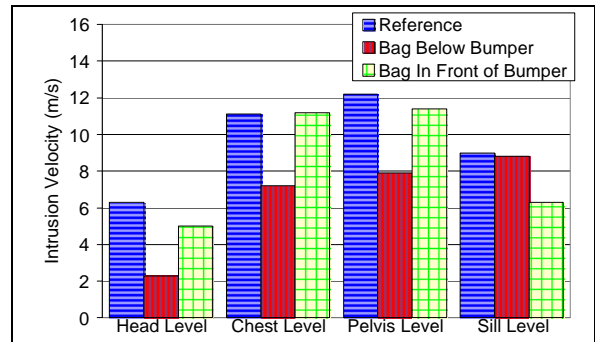


Figure 12
Intrusion Velocity, Peak Values (m/s), Location of Bumper Bag

For the peak intrusion distance significant reductions were also obtained for a bag mounted below the bumper for all sensor locations but the sill location (Figure 13). For the sill sensor location no reductions in intrusion distance was obtained for a bag mounted below the bumper relative to when no bag was used.

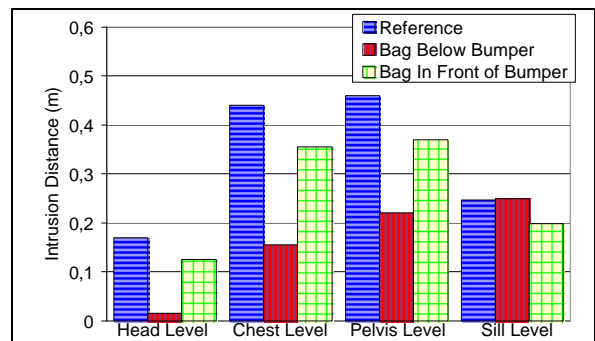


Figure 13
Intrusion Distance, Peak Values (m), Location of Bumper Bag

For the bag pressure evaluation it was found that for the chest and pelvis sensor location the higher the pressure the lower the intrusion velocity (Figure 14). For the sill sensor location the intrusion velocity increased significantly for all bag pressures but 10 bars. For 10 bar pressure intrusion velocity was reduced also for the sill sensor location. For the head sensor location significant reductions were obtained by adding a bag. However only minor variations in intrusion velocity was obtained for the various bag pressures.

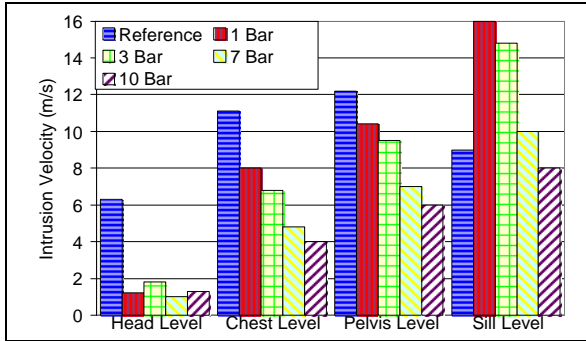


Figure 14

Intrusion Velocity, Peak Values (m), Bag Pressure

In the bag pressure evaluation it was found that for the chest and pelvis sensor locations the higher the pressures the lower the intrusion distance (Figure 15). For the head and sill sensor locations only small differences in intrusion distance for the various bag pressures was observed. However, significant reductions in intrusion distance relative to when no bag was used was obtained.

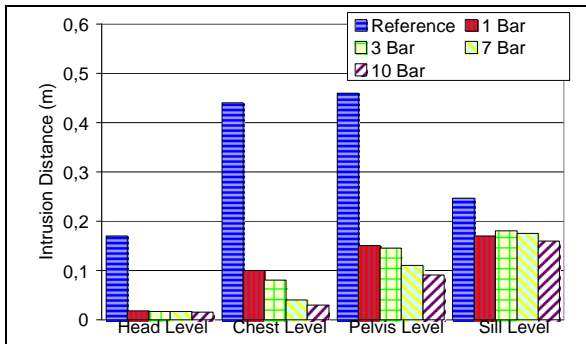


Figure 15

Intrusion Distance, Peak Values (m), Bag Pressure

For the bag volume evaluation greatest reductions in intrusion velocity was obtained for the large volume airbag. The volume of that airbag was 189 liters (Figure 16). For the smallest bag, 47 liters, an increase in intrusion velocity for the sill sensor location was obtained and for the pelvis sensor location no reduction in intrusion velocity was obtained. For the bag with 102 and 147 liter volume reductions in intrusion velocity was obtained for the pelvis sensor location. For the sill sensor location there was an increase in intrusion velocity for 102 and 147 liter bag volume.

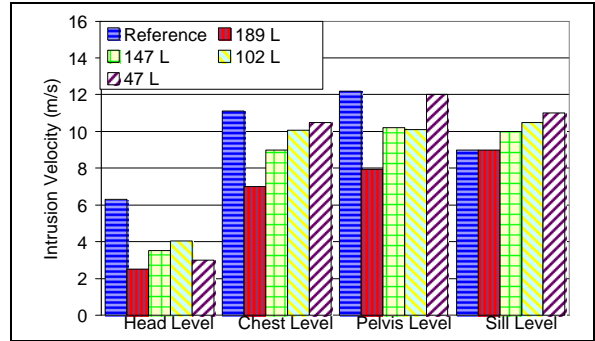


Figure 16

Intrusion Velocity, Peak Values (m), Bag Volume

For the intrusion distance greatest reductions was obtained for the bag with greatest volume 189 liter (Figure 17). For all bag volumes but one peak intrusion distance was reduced significantly. For the sill sensor location there was no reduction in intrusion distance for the various bag pressures.

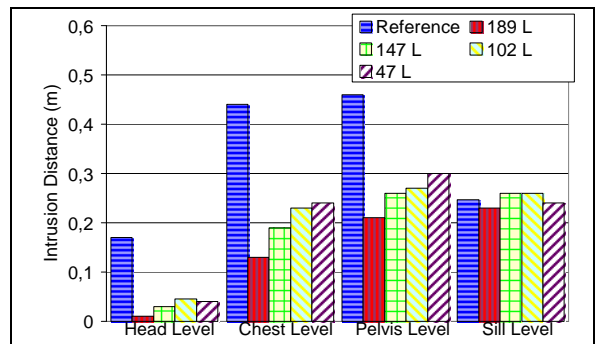


Figure 17

Intrusion Distance, Peak Values (m), Bag Volume

From the mathematical simulation results a bumper bag system was proposed. The preferred location of the bumper bag was below the bumper, the volume was 189 liters and the pressure was 10 bars.

MECHANICAL BUMPER BAG

Based on the results from the mathematical model a mechanical bumper bag was designed and a prototype made (Figure 18). The bag was of tubular shape. The length of the bag was 2.4 m, the width was 0.3 m and the volume was 134 liters. The bag was covered with 53 circular seat belt elements. Half of the bag diameter (0.15 m) was extending in front of the bumper when the bag was inflated. The bag was inflated using 3 passenger side airbag gasgenerators. The peak pressure obtained was 7 bars.

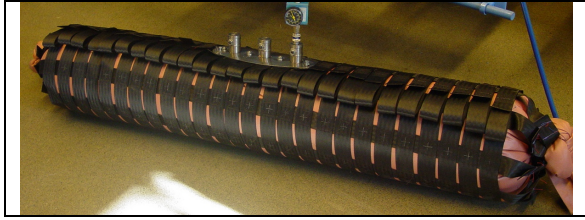


Figure 18
Mechanical Bumper Bag

For the bumper bag to transfer load from the SUV to the passenger car, in a side impact, a load carrying support structure was needed. The support structure was mounted with a hinge joint to the SUV. The bumper bag was mounted on the support structure (Figure 19). When not used the bumper bag was folded and the support structure with the bag was located behind the bumper. In the crash the bumper bag was expanded and pushed the support structure downwards. When in position, the bumper bag support structure was locked providing the bumper bag with a load carrying support structure.

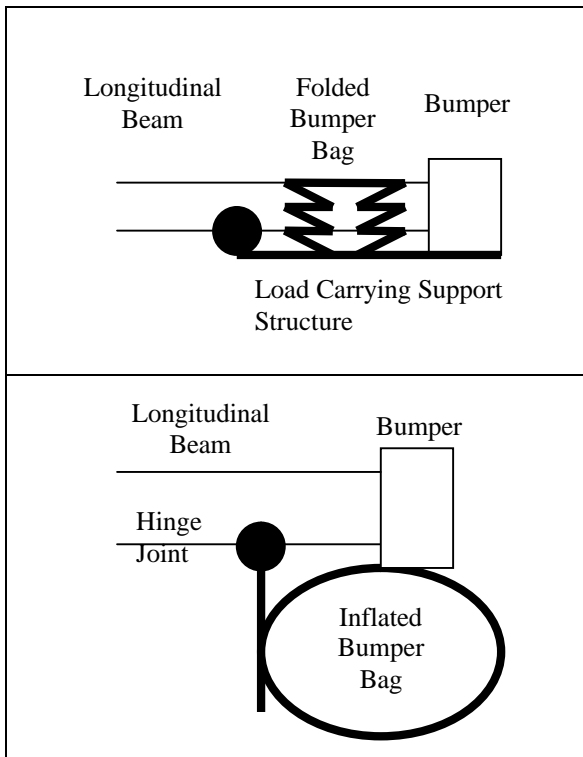


Figure 19
Bumper Bag Schematic

MECHANICAL SUV TO CAR CRASH TEST

The potential compatibility benefits of the mechanical prototype bumper bag were evaluated by means of Ford Explorer to Toyota Corolla crash tests (Figure 20). In the tests the Ford Explorer was impacting the side of the Toyota Corolla at an impact angle of 90 degrees and an impact velocity

of 48 kph (30 mph). The mid point of the Ford Explorer bumper was impacting at the H-point of the Toyota Corolla. The Toyota Corolla was MY 1992 and the Ford Explorer was MY 1993. The mass of the Ford Explorer was 2043 kg and the mass of the Toyota Corolla was 1100 kg. Two crash tests were carried out. One reference test without bumper bag and one test with bumper bag. Accelerations and Intrusion distances at 4 sensor locations on the b-pillar were recorded. The intrusion distances were recorded by means of string potentiometers. The same locations as were used in the mathematical model were used in the mechanical tests. In addition, accelerations were recorded at numerous locations on the impacted and non-impacted side of the Toyota Corolla and acceleration was recorded at the tunnel of the Ford Explorer. No crash test dummies were used in the crash tests



Figure 20
SUV to Car Side Impact

RESULTS FORD EXPLORER TO TOYOTA COROLLA CRASH TESTS

For the impacting vehicle, the Ford Explorer, The acceleration, at an undeformed location (tunnel) of the vehicle, was altered somewhat by the addition of a bumper bag (Figure 21). The first local peak acceleration was increased, when a bumper bag was added, from 75 m/s^2 to 100 m/s^2 . Peak global acceleration was increased from 136 m/s^2 to 146 m/s^2 .

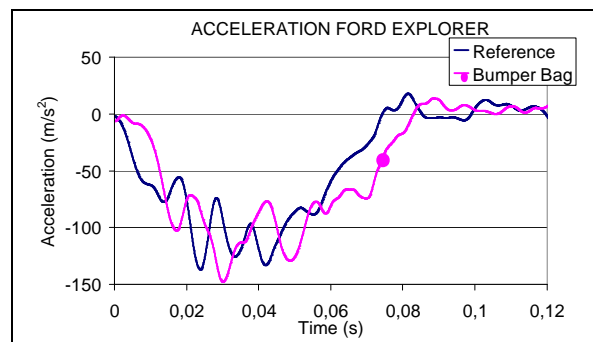


Figure 21
Tunnel Acceleration Ford Explorer

The final velocity at an undeformed location (tunnel) of the Toyota Corolla was 10 m/s for the reference test (Figure 22). For the test with a bumper bag the final tunnel velocity was 11 m/s.

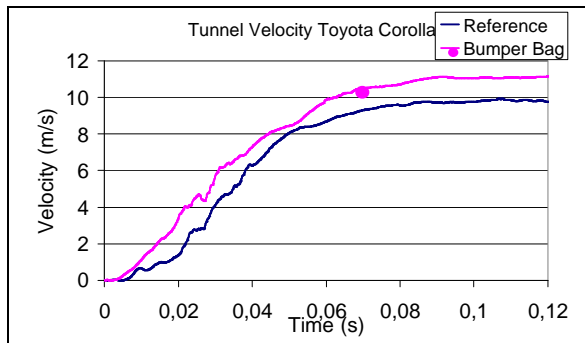


Figure 22
Tunnel Velocity Toyota Corolla

Peak intrusion velocity was very small at the head sensor location for both the reference test and the test with the bumper bag (Figure 23). For the chest and pelvis sensor location peak intrusion velocity was reduced when a bumper bag was added. At the chest sensor location peak intrusion velocity was reduced from 12.5 m/s to 10.0 m/s and at the pelvis sensor location peak intrusion velocity was reduced from 12.0 m/s to 11.0 m/s. At the sill sensor location, however, peak intrusion velocity was increased from 5.0 to 8.5 m/s when a bumper bag was added.

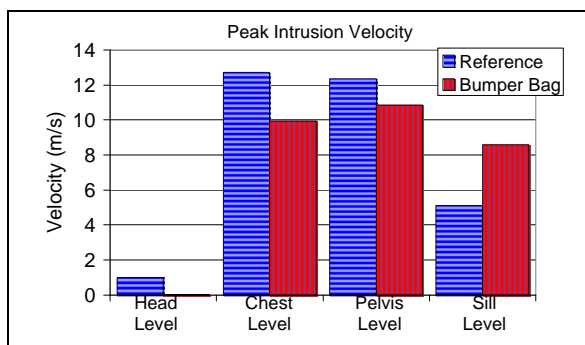


Figure 23
Peak Intrusion Velocity

Peak intrusion distance at the head, chest and pelvis sensor location was reduced with the bumper bag (Figure 24). At the head sensor location peak intrusion distance was reduced from 0.12 m to 0.07 m. At the chest location it was reduced from 0.32 m to 0.28 m and at the pelvis location it was reduced from 0.32 m to 0.24 m. At the sill location it was increased from 0.14 m to 0.24 m.

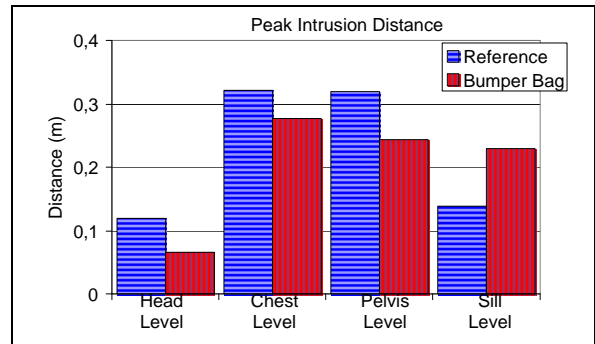


Figure 24
Peak Intrusion Distance

PEDESTRIAN TESTS

A pedestrian evaluation of the bumper bag was also carried out. In the evaluation a pedestrian leg form was used [12]. The tests were a reference without bumper bag, an impact test with an inflated bumper bag and an inadvertent firing test. In the impact test the leg form was impacting the front of the Ford Explorer at 40 kph (25 mph) with and without bumper bag. In the inadvertent firing tests a leg form was positioned in front of the bumper bag when inflation of the bag was initiated.

RESULTS PEDESTRIAN TESTS

In the results from the leg form tests it can be observed that the bending angle was significantly reduced with the bumper bag (Figure 25). There was a significant difference in the bending angle between the two reference tests and the two tests with bumper bag. However, in both reference tests the bending angle was greater than the EuroNCAP injury criteria level. In one of the tests, with the bumper bag, peak bending angle was greater than the injury criteria level. For the inadvertent firing test the bending angle was significantly lower than the injury criteria level.

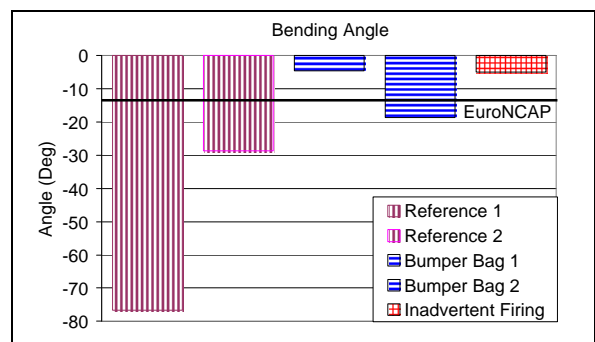


Figure 25
Peak Bending Angle

The shearing displacement in the reference test was 5 mm (Figure 26). In the tests with the bumper bag peak shearing displacement was less than 1 mm.

The shearing displacement was significantly reduced with the bumper bag. However, all test results were below the EuroNCAP injury criteria level of 6 mm. The shearing displacement in the inadvertent firing test was very low.

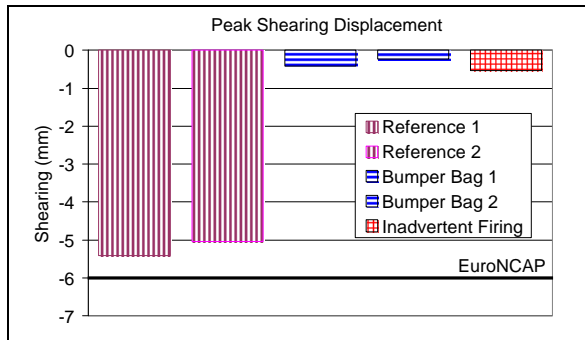


Figure 26
Peak Shearing Displacement

The tibia acceleration in the reference tests were 250 g's (Figure 27). For the bumper bag the tibia accelerations were 120 g's. Therefore great reductions in tibia accelerations were obtained with the bumper bag. The tibia accelerations in the reference tests were significantly greater than the EuroNCAP injury criteria level. The tibia acceleration in the inadvertent firing test was 100 g's which was significantly lower than the EuroNCAP injury criteria level.

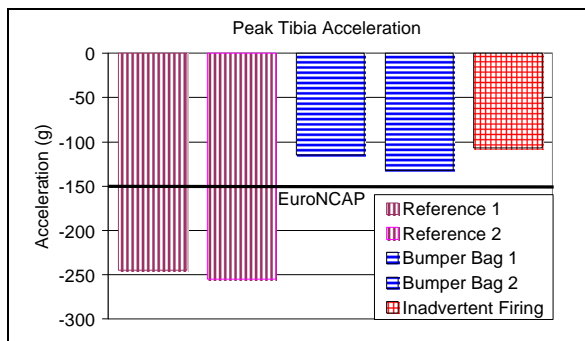


Figure 27
Peak Tibia Acceleration

DISCUSSION

The potential compatibility and pedestrian protection benefit of mounting a bumper airbag on an SUV was evaluated. It was found that the intrusion velocity and displacement was significantly reduced by adding a bumper bag. An added benefit with a bumper bag was that the time available to inflate a side airbag was also increased.

In the modelling results in which the pressure of the bumper bag was evaluated it was observed that the sill sensor location velocity was increased for all pressures but for the bag with 10 bar pressure.

The reason was that for all other evaluated pressures the bumper bag was bottoming out and the support surface was impacting the sill of the passenger vehicle resulting in high peak intrusion velocities.

The mechanical prototype bumper bag that was made was not exactly the same as the bumper bag that was proposed based on the mathematical simulations. This was due to the fact that in the mathematical simulations a model of a pickup truck was used and in the mechanical test a Ford Explorer was used. The bag was modified to fit the Ford Explorer geometry. In addition, in the prototype bumper bag the pressure was 7 bar resulting in improved bag integrity. Also less powerful gasgenerators were used in the mechanical test relative to the gasgenerator used in the mathematical model.

In the crash tests no dummies were used. For geometrical reasons it was not possible to both measure intrusion and include dummies. The intrusion measurements using string potentiometers were considered to be more important than dummy measurements.

The acceleration of the Ford Explorer was not altered by adding a bumper bag. However, in both crash tests, the acceleration was at a very low level exposing an occupant to a minor risk of sustaining an injury.

Generally small improvements in intrusion velocity and intrusion distance were observed for the sill sensor location. The aim of the bumper bag was to load the lower stiff structures of a passenger car in a side impact. Therefore the sill sensor location velocity and intrusion distance was not reduced to a great extent. In addition the velocity of an undeformed location of the Toyota Corolla increased when a bumper bag was used due to the fact that the bumper bag loaded the lower stiff structures.

For the bumper bag generally smaller reductions in intrusion velocity and intrusion distance of the b-pillar of the impacted passenger car was obtained in the mechanical tests compared to the mathematical model predictions. One explanation can be that the support structure was also used in the crash test without the bumper bag. Another explanation can be that the impacted vehicle in the mechanical test was a Toyota Corolla which seems to have stiffer side structures than the Ford Taurus.

The reason for using the support structure in the crash test without the bumper bag was to investigate the influence of only the support structure. Therefore, the reductions in intrusion

velocity and displacement can be even greater if the result from a test with a bumper bag is compared to the result with a standard Ford Explorer without support structure for the bumper bag.

In the crash tests carried out the bumper bag was unventilated. The energy absorption of the bumper bag can be increased if ventilation is used. In future analysis the potential improvement of a bumper bag system with ventilation will be evaluated.

The potential injury reducing benefits for an occupant by adding a bumper airbag was evaluated by means of mechanical sled tests. The intrusion velocity from both crash tests, without and with bumper bag, was used to drive the sled in the sled tests (Figure 28).

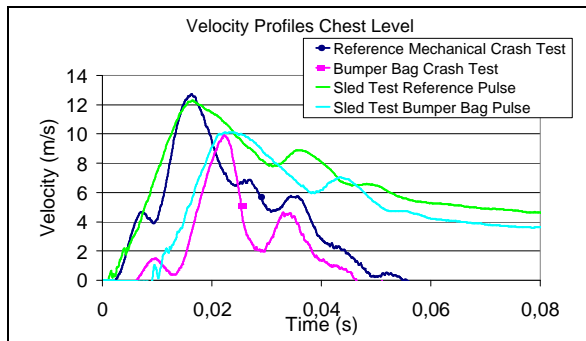


Figure 28
Intrusion Velocity in Crash Tests and Sled Tests

In the sled test a belted ES-2 dummy was positioned in a seat. A rigid wall with 50 mm foam material (Ethafom 220) with a state of the art side airbag was impacting the dummy (Figure 29).

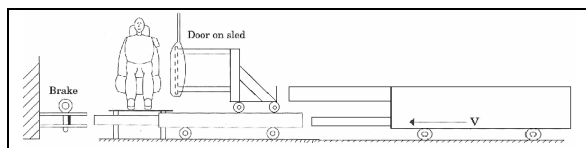


Figure 29
Mechanical Sled Test Set Up

The chest deflection for all ribs was reduced with the bumper bag (Figure 30). For the upper rib the deflection was reduced from 49 to 42 mm. For the middle rib it was reduced from 47 to 37 mm and for the lower rib it was reduced from 42 to 33 mm.

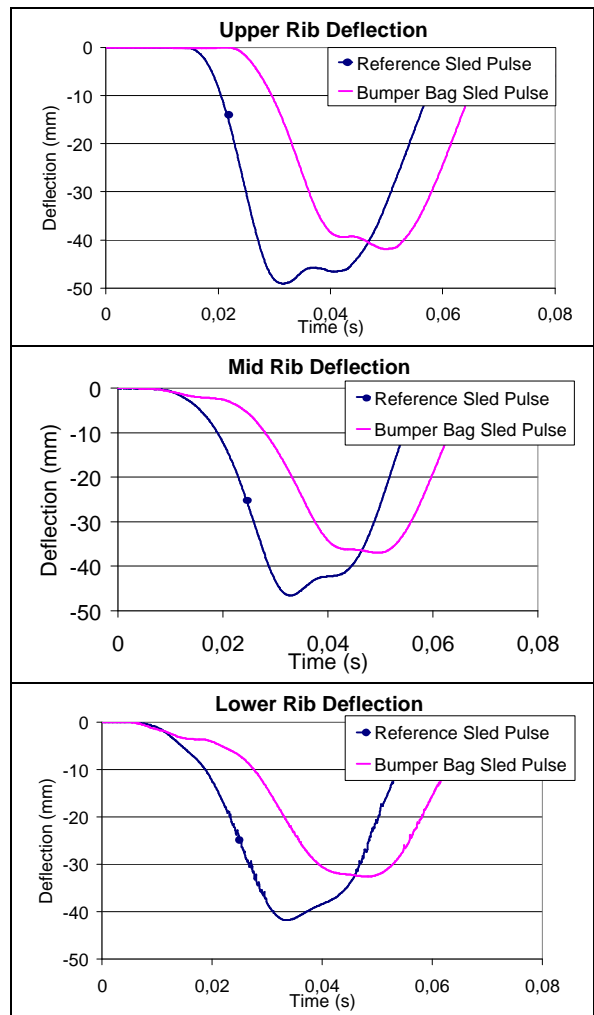


Figure 30
Upper, Mid and Lower Chest Deflection

The sled method used to evaluate the potential occupant injury reductions by using a bumper bag was a simplification of a side impact. The crash pulses used to drive the sled in the sled tests mimicked the corresponding crash pulse up until peak velocity was reached (Figure 28). After peak velocity the curves diverged. The sled velocities remained at a higher level than the velocities from the crash tests. However, the method will serve as an indication of the potential benefits that can be obtained with a bumper bag.

In the pedestrian legform test results there were significant variations in peak bending angle. The reason for the variations was not clear. In the high speed movie a bending angle of 75 degrees, as was measured in the first reference test, was not observed. Therefore the variations are likely to be due to unreliable measurements.

When the bumper bag is used in a pedestrian impact the kinematics of the occupant is altered compared to when the occupant is impacted by the bumper without bumper bag. In future evaluations

of the bumper bag system the kinematics of a pedestrian impacted by a bumper bag will be evaluated.

The injury reducing benefits for the lower extremity of pedestrian with a bumper bag is not limited to SUVs. The benefits can also be obtained for a passenger car with a bumper bag.

There are legal requirements (approach angle) for the angle between the bumper structure and the front wheel of an SUV [18]. Mounting a load carrying beam below and in front of the bumper structure, at the same location as an inflated bumper bag, infringes the legal requirements. Therefore, an advantage with the bumper bag is that it fulfills these requirements due to the fact that the bag is located behind the bumper when not inflated. A bumper bag increases the design freedom for the bumper structure of an SUV and also improves the compatibility between an SUV and a passenger car.

For the bumper bag to work properly in a crash it has to be triggered prior to impact. Such triggering systems are now being developed [19 and 20]. They have to be able to reliably trigger irreversible systems such as the bumper bag.

CONCLUSIONS

- A bumper bag reduces the intrusion velocity of the door structure of a impacted passenger car significantly in a SUV to passenger car side impact
- A bumper bag reduces the injury measures for the lower extremity of a pedestrian impacted by a SUV equipped with a bumper bag.

ACKNOWLEDGEMENT

The author acknowledges Yannick Schroeder for carrying out most of the mathematical modeling work.

REFERENCES

[1] Summers, S., Hollowell, T., Prasad, A. "NHTSA's Research Program for Vehicle Compatibility", Proceeding of the Eighteenth Conference on Enhanced Safety of Vehicles, Nagoya, Japan, 2003.

[2] Insurance Institute for Highway Safety "Putting the Crash Compatibility in Perspective". Insurance

Institute for Highway Safety Status Report 34 (9), 1-11, 1999.

[3] Crain Communication Inc. Automotive News, no. 6129, Detroit, USA, 2005.

[4] Hollowell, T., Summers, S., Prasad, A., "NHTSA Research Program for Vehicle Aggressivity and Fleet Compatibility", ImechE, 2002.

[5] Summers, S., Prasad, A., Hollowell, T., "NHTSAs Vehicle Compatibility Research Program", SAE Paper 1999-01-0071, 1999.

[6] Acierno, S., Kaufmann, R., Rivara, F. P., Grossman, D. C., Mockb, C., "Vehicle Mismatch: Injury Pattern and Severity", SIREN, Seattle, 2003.

[7] ECE 95, "Status of United Nations Regulation" E/ECE/234, E/ECE/TRANS/505, February 21, 2005.

[8] Federal Motor Vehicle Safety Standard (49 DFR Part 571) MVSS 214 Side Impact Protection, As Amended F.R. Vol. 68 No.230 – 01.12.2003

[9] Arbelaez, R. B., Baker, B. C., Nolan, J. M., "Delta VS for IIHS Side Impact Crash Tests and Their Relationship to Real World Crash Severity", ESV Paper 05-0049.

[10] Ludo, M., Careme, M., "Occupant Kinematics and Injury Causation in Side Impacts – Field Accident Experience", SAE Paper 910316, 1991.

[11] Clarke, C., "The Crash Anticipating Extended Airbag Bumper", ESV 1994, 1994.

[12] Clarke, C., William, Y. A., "Airbag Bumper just Inflated Before the Crash", SAE Paper 941051, 1994.

[13] Clarke, C., William, Y. A., "Car Crash Theory and Tests of Airbag Bumper Systems", SAE Paper 951056 1995.

[14] European Experimental Vehicles Committee, "Improved test methods to evaluate pedestrian protection afforded by passenger cars", EEVC Working Group 17 Report, December 1998.

[15] Longhitano D, Henary B, Bhalla K, Ivarsson J, Crandall J, "Influence of vehicle body type on pedestrian injury distribution", SAE World Congress, paper no 2005-01-1876, Detroit, USA, 2005.

[16] Lefler DE, Gabler HC, "The fatality and injury risk of light truck impacts with pedestrians in the

United States”, Accident Analysis and Prevention
36, pp 295-304, 2004.

[17] <http://www.ncac.gwu.edu/vml/models.html>

[18] 70/156/EEC amendment 92/53/EEC “Motor
Vehicle type Approval”, Issue:1, May 1990.

[19] Nitsche, S., “Integrated Safety: Linking Active
and Passive Safety”, Proceedings Airbag 2006 8th
International Symposium and Exhibition on
Sophisticated Car Occupant Safety Systems, 2006.

[20] Wohlebe, T., Gonter, M. M., “Potential of
Pre-Crash Restraints in Frontal Collisions.
Proceedings Airbag 2006 8th International
Symposium and Exhibition on Sophisticated Car
Occupant Safety Systems, 2006.

CURRENT STATUS OF THE FULL WIDTH DEFORMABLE BARRIER TEST

Mervyn Edwards

Richard Cuerden

Huw Davies

TRL Limited (Transport Research Laboratory)

United Kingdom

Paper Number 07-0088

ABSTRACT

To improve compatibility in car frontal collisions it is generally agreed that better structural interaction, matching frontal forces (stiffnesses) and a strong occupant compartment, in particular for small cars, are required. The Full Width Deformable Barrier (FWDB) test is part of a portfolio of tests being considered to assess a vehicle's frontal impact performance, including its compatibility. For compatibility, it aims to assess a vehicle's structural interaction potential using measurements from a high resolution Load Cell Wall behind the deformable element. For self protection, it aims to provide a high compartment deceleration pulse, similar to the current US NCAP test, to assess a vehicle's restraint system.

This paper describes the benefit predicted for the implementation of improved compatibility in GB and the current status of the FWDB test. For the FWDB test, it clarifies remaining issues including test repeatability and describes the new 'Structural Interaction' (SI) criterion. The SI criterion is designed to ensure that vehicles have an adequate structure in a common interaction area to interact with their collision partners and to encourage stable multi-load path structures. It consists of vertical and horizontal components that are divided into parts that could be adopted in a stepwise manner, to allow the gradual development of more compatible vehicles, appropriate for application in a regulatory framework.

INTRODUCTION

Following the introduction of the European frontal and side impact Directives and EuroNCAP, car safety has made a major step forward. Even so, there are still about 1,500 car occupants killed and 15,000 seriously injured in GB annually [1]. Approximately 60 percent of these occur in frontal impacts. The next step to improve frontal impact protection further is to improve compatibility in vehicle-to-vehicle impacts. Much research has been performed to understand compatibility, which has identified three main influencing factors: structural interaction, frontal force matching and compartment strength.

Structural interaction is relevant for all frontal impacts and describes how well vehicles interact with their impact partner, either another vehicle or a roadside obstacle [2]. If the structural interaction is poor, the energy absorbing front structures of the vehicle may not function as efficiently as designed, leading to an increased risk of compartment intrusion at lower than designed impact severities and a less optimum (more back-loaded) compartment deceleration pulse. Also, 'triggering' of the restraint system may be less effective due to a less predictable crash pulse. Examples of poor structural interaction are override and the fork effect [2].

A vehicle's frontal force levels are related to its mass. In general, heavier vehicles have higher force levels as a result of the current test procedures and manufacturer's desire to keep crush space to a minimum [3]. As a consequence, in a collision between a light vehicle and a heavy vehicle, the light vehicle absorbs more than its share of the impact energy as it is unable to deform the heavier vehicle at the higher force level required. Matched frontal force levels would ensure that both vehicles absorb their share of the kinetic energy, which would reduce the risk of injury for the occupant in the lighter vehicle.

Compartment strength is an important factor for self-protection, especially for light vehicles. In the event where vehicle front structures do not absorb the impact energy as designed the compartment strength needs to be sufficiently high to ensure minimal compartment intrusion. Beyond this, there is scope for better optimisation of the car's deceleration pulse to minimise restraint induced deceleration injuries.

To assess a car's frontal impact performance, including its compatibility, an integrated set of test procedures is required. The set of test procedures should assess both the car's partner and self protection. To minimise the burden of change to industry the set of procedures should contain a minimum number of procedures which are based on current procedures as much as possible. Also, the procedures should be internationally harmonised to reduce the burden further. Above all, the procedures and associated performance limits should ensure that the current self protection levels are not decreased as good self protection is required for impacts with roadside obstacles. Indeed, if possible, for light vehicles they should be increased. The set of test procedures should contain both a full overlap test and an offset (partial overlap) test as recommended by the IHRA

frontal impact working group [4]. A full width test is required to provide a high deceleration pulse to control the occupant's deceleration and check that the vehicle's restraint system provides sufficient protection at high deceleration levels. An offset test is required to load one side of the vehicle to check compartment integrity, i.e. that the vehicle can absorb the impact energy in one side without significant compartment intrusion. The offset test also provides a softer deceleration pulse than the full width test, which checks that the restraint system provides good protection for a range of pulses and is not over-optimised to one pulse.

The European Enhanced Vehicle-safety Committee (EEVC) Working Group 15 is working to develop an integrated set of test procedures to assess a vehicle's frontal impact performance [5]. One of the main candidate procedures is the Full Width Deformable Barrier (FWDB) test, the development of which is being led by the UK. The other is the Progressive Deformable Barrier (PDB) test, led by France [6].

This paper describes an estimation of the benefit for the implementation of improved compatibility in Great Britain (GB) and the current status of the Full Width Deformable Barrier (FWDB) test

GB BENEFIT

The GB national accident data (STATS19), averaged for the years 1999 to 2003, shows that about 60% of the car occupant casualties occur in frontal impacts [Table 1].

Table 1.
Average casualties from RAGB 1999 to 2003
inclusive, front car occupants

First point of impact	Car Occupant Police Injury Severity	
	Fatal	Serious
Did not impact	29	328
Front	898	10055
Back	54	1200
Offside	257	1899
Nearside	252	1459
Total	1490	14941

Of these casualties about 70% occur in collisions with another vehicle, a collision type which compatibility directly addresses [Table 2].

Table 2.
Average casualties from RAGB 1999 to 2003
inclusive, front car occupants, front collisions

Number of Vehicles	Police Casualty Injury Severity	
	Fatal	Serious
Single vehicle	281	2823
1 other vehicle	415	5494
At least 2 other vehicles	202	1738
Total	898	10055

To determine the benefit of implementing improved compatibility both the national and in-depth accident databases were used. The in-depth data used were from the UK Co-operative Crash Injury Study (CCIS) collected from 1998 to 2006. CCIS is a sub-sample of the STATS19 database and can be weighted to describe national trends.

The methodology used to estimate the benefit was as follows:

- Divide occupants in STATS19 national accident database involved in frontal impacts into the following groups categorised by object struck.
 1. Another car
 2. A 'heavy' vehicle (e.g. Light Goods vehicle, Heavy goods vehicle)
 3. An object (roadside)
- Form equivalent data sets for CCIS in-depth data and estimate the benefit for each individual occupant.
- Scale STATS19 national accident data using benefit proportions calculated from CCIS data sets.

A total of 4,061 front seat occupants who experienced frontal impacts to their cars and whose injury information was known were selected for inclusion in the CCIS equivalent data sets. All the selected occupants were seated in cars registered in 1996 or later. 40% of the cars were registered after 2000.

Two distinct processes were used to determine the individual benefit for each occupant. Firstly, the nature and severity of damage that their car experienced was evaluated to determine if it is realistic for a future improved compatible vehicle to manage such a crash and offer improved occupant protection. This was achieved by determining if the occupant was included in the target population defined by the crash selection criteria shown in Table 3. If occupants were not in the target population, it was assumed that they would experience no benefit.

Table 3.
Target population selection criteria

Selection criteria	Cases included
Belt Restraint System Use	Only restrained occupants
Occupant Seating Position	Only front seat occupants
Overlap	> 20%
Principle Direction of Force	10, 11, 12, 1 and 2 o'clock
Accident severity (Estimated Test Speed)	All accidents up to 56 km/hr
Mass ratio	All mass ratios
Under-run	Exclude under-run cases for Larger Vehicles (Group 2)

Secondly, for occupants in the target population each injury experienced by each occupant was evaluated to decide whether the injury and associated mechanism would be mitigated by compatibility improvements to the frontal car structure. To do this two injury models were applied to estimate which injuries, if any, would be mitigated or removed from the database.

The models were constructed on the assumption that for frontal collisions up to a severity of 56 km/h ETS (approximately the severity of the EuroNCAP frontal impact test), improved compatibility should result in a car being able to absorb the impact energy in its frontal structure with minimal occupant compartment intrusion and an improved deceleration pulse with better restraint triggering. To represent minimal occupant compartment intrusion Model (1) {Intrusion based} removed all injuries caused by contact with an intruding internal front structure. To represent the improved deceleration pulse and restraint triggering as well, Model (2) {Contact based} removed all injuries caused by contact with any internal front structure, regardless if it had intruded or not. Model (1) produces a sub-set of the benefit seen in Model (2).

Using these injury reduction models the MAIS¹ for each occupant was re-calculated and compared with the original MAIS to estimate a benefit in terms of MAIS reduction as illustrated in Table 4 for the Group 1 equivalent data set (struck another car) for Model 1 {Intrusion based}.

¹ MAIS: Maximum Abbreviated Injury Score.

Table 4.
MAIS distribution for car-car (Group 1), before and after application of compatibility intrusion Model 1

MAIS	Original	Model (1)	
	CCIS Occupant Sample Group 1 No.	Occupants, assuming prevention of intrusion-caused injuries No.	Change
6	6	6	0
5	26	19	-7
4	31	31	0
3	126	97	-29
2	304	288	-16
1	1227	1251	+24
0	311	339	+28
Total	2031	2031	-

The distribution of AIS 3+ injury by body region is shown for the original data and after the application of the injury reduction models [Figure 1].

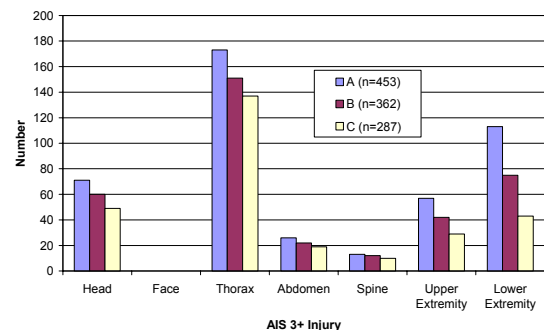


Figure 1. Distribution of AIS 3+ Injuries for original data and after application of injury reduction models.

This Figure illustrates the high frequency of thoracic injuries. Also illustrated is the fact that the compatibility benefit models do not significantly reduce this because the principal cause of injury to the thorax was found to be seat belt loads and not contact with the vehicle interior. This issue requires further investigation because thoracic injuries are known to be associated with fatal outcomes.

To convert the proportional benefit estimated using the CCIS database in terms of MAIS into the police

injury classifications of fatal and seriously injured a transfer function was developed. This was done by correlating the original MAIS 2+ distribution for all occupants within the target population against the casualties' injury outcome with respect to the police injury classifications to give a percentage risk of sustaining fatal or serious injury for a given MAIS [Table 5].

Table 5.
Derivation of transfer function between injury classifications

MAIS	Percent of Casualties (%)		Original number of casualties		
	Fatal	Serious	Total	Fatal	Serious
6	100	0	15	15	0
5	89.4	10.6	47	42	5
4	58.7	41.3	63	37	26
3	5.2	94.8	213	11	202
2	0.7	99.3	460	3	448
Total	-	-	798	108	681

Following this, the CCIS calculated proportional benefit, in terms of fatal and seriously injured, was scaled using the national accident data to give the benefit for GB. It was predicted that between approximately 5% (67) and 8% (124) front seat car occupants killed in GB would be saved and between 5% (732) and 13% (1876) of seriously injured casualties would be prevented if improved frontal impact compatibility were implemented.

The authors believe that this is a reasonable and conservative estimate of the benefit for the following reasons. Firstly, no account is made for the possible benefit that improved compatibility may give to side impact casualties. Secondly, the models do not account for any benefit for a reduction in the number of injuries to different body regions, if there are other injuries of the same severity that are not mitigated. For example, if a driver has sustained a fracture to his right femur (AIS score 3) due to contact with the intruding fascia and multiple rib fractures (AIS score 3) due to seat belt loading, only the femur fracture will be prevented in the model. Therefore, when the most severe injury is assessed, his overall injury severity remains the same. However, in contrast it is accepted that not all contact based injuries would in reality be mitigated. It is known that significant numbers of lower limb injuries result from contact with a car interior that has not intruded.

Another significant finding of the work was the high frequency of moderate (AIS2) and life threatening (AIS 3+) injuries sustained by car occupants due to seat belt induced loading. Also, the majority of

thoracic injury was not prevented by the injury reduction models. There is an argument that a more compatible vehicle would benefit from an improved crash pulse and therefore it would be expected to see lower seat belt loads and a reduced risk of thoracic injury. The injury models, by their design, did not account for injury attributed to seat belt loading, and therefore possibly underestimate the potential benefit that could be seen for this body region. This is an area which requires further work, as head and thoracic injuries are known to be associated with fatal outcomes.

In summary, the model finds significant benefits, and on balance can be argued to both over and under estimate injury reduction, dependant on the specific body region injured. A verification of the model was undertaken by reviewing individual crashes and evaluating the model's predicted benefits with respect to the actual crash characteristics.

FULL WIDTH DEFORMABLE BARRIER TEST

The Full Deformable Barrier (FWDB) test forms part of an integrated set of two procedures proposed to assess a car's frontal impact crash performance, including its compatibility:

FWDB test:

- (1) To assess structural interaction potential.
- (2) To provide a high deceleration pulse to test the restraint system.

Offset Deformable Barrier (ODB) test with EEVC barrier:

- (1) To assess frontal force levels.
- (2) To load one side of the car to check its compartment integrity.
- (3) To provide a softer deceleration pulse than the FWDB test to check the restraint system performs over a range of decelerations.

Originally the approach also included a high speed (80 km/h) ODB test to measure compartment strength using a Load Cell Wall (LCW). This test is not currently included in the approach because it is thought that adequate control of the compartment strength should be possible using a lower speed (e.g. regulatory or EuroNCAP) ODB test or the PDB test [6]. However, if an absolute measure of compartment strength is required then a high speed test will be necessary. This is because in the lower speed test the car may not be deformed sufficiently to load the compartment fully, so the LCW measure in these tests will only give an indication of the load the compartment has withstood in that test, which is not

necessarily the maximum load that the compartment can withstand. A high speed test ensures sufficient deformation of the car to load the compartment fully so that the LCW measure gives a true indication of the compartment strength.

The FWDB test is effectively a modification of the US FMVSS208 test, the modifications being the addition of a deformable element and a high resolution Load Cell Wall. The LCW consists of cells of nominal size 125 mm by 125 mm. The load cells are mounted 80 mm above ground level so that the division line between rows 3 and 4 is at a height of 455 mm which is approximately mid-point of the US part 581 bumper beam test zone² [Figure 2]. The reason that this particular height was chosen was to be able to detect whether vehicles had structures in alignment with the top and bottom halves of the Part 581 zone by examining the loads on rows 3 and 4 of the LCW. The intention is to enable the test procedure to be used to encourage all vehicles to have crashworthy structures in a common interaction zone that spans the part 581 zone. This should ensure structural interaction between high SUV type vehicles and cars as most cars have their main longitudinal structures in the Part 581 zone to meet the US bumper beam requirement.

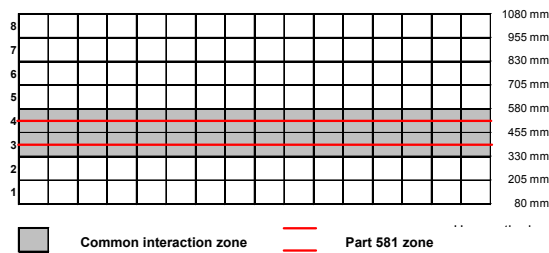


Figure 2. FWDB test LCW configuration showing row number and height above ground level.

The purpose of the deformable element has been discussed previously, [3], the main purpose being to improve detection of crossbeam structures which may not be strained in an impact with a rigid wall and to reduce engine dump loading that may otherwise confound the measured force distribution.

The intention of the FWDB test is to control both self and partner protection. For self protection the occupants deceleration and restraint system performance will be assessed using dummy measures in a similar way to the current FMVSS208 test. For

² Part 581 zone: Zone from 16” to 20” above ground established by NHTSA in its bumper standard (49 CFR 581) for passenger cars.

partner protection the car’s structural interaction potential will be assessed using the measures from the LCW. The premise is that cars that exhibit a more homogeneous force distribution on the LCW should have a better structural interaction. To assess the LCW force distribution a new Structural Interaction assessment criterion has been developed, which is described below.

Structural Interaction (SI) Criterion

The Structural Interaction (SI) criterion has been developed to resolve issues with the previous Homogeneity Criterion [3]. Its development was based on the following requirements:

- An ability to be applied in a stepwise manner to allow manufacturers to gradually adapt vehicle designs
- To encourage better horizontal force distribution (crossbeams).
- To encourage better vertical force distribution (multi-level load paths).
- To encourage a common interaction area with minimum load requirement.

The SI criterion is calculated from the peak cell loads recorded in the first 40 ms of the impact. Compared to using peak cell loads recorded throughout the duration of the impact (as with the previous Homogeneity Criterion), this has the advantage of assessing structural interaction at the beginning of the impact when it is more important and minimising the loading applied by structures further back into the vehicle such as the engine. The 40 ms time interval corresponds to a B-pillar displacement of approximately 550 mm for most cars [Figure 3].

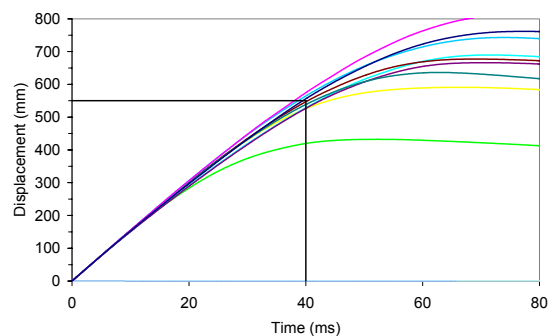


Figure 3. B-pillar displacement vs time plots for FWDB tests. Outlier is a supermini car with unique short stiff frontal structure which restricts its deformation.

Based on the assumption that structure which only crushes the 150 mm softer front layer of the barrier

will not apply sufficient load to the LCW to be adequately detected, this should allow the detection of structures up to 400 mm (550 mm -150 mm) from the front of the vehicle. This is adequate for detection of most Secondary Energy Absorbing Structures (SEAS), such as subframes, that interact with the partner vehicle in a crash. In addition, 400mm aligns with a recent NHTSA proposal to assess the Average Height of Force (AHOF) over the initial 400mm vehicle displacement.

To allow manufacturers to gradually adapt vehicle designs to become more compatible, the criterion consists of two parts which could be adopted in a stepwise manner. The first part assesses over a common interaction area (Area 1) which is from 330 mm to 580 mm above ground level and consists of LCW rows 3 and 4. The intention of this part of the assessment is to ensure that all vehicles have adequate structure in alignment with this area to ensure interaction. The second part assesses over a larger area (Area 2) which is from 205 mm to 705 mm above ground level and consists of LCW rows 2, 3, 4 and 5. The intention of this part of the assessment is to encourage cars to distribute their load more homogeneously over a larger area to reduce the likelihood of over/under-ride and the fork effect. However, further work is needed to ensure that the structural changes encouraged by this are not detrimental for side impact collisions. For example, although a strong shotgun type structure that extended to the front of the car should improve frontal impact compatibility performance it could be detrimental in side impact. If this was found to be the case, additional measures that limited the loads applied to specific areas of the LCW early in the impact may be needed to discourage this type of structure.

Each part of the SI criterion consists of two components, a vertical component (VSI) and a horizontal component (HSI). An outline of the steps to calculate these components for each part (Area 1 and Area 2) and the underlining concepts are described below. Further details of how to perform the calculations together with the supporting equations are given in the FWDB test and assessment protocol [7].

Vertical Component (VSI)

Area 1 (rows 3 & 4)

The intention of VSI Area 1 is to assess if the vehicle has structure capable of generating a minimum load within the common interaction zone. The calculation steps are:

- Determine row loads by summing the peak cell loads that occur before 40 msec.
- Set row load target. The current proposal is that this should be capped at 100 kN and mass dependent to ensure that lighter cars which cannot generate average loads of 100 kN are not unduly penalised.
- Determine negative deviation by summing the amount by which each row load fails to meet the row load target.
- VSI Area 1 is equivalent to the negative deviation.

Examination of the FWDB test data set available at TRL shows that a minimum row load requirement of 100 kN (i.e. target load of 100 kN with VSI area 1 score of 0) is a good indicator that vehicles have structure in alignment with rows 3 and 4, (the common interaction zone).

Area 2 (rows 2 to 5)

The intention of VSI Area 2 is to assess whether the vehicle has structure capable of generating a minimum row load within the larger assessment area and how evenly the load is applied vertically. The calculation steps are:

- Determine negative deviation for Area 2 in a similar way as for Area 1 above.
- Determine row load distribution using Coefficient of Variance.
- Determine VSI Area 2 by summing normalised values of negative deviation (minimum load) and Coefficient of Variance (load balance).

An example of how the VSI Area 2 distinguishes between vehicles is seen by examining the FWDB test data set in Figure 4. VSI Area 2 can correctly distinguish between two small family cars with different structures labelled 'small family 1' and 'small family 2'. 'Small family 1' was a multi-load path level design which showed better structural interaction performance in car to car tests compared to 'small family 2' which was a single load path design [8]. However, if a performance limit was set to distinguish between these cars, large SUV type vehicles may find it difficult to achieve because their design requires large approach angles which makes it difficult to design them to apply load to the lower part of the assessment area (row 2). Therefore, it may be necessary to have separate performance limits for large SUVs, but this should be avoided if possible.

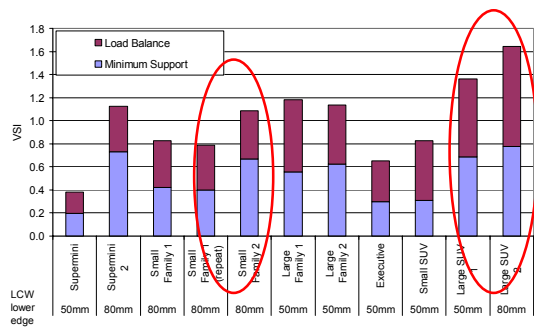


Figure 4. VSI Area 2 scores for VC-COMPAT FWDB test data set. (Note: lower score is better.)

Horizontal Component (HSI)

Area 1 and Area 2

The main intention of the HSI component is to encourage strong crossbeam structures to adequately distribute the rail loading in the assessed area. Also, because vehicle structural width has been seen to be a major influencing factor in vehicle to vehicle tests performed in the VC-COMPAT project [9], an option exists for the HSI component to be used to encourage wider structures for better structural interaction in lower overlap impacts. However, this part of the component is not currently included in the assessment and will not be included until it has been confirmed that wider structures have a significant benefit in real world accidents.

The calculation steps are:

1) For the crossbeam / rail strength balance part:

- Determine the peak cell loads that occur before 40 msec.
- Determine target cell load which is based on row load for each row. The target cell load is limited to a maximum [20kN], independent of vehicle mass. Crossbeams cannot apply loads greater than this to a cell without bottoming out the barrier because of the limit imposed by the crush strength of the barrier rear layer.
- Determine negative deviations from target cell load for centre 4 load cells in each row, sum and average. Note HSI Area 1 includes only rows 3 and 4 whereas HSI Area 2 includes rows 2, 3, 4 and 5.

2) For the structural width part: (currently not part of assessment but option for future)

- Determine negative deviations from target load for load cells aligned with outer structure in each row, sum and average.

At present the HSI is defined as the value of the crossbeam / rail strength balance as defined above. However, in the future the structural width part may be included in the HSI component.

Examination of the FWDB test data set shows that HSI Area 1 can correctly distinguish between two small family cars with different crossbeam structures labelled ‘small family 1’ and ‘small family 2’ in Figure 5. ‘Small family 2’ had a stronger crossbeam than ‘small family 1’ and showed better structural interaction performance in car to car tests [8].

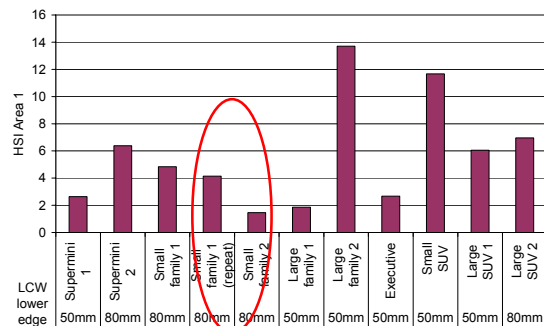


Figure 5. HSI Area 1 scores for VC-COMPAT FWDB test data set. (Note: lower score is better.)

HSI Area 1 also correctly ranks the bumper crossbeam strength correctly for a series of FWDB tests performed by ACEA with a large family car with different strength bumper crossbeams [Figure 6].

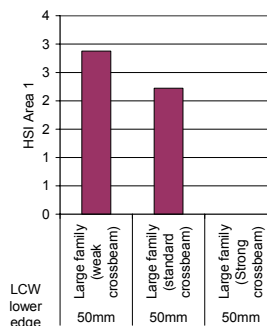


Figure 6. HSI Area 1 scores for FWDB tests performed by ACEA with large family car with different strength bumper crossbeams.

For implementation of the SI criterion the following two phases are proposed to allow manufacturers to gradually adapt vehicle designs to become more compatible:

- Phase 1 – the vertical and horizontal components of the criterion are applied over assessment area 1 to ensure that all vehicles have adequate structure in a common interaction zone.

- Phase 2 – in addition to the requirement of Phase 1, the vertical component of the criterion is applied over assessment area 2 to encourage vehicles to spread their load better vertically.

Repeatability

In the FWDB test the vehicle alignment with the Load Cell Wall (LCW) at the point of impact can vary from test to test, which can cause changes in the loads measured on the individual cells on the wall, which in turn can affect test repeatability. Change of the vehicle alignment with the wall can be caused by two factors. These are changes in the ride height of the vehicle and the test impact accuracy. It has been estimated that a vertical impact alignment tolerance of +/-10mm is required to achieve acceptable test repeatability with current vehicle designs that demonstrate poor compatibility. As the compatibility of vehicles improves and they spread their load more homogeneously over the LCW it should be possible to relax this tolerance.

Two tests within the +/-10mm impact alignment tolerance with a small family car were performed to assess repeatability. Also flat rigid plate impactor tests were performed to test the response of the deformable element and LCW to uniform loading.

For the car tests, the difference in the impact alignment was less than 1 mm in the vertical direction and 7 mm in the horizontal direction. The peak load cell wall (LCW) force was similar for the two tests, 549kN for the repeat test compared to 557kN for the first test. A difference in the B-Pillar displacement for the two tests resulted in a 22kJ difference in the absorbed energy [Figure 7]. However, in both tests the absorbed energy was within +/- 5% of the change in the vehicle kinetic energy. A +/- 5% difference, given the assumptions made when calculating the absorbed energy, was considered to be acceptable when considering energy balance.

The test results showed the majority of peak cell loads were within 5kN, whilst the row and column loads were within 10kN indicating good repeatability of the force measurement [Figure 10].

The Structural Interaction criterion difference was 4% for VSI Area 2 [Figure 4] and 15% for HSI Area 1 [Figure 5] indicating reasonable repeatability. Note car is labelled ‘small family 1’ in these figures.

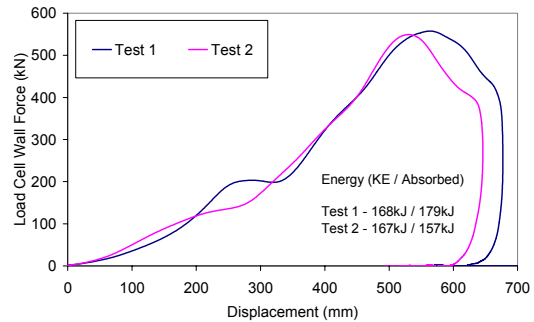


Figure 7. Load Cell Wall force against B pillar displacement for repeat tests with ‘small family 1’ car.

For the rigid impactor tests, an impactor (size 500 mm x 500 mm) was mounted on a sled, aligned with 16 load cells and impacted into the barrier as shown [Figure 8].

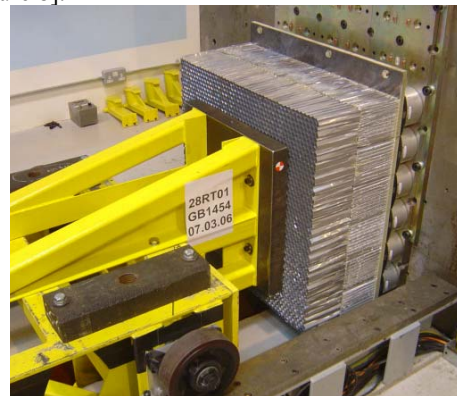


Figure 8. Sled test set-up, showing the sled, impactor face, deformable element and LCW.

The results of 2 tests showed that the LCW global force measurement was repeatable [Figure 9].

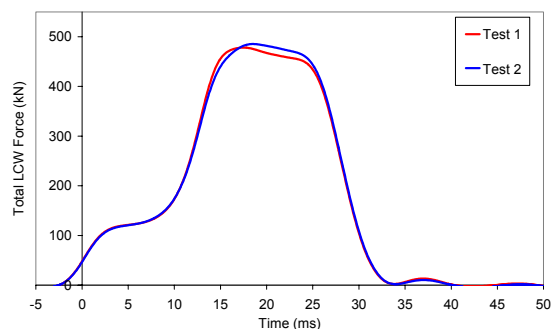


Figure 9. Comparison of total LCW force from sled tests showing good repeatability. (Note: Data filtered at CFC60 which causes non-zero load at time zero).

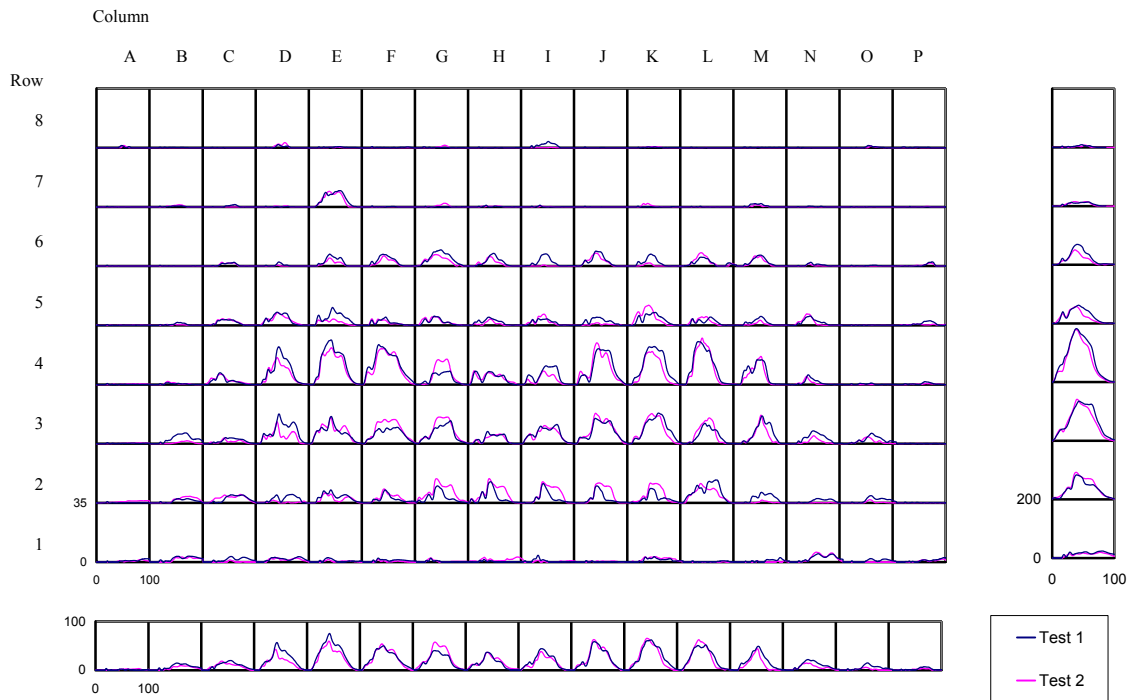


Figure 10. Load (scale 0 –35 kN) against time (scale 0-100ms) curves for complete Load Cell Wall for repeat tests with ‘small family 1’ car.

However, in both tests a greater than expected difference was observed between the peak cell loads recorded for the 16 load cells in alignment with the impactor [Figure 11].

Test2	A	B	C	D	E	F
3	2	3	4	5	2	1
4	0	26	27	28	26	1
5	3	31	29	30	29	4
6	1	27	28	35	28	0
7	0	28	28	30	31	0
8	2	2	0	1	2	0

Figure 11. Peak cell loads sled test 2. The shaded area indicates the cells which were in alignment with the impactor.

The reason for this is unclear and could be due to a number of factors, such as load spreading by the rear face of the barrier. However, differences of this magnitude should not substantially effect a vehicle’s Structural Interaction criterion score, as they are much smaller than the differences seen with a car structure. Even so, further work is recommended to identify the cause of them and ideally reduce them.

In summary, from the work performed to date test repeatability was found to be adequate. However, further work is recommended to check test repeatability with greater impact alignment differences and investigate the greater than expected cell load differences seen in tests with a flat rigid impactor.

WAY FORWARD

This section proposes a route map for the implementation of the FWDB set of tests into regulatory and/or consumer testing in Europe. It also outlines the main outstanding issues for compatibility, in particular for the FWDB test, and the work recommended to address them.

Route Map

A possible route map for the implementation of the FWDB set of tests in Europe is described below:

Step 0 – Use LCW to monitor force levels in ODB test

At present evidence exists that the frontal force levels of newer vehicles are increasing, especially for heavier vehicles, which could worsen the current compatibility problem. To monitor this situation, it is proposed that a LCW is introduced into current regulation and consumer ODB tests to measure vehicle frontal force levels. This information could be used to determine if vehicle frontal force levels are changing or not and help determine future priorities for compatibility.

Step 1 - Introduce FWDB test to improve self protection and structural interaction

As a first step to improve a car's self protection capability and structural interaction potential, it is proposed to introduce the FWDB test. There are a number of options for introducing this test depending on what level of structural interaction improvement it is decided to enforce.

Option 1

- Improve self protection by controlling occupant deceleration using enforcement of dummy measures similar to the US FMVSS208 test.
- Monitor structural interaction measures for research purposes.

Option 2

- Option 1 plus improvement of structural interaction by ensuring that all vehicles have adequate structure in a common interaction area using enforcement of the criteria VSI Area 1 and HSI Area 1 with appropriate performance limits.

Option 3

- Option 2 plus further improvement of structural interaction by ensuring that vehicles spread their

load better vertically using enforcement of the VSI Area 2 criteria with appropriate performance limits.

Step 2 - Improve frontal force matching

Currently, without further research it is difficult to determine precisely what this step may be. However, possible options at this point are:

Option 1

- Further improve self-protection by increasing test speed to 60 km/h for regulation as proposed by EEVC WG16. However, this option would not be acceptable unless measures could be taken to ensure this increased test severity would not increase the frontal force mismatch between light and heavy cars.
- Improve frontal force matching by controlling LCW force measured in ODB test.

Option 2

- Replace ODB test with PDB test and improve self protection and frontal force levels using measures as proposed in PDB approach.

Main Outstanding Issues

The main outstanding issues for compatibility, in particular for the FWDB test, and the work recommended to address them are:

Accident analysis

- Thoracic injury

In the GB benefit analysis it was observed that a high frequency of moderate (AIS2) and life threatening (AIS 3+) thoracic injuries were sustained by car occupants due to seat belt induced loading. The benefit models did not predict a significant reduction in these injuries. As thoracic injuries are known to be associated with fatal outcomes further work is recommended to understand more precisely the nature and cause of these injuries and their relationship to compatibility and its benefit. This work should consider the influence of improved restraint systems, in particular load limiters, on these injuries.

- Vehicle structural width

In laboratory testing a vehicle's structural width has been shown to have a large influence on its performance in vehicle to vehicle tests [9]. However, its relevance in real-world accidents is not known, so a decision whether or not tests should assess it cannot be made. Further accident analysis is recommended to answer this question.

FWDB test

Partner protection (LCW based measurements)

- Criteria and performance limits

A new criterion to assess a vehicle's structural interaction potential has been developed and shown to correctly rank different vehicles. Further work is recommended to validate the criterion and set performance limits. This work should include a test series to show that changing the vehicle to meet the performance requirement correlates to better performance in car to car impacts, which could then be used to help perform a benefit analysis for the introduction of this test procedure.

- Test repeatability / reproducibility

A limited number of tests to investigate repeatability have been performed to date, which found no significant problems. Further work is recommended to check the validity of this conclusion with different vehicle types and confirm the appropriateness of the proposed vertical impact alignment tolerance of +/- 10 mm.

In sled component tests using a flat rigid impactor, the load distribution measured on the LCW for cells in alignment with the impactor showed a greater variation than expected. Even though it was shown that this variation should not have a substantial effect on test repeatability it is recommended that further work is performed to understand why this variation occurred and ideally to minimise it.

Self-protection (Dummy based measures)

- Dummy

Work to determine the most appropriate dummy (THOR or HYBRIDIII), seating positions and size of dummy for inclusion in this test is recommended.

- Criteria and Performance limits

Further work is recommended to determine appropriate criteria and performance limits. However, if the HYBRIDIII dummy is used as in the current FMVSS208 test, then criteria and limits could be based on those in FMVSS 208.

ODB test

- Criterion

Work to complete the development of a criterion to control a vehicle's frontal force levels is recommended.

Cost Benefit

A cost benefit analysis for the implementation of the chosen procedures will be required.

ACKNOWLEDGEMENTS

The authors acknowledge the support of the UK Department of Transport DfT and the European Commission DG-TREN for funding this work.

This paper uses accident data from the United Kingdom's Co-operative Crash Injury Study (CCIS) collected during the period 1998 to 2006 (Phases 6 and 7).

Currently CCIS is managed by TRL Limited, on behalf of the United Kingdom's Department for Transport (DfT) (Transport Technology and Standards Division) who fund the project along with Autoliv, Ford Motor Company, Nissan Motor Company and Toyota Motor Europe. Previous sponsors include Daimler Chrysler, LAB, Rover Group Ltd, Visteon, Volvo Car Corporation, Daewoo Motor Company Ltd and Honda R&D Europe (UK) Ltd.

Data was collected by teams from the Birmingham Automotive Safety Centre of the University of Birmingham; the Vehicle Safety Research Centre at Loughborough University; TRL Limited and the Vehicle & Operator Services Agency (VOSA) of the DfT

Further information on CCIS can be found at <http://www.ukccis.org>

REFERENCES

1. Road Casualties Great Britain: 2005, DfT National Statistics, see <http://www.dft.gov.uk>
2. Edwards M, et al. (2001). 'The Essential Requirements for Compatible Cars in Frontal Impacts', 17th ESV conference, Amsterdam 2001.
3. Edwards M et al. (2003). 'Development of Test procedures and Performance Criteria to Improve Compatibility in Car Frontal Collisions', Paper No. 86, 18th ESV conference, Nagoya, 2003.
4. Lomonaco C and Gianotti E (2001). '5-years Status Report of the Advanced Offset Frontal Crash Protection', 17th ESV conference, Amsterdam, Netherlands, 2001.
5. Faerber E (2005). 'EEVC Approach to the Improvement of Crash Compatibility between Passenger Cars', 19th ESV conference, Washington DC, USA, 2005.

6. Delannoy P et al. 'Comparative Evaluation of Frontal Offset Tests to Control Self and Partner Protection', 19th ESV Conference, Washington 2005, Paper no 05-0010.
7. Full Width Deformable Barrier Test and Assessment Protocol, Version 1.9, August 2006.
8. Thomson R and Edwards M (2005). 'Passenger Vehicle Test Procedure Developments in the VC-COMPAT project', Paper No. 05-0008, 19th ESV conference, Washington DC, USA, 2005.
9. Thomson R et al (2006). 'Car-Car Compatibility: Development of Crash Test Procedures in the VC-COMPAT Project', Paper No. 2006-64, ICrash 2006 conference Athens, Greece, June 2006.

© Copyright TRL Limited 2007.

THE STUDY OF THE FRONTAL COMPATIBILITY WITH CONSIDERATION OF INTRERACTION AND STIFFNESS.

Takeo Mori

Toshiya Kudo

Naoya Kosaka

Harutoshi Motojima

Toyota Motor Corporation

Japan

Paper Number. 07-0105

ABSTRACT

To reduce the amount of casualties in traffic accidents that involve various types of vehicles, the improvement of compatibility performance is important. In case of accidents, there are mismatches between colliding vehicles, which are in structural geometry, vehicle frontal stiffness and so on. For improving compatibility, helping minimize these mismatch issues as the first step.

The concept investigated in this research study, has three aspects. The first one is “Multi load path including mechanical parts”. To ensure good interaction between colliding vehicles under existing mismatch of structure parts, it is effective to make use of mechanical parts as ‘a substitute’ load path, such as an engine with transmission or tire. The second is “To increase the amount of energy absorption (EA) of front body parts”. The third is “Sufficient stiffness of the passenger compartment”. To crush the front body parts for attaining additional EA, a proper stiffness of the passenger compartment is the prerequisite.

For improving compatibility, to satisfy above three items simultaneously is effective. According to the results of crash analysis, the concept for improving compatibility is investigated. Then structures applied for this concept are studied from the viewpoint of load flow and energy absorption, mainly by conducting CAE simulation. The improved structures were subsequently tested using actual vehicles for verification and the effectiveness of the concept is confirmed.

INTRODUCTION

In general, frontal crash performance of a vehicle is significantly affected by interaction and stiffness of frontal structures as already shown in previous publications. [1], [2]

In case of a crash between actual vehicles, crash members, like front rails, do not always have a good interaction with each other because of their mismatch in design layout. When crash members miss each other, not enough crash load for energy absorption is generated and could cause a severe deformation of the passenger compartment. Crash members, here, mean members that carry crash load and dissipate kinetic energy. The design concept to improve structural interaction was proposed in [3].

Vehicle frontal stiffness correlates mainly with the mass as shown in Figure 1. The stiffness is obtained from FRB (full overlap rigid barrier) test results, by supposing the kinetic energy is equal to the strain energy of linear stiffness structure. The tendency to increase with vehicle mass is influenced by the barrier test with constant speed, regardless of the vehicle mass. Considering these differences in stiffness, a lightweight, small car will suffer more severe damage in a collision with a large, heavy vehicle.

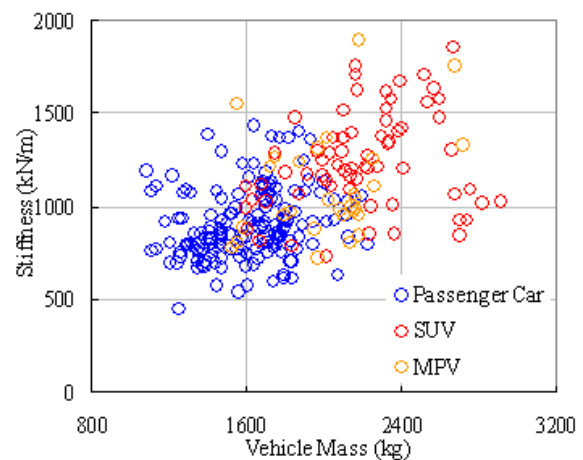


Figure1. Vehicle Mass and Frontal Stiffness.

(Source: US/JPN NCAP results & TMC inside tests)

To explain a crash phenomenon simply, momentum of a vehicle decreases by a reaction force that is generated in

the crash of both vehicles. This is shown in the equation 1:

$$\Delta m \cdot V = m \cdot V_o - m \cdot V_a = \int F dt \quad (1).$$

$\Delta m \cdot V$:Variation of momentum.

m : Mass of a vehicle.

V_o :Velocity before crash.

V_a : Velocity after crash.

F : Force generated during crash.

The reaction force is determined by a structural strength or inertia force of the vehicle. This force deforms the vehicle structures. The deformation continues until the kinetic energy of the vehicles is reduced to the final quantity that is determined according to physical law. In a crash event, the vehicles absorb the kinetic energy as deformation energy. This is shown in the equation 2:

$$\frac{1}{2} M_s \cdot V_s^2 + \frac{1}{2} M_l \cdot V_l^2 = \int_{small} F ds + \int_{large} F ds + E_r \quad (2).$$

M_s : Mass of a small car.

M_l : mass of a large vehicle.

V_s : Velocity of a small car.

V_l : Velocity of a large vehicle.

E_r : Remaining kinetic energy after crash, etc.

The deformation energy is determined by deforming force and length, in terms of their product. This means that the kinetic energy to be absorbed increases in proportion to the vehicle mass. Frontal crash compatibility of the heavier vehicle means to better balance the energy, i.e. absorb more energy. Compatibility of the small car means same stiffness to reduce vehicle deformation at higher crash load. For that purpose, an improved interaction is important.

Large deformation of a vehicle in a frontal crash can be caused by insufficient front-end energy absorption. When a vehicle, of 2070 kg mass crashes a car of 1160 kg mass with 50km/h closing speed, the total kinetic energy of both vehicles is 310 kJ. The vehicle run-out kinetic energy would be approximately 100 kJ. 210 kJ of the energy should be absorbed as strain energy of both vehicles, in case of a frontal offset crash. The energy should be absorbed before the cabin to help minimize the intrusion.

During ride-down, it is also important to control deceleration G for not to exceeding human tolerance levels. In general, the vehicle front should be designed as an energy absorbing area to absorb the energy effectively.

From the above, to improve compatibility, 1) Good interaction of crash members to generate crash load, 2) Adequate stiffness balance of energy absorbing area of both vehicles, 3) Cabin stiffness high enough to limit deformations to the front area, are seemed to be important. From this point of view, the study of improving the compatibility is conducted as follows.

ANALYSIS OF CRASH PHENOMENON

Analysis of crash phenomenon was carried out with crash tests between a small car and various large vehicles. There were 3 types of large vehicles, one is a large passenger car, the second was a SUV with frame structure (SUV-A), and the third was a SUV of unitized body (SUV-B). The weight of the large vehicles was about 2000 kg and that of the small car was ~1200 kg. Such the mass ratio was is in the range of 1.7. To represent a severe offset crash condition, the frontal offset tests were conducted with 50% overlap, at a closing speed of 55km/h each.

Vehicle deformation and crash load

The deformation of the small car was severe after the crash with the SUVs, especially in case of SUV-B. In case of the large passenger car, the deformation of the small car was much less as shown in Figure 2.



Crash to a Large Car.

Crash to SUV-B.

Figure 2. Deformation of a Small Car.

Comparison of the crash load is shown in Figure 3. Here, crash loads were calculated by multiplying vehicle deceleration G and mass. In Figure 3, the corresponding curves of the small car and the large vehicles that impacted each other are shown in the same color. The left

side of the figure shows curves of the large vehicles, and right side shows those of the small car. The load of the large passenger car (shown in green, left) is relatively low and its deformation is larger than the SUVs. Therefore, the deformation of the small car that crashes into SUV-B (shown in red, right) is larger than in the large passenger car's case.

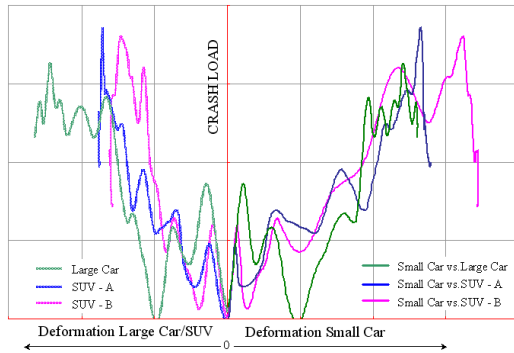


Figure 3. Comparison of Crash Load.

Energy absorption

Energy absorption ratio estimated from the load-deformation curve is shown in Figure 4.

In a crash between large passenger car and small car, the EA amount of the large car is larger than that of the small car. The compatibility of the large passenger car is very good. For the tests with SUVs, the EA amounts of both SUVs are smaller than that of a small car.

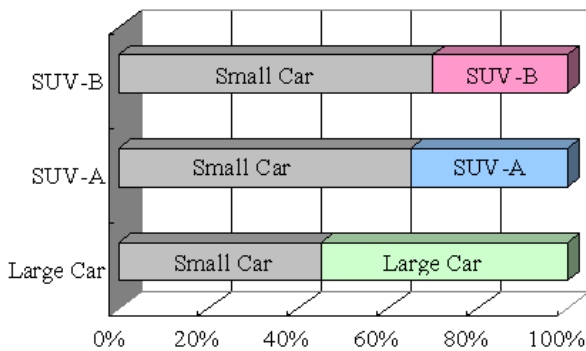


Figure 4. Ratio of the Energy Absorption.

The front body structures of the small car and the large passenger car were well deformed as shown in Figure 2 and Figure 5 left. On the other hand, the front body of the SUV was less deformed, shown in Figure 5 right, and it seemed that the EA amount of this section was not fully utilized. One of the reasons of less deformation is

due to the difference of frontal stiffness between small car and SUV. The structure of the small car that has lower stiffness deformed one-sidedly. Another reason may be due to the misalignment of crash members, resulting in reduced crash loads for energy absorption. One of the reasons is the difference in ground clearance of front rails between SUV and small car, of about 75mm. An aggressiveness of SUV was shown in previous study. [4]



Large car.

SUV-B.

Figure 5. Deformation of Large Car/SUV.

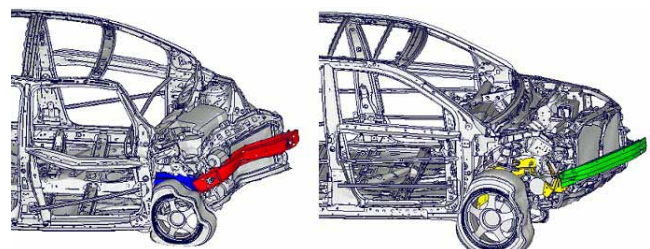
ANALYSIS BY CAE SIMULATION

To further comprehend the results of test analysis, a study using CAE simulation was conducted. The crash between small car and SUV-B was simulated, which represents the most severe case. The investigation was conducted from the viewpoint of interaction, load flow and energy absorption. The crash condition is given below:

- 50% Overlap, Closing speed each: 50 km/h,
- Mass : small car 1162 kg, SUV-B 2078 kg.

Vehicle deformation

The deformation of the small car was severe as predicted from above analysis. It extended into the cabin area. As for the SUV, its deformation was limited to the front end only.



Small car.

SUV-B.

Figure 6. Body Deformation in CAE simulation.

Crash load and interaction

A crash load is analyzed from the viewpoint of interaction. The load is classified in to three stages according to the characteristics,

First stage-Low load term from the beginning up to ~20 ms. Front-end structures hit each other. In this case, the interaction of front rails of both vehicles is not sufficient because of geometry mismatch.

Second stage-Load increasing term from 20 ms to 35 ms. Front structures are proceeding their deformation and starting to interact with opposite mechanical parts, like power train unit, tire and so on. With progressing interaction of these mechanical parts, the crash load increases drastically. The tires of both vehicles start to hit the opposite bumper beam. However, these interactions are not satisfying because of over-riding or bending of the beams.

Third stage-High load term from 35ms. Mechanical parts, such as tire and power train unit, are slightly deformed and pushed back, and some cabin structures become deformed.

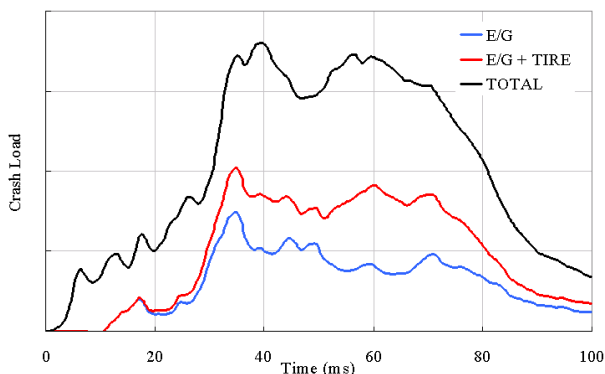


Figure 7. Crash Load – Time Curve.

Load Path

There are three load paths in this combination of the vehicle. The first one is the structural load path, mentioned in many papers. The second path is the power train path through the engine and transmission. The third path is the suspension path that consists of tire, wheel and suspension arms, etc. These paths are shown in Figure 8. The loads in the paths are changing during the crash, as described below. Only the load path of the small car will be mentioned here.

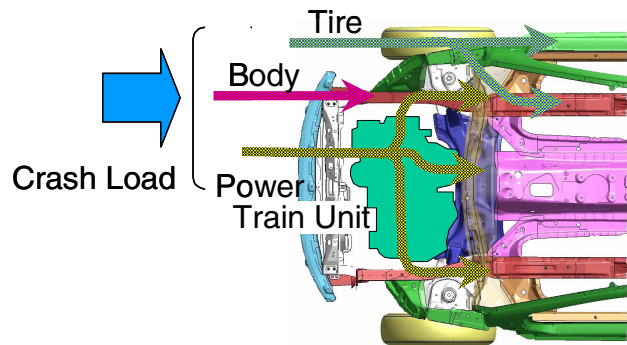


Figure 8. Load Path.

First stage - The structural load path is a main path at this stage. The front bumper beam hits the opposite structures and/or parts like the radiator, and generate a crash load. Crash load is translated to the front members. The load deforms these rails, and the load flows through cabin structures distributed to upper and under structures, shown in Figure 9. The bumper beam was not able to translate a satisfactory crash load to the front rail, because of its smaller cross section.

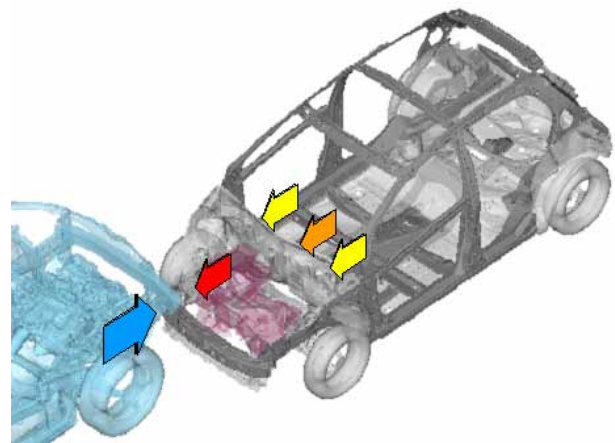


Figure 9. Load Path of the First Stage.

Second stage – In addition to the structural parts, mechanical parts e.g. tire, power train unit of both vehicles push each other through the crushed front-end structures. Load translation to cabin parts through body structures continues, and the load through a mechanical path is increasing rapidly. The load is translated to the rearward parts through mounting portion of the mechanical parts. At half of this stage, a tire impacts the opposite structures hard and the load through suspension is increasing. This load goes through suspension parts to under body structures. The load paths are shown in Figure 10.

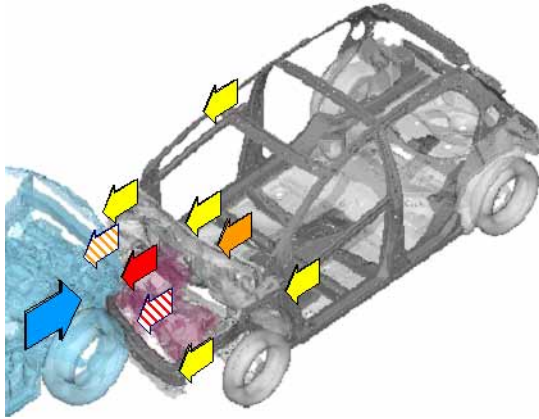


Figure 10. Load Path of the Second Stage.

Third stage - Mechanical path becomes a main path at this stage. After the deformation of the body has progressed, the tire starts to hit the side sill. The power train unit is pushed back into the dash panel and the sub frame. In this case, the bumper beam of the SUV hits the small car's strut. The load flow of the third stage is shown in Figure 11.

According to the above investigation, the mechanical load path should be considered to improve compatibility performance.

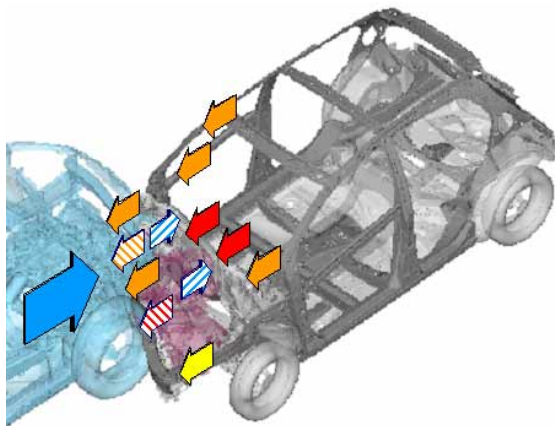


Figure 11. Load Path of Third Stage.

Crash Energy Absorption

As mentioned before, it is important to make a careful design of the energy absorption area. In other words, increasing the amount of energy absorption of front structures can help reduce the cabin intrusion in turn. Figure 12 shows the variation of strain energy per unit of time, absorbed by the parts of the small car. In this graph, the vertical axis is differentiation of EA amounts with respect to time and horizontal axis is time, so an area below the curve means EA amount of the parts. The blue

line means EA amount differentiation of front body parts, the red line means the sum of the differentiation of front body parts and that of cabin parts.

Front body parts start to absorb the energy from the beginning of the crash and continue to the third stage. As for the cabin parts, strain energy starts to be absorbed after 30 ms. In case of the small car in this study, some 70 % of the strain energy of body structures was shared by the front structures, and 30 % by the cabin structures. The EA amount of the small car cabin absorbed is 1.4 times as much as that of the cabin structures absorbed in an Euro NCAP 64km/h ODB crash. On the contrary, in case of the SUVs, most energy was absorbed by front structures only.

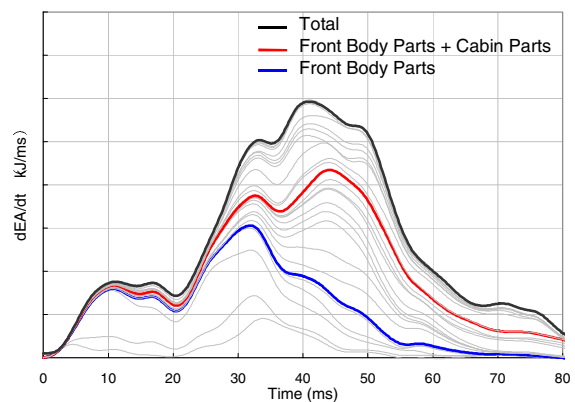


Figure 12. Energy Absorption History.

How to improve the Energy Absorption

It is important to crush the front structures effectively. For this purpose, it is needed to direct the crash load to energy absorbing parts, and to back up these parts from behind with stiffness higher than the actual crushing load. Requirement for the parts is shown below,

Front bumper beam - The cross beam should have a large area under load to transmit it to the front rails. This helps the front rail to deform well and as a result, it can absorb higher energy. Moreover, in case of a crash with misalignment in longitudinal members, a better interaction in lateral direction is expected, if the beam has enough stiffness. The effectiveness of a bumper beam is described in [5].

Front body structure parts - It is important to ensure a good balance in stiffness of each vehicle's front structures. To stiffen the cabin front area will allow deforming parts in the engine compartment, thus in turn maintaining the integrity of the cabin. In addition, it is

important to improve the front rail deformation mode as described in previous work. [6]

Mechanical Parts - The power train unit plays an important role in the load translation in the second and third stage of crash. The unit itself represents a rigid block, and could be rather considered as an interaction part. There is a possibility to make use of it as a load distributing part. Tire and suspension parts can also provide the same kind of function. By utilizing these mechanical parts, it seems possible to prevent weight increase for structural reinforcement. The effect of mechanical parts utilization is more effective, when the bumper beam stiffness is increased.

According to the above, subjects for improving energy absorption of the front structures are,

- 1) Direct crash load adequate to the members,
- 2) Enough supporting stiffness of front structures,
- 3) A tuned, progressive balance of frontal stiffness of each vehicle.

STUDY FOR IMPROVING STRUCTURES

Studied Structures

The concept for improving crash compatibility, described above, is checked by conducting a structural study using CAE simulation. Condition of the simulation is the same as mentioned before. Only the small car structures were modified, here. Modified parts are shown in blue color in Figure 13.

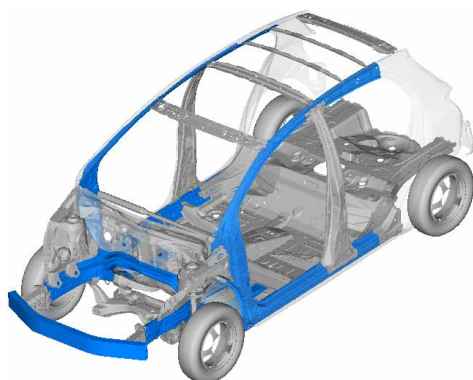


Figure 13. Modified Parts of the small car.

Items studied are listed below:

- 1) Increase the bending stiffness of bumper beam,
- 2) Optimize a deformation mode of front rail,
- 3) Increase the supporting stiffness of front rail,

- 4) Increase the cabin stiffness,
- 5) Stiffen the power train unit mounting.

Improvement of Crash Load and Interaction

Load curve of the modified structure is shown in Figure 14. In the first stage, no significant change has occurred in spite of increased bumper beam stiffness. Obviously, the reason is mismatch of the beams. On the contrary, there is a great increase of crash load in the second stage.

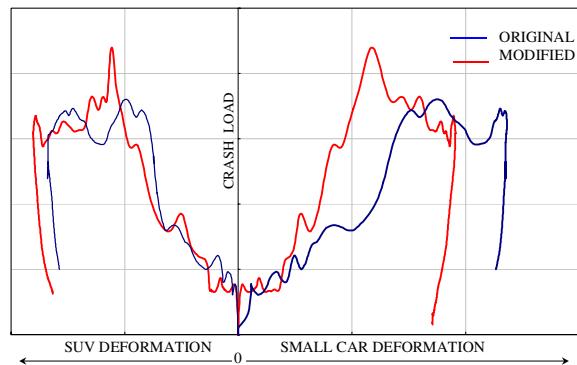


Figure 14. Comparison of Crash Load.

This is caused by the interaction improvement of the bumper beam. The beam kept its function during crash, and generates high load activating the opposite structure and hitting tire and power train unit, etc. Increase of the interaction force during the latter stage of crash is shown in Figure 15.

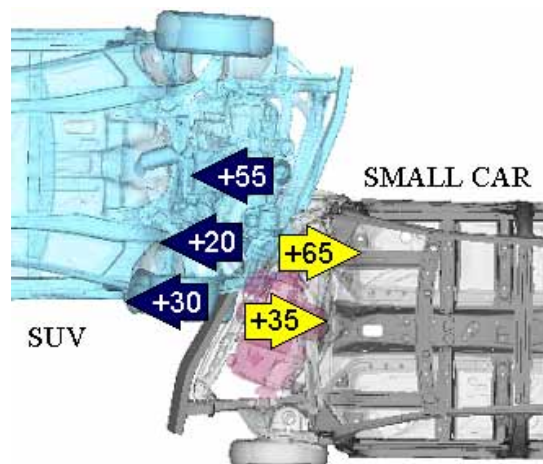


Figure 15. Increase of Interaction Force.

The bumper beam with increased stiffness works as a bridge among front rail, tire and power train unit, and increases the crash load significantly. To continue the crash load, supporting stiffness of the beam mainly pro-

vided by a front rail, is also important. The maximum load value increased about 20%. This seems caused by the higher cabin stiffness. The improvement of load flow mentioned above drastically decreased the cabin intrusion of the small car. Comparison of the body deformation is shown in figure 16. For the test conditions analyzed, the integrity of the cabin of the small car has greatly improved. Intrusion of toe-board and A-pillar is reduced to under the half. The deformation of the SUV, remained in the front body area. Though, it has somewhat increased, it is not significant because of the initial deformation was fairly small.

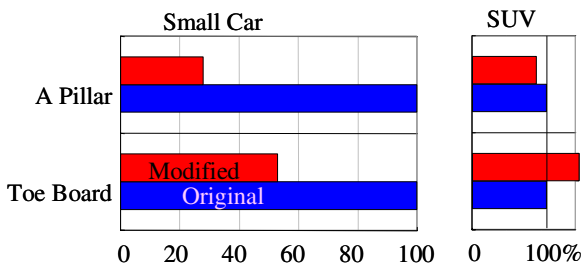


Figure 16. Comparison of Body Deformation.

Comparison of the energy absorption is shown in figure 17. The amount of energy absorption of only the small car cabin has decreased by nearly 10%, whereas the SUV has increased about 10% in total.

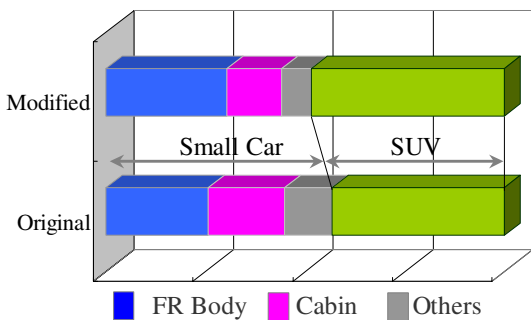


Figure 17. Comparison of Energy Absorption.

According to the above research, the concept to improve frontal compatibility is summarized below.

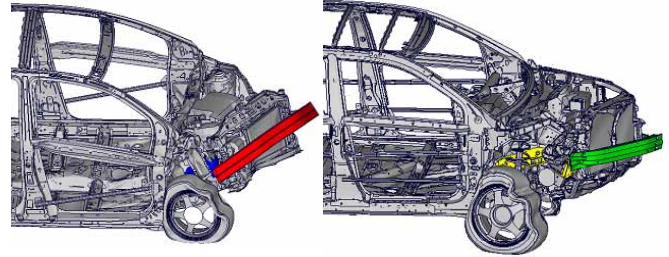
- 1) Improve the interaction. Not only structural interaction but also mechanical interaction should be considered. Especially, applying a bridging effect of the cross beam is necessary.
- 2) Balance the frontal stiffness of each vehicle. This makes it possible to adjust each energy absorption area more effectively.

- 3) Increase cabin stiffness of the small car. This is a requisite to crush vehicle front structures and, of course, contributes to the cabin integrity.

Small Car.

SUV.

Figure 18. Deformation of Studied Structure.



CONFIRMATION BY CRASH TEST

To confirm the above concept, a crash test was conducted using a modified car. The test condition is given below. It is the same as used in CAE simulation:

50% Overlap, Closing speed each: 50 km/h,

Mass: small car 1218kg, SUV 2078kg.

Only the small car was modified and almost the same like the structure studied in CAE investigation.

Crash Load and Interaction

Crash load estimated from deceleration and actual mass involved is shown in Fig-19. As well as the CAE result, the load of the second stage has increased significantly. Film analysis confirmed that this increase of the load is due to the improvement of bumper beam interaction.

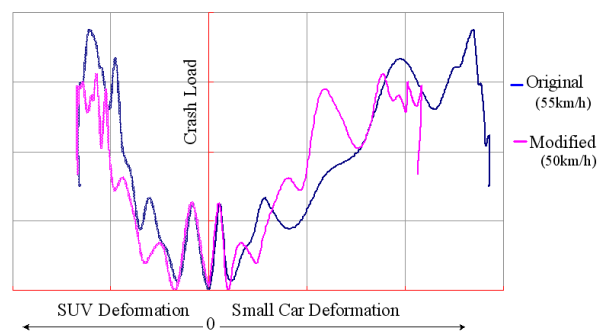


Figure 19. Comparison of the Crash Load Curve.

The bumper beam with improved stiffness had a good interaction with the other vehicle. The interaction among power train unit, tire, and bumper beam has proved to be effective in the earlier stage of the crash. It generated a

high load by hitting an opposite tire. To keep the beam from deforming away can make it possible to transmit additional load to the front rail during the crash.

Modified Structure. Original Structure.

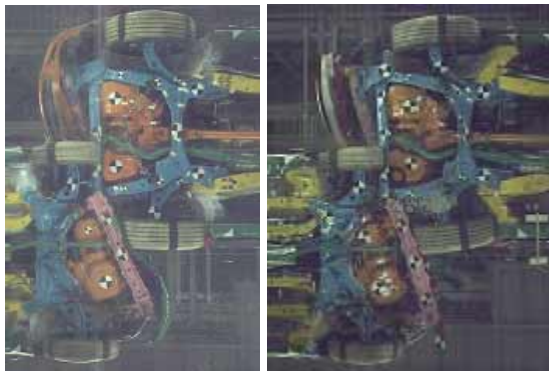
Figure 20. Bumper Deformation after Crash.



The higher stiffness of the supporting member of the power train unit helped to raise the overall front end stiffness. This might contribute to the improvement of mechanical interaction.

Modified structure. Original structure.

Figure 21. Interaction of Mechanical Parts.



VEHICLE DEFORMATION

The vehicle deformations are shown below.



Small Car.

SUV.

Figure 22. Deformation of the Vehicles (Side view).

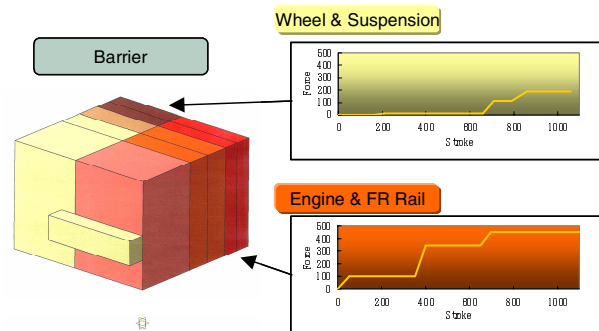
The front-end structure showed the expected deformation by generating high crash load in the middle stage of the crash. Both the intrusion of toe-board and A - pillar were satisfying the deformation target.

The above mentioned concept confirmed that it allows to improve frontal compatibility.

BARRIER FOR COMPATIBILITY EVALUATION

A barrier can be used for evaluation of compatibility in the vehicle development process. It is necessary to be representative of frontal stiffness of actual vehicles including its distribution both in width and height. The load paths of the frontal crash were composed of three parts, structure path, power train unit path and suspension path, as mentioned before. Of course, due to different stiffness, the reaction load from each path is different. Therefore, it seems to be reasonable that a barrier could have a stiffness distribution adjusted to represent actual vehicles. An example of barrier composition, which is basis of the above idea, is shown in Figure 23.

Figure 23. Barrier Composition.



The barrier concept is under investigation. It could be used to help develop compatible structures within TMC in the future.

CONCLUSION

To improve frontal compatibility, it is essential to properly define the energy absorption area of both vehicles. For the test conditions analyzed in this research, the concept below has proved to be reasonable:

1. A stiff cross beam at the bumper is effective to improve early interaction.
2. To improve the interaction, not only structural interaction but also the mechanical parts interaction should be considered.
3. A good balance of frontal stiffness of each vehicle is required for sufficient energy absorption in the front-end.
4. Proper stiffness of the cabin structure is prerequisite

for improving the energy absorption of the front structure.

The structure studied in this research is only analyzed under limited conditions. However the way of thinking is available for other crash conditions.

Improvement of crash safety performance is associated with weight increase in most cases. Of course, it is desirable to improve the performance without adding mass from the viewpoint of ecology. In view of this, to make use of the mechanical load path effectively is preferable.

REFERENCE

[1] Edward, M. et al. 2001. "The Essential Requirements for Compatible Cars in Frontal Collisions." ESV 2001 No.158.

[2] Zobel, R. and Schwarz, T. 2001. "Development of Criteria and Standards for Vehicle Compatibility." ESV 2001. No.140

[3] Saito, M. et al. 2003. "Innovative Body Structure for the Self-Protection of a Small Car in a Frontal Vehicle-To-Vehicle Crash." ESV 2003. No.239.

[4] Summers, S.M. et al. 2003. "NHTSA's Research Program for Vehicle Compatibility." ESV 2003. No.307

[5] Hasegawa, T. 2007. "Study of Vehicle-to-Vehicle Collision Performance which is based on a Balance of Front End Strength." SAE 2007. World Congress. 2007-01-1175.

[6] Schoeneburg, R. and Pankalla, H. 1998. "Implementation and Assessment of Measures for Compatible Crash Behavior Using the Aluminum Vehicle as an Example." ESV 1998. 98-S3-O-07.

EVALUATION OF STIFFNESS MATCHING CONCEPTS FOR VEHICLE SAFETY IMPROVEMENT

Krishnan Subramaniam

Mukul Verma

Rajesh Nagappala

Ronald Tedesco

Louis Carlin

General Motors Corporation, USA

Paper Number 07-0112

ABSTRACT

The concept of ‘stiffness mismatch’ between front structures of colliding vehicles has been viewed as one of the important factors in collision incompatibility in front-to-front crashes between vehicles of different size. Consequently, it has been hypothesized that ‘better matching’ of stiffness properties of the front structure of the colliding pair of vehicles may improve the safety of the occupants of the smaller vehicle in such crashes. However, since the front structures of automobiles are designed to meet the protection requirements for their occupants in various frontal impacts, any changes in these properties need to be evaluated for possible influence on all requirements of self-protection as well as of improved compatibility. This paper examines statistical data to estimate the portion of the vehicle front end that may be of significance in front-to-front collision compatibility. The structural properties of an LTV’s front structure were modified to reduce the force and energy levels during the front four hundred millimeters of its crush in order to bring its stiffness properties closer to that of a representative mid-sized car in the US fleet. Detailed studies were conducted for this modified LTV utilizing finite-element based simulations of frontal NCAP test as well as of frontal impact with a passenger car in a field-representative test configuration. Results of these studies show that changing the structural properties of the LTV to be closer to that of the passenger car may have negative consequences for the protection of the LTV occupants. Alternative scenarios for achieving the proper balance in vehicles’ structural properties to improve overall safety are proposed.

INTRODUCTION

Collision compatibility between vehicles of dissimilar sizes has been the subject of research by several investigators [1-3] in recent years. Statistics for such crashes in the US show that impacts between the front of a large vehicle to the side of a smaller vehicle account for a large part of the societal harm

in LTV-to-car crashes, followed in order of magnitude by that in front-to-front impacts between such vehicles. Several hypotheses have been presented in literature [4] regarding possible solutions for improving collision compatibility in front-to-front impacts and one of such proposals is that of ‘stiffness matching’ of the front structures of the colliding automobiles. But, since the front structure of an automobile is a nonlinear structure with speed- and time-dependent response characteristics, the definition of a ‘vehicle stiffness’ is not straightforward [5]. A recent proposal [6] of ‘stiffness matching’ has been to match the slope of a predefined initial portion of force-versus-displacement response of a vehicle (as measured in a US NCAP test of 35 mph impact into a rigid barrier) to a ‘medium range’ as a possible solution for improving compatibility in frontal impacts. Such a concept is examined in detail in this paper by modifying the front end structure of a larger vehicle and evaluating its self-protection as well as partner protection.

CONCEPT OF STIFFNESS MATCHING FOR FRONT STRUCTURES

Front structures of automobiles are designed to meet many different functional and operational requirements. Protection of the occupants in case of a crash is one such requirement and therefore, one of the primary structural functions is to efficiently dissipate the impact energy in the available crush distance and thereby minimize the injury potential to the occupants. The degree of crash protection is usually evaluated in tests specified by regulations (e.g. FMVSS) as well as by various consumer information programs (e.g. NCAP, IIHS tests) which consist of impacts into a fixed barrier at specified speeds.

For such test conditions, the pre-impact kinetic energy of the vehicle (‘impact energy’) is proportional to its mass. The post-impact kinetic

energy is zero (i.e., the vehicle comes to a stop). The impact energy is dissipated in deforming the vehicle (ignoring second order effects such as acoustic and thermal energies) and from mechanical principles, the mechanical work (which equals force times displacement) must equal the impact energy. Thus, the area under the force versus deformation curve for the vehicle must equal its impact energy which is proportional to the vehicle's mass.

To illustrate this, test results for several vehicles are shown in Figures 1 and 2 for US NCAP tests (frontal impact into a rigid barrier at 35 miles per hour). Figure 1 shows plots of measured forces on the barrier versus the vehicle displacement. Since the front end structure of each vehicle is usually optimized subject to the particular vehicle's constraints of that vehicle, no general observations regarding the vehicle properties can be made from such data alone.

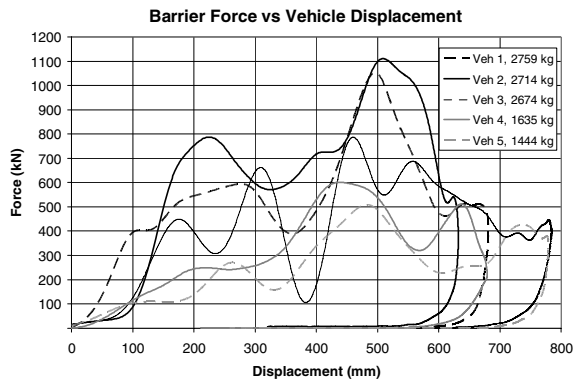


Figure 1: Force and Deflection Measurements in Frontal Impact Tests

Shown in figure 2 are calculated values of work (area under the force-deflection curve) for each vehicle.

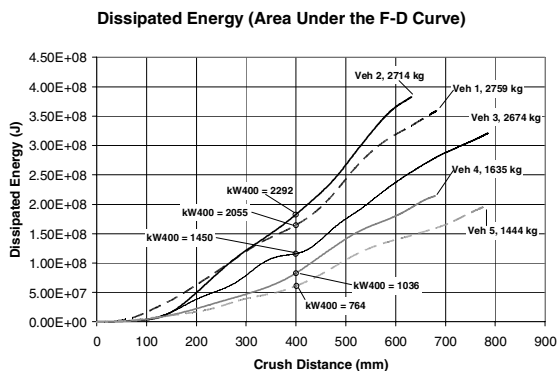


Figure 2: Relationship of Vehicle Mass and Total Work in Frontal Impact Tests

It is observed that, in accordance with the principles of mechanics, the area under each vehicle's curve (or

the mechanical work) is proportional to the mass of that vehicle [7]. Thus, the total area under the barrier force versus vehicle displacement plot is a property of the vehicle, is proportional to the vehicle's mass (assuming a fixed impact speed) and cannot be changed unless vehicle mass is changed.

We will now evaluate the impact of altering a specific portion of the force-versus-displacement property of a given vehicle. Since an automobile's front structure is usually optimized for its multiple functional and operational requirements and constraints, it can be hypothesized that isolated changes to alter specific portions of its force versus displacement property will render the front structure suboptimal in overall protection in frontal impacts.

It can also be hypothesized that if changes were made to reduce force levels in specific parts of the front structure, the consequence is likely to be an increase in force levels in the rest of the structure such that the total area under the curve remains constant. This is illustrated in figure 3 for force-displacement responses of two vehicles in US NCAP tests at 35 mph. Vehicle 1 has a larger mass than vehicle 2. If the front end of (the heavier) vehicle 1 were modified to lower its force levels to be similar to that of (the lighter) vehicle 2 over a distance 'd', the consequence

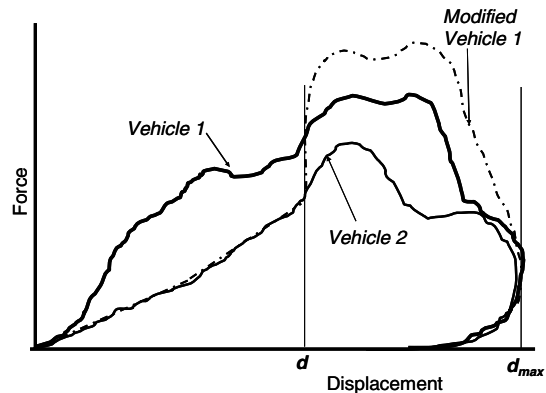


Figure 3: Concept of Stiffness Matching Between Vehicles of Different Sizes

will be that the structural force levels of vehicle 1 are higher for the rest of the crush (shown by dash lines) than that of the original vehicle 1.

This is an important consideration because concepts of 'stiffness matching' usually denote lowering the force levels in the earlier part of the crush of the heavier vehicle and as shown above, this is likely to cause higher force levels in the remaining portion of the front end of the heavier vehicle, so that the calculated work is the same in both cases.

The above reasoning is based on the assumption that available crush distance remains essentially unchanged as the vehicle's front end is altered for 'stiffness matching'. This is a valid assumption since the possibility of significantly increasing available crush space in a vehicle may not be feasible due to the following constraints:

- Increase in total crush distance by allowing higher values of d_{max} may imply more intrusion into the passenger compartment of the vehicle ;
- Increase in available crush distance by adding more length to the front of the vehicle requires additional structure and will increase the mass of the heavier vehicle more (leading to higher values of impact energy).

ANALYSIS OF STRUCTURAL CHANGES FOR STIFFNESS MATCHING

A detailed study was conducted for changes required to lower the frontal force levels (measured in a 35 mph front impact into a rigid barrier) of a light truck-based vehicle (LTV) in the first 400 mm of crush. One of the parameters used in this study is KW400 [6] which is defined as the stiffness of a hypothetical linear spring selected such that the work done by this spring over the first 400 mm of crush equals the energy dissipated by the vehicle in the same distance of crush in a 35 mph frontal impact into a rigid barrier (US NCAP test).

The LTV used for this study was approximately 2300 kilograms and its front end structure is modified so as to lower the value of KW400 for the LTV and bring it closer to that of a car (approximately 1650 kilograms). The consequence of such modification was evaluated by finite element simulation of the following impact conditions:

- LTV frontal impact into a rigid barrier at 35 mph;
- LTV impact into a compact size car with a ΔV of 35 mph in the car.

The first impact condition (LTV impact into a rigid barrier at 35 mph) is assumed for the purpose of this study to represent the self-protection of the LTV and the second case (LTV impact into a compact size car) is a measure of collision compatibility ('partner protection').

Shown in figure 4 is the front structure (shown without the engine) of a typical automobile and the complexity of such structures indicates that numerous changes need to be made in the geometric as well as in the material properties of multiple components to achieve the goal of lowering front 'stiffness'.

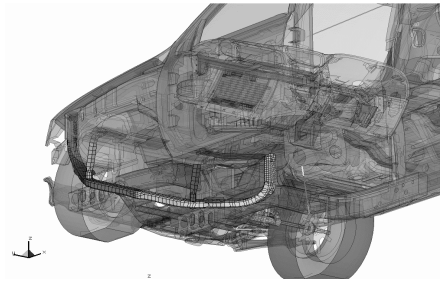


Figure 4: Front End Structure of a Vehicle

In this study, several iterations in LTV's structural design were necessary to achieve the above-mentioned goal of matching KW400. The effect of these iterations was to progressively lower the force levels in the front 400 mm of the vehicle. The total mass of the LTV changed only slightly during these iterations.

Results from the final iteration are shown in Figure 5 as barrier force-versus-vehicle displacement responses of the modified LTV structure, the baseline LTV and the car in 35 mph front barrier impacts. As expected from the discussion in figure 3 above, the effect of lowered forces in the first 400 mm of the crush space ('stiffness matching') is a significant increase in force levels in the rest of the vehicle structure. The implications of this on the protection of vehicle occupants are examined in the following sections.

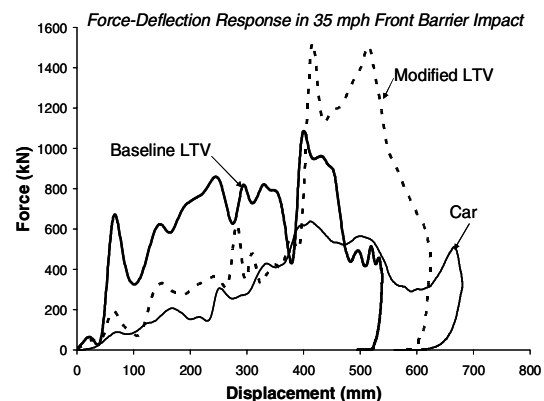


Figure 5: Force Deflection Response of Base LTV and Modified LTV

EFFECT ON OCCUPANT PROTECTION IN RIGID BARRIER IMPACTS

Results from finite element simulation of vehicle front impact into a rigid barrier at 35 mph are presented below for the baseline LTV, the modified LTV and the car.

Figure 6 is a plot of vehicle velocity as a function of time ('deceleration plot') for each of the vehicles. It is observed that when the LTV is modified to reduce the force levels in earlier part of the crush, the effect in the barrier test is to reduce the slope in the earlier part of the deceleration plot and increase the slope in the later part.

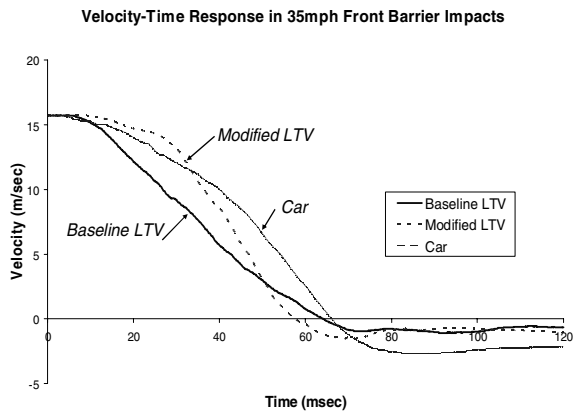


Figure 6: Velocity-Time Response of Base LTV and Modified LTV in 35mph US NCAP Test

One measure of this change is the 'effective deceleration' of the vehicle, defined as the slope of a linear approximation of a large portion of the deceleration plot. This is shown in figure 7 for the baseline LTV as well as for the modified LTV. The maximum effective deceleration in the baseline vehicle is approximately 30 g but this 'effective deceleration' increases to 54 g when the LTV is modified as mentioned above.

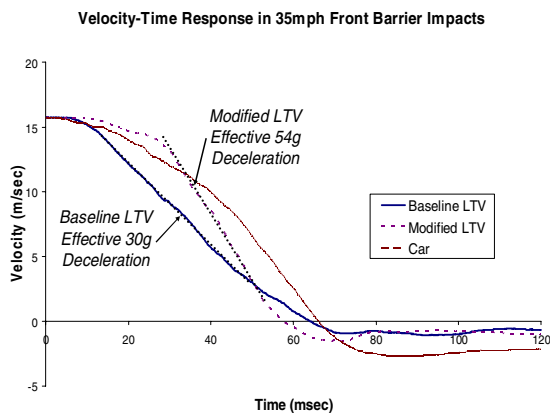


Figure 7: Maximum Effective Deceleration in 35 MPH Front Barrier Test

Figure 8 is a plot of the deceleration of the vehicles showing higher peak deceleration in the modified LTV (60 g) than in the baseline LTV (41 g).

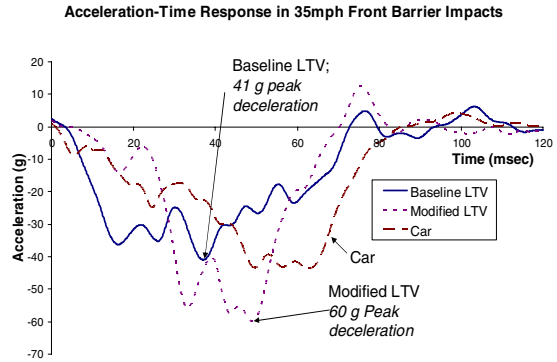


Figure 8: Deceleration Response in 35 mph Front Barrier Test

Similar conclusions are drawn from the calculated intrusions into the passenger compartment of the vehicles. As shown in figure 9, the calculated intrusions in the modified LTV (with lower KW400 value) are higher than those in the base LTV.

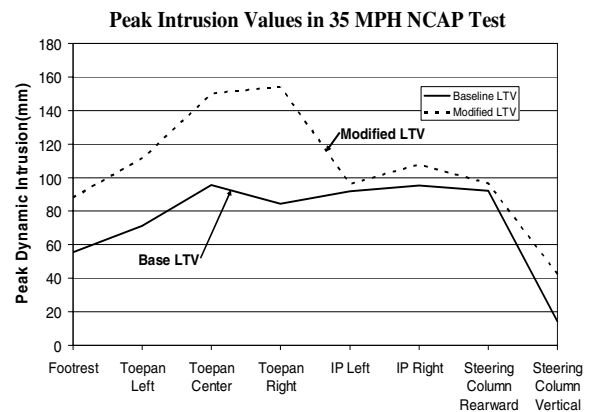


Figure 9: Peak Intrusion Values in 35 MPH Front Barrier Test

Further evaluation of the effect of these front structure changes in the LTV on the kinematics of the vehicle occupant was also obtained by finite element simulations. The driver was represented by a fiftieth percentile Hybrid III anthropomorphic test device, restrained by seatbelts and front airbag. The calculated decelerations of the head and the chest as obtained from the finite element model are shown in figure 10 and it is observed that these deceleration levels for driver ATD are higher in the modified LTV than in the base vehicle. The HIC (calculated from the head acceleration shown in Figure 10) for the driver ATD also increases from approximately 700 in the baseline LTV to about 1200 in the modified LTV.

It can therefore be summarized from the above results that force-reduction modifications to the

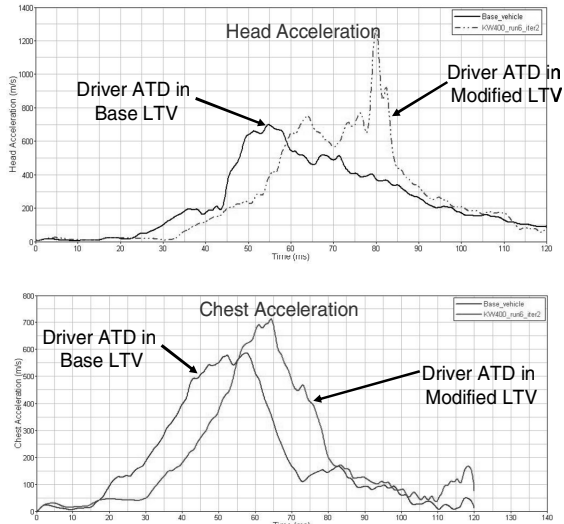


Figure 10: Estimated ATD response in Baseline LTV and Modified LTV

front structure of the LTV result in significant reduction in occupant protection in the 35 mph frontal crash. This is due to the modifications for stiffness matching reducing the front structure’s ability to dissipate the crash energy.

EFFECT ON OCCUPANT PROTECTION IN LTV-TO-CAR IMPACTS

The effect of stiffness matching on collision compatibility was also evaluated by simulating a frontal impact between the LTV and a passenger car of mass approximately 1650 kg. This was done by utilizing finite element models of both the LTV and the car in a full frontal collision with approximately

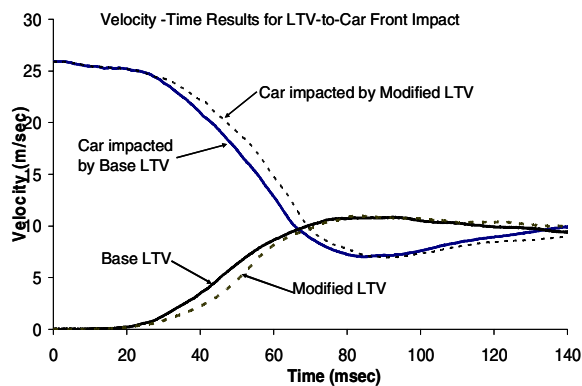


Figure 11: Velocity versus Time Plot for LTV-to-Car Impacts

35 mph change in velocity (ΔV) in the struck car. This simulation was conducted for the baseline LTV

as well for the modified LTV. The plot of vehicle velocities as functions of time is shown in Figure 11. The calculated responses in both the car and the LTVs are shown below.

Figure 12 is the plot of the deceleration in the vehicles. The result of modifying the front structure of the LTV to lower the force levels in the first 400 mm of its crush is observed to be insignificant in

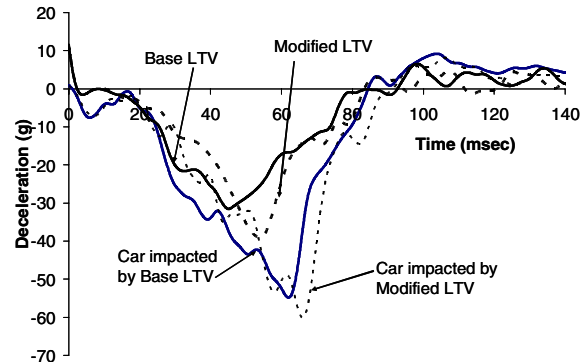


Figure 12: Deceleration versus Time Plot for LTV-to-Car Impacts

terms of the deceleration response of the vehicles because the small changes observed in the peak deceleration values are likely to be filtered by airbags and seatbelts and not likely to affect the response of the vehicle occupants.

The effect of modification in the front structure of the LTV is observed in Figure 13 which shows the calculated intrusion levels in the car when impacted by the baseline LTV and by the modified LTV. The reduction in force levels in front part of the LTV is shown to lead to reduced intrusions of the instrument panel and the steering column and slightly increased intrusions in the toe pan area.

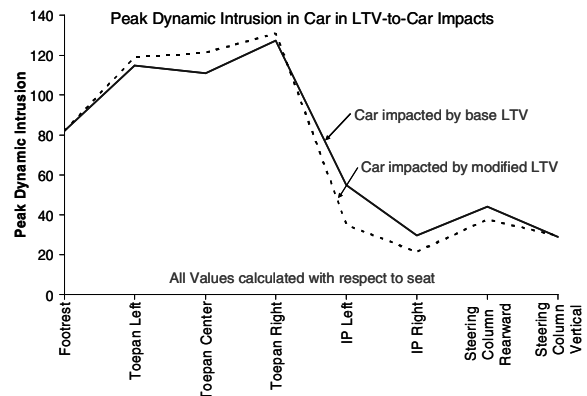


Figure 13: Peak Intrusion Values in Car in LTV-to-Car Impacts

CONCLUSIONS

The effect of modifying front structure of a heavier vehicle (an LTV in this case) has been examined for its self-protection (protection of its driver in 35 mph front crash against rigid barrier) as well as for collision compatibility (protection of driver of a smaller vehicle in front-to-front crash). The front structure of the LTV was modified to reduce its force levels in the first 400 mm of crush and thus to bring its 'stiffness' (KW400) to be closer to that of the lighter mass car.

The effect of such modifications is observed to be a significant increase in the modified LTV's deceleration levels as well as in the peak intrusion value in passenger compartment and in the calculated ATD response in the LTV in frontal impacts against a rigid barrier. All of these are indicative of reduced self-protection in the modified LTV. For the case of the car driver when the car is impacted by the modified LTV, it is observed that the modified LTV is likely to reduce the peak intrusions inside the car at the instrument panel and the steering column and increase these values in the toe pan area.

Thus, this study for a specific LTV and a specific passenger car shows that reducing force levels in front part of LTV structure may have benefits in compatibility but has significant reduction in self-protection. Further studies are needed to assess the effects for the national fleet and determine if such measures have any possibility of improving the safety of automobile occupants. However, a preliminary assessment of the fraction of LTV-to-car crashes where the above changes in LTV design may be beneficial may be made from the 1999-2005 NASS data (Figure 14) for front crashes.

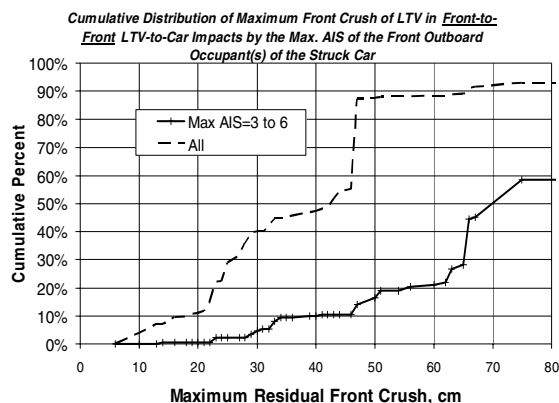


Figure 14: NASS Data on Maximum Residual Crush of LTV in LTV-to-Car Crashes

Figure 14 shows that 400 mm crush of the LTV corresponds to approximately 10% probability of injury levels of 3 to 6 in the struck car. It can therefore be hypothesized that softening the first 400 mm of the LTV front structure will affect only 10% of crashes.

As a recommendation, it is necessary that any proposed changes in automobile structures for 'stiffness matching' be evaluated for impact on protection of occupant in all types of crashes in the national automotive fleet before any decision is made regarding implementation.

ACKNOWLEDGEMENT

We are grateful to Mr. Sairam Peddi for his help and guidance during this study.

REFERENCES:

1. Backaitis, S. (editor), 'Vehicle Compatibility in Automotive Crashes', SAE Publication PT-102, 2005.
2. Barbat, S., 'Status of Enhanced Front-to-Front Vehicle Compatibility Technical Workgroup Research and Commitments', Paper 05-0463-O, 19th International ESV Conference, 2005.
3. Summers S., 'Recent NHTSA Compatibility Research – Repeatability Evaluations for Recent Compatibility Test Procedures', SAE Government Industry Meeting, 2005.
4. Takizawa S., Higuchi E., Iwabe T., Sugimoto T., Kisai T., Suzuki T., 'Evaluation of Test Procedures for Frontal Collision Compatibility', Paper 2001-01-1162, SAE Annual Congress, 2004.
5. Mostafa K., Digges K., Bahouth G., Morgan R., 'Vehicle Frontal Stiffness in a Front-to-Front Crash', Paper 2005-01-1375, SAE Annual Congress, 2005.
6. Smith D., 'NHTSA Compatibility Research Update', SAE Government Industry Meeting, 2006.
7. Verma M., Lange R., Lavelle J., 'Relationship of Crash Test Procedures to Vehicle Compatibility', Paper 2003-01-0900, SAE Annual Congress, 2003.

INVESTIGATION OF STRUCTURAL FACTORS INFLUENCING COMPATIBILITY IN VEHICLE-TO-VEHICLE SIDE IMPACTS

Satoshi Takizawa

Eisei Higuchi

Tatsuo Iwabe

Masahiko Emura

Honda R&D Co., Ltd.

Takayuki Kisai

Takayuki Suzuki

PSG Co., Ltd.

Japan

Paper Number 07-0180

ABSTRACT

The aim of this study is to identify how vehicle safety during side impacts may be enhanced by changes to the structures of bullet vehicles. Side impact tests being conducted around the world are focusing on the improvement of self-protection performance of target vehicles, based on existing vehicle fleets. However, the protection of occupants in the target vehicle is influenced both by the characteristics of the target vehicle and the characteristics of the bullet vehicle. Since test procedures for frontal impact compatibility are currently being planned, those that encourage homogeneity and good structural interaction among vehicles may also be beneficial for side impacts. Thus, it is necessary to investigate the design factors of the bullet vehicle in terms of side impact compatibility.

First, a study using FE simulation was carried out to develop an understanding of the major influencing factors relating to side impact compatibility. From this understanding, concept ideas for enhancing vehicle side impact compatibility were proposed. Second, FE simulation of a Full Width Deformable Barrier test was conducted with unmodified and modified vehicles to check that the test and assessment technique could correctly distinguish the improved performance of the modified vehicle. Finally, vehicle-to-vehicle tests using modified bullet vehicles were performed to demonstrate the principles identified in the FE simulation.

The results showed that the matching of geometry and stiffness in vehicle front-end structure contributes significantly to vehicle safety during side and frontal impacts.

INTRODUCTION

In recent years, front-to-front impact compatibility has been discussed by a wide variety of governments, researcher organizations and automakers. In the United States, the Enhancing Vehicle-to-Vehicle Crash Compatibility Technical Working Group (EVC TWG) has developed performance criteria to further enhance occupant protection in both front-to-front and front-to-side crashes. In front-to-front TWG, Phase 1

commitment was announced on December 3, 2003 as a first step towards improving geometrical compatibility⁽¹⁾. By production year 2006, approximately 75 % of applicable vehicle have been designed in accordance with the front-to-front criteria. In the recent Insurance Institute for Highway Safety (IIHS) study which measured the benefit from front-to-front compatibility as determined through the EVC Phase I Commitment, the simple geometric alignment prescribed in this Commitment has resulted in an impressive real world improvement in front-to-side compatibility⁽²⁾.

Side impact tests being conducted around the world are focusing on improving the self-protection performance of target vehicles, based on existing vehicle fleets. However, the protection of occupants in the target vehicle is influenced both by the characteristics of the target vehicle and of the bullet vehicle. There appears to be few published literature on the reduction of bullet vehicle aggressivity as a factor in side impact. Side impact compatibility can be considered the next subject to examine, to further reduce harm in side impacts. The National Highway Traffic Safety Administration (NHTSA) reported the issue of aggressivity in sport utility vehicles (SUV) and light trucks and vans (LTV) in their U.S. fleet. In side impacts, the drivers of the struck vehicles are much more likely to be killed than those in frontal impacts. In the U.S., the emphasis is on LTV-to-car impact compatibility, whereas car-to-car impact appears to take on significance in Europe and Japan. According to the NHTSA report, the driver in the struck passenger car is 8.2 times more likely to be killed as the driver in the striking passenger car⁽³⁾. Since test procedures for frontal impact compatibility are currently being developed, not only in the U.S., but in Europe and Japan as well, procedures that encourage good structural interaction and homogeneity among vehicles may also provide an opportunity to enhance side impact compatibility. Thus, investigation into the design factors of the bullet vehicle would be beneficial for both side impact and frontal impact compatibility.

In general, three different factors are relevant to impact compatibility; namely mass, stiffness and geometry. According to Hobbs et al., increased striking vehicle mass had little effect on struck vehicle driver injuries and front structure

homogeneity, rather than simple stiffness dominating the injury risk in side impacts (4), (5). IIHS reported that that front-end geometry was the most consistent factor influencing vehicle aggressivity (6). Regarding modification of vehicle front-end structures, several studies have been made on reducing the aggressivity of striking vehicles based on the basic understanding of relevant factors to side impact compatibility (7), (8). Better understanding of these design factors may present opportunities to reduce side impact harm, by modifying side structure and restraint systems, and by modifying front-end structures.

This paper reports on a study that was conducted to examine side impact compatibility and the factors influencing occupant injuries in side impact. Computer simulation was utilized to understand the factors influencing side impact compatibility. In addition, physical crash testing was performed to demonstrate the effect of a modification, obtained from the computer simulation, for the bullet vehicle. This paper attempts to contribute to a better understanding of side impact compatibility by means of observations gained through computer simulation and physical crash testing.

COMPARISON OF MDB-TO-CAR TEST AND CAR-TO-CAR TEST

New Car Assessment Program (NCAP) tests are currently being carried out to assess side impact occupant protection performance in various countries. In the NCAP testing, a Moving Deformable Barrier (MDB), which has an aluminum honeycomb component mimicking the front-end stiffness of vehicles, collides into the stationary target vehicle to assess dummy injury measures and target vehicle body deformation. However, the stiffness distribution of the MDB is generally more homogeneous than that of actual vehicles. Therefore, a MDB-to-Car test and a Car-to-Car test were carried out to identify the difference by comparing the body deformation and dummy injury measures. A small 5-door hatchback car, which performs well in ECE R95-type tests without side airbags, was selected as the target vehicle. A car with no side airbag was specified, as a side airbag is considered a supplemental restraint that could hinder improvement on what could be achieved with the structure of the bullet vehicle, likely complicating the interpretation of the research results.

Figure 1 shows the side impact test configuration in this study. The test configuration of the Euro-NCAP, where a bullet vehicle collides into the stationary target vehicle at a collision velocity of 50km/h, was chosen as the basis from which to compare the test results. In the MDB-to-Car test, the MDB, as specified by ECE -R95, collided into the small 5-door car, and in the Car-to-Car test, an identical small 5-door car was used as the bullet vehicle to compare to the MDB-to-Car test. The

EuroSID-2 dummy was used to measure the injury criteria. Body deformation and the dummy injury measures of the target vehicle were compared between the MDB-to-Car and Car-to-Car tests.

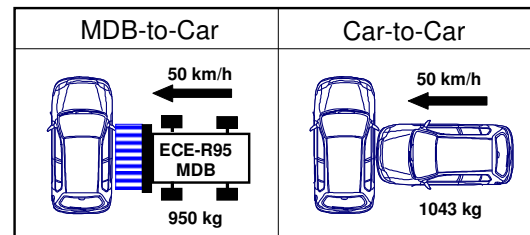


Figure 1. Side impact test configuration

Body Deformation

Body deformation of the target vehicle in the MDB-to-Car test and in the Car-to-Car test is shown in Figure 2. The stiffness distribution in the front-end of the bullet vehicle actually affects the deformation mode of the target car. There was localized deformation on the target vehicle that was aligned with the position of the bullet car's front side member in the Car-to-Car test, whereas relatively flat deformation was seen in the MDB-to-Car test.

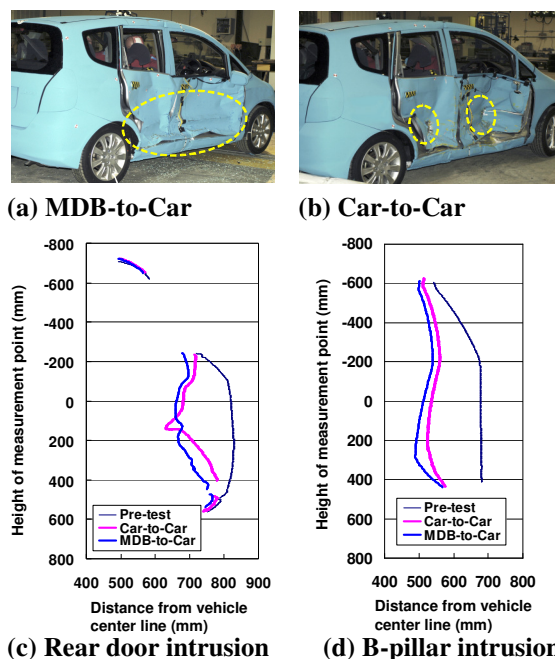


Figure 2. Comparison of body deformation

Dummy Response

Injury measures were normalized by the injury values of the MDB-to-Car test, and shown in Figure 3. Comparison of the driver dummy results from the MDB-to-Car and Car-to-Car tests showed that the injury values on the upper torso were almost similar between the two tests, whereas significant differences were seen for the pubic symphysis force, the driver's right femur load and

femur bending moment. The intrusion into the passenger compartment resulted in some higher driver dummy injury values, especially for the femur, which was aligned with the main bullet vehicle structure.

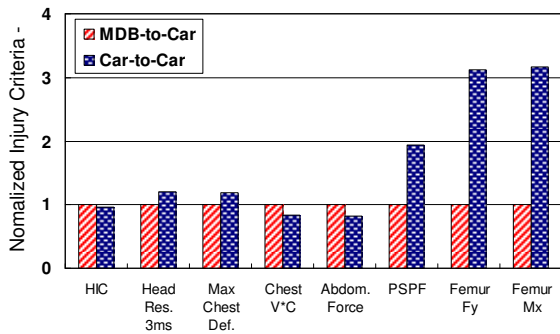


Figure 3. Comparison of injury measures

The overall levels of deformation indicated that the bullet vehicle's front structure was stiffer, relative to the target vehicle's side structure. The lack of deformation of the bullet vehicle's frontal structure showed that little energy was absorbed by the bullet vehicle in the impact, resulting in high levels of deformation of the target vehicle, as shown in Figure 4.



Figure 4. Comparison of bullet vehicle and MDB deformation

COMPUTER SIMULATION

The capability of improvements to side impact compatibility was investigated using an FE model. A parametric study was carried out using full-car finite element models that corresponded to the Car-to-Car test. The aim of this work was to aid our understanding of the effects of the bullet vehicle's structural characteristics that will enhance compatibility. To enhance side impact compatibility, the front-end of the bullet vehicle should effectively absorb impact energy to reduce the intrusion into the target vehicle. In this study, main energy-absorbing structures, e.g., front side members, bumper crossbeams, and sub-frames etc., were modified to enhance the side impact compatibility of the bullet vehicle. Originally, the baseline model, which is the same vehicle as that used in the Car-to-Car tests, did not have a sub-frame. In this study, a simple sub-frame extended to the vehicle front-end for the purpose of creating good structural interaction between the side sill of the target vehicle and front-end structure of the bullet vehicle has been designed for the FE analysis. The FE model of

the small 5-door car and EuroSID-2 dummy model used for this study are shown in Figure 5. The models were validated for a European side impact test and shown to give reasonable agreement (Figure 6).

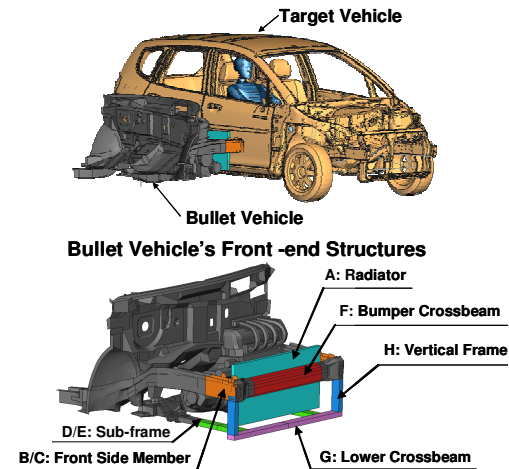


Figure 5. Full vehicle FE simulation model

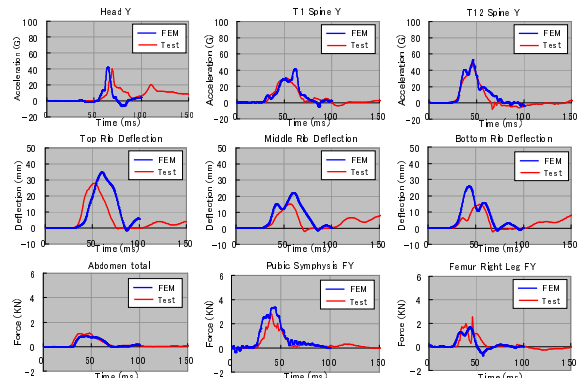


Figure 6. Comparison of FE simulation and crash test injury values

SIMULATION RESULTS

Orthogonal arrays were utilized for the matrix experiments in the design of experiments (DOE). Since there were five design variables and three levels, $L_{18} (2^1 \times 3^7)$ standard orthogonal arrays were selected for the frontal structures (Table 1).

Table 1. Orthogonal arrays of L_{18}

Discription	Levels	Simulation Run Number & Levels			~	18		
		1	2	3				
A Radiator	Strength	0.34 MPa 1	1.71 Mpa 2		1	1	1	2
B Front Side Member	Thickness	2.0 mm 1	1.5 mm 2	1.0 mm 3	1	1	1	3
C	Height	Baseline 1	+75 mm 2	+150 mm 3	1	2	3	3
D Sub-frame	Thickness	1.2 mm 1	0.8 mm 2	1.6 mm 3	1	2	3	2
E	Height	Baseline 1	+75 mm 2	-75 mm 3	1	2	3	1
F Bumper C/Beam	Thickness	1.0 mm 1	1.5 mm 2	2.0 mm 3	1	2	3	2
G Lower C/Beam	Thickness	1.2 mm 1	0.8 mm 2	1.6 mm 3	1	2	3	3
H Vertical Frame	Thickness	1.2 mm 1	0.8 mm 2	1.6 mm 3	1	2	3	1

Table 2.
FE simulation results

			Rib_Top	Rib_Mid	Rib_Bot	Abdomen	Pubic	Backplate	T12	Femur	T12	Femur	HIC
			Compression			Fy					Mx		
Radiator	Stronger	A											
Front Side Member	Stronger	B	↗	↗		↗	↗			↗		↗	↗
	Heigher	C	↗	↗	↗	↗	↗	↗		↗	↘	↗	↗
Sub-frame	Stronger	D	↘	↘	↘	↘				↘			
	Heigher	E									↗		↗
Bumper Cross Beam	Stronger	F			↗			↗				↘	
Lower Cross Beam	Stronger	G											
Verical Frame	Stronger	H											

After the row experiments were performed, design parameters were analyzed using analysis of variance (ANOVA) techniques. Effective design factors for the characteristic values, obtained from the ANOVA analysis, are summarized in Table 2. The significance level was set at 5 %, although lower levels are sometimes specified. Red arrows show significant factors, while also indicating a dummy injury response. The upward direction of the arrow means that the dummy injury value increases when the magnitude of each design factor enlarges, and vice versa. It was found from ANOVA that the radiator strength, side member thickness and height, sub-frame thickness and height, and bumper crossbeam thickness were dominant for each characteristic value, as shown in Table 2. It is seen that stiffening and raising the height of the front side member increases almost all of the injury parameters and stiffening the bumper crossbeam causes an even larger increase in the chest injury values. In contrast, stiffening the sub-frame reduces the injury value. These results can be explained by the load share between the load path into the door and the path into the floor. Stiffening the front side member directly increases the load through the door into the occupant and hence increases injury. In contrast, stiffening the sub-frame increases the load into the floor and decreases the load through the door into the occupant. Thus, it is reasonable to suppose that reducing the direct load into the occupant resulted in reducing the injury value. Hence, the load share between the two major load paths should be considered so as to enhance side impact compatibility.

Observation of Body Deformation

Influence on Front Side Member Strength and Height

Figure 7 shows the deformation modes of the side of the target vehicle and the front end structure of the bullet vehicle. In the stiffer side member model, little front side member deformation was identified. However, the weaker side member was more deformed and absorbed more impact energy, along with a reduction in the localized intrusion of the door.

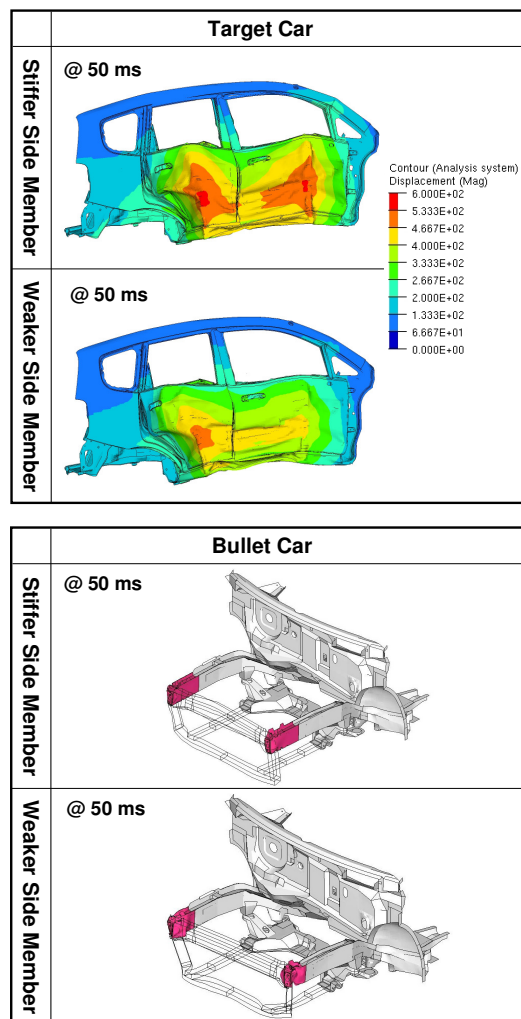


Figure 7. Deformation of side panel and front-end structure

Influence on Bumper Crossbeam Strength

In Car-to-Car frontal impact, stiff front structures, such as front side members, are more likely to penetrate into the weak structures of the struck vehicle (fork effect). It is said that the homogeneity of a crash force is an important factor in preventing the fork effect. The same thing may be said of side impact. Therefore, the horizontal homogeneity of front-end structures was

investigated by changing the stiffness of the bumper crossbeam of the vehicle equipped with a weaker bumper crossbeam (less homogeneous), which was then compared to the vehicle with a stiffer bumper crossbeam (more homogeneous).

Figure 8 shows the deformation modes of the side of the target vehicle and the front-end structure of the bullet vehicle. In the model equipped with the weaker bumper crossbeam, since the bumper crossbeam deformed greatly and pulled the front side member, a bending load was applied to the front-end of the front side member in addition to the compression load from the side structure of the target vehicle. Therefore, the front side member deformed inward. In the model equipped with the stiffer bumper crossbeam, the deformation of the bumper crossbeam was smaller than that of a weaker crossbeam. In such case, the load input from the B-pillar is transmitted to the front side member of the target vehicle as a compression load. The front side member crushed axially in response to the compression load.

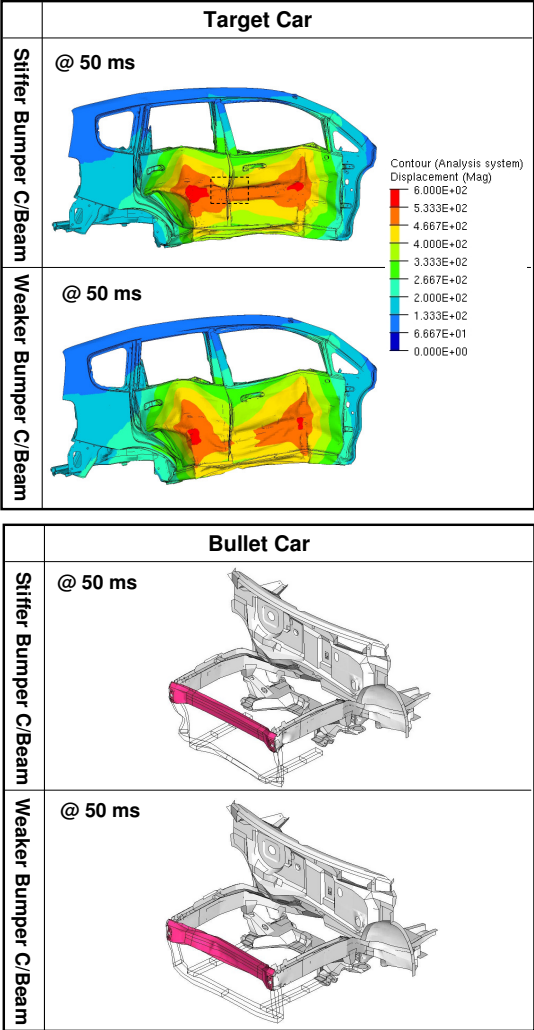


Figure 8. Deformation of side panel and front-end structure

The critical issue was that the deformation of the B-pillar increased as the stiffness of the bumper crossbeam became higher. Namely, although the deformation mode of the target car’s body side structure became uniform and prevented localized intrusion by the increased stiffness of the bumper crossbeam, the average deformation of the target vehicle increased due to a larger intrusion into the B-pillar of the target vehicle. Generally speaking, vehicles with a more homogeneous frontal stiffness will appear to avoid concentrated loading. A vehicle with a stiff homogeneous front may bridge the gap between the door and pillars. If the stiffness is lower, the bridging effect is lowered and loading through the door to the occupant increases. However, a stiffer bumper crossbeam would likely overload the B-pillar. Therefore, stiffness matching, in addition to structural interaction, is important in side impact compatibility.

Influence on Sub-frame Strength and Height

It is appropriate to consider the two load paths for side impact compatibility, which are the load path through the door into the occupant and through the vehicle’s side sill. A sub-frame achieves this by giving better structural engagement with the sill. When structural interaction between the side sill of the target vehicle and sub-frame of the bullet vehicle is possible, impact energy is absorbed further by these structures, which would thus enhance side impact compatibility.

Figure 9 shows the deformation of the body side structure of the target vehicle and of the front-end structure of the bullet vehicle. The weaker sub-frame was able to decrease the localized door intrusion because the crash force was directly transmitted from a sub-frame to a side sill with the side sill absorbing the impact energy. Equipping the model with a stiffer sub-frame further reduced dummy injury values. However, the larger intrusion into the bottom of the B-pillar was seen in the case of the stiffer sub-frame, which produced little deformation; deformation of the front side member was also minimal, compared to the weaker sub-frame. That is, less energy was absorbed by the target vehicle than by the model equipped with the weaker sub-frame. Since a stiffer sub-frame would likely overload to the side sill, which was the same effect produced in the stiffer bumper cross beam simulation, stiffness matching is an important factor in both side impact compatibility and structural interaction.

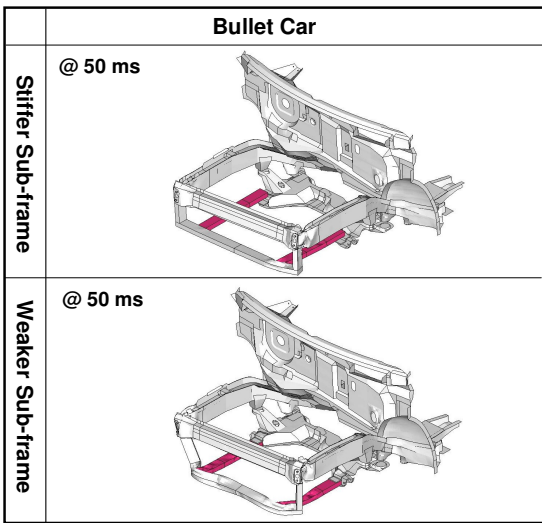
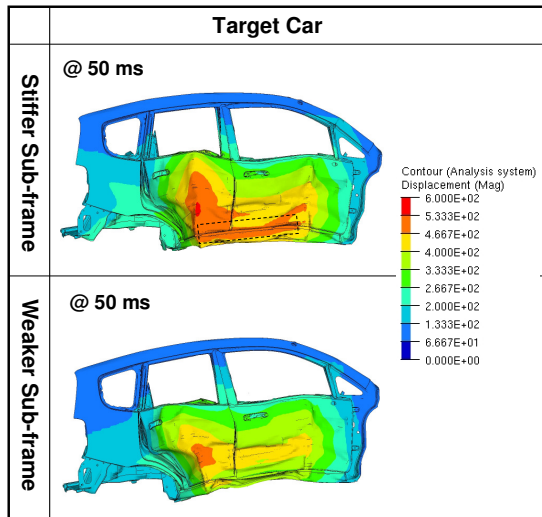


Figure 9. Deformation of side panel and front-end structure

From these simulation results, it is thought that in a Car-to-Car side impact, the structural interaction between vehicles has a big effect on the reduction of the body deformation. However, it is possible that if the stiffness of the sub-frame is greater than that of the floor of the target vehicle, the floor of the target vehicle deforms to a large extent and subsequently, the sub-frame may not effectively help protect the occupants. That is, the stiffness of the side sill and of the floor of the target vehicle should match with the stiffness of the sub-frame of the bullet vehicle for side impact compatibility.

OPTIMIZATION OF THE FRONT-END STRUCTURES

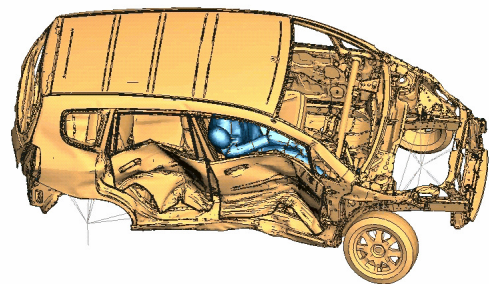
This study involves; modeling the Car-to-Car side impact using the finite element method and validating the modeling results with a Euro-SID2 dummy model, identifying influential parametric effects using DOE and ANOVA analysis and optimizing the identified influential parameters to

achieve better vehicle side impact compatibility performance. An optimized vehicle frontal structure was created by choosing the dominant factors of vehicle design obtained from ANOVA as is shown in Table 3.

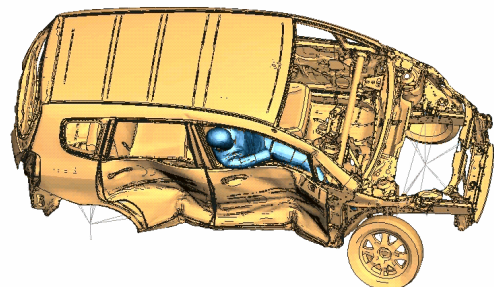
Table 3. Comparison of baseline model and optimal model

Discription		Baseline	Optimal
Radiator	Strength	0.34 Mpa	0.34 Mpa
Front Side Member	Thickness	2.0mm	1.0mm
	Height	Baseline	Baseline
Sub-frame	Thickness	Without Sub-frame	1.6mm
	Height	Without Sub-frame	-75mm
Bumper Crossbeam	Thickness	1.0mm	1.0mm
Lower Crossbeam	Thickness	Without Crossbeam	1.2mm
Vertcal Frame	Thickness	Without V-Frame	1.2mm

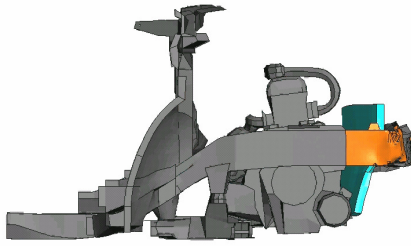
Figure 10 shows the deformation mode of the side of the target vehicle and front-end structure of the bullet vehicle. The Optimal Model was equipped with the stiffer sub-frame that was positioned -75 mm lower than that on the Baseline Model. Therefore, the Vertical Frame impacted the side sill, enabling the localized deformation in the sill to be identified. In this study, this sub-frame gave the better dummy injury values compared to the Baseline Model. However, generally the height of the sub-frame in alignment with the sill would provide better performance in terms of energy absorption



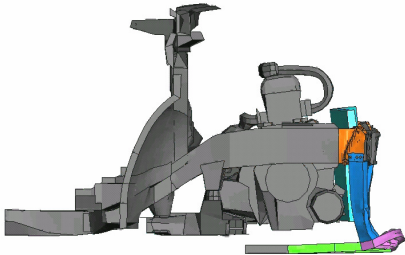
(a) Baseline target car



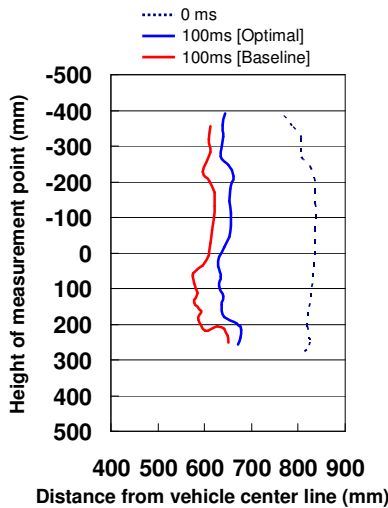
(b) Optimal target car



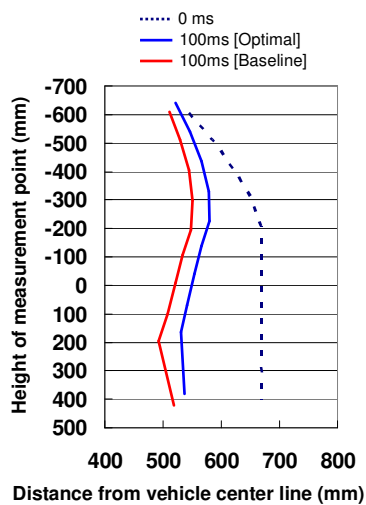
(c) Baseline bullet car



(d) Optimal bullet car



(e) Front door intrusion



(f) B-pillar intrusion

Figure 10. Comparison of modified Car-to-Car test and Baseline Car-to-Car test in FE simulation

Figure 11 compares injury values between the optimized and original target car. The modification of the front-end depicted in Fig. 10 was meant to improve the structural interaction and as such reduce intrusions. The results indicate that almost all of the injury values were reduced significantly. The reduction of intrusion can be clearly seen in Fig. 10, which shows deformed configurations for the target vehicle.

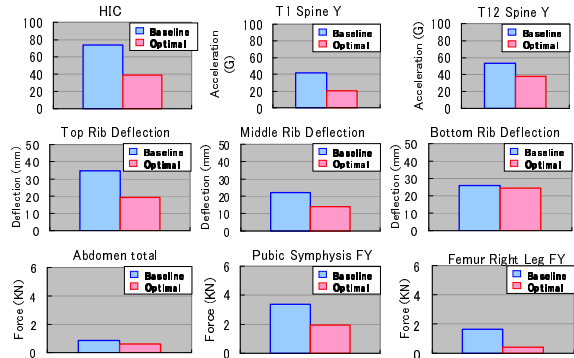
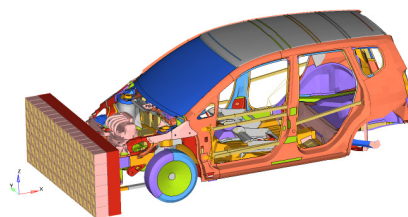


Figure 11. Comparison of injury values

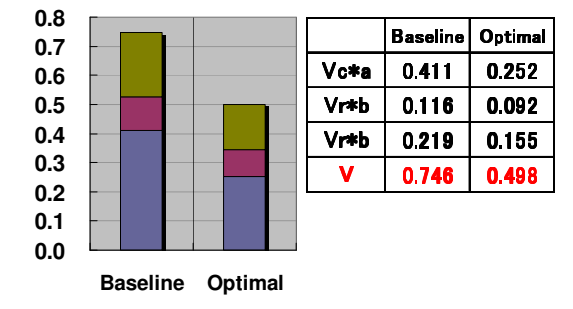
OPTIMIZED STRUCTURE IN FRONTAL IMPACT

FE Analysis

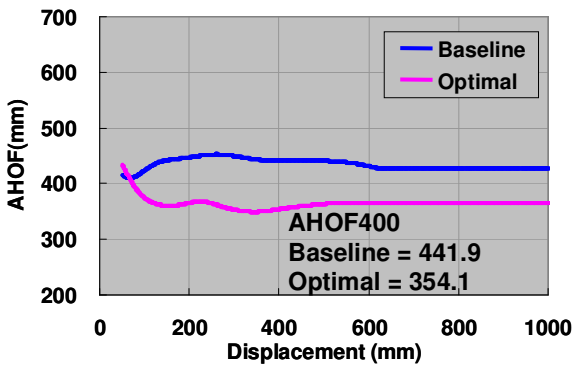
The effect of optimized structure in FE analysis, which was found to enhance compatibility in side impact, was studied in terms of frontal impact compatibility. The Full Width Deformable Barrier (FWDB) test, proposed by Transport Research Laboratory (TRL), was used to compare the compatibility metric in frontal impact at an impact velocity of 56 km/h. The compatibility metrics used for FWDB test simulation were Relative Homogeneity Criteria (RHC) and Average Height of Force (AHOF), which are calculated from load cell wall data^{(9), (10)}. RHC and AHOF were compared between the Optimized Model and Baseline Model (Figure 12). The RHC for the Optimized Model indicated a lower RHC value than that of the Baseline Model, which means that the Optimized Model has more homogeneous force distribution in its front-end structure. As for AHOF, the Optimized structure lowered the AHOF400 by 87.8 mm, compared to the Baseline Model. These simulation results indicate that the metrics for frontal impact compatibility can discriminate the difference between the Optimal and Baseline models.



(a) Full Width Deformable Barrier test simulation



(b) Relative Homogeneity Criteria

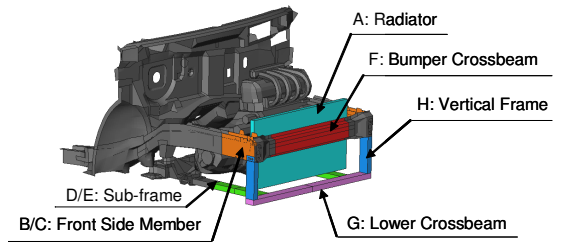


(c) Average Height Of Force

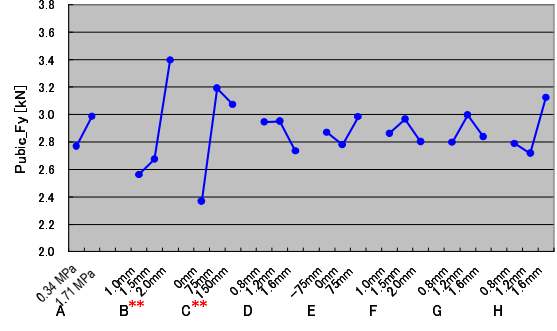
Figure 12. Comparison of frontal compatibility metrics in FWDB test simulation

MODIFIED VEHICLE-TO-VEHICLE CRASH TEST

In the Baseline Car-to-Car test, the intrusion into the passenger compartment resulted in some higher pelvis and femur injury values, which were similar to those in the main bullet vehicle structure. In the FE analysis, the influence on those main structures was investigated in an effort to reduce injury values for the pelvis and femur. Figure 13 shows the variation in injury values between the pelvis and femur. These graphs indicate that the stiffness of the front side member was the most significant factor.

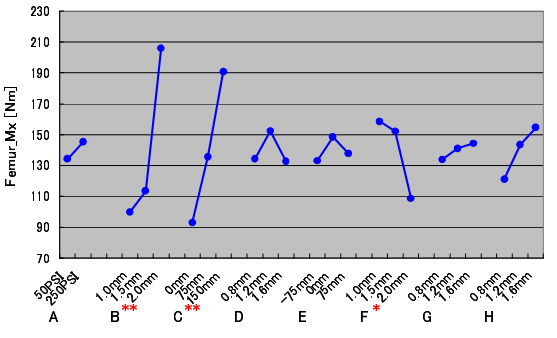


(a) Structural factors



Significant factors
B: Front Side Member Thickness
C: Front Side Member Height

(b) Influence on pubic symphysis force



Significant Factors
B: Front Side Member Thickness
C: Front Side Member Height
F: Bumper Crossbeam Thickness

(c) Influence on femur moment

Figure 13. Influence on each design factor

Since modification of the front side member significantly reduced the pelvis and femur injury values in FE analysis, a physical Car-to-Car test was performed. The modified Car-to-Car test aims to demonstrate the principles behind improved side impact compatibility, as identified in the FE simulation of this study, by modifying existing structures on the bullet vehicle. The results from tests with the modified bullet vehicle were compared to the results from the Baseline Car-to-Car test to demonstrate how the modifications affected the target vehicle's performance. A reduction in the crush strength of the front side member to prevent localized loading of the target vehicle was implemented to increase the amount of energy absorbed by the bullet vehicle in the impact. The modifications to the front section of the front side members were designed as the result of computer simulations, which indicated the optimum target vehicle performance could be achieved by reducing the thickness of the steel in the front side member from 2 to 1 mm. The modified section was approximately 250 mm in length, 100 mm high, excluding flanges, and 50 mm wide. The addition of a strengthened bumper cross beam was not implemented as the simulation work

indicated that this would likely overload the B-pillar. The modified section of the front of the lower rails is shown in Fig. 14. The reparability issue associated with low speed impacts is not our present concern.



Figure 14. Modification of front side member for Car-to-Car test

Dummy Injury Measures

Comparison of the driver dummy’s results from Modified Car-to-Car test with the Baseline Car-to-Car test showed that there were only slight differences in the chest injury levels. However, the most significant difference between the two tests was the force of impact on the pubic symphysis, which was approximately 60 % lower in the modified car. Comparison of the additional dummy injury parameters showed that there was a significant reduction in femur load and bending moment in the modified car, compared to those in the Baseline Car-to-Car test.

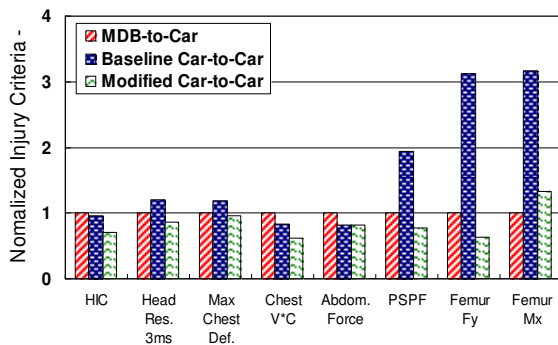


Figure 15. Comparison of injury measures

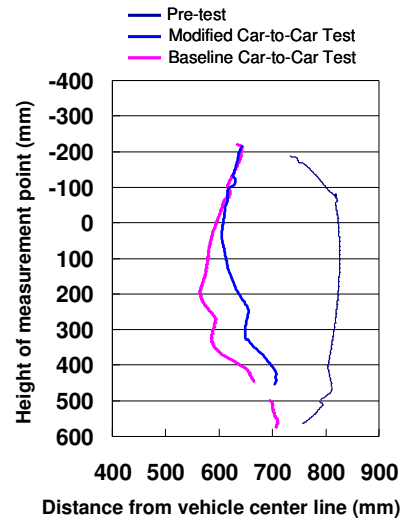
Body Deformation

A comparison of the deformation of the target cars from the Modified Car-to-Car test and Baseline Car-to-Car test is shown in Fig. 16. It can be seen that there was a significant difference in the deformation between the two test cars. The localized intrusion of the target car in alignment with the bullet vehicle’s front side member was significantly reduced in the test with the modified bullet car. The B-pillar intrusion of the target car in

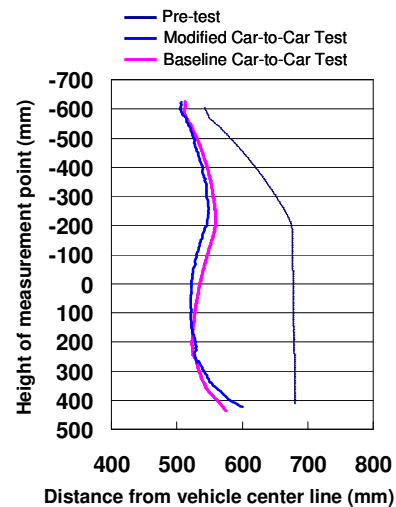
the Modified Car-to-Car test was also reduced, compared to the Baseline Car-to-Car test.



(a) Baseline Car-to-Car (b) Modified Car-to-Car



(c) Front door intrusion



(d) B-pillar intrusion

Figure 16. Comparison of body deformation between two Car-to-Car tests

Comparison of the left-side front side member for the modified and unmodified vehicles showed a similar pattern (Fig. 17). The modified front side member section exhibited approximately 150 mm of axial crush, whilst the unmodified front side member had bent slightly inward. The deformation patterns indicated that there had been more energy absorbed by the modified bullet car’s front side member in impact than there had been in the

Baseline Car-to-Car test. In addition, the overall deformation of the bullet vehicle's front side member and bumper cross beam was more homogeneous, as compared to the unmodified vehicle. These appeared to be significant factors in the reduction of localized deformation and target car intrusion. This reduction in intrusion appears to have most likely been the main contributory factor in the reduction of the driver's femur load and bending moment observed in the Modified Car-to-Car test.



Modified car's front side members (post-test)



Unmodified car's front side members (post-test)

Figure 17. Comparison of front side member deformation mode between two Car-to-Car tests

The optimized structure by FE simulation calls for further investigation into the stiffness and geometric properties of the sub-frame in order to achieve good structural interaction and stiffness matching. A further direction of this study will be to perform physical Car-to-Car testing with a modified sub-frame.

DISCUSSION

According to the International Harmonized Research Activity (IHRA) report, relevant aspects for compatibility in a frontal impact are ⁽¹¹⁾

- Good structural interaction
- Frontal stiffness matching
- Occupant compartment strength
- Control of the deceleration time histories of impacting vehicles

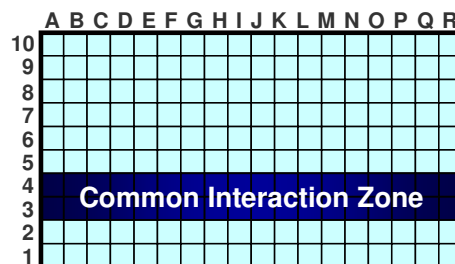
Since these four factors had been proposed for an improvement of frontal impact compatibility, other impact configurations were not taken into account. However, it was found from this study that these factors could be considered for side impact compatibility as well as for frontal impact compatibility. From the results of a numerical simulation, side impact compatibility was able to be achieved when the front-end structures of the bullet vehicle interacted well with the body side structure of the target vehicle with stiffness matching

between those structures. This is in agreement with items 1 and 2, in relation to compatibility improvement in frontal impact, as reported in the IHRA report. In the real world, there are vehicles with various structures and stiffnesses. As such, how structural interaction and stiffness matching are realized to enhance side impact compatibility should be further examined. Currently, test procedures for frontal impact are being studied in various countries. The role of side compatibility, however, has yet to be examined as a contributing factor. Therefore, development of the test procedure and assessment criteria for side impact compatibility is needed.

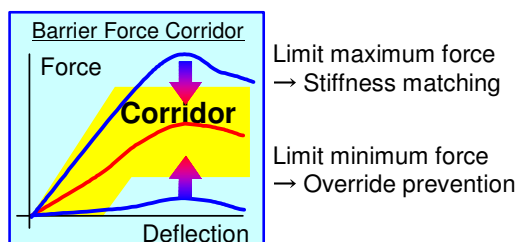
Note that in addition to the various crash directions, such as in the frontal and side directions, the benefits for/detriment to pedestrian protection and damageability ultimately need to be addressed as well. The future may require some portion of the vehicle front structure be developed to accommodate pedestrian protection, damageability, side impact and frontal impact, with corresponding crush displacement. To achieve this, controlling force-displacement characteristics by load cell wall data within the common interaction zone in the FWDB test may be one way of managing crash energy (Fig. 18) ⁽¹²⁾.



(a) Full Width Deformable Barrier test



(b) 125 mm x 125 mm barrier load cell wall



(c) Barrier force corridor for each load cell

Figure 18. Common interaction zone and interaction force

The structural geometry and stiffness characteristics of the front of a bullet vehicle play a role in influencing the risk of injury. For good occupant protection, it is desirable for the main impact loads to be transferred to the target vehicle through the side sill and door pillars. To be fully effective, strengthening the target vehicle's side structures will also be necessary for stiffness matching.

CONCLUSION

In this research, to clarify the factors that influence side impact compatibility, actual-vehicle crash tests and computer simulations were performed. Moreover, computer simulations were utilized to investigate the influence on vehicle deformation and injury values of the target vehicle when the stiffness of the front side member, bumper crossbeam and sub-frame of the bullet vehicle were altered.

In summary,

- Localized deformation was observed in the Car-to-Car test due to a concentrated loading effect imparted from the front side member, whereas the B-pillar deformed uniformly in the MDB-to-Car test. It was found from the results that the localized intrusion into the door produced higher pelvis and femur injury values.
- In order to enhance side impact compatibility, structural interaction between the target vehicle body side structure and bullet vehicle front-end structure as well as stiffness matching of those structures are important, and are the same contributing factors for frontal impact.
- When the front side member was modified by the FE analysis, there was a significant reduction in the localized intrusion of the target vehicle in alignment with the bullet vehicle's front side members, as compared to the Baseline Car-to-Car test. The performance of the driver dummy was significantly improved in the Modified Car-to-Car test for the body regions in alignment with the bullet vehicle's structure, as compared to the Baseline Car-to-Car test.

The results of this study indicate that to improve compatibility for side impact, the bullet vehicle should be designed in such a way that it engages the structure of the target vehicle more effectively, through improved geometrical interaction. The results also showed that matching the geometry and stiffness between front-end structures of the bullet vehicle and body side structures of the target vehicle contributed significantly during side and frontal impacts.

REFERENCES

- [1] Barbat, S., "Status of Enhanced Front-to-Front Vehicle Compatibility Technical Working Group Research and Commitment", 19th International Conference on the Enhanced Safety of Vehicles Paper No. 05-463, Washington DC, USA, June 2005
- [2] Insurance Institute for Highway Safety, "Incompatibility between cars and light trucks are being lessened by steps automakers are taking to improve geometric matchups of vehicles' front ends", Status Report Vol. 41, No. 1, Jan. 28, 2006
- [3] Summers, S., et al., "NHTSA's Research Program for Vehicle Compatibility", 18th International Conference on the Enhanced Safety of Vehicles Paper No. 307, Nagoya, Japan, May 2003
- [4] Hobbs, C.A., "The Influence of Car Structures and Padding on Side Impact Injuries", 12th International Conference on the Enhanced Safety of Vehicles, 954-62, Washington DC, USA, June 2005
- [5] Hobbs, C.A., et al., "Compatibility of Cars in Front and Side Impact", 15th International Conference on the Enhanced Safety of Vehicles, 617-24, Melbourne, Australia, May 1996
- [6] Nolan, M.J., et al., "Factors Contributing to Front-Side Compatibility: A Comparison of Crash Test Results", Society of Automotive Engineers Paper No. 99sc02, Detroit, USA, March 1999
- [7] Abe, A., et al., "Aggressivity-Reducing Structure of Large Vehicles in Side Vehicle-to-Vehicle Crash", Society of Automotive Engineers Paper No. 2005-01-1355, Detroit, USA, April 2005
- [8] Emura, M., et al., "Research on Compatibility in Car-to-Car Side Impacts", J-SAE Paper No. 20065648, Sapporo, Japan, September 2006
- [9] Summers, S., et al., "Design Consideration for a Compatibility Test Procedure", Society of Automotive Engineers Paper No. 2002-01-1022, Detroit, USA, March 2003
- [10] Edwards, M., et al., "Development of Test Procedures and Performance Criteria to Improve Compatibility in Frontal Collisions", 18th International Conference on the Enhanced Safety of Vehicles Paper No. 86, Nagoya, Japan, May 2003
- [11] O'Reilly, P., "Status Report of IHRA Vehicle Compatibility Working Group" 17th International Conference on the Enhanced Safety of Vehicles Paper No. 337, Amsterdam, the Nether lands, June 2001
- [12] Takizawa, S., et al., "Experimental Evaluation of Test procedures for Frontal Collision compatibility", Society of Automotive Engineers Paper No. 2004-01-1162, Detroit, USA, April 2004

FULL-WIDTH TESTS TO EVALUATE STRUCTURAL INTERACTION

Yuji Arai

Kunio Yamazaki

Japan Automobile Research Institute

Koji Mizuno

Nagoya University

Hidenobu Kubota

Ministry of Land, Infrastructure and Transport

Japan

Paper Number 07-0195

ABSTRACT

This paper discusses the improvement and assessment of structural interaction in SUV-to-car frontal collisions. For this purpose, a series of crash tests using SUVs and small cars was conducted. The results of the SUV-to-small car crash tests indicated that the aggressiveness of SUVs can be reduced by equipping the SUV with a secondary energy absorbing structure (SEAS) or by aligning the height of the SUV's longitudinal members with that of the small car's longitudinal members. The full-width tests, which had been proposed for the assessment of structural interaction, were conducted to detect and assess SEAS reaction force. The test results indicated that SEAS reaction force is detected in the full-width deformable barrier test and also suggested that vertical structural interaction (VSI) will be a useful criterion for assessing SEAS reaction force.

INTRODUCTION

To improve the compatibility of vehicles of different sizes in a frontal crash, it is necessary to improve the structural interaction in front. Accordingly full-width tests have been proposed to measure barrier force distributions for the improvement and assessment of structural interaction [1-3].

In vehicle crash compatibility, the aggressiveness of the SUV is an important subject to be addressed [4]. The longitudinal members of SUVs are inclined to be higher than those of cars, and a vertical mismatch of longitudinal members between an SUV and a car can occur. This vertical mismatch can lead to an override by the SUV, and cause a large intrusion into the upper part of the passenger compartment of the struck car. Therefore, to prevent the override, it is important to improve structural interaction in the vertical direction. For such improvements, two means are conceivable: a) aligning the height of longitudinal members between

car and SUV or b) equipping a SEAS below the longitudinal members of the SUV.

The present study, part of the compatibility research project organized by Japan's Ministry of Land, Infrastructure and Transport, was focused on the structural interaction of SUVs and was intended to examine the vehicle deformation and occupant injury of a small car in a frontal crash with an SUV where the SUV is equipped with a SEAS or the height of the SUV's longitudinal members is aligned with that of the small car's longitudinal members. In addition, full-width rigid barrier test and full-width deformable barrier test were carried out using SUVs with and without SEAS, and the barrier force distributions were examined to detect and evaluate SEAS. Further, repeatability of the full-width deformable barrier test was investigated.

SUV-TO-CAR CRASHES

The SUV-to-small car test was performed in two crash configurations: offset frontal crash and full frontal crash, the latter test conducted by the Japan Automobile Manufacturers Association, Inc. (JAMA). Table 1 shows the test matrix. The impact velocity was 50 km/h with both vehicles traveling. Hybrid III test dummies were used for the front seat driver and passenger positions in each vehicle. The offset frontal crash test was divided into Test 1 and Test 2. In Test 1, the normal SUV with SEAS was used, and in Test 2, the modified SUV with SEAS removed was used. In both Test 1 and Test 2, the overlap ratio was 50% of the small car.

The full frontal crash test was divided into Test 3 and Test 4. In Test 3, the normal SUV with SEAS was used, and in Test 4, the SUV's longitudinal members were located at a lower position aligning with the center height to the small car's longitudinal members. In full frontal crash Test 3, there was a 57 mm vertical gap between normal SUV and small car as measured at the center of the longitudinal member. The overlap ratio was 43% between the longitudinal

members of the two vehicles.

Table 1.
Test matrix of SUV-to-car crash tests

Test configuration	Test vehicle	Impact velocity (km/h)	Test mass (kg)	Overlap ratio (%)	Longitudinal member height difference (mm)
SUV-to-car offset frontal crash (Test 1)	Normal SUV w/ SEAS	50.5	2076	50	63
	Small car		1091	(Small car)	
SUV-to-car offset frontal crash (Test 2)	Modified SUV w/o SEAS	50.1	2076	50	63
	Small car		1091	(Small car)	
SUV-to-car full frontal crash (Test 3)	Normal SUV w/ SEAS	50	2076	100	57
SUV-to-car full frontal crash (Test 4)	Lowered SUV w/ SEAS	50	2076	100	0
	Small car		1074	(Small car)	

Figure 1 shows the front structural components of the normal SUV and small car. The normal SUV is a frame-type vehicle with stiff longitudinal members. The SEAS is mounted directly on the longitudinal members. The distance from the front edge of the bumper cover to the SEAS was 377 mm in a longitudinal direction. The small car has a simple body structure with longitudinal members and bumper beam.



(a) SUV



(b) Small car

Figure 1. Front structure of test vehicles.

Offset Frontal Crashes

Figure 2 shows the deformation of the small cars in the SUV-to-car offset frontal crash tests. In the crash tests, geometric misalignments of the longitudinal members existed in the horizontal and vertical directions between SUV and small car. Consequently, the longitudinal member of the SUV

impacted the suspension strut and A-pillar of the small car in the two tests. As shown in Figure 3, the SEAS engaged the front wheel of the small car. In contrast, the longitudinal member of the SUV without the SEAS did not engage the front wheel but impacted the A-pillar of the small car. As a result, the A-pillar beltline deformation of the small car in the crash into the SUV without the SEAS was as large as 350 mm, and the small car in the crash into the SUV without the SEAS caused more intrusion at the brake pedal and toe board than the small car in the crash into the SUV with the SEAS (Figure 2).

From the two tests, it was demonstrated that the SEAS of the SUV is quite effective for structural interaction improvement even in a case of lateral mismatch.



(a) Test 1 (vs. normal SUV w/ SEAS)



(b) Test 2 (vs. modified SUV w/o SEAS)

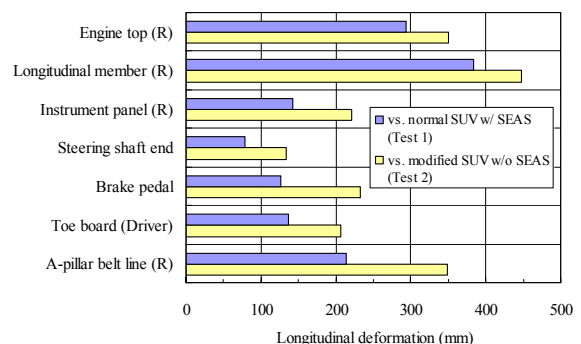


Figure 2. Deformations of small car in Test 1 and Test 2.

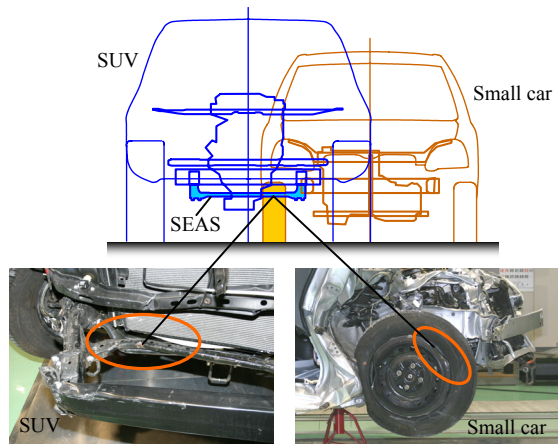


Figure 3. Structure alignment (Test 1).

Figure 4 shows the injury measures of the driver dummy in the small car. In Test 2, the lower extremity injury criteria of the driver dummy, such as femur force, knee displacement and tibia index, exceeded the injury assessment reference values (IARV) due to a greater intrusion. On the other hand in Test 1, the lower extremity injury criteria of the driver dummy were much lower than those in Test 2, although two of the lower extremity injury criteria exceeded their standard values.

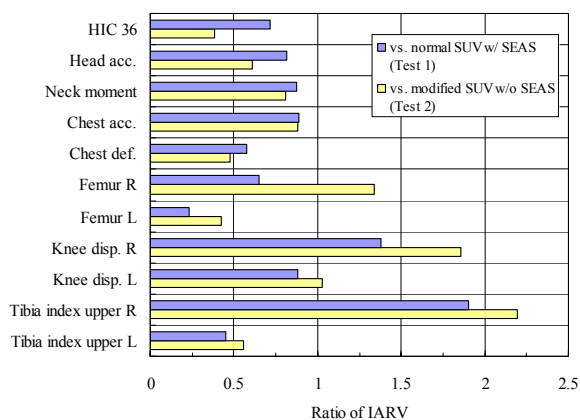


Figure 4. Injury measures of driver dummy in small car in Test 1 and Test 2.

In Test 1, the head injury criterion (HIC) was much higher than that in Test 2 (Figure 4). From a high-speed video, the driver airbag of small car was seen to deploy at 28 ms in the crash into the SUV without SEAS, against 40 ms in the crash into the SUV with the SEAS. In the crash into the SUV with SEAS, it was considered that there was a greater delay in the crash sensor response, which delayed the airbag and seatbelt pretensioner activation and caused higher head acceleration due to contact with the airbag which did not deploy completely and then with the compartment interior. It was guessed that the difference of the crash sensor response between the two tests was caused by the difference of the deformation mode of the longitudinal members.

Full Frontal Crashes

From the SUV-to-car full frontal crash tests (Test 3 and Test 4), it was observed that the normal SUV with a regular longitudinal member height overrode the small car in Test 3 but that the SUV with a lowered longitudinal member height (lowered SUV) did not override the small car in Test 4 as the longitudinal members of the two vehicles interacted effectively. Figure 5 shows the deformations of the small car in the two tests. In Test 3, the small car's longitudinal members deformed upward while its bumper beam intruded and was sheared between the normal SUV's bumper beam and SEAS. In Test 4 with the lowered SUV, the front of the small car exhibited a flat deformation. In the crash into the lowered SUV, the intrusions of the small car's upper components such as the steering wheel and instrument panel were smaller but the intrusion of the toe board was greater than that in the crash into the normal SUV.

The force-deformation characteristics of the small car was compared for the crash into the lowered SUV and for the full-width rigid crash at 55 km/h (Figure 6). To determine the deformation of the car in SUV-to-car crash, it is needed to identify the crash interface. In the lowered SUV-to-car full frontal crash test (Test 4), the crash interface could be determined based on the high speed video from the side view. However, in the normal SUV-to-car test (Test 3), the crash interface could not be determined because the override of the SUV occurred. As shown in Figure 6, the force-deformation characteristics are similar between two tests. Accordingly, when the members of both vehicles in car-to-car crash are in alignment, it is likely that the car deforms similar to the full-width test and the structural behavior can be predicted.

Figure 7 shows the injury measures of the driver dummy in the small car. It was found that the

dummy's right lower extremity generated higher injury measures with the lowered SUV than with the normal SUV but that its left lower extremity generated higher injury measures with the normal SUV. Also, head and neck injury criteria were lower with the lowered SUV than with the normal SUV.



(a) Test 3 (vs. normal SUV w/ SEAS)



(b) Test 4 (vs. lowered SUV w/ SEAS)

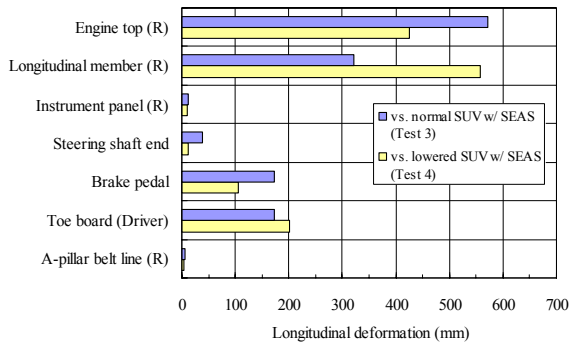


Figure 5. Deformations of the small car in Test 3 and Test 4.

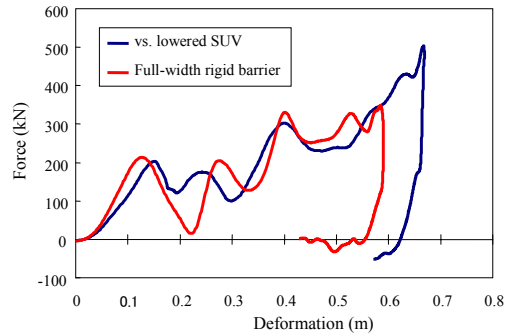


Figure 6. Force-deformation characteristics of small car in crash test into the lowered SUV and in full-width rigid barrier test (55 km/h).

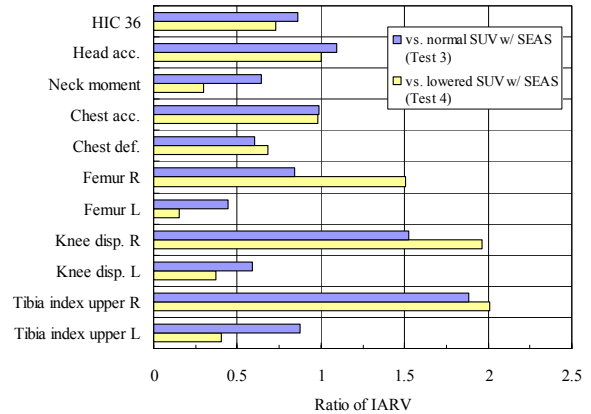


Figure 7. Injury measures of the driver dummy in the small car in Test 3 and Test 4.

Overall, the SUV-to-car full frontal crash tests indicated that structural interaction is an important factor for vehicle compatibility and that an effective means to enhance structural interaction is to improve the geometric alignment of longitudinal member height between vehicles. However, since the injury of the lower legs was increased, this point could be considered to be the problem which it should take notice of.

Although the normal SUV overrode the small car, structural interaction was observed between the SEAS of the normal SUV and the bumper beam of the small car. Assuming the removal of SEAS from the SUV, there may be a more intense overriding of the small car by the SUV. Therefore, it is clear that a SEAS is an important structural component for improving the structural interaction of vehicles.

FULL-WIDTH RIGID AND DEFORMABLE BARRIER TESTS

In order to clarify whether the SEAS can be detected in full-width tests, the barrier force distributions of the normal SUV (with SEAS) and modified SUV (without SEAS) were examined. Table 2 shows the test matrix. Hybrid III test dummies were used for the front seat driver and passenger positions in each vehicle. The barrier force distributions were compared in a full-width deformable barrier (FWDB) test and a full-width rigid barrier (FWRB) test, using 125 x 125 mm high resolution load cells (Figure 8). In the tests, the ground clearance of the load cell barrier was 125 mm, which was different from the 80 mm recommended by IHRA (International Harmonized Research Activities) Phase 1a [1]. The SEAS was aligned with row 2 in the load cell barrier. Thus, the barrier force in row 2 was compared between normal and modified SUVs. The impact velocity was set at 55 km/h. The deformable barrier face used in the FWDB test has two layers [3]. The first layer consists of a 0.34 MPa aluminum honeycomb element, and the second layer consists of a 1.71 MPa element (Figure 9).

Table 2.
Full-width test matrix

Test configuration	Test vehicle	Impact velocity (km/h)	Test mass (kg)
FWDB	Normal SUV w/ SEAS	54.9	2076
FWDB	Modified SUV w/o SEAS	55.0	2076
FWRB	Normal SUV w/ SEAS	54.8	2076

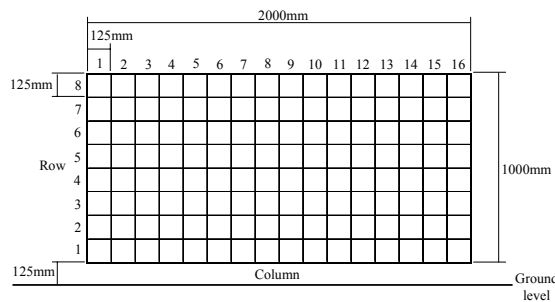


Figure 8. Load cell wall.

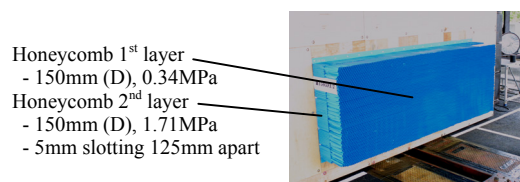


Figure 9. Deformable barrier face.

Figure 10 shows the vehicle deformation of the normal SUV with the SEAS in the FWDB and FWRB tests. In the FWDB test, the SEAS deformed rearward, the front end of the longitudinal members bent downward, and the bumper beam bent backward at its center. In the FWRB test, the front body of the SUV exhibited a flat deformation. The SEAS did not deform rearward in accordance with the axial collapse of the longitudinal members. Thus, SUV deformation differed between deformable and rigid barriers.

Figure 11 shows peak cell force distributions of the SUV with and without the SEAS in the FWDB tests. It was observed that the force on the longitudinal members was extremely large in both vehicles. In the SUV with the SEAS, the front end of its left longitudinal member came into contact with two load cells. The SUV without the SEAS came in contact with three load cells and recorded a high impact force on its engine due to the outward deformation of the left-longitudinal member.

Row 2 with columns from 5 to 12 are the load cells which are in alignment with the SEAS. In row 2 where the SEAS made contact, the row load was 120 kN, against 87 kN in row 2 of the SUV without the SEAS. Comparing Figure 11(a) and (b), it may still be difficult to conclude that the forces of row 2 were generated from the SEAS deformation, because they are spread by the honeycomb. Thus, the force in row 2 was examined according to the vehicle deformation.



(a) with SEAS in FWDB test



(b) with SEAS in FWRB test

Figure 10. Deformations of normal SUV with SEAS in FWDB and FWRB tests.

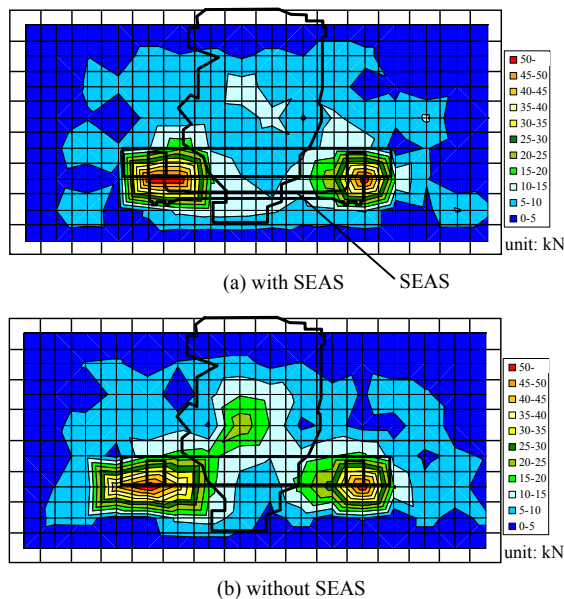


Figure 11. Peak cell force distributions of SUV with and without SEAS in FWDB tests.

The sum of the barrier force in row 2 where SEAS made contact was plotted against the vehicle displacement, which was calculated from a double integral of the passenger compartment acceleration (Figure 12). In the FWDB test, the force increases from the vehicle displacement of 0.4 m, where the SEAS began to contact the barrier. In the SUV without the SEAS, the force level was small in the initial stage, and increased after 0.5 m where the lateral suspension structures started to contact the barrier. Thus, it was demonstrated that the barrier force in row 2 shows the SEAS reaction force in the FWDB test. The result of SUV (with SEAS) in a FWRB test is also shown in Figure 12. The force in row 2 does not increase until the deformation of 0.5 m. Since the vehicle deformation was flat in the FWRB test, the SEAS did not deform rearward and did not generate the reaction force against the rigid barrier. Thus, it will be difficult to measure a SEAS reaction force in FWRB tests.

SEAS detection was examined using the criteria of structural interaction such as average height of force (AHOF) and vertical structural interaction (VSI). The AHOF is a measure of the average height from the ground that a vehicle applies force to the load cell wall, and the intent is to promote structural interaction between vehicles by aligning their stiffest members in the vertical direction [5]. The aim of the VSI is to encourage sufficient vehicle structure in alignment with a

common interaction zone, i.e. rows 2 to 5.

Height of force (HOF) was plotted with vehicle displacement (Figure 13), and was almost constant after the bumper beam had come into contact with the barrier because the SUV had a simple frame-type longitudinal member. The AHOF, which was calculated from displacement up to 400 mm (AHOF400), was 551 mm for the SUV with the SEAS, and it increased to 567 mm for the SUV without the SEAS. However, it can not be concluded that the AHOF400 decreased by the SEAS reaction force due to its small force. The engine impact force of the SUV without the SEAS was large as indicated by the collapse of the left-longitudinal member, and it may be more reasonable to consider that a number of factors including engine impact affected the HOF.

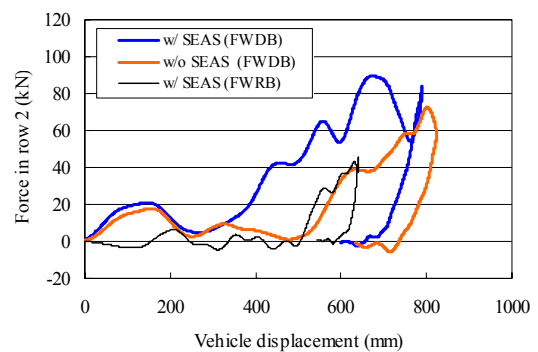


Figure 12. Barrier force in row 2 vs. vehicle displacement for SUV with and without SEAS in FWDB and FWRB tests

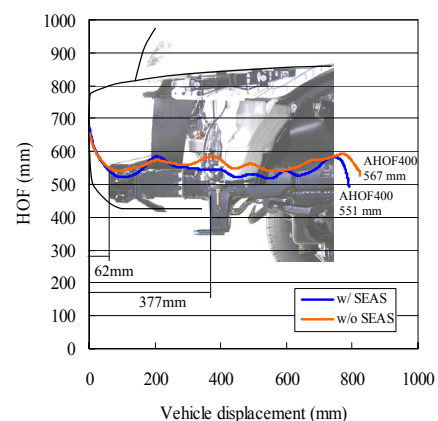


Figure 13. HOF-displacement curves in FWDB tests of SUV with and without SEAS.

Figure 14 shows the peak row load (based on sum of peak load cell forces up to 40 ms) for rows 2 to 5 in the FWDB tests. In row 2 where the SEAS made contact, the row load was 71 kN, against 27 kN in row 2 of the SUV without the SEAS. According to VSI proposed by the Transport Research Laboratory (TRL), which defines rows 2 to 5 as the assessment area, the score was 1.3 for the SUV with the SEAS and 2.0 for the SUV without SEAS. As a result of the FWDB test, it was demonstrated that the SUV with the SEAS is better than the SUV without the SEAS as a structural interaction evaluation. Thus, the VSI will be a useful criterion for assessing the reaction force of SEAS.

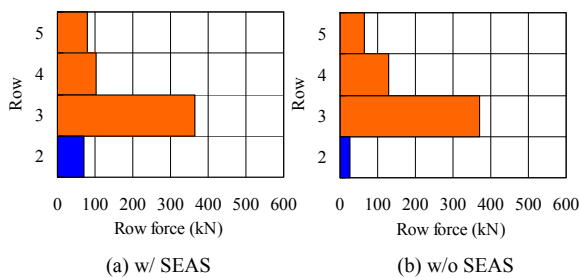


Figure 14. Peak row load in FWDB tests of SUV with and without SEAS.

REPEATABILITY ASSESSMENT OF THE FULL-WIDTH DEFORMABLE TEST

In order to assess the repeatability of the FWDB test, two identical FWDB tests were conducted and vehicle deformations, dummy responses and barrier force distributions were compared between the two tests. In the tests, the ground clearance of the load cell barrier was 80 mm. Table 3 shows the test matrix, using a SUV (with SEAS). Hybrid III test dummies were used for the front seat driver and passenger positions in each vehicle. The impact velocity was 54.9 km/h in the first test (Test 1) and 54.8 km/h in the second test (Test 2). Differences of target location on the barrier were 2 mm left in horizontal direction and 0 mm in vertical direction in Test 1, and 13 mm right in horizontal direction and 0 mm in vertical direction in Test 2.

Table 3. FWDB test matrix

Test configuration	Test vehicle	Impact velocity (km/h)	Test mass (kg)	Impact accuracy
FWDB (Test 1)	SUV (w/ SEAS)	54.9	2076	2mm left 0mm vertical
FWDB (Test 2)		54.8		13mm right 0mm vertical

Barrier deformations after tests are shown in Figure 15. The honeycomb block deformations caused by the SUV's bumper beam of the SUV substantially differed between the two tests. In the case of Test 1, honeycomb blocks which contacted with the bumper beam were completely deformed. However, in Test 2, the second layer of honeycomb blocks were hardly deformed. They dropped during crashes, and the bumper beam contacted to the back plate directly.

Figure 16 shows the vehicle deformations in the two tests. The vehicle deformations were almost the same in Test 1 and Test 2. However, there was a difference in the deformation mode of the bumper beam between two tests. While the bumper beam bent in Test 1, there was no such bending in Test 2. This difference was considered to be caused by the difference of barrier deformation.

The injury measures of the driver and front passenger dummies are presented in Figure 17. As shown in Figure 17, there were no large differences for injury measures between two tests. The maximum difference was 11.4% for the right upper tibia force of the front passenger, and the difference was less than 5% for many other body parts.



(a) Test 1



(b) Test 2

Figure 15. Barrier deformations.



(a) Test 1



(b) Test 2

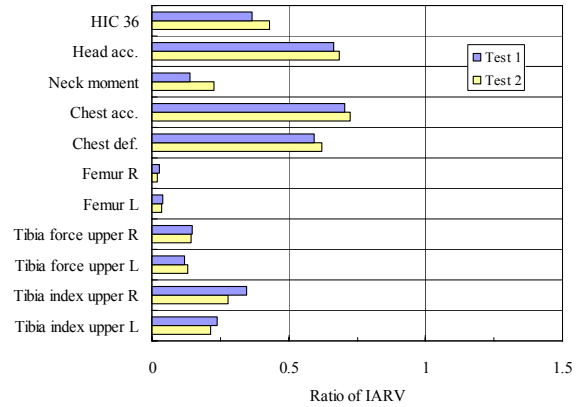
Figure 16. Vehicle deformations.

The barrier force-time history is shown in Figure 18. The force curve was almost the same in Test 1 and Test 2, and the maximum force was 657 kN for Test 1 and 672 kN for Test 2. However, the force about 40 ms was greater in Test 2 than in Test 1. In Test 2, since the second layer of honeycomb blocks dropped during crashes, the force generated by the contact with the front end of longitudinal members became great.

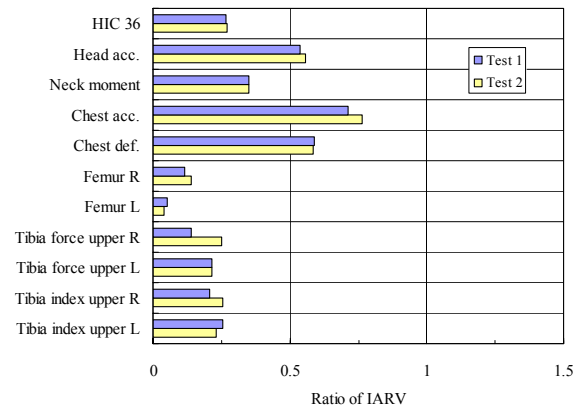
Several criteria of structural interaction such as AHOF were compared between two tests. Figure 19 shows HOF-vehicle displacement curve. HOF was almost the same in Test 1 and Test 2. AHOF400 was 546 mm for Test 1 and 555 mm for Test 2, and the difference was small as 9 mm.

The VSI and horizontal structural interaction (HSI) in the assessment area for rows 2 to 5 are shown in Figure 20. The aim of the HSI is to encourage strong crossbeams to adequately distribute rail load and wider structures for lower overlap impacts. As shown in Figure 20, the VSI score was almost the same in Test 1 and Test 2. As for HSI, the outer support measure was equivalent between the two tests. However, the center support measures of the HSI clearly differed between 5.0 for Test 1 and 11.3 for Test 2. The reason for this is that the distributions of the peak cell forces in row 3 are greatly different between the two tests. In Test 2, due to the high force of the longitudinal members, target cell load level was set higher than that in Test 1, while the forces of the 4 cells in the assessment area for the center support were small as a whole

compared to Test 1 (Figure 21). These differences were considered to be caused by the difference of barrier deformation.



(a) Driver



(b) Front passenger

Figure 17. Injury measures of driver and front passenger dummies.

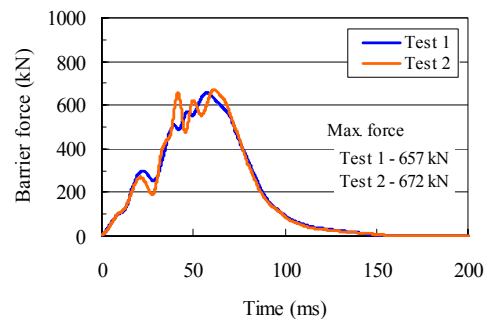


Figure 18. Barrier force-time histories.

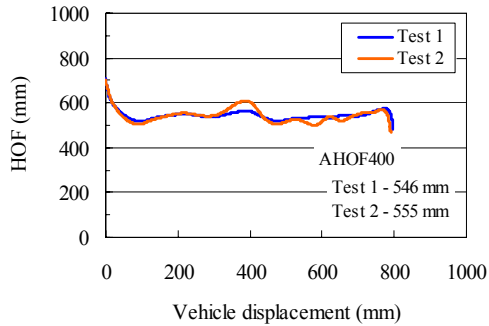


Figure 19. HOF-displacement curves.

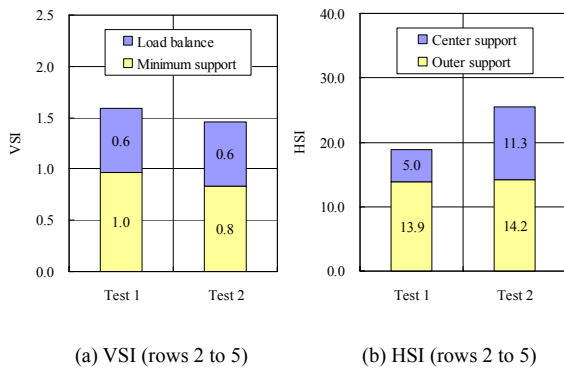


Figure 20. VSI and HSI (rows 2 to 5).

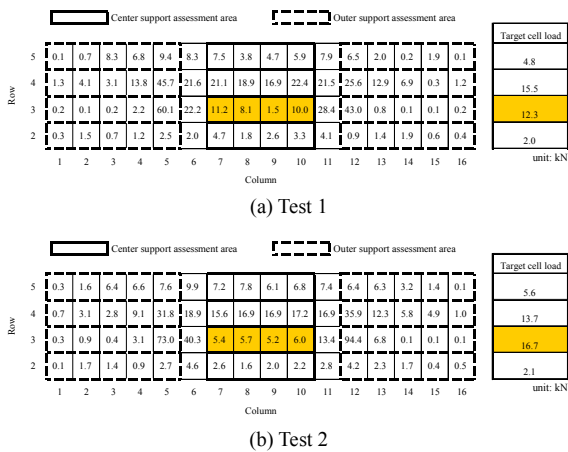


Figure 21. Peak cell force (up to 40 ms).

CONCLUSIONS

For the improvement and assessment of structural interaction in vehicle-to-vehicle frontal collisions, a series of crash tests using SUVs was conducted. The results are summarized as follows:

1. In SUV-to-small car crash tests, structural interaction was improved by equipping the SUV with a SEAS or by aligning the height of the SUV's longitudinal members with the height of the small car's longitudinal members.
2. SEAS reaction force was detected in a full-width deformable barrier test, and it was demonstrated that VSI will be a useful criterion for assessing structural interaction including SEAS reaction force.
3. Full-width deformable barrier tests indicated a generally good repeatability with regard to dummy responses and vehicle deformations. As compatibility assessment criteria, AHOF and VSI, which are parameters for vertical structural interaction, exhibited good repeatability. However, HSI results were not good due to the difference of barrier deformation.

ACKNOWLEDGEMENT

The authors gratefully acknowledge JAMA for providing crash test data.

REFERENCES

- [1] O'Reilly, P., "Status Report of IHRA Compatibility Working Group," 19th International Conference on the Enhanced Safety of Vehicles, Paper No. 365, 2005
- [2] Edwards, M., et al., "The Essential Requirements for Compatible Cars in Frontal Collisions," 17th International Conference on the Enhanced Safety of Vehicles, Paper No. 158, 2001
- [3] Edwards, M., et al., "Development of Test Procedures and Performance Criteria to improve Compatibility in Car Frontal Collisions," 18th International Conference on the Enhanced Safety of Vehicles, Paper No. 86, 2003
- [4] Hollowell, W.T., et al., "NHTSA's research program for vehicle aggressivity and compatibility," ImechE Conference, 2002
- [5] Summers, S., et al., "Design Considerations for a Compatibility Test Procedure," Society of Automotive Engineers, Paper No. 2002-01-1022, 2002

NHTSA's RECENT VEHICLE CRASH TEST PROGRAM ON COMPATIBILITY IN FRONT-TO-FRONT IMPACTS

Sanjay Patel, David Smith, Alope Prasad

U.S. National Highway Traffic Safety Administration (NHTSA)

Pradeep Mohan

FHWA/NHTSA National Crash Analysis Center,

The George Washington University

United States of America

Paper Number 07-0231

ABSTRACT

This paper presents results from NHTSA's light vehicle compatibility crash testing program during 2005 and 2006. During these years, NHTSA Research has continued to collect full frontal rigid wall data in conjunction with the U.S. New Car Assessment Program (USNCAP), it has supplemented this with additional rigid barrier data to explore barrier design options, and it has developed and conducted vehicle-to-vehicle crash tests to explore the potential for reducing injuries by improving the crash compatibility between light vehicles. This effort was begun by first identifying the most promising metrics to characterize full frontal crash compatibility using data taken during frontal USNCAP testing, selecting crash test vehicles based on the metrics, and finally, performing full-frontal vehicle-to-vehicle crash tests to evaluate the probability of belted occupant injury and fatality in the crash vehicles. The test series provided evidence that by maintaining structural alignment and matching frontal energy absorptions, the probability of injuries/fatalities in both the Light Trucks and Vans (LTVs) and passenger car can be significantly reduced.

Carmakers are now voluntarily addressing compatibility in the U.S. by aligning their structures and implementing Secondary Energy Absorbing Structures (SEAS) and Advanced Compatibility Engineering (ACE). Vehicle-to-vehicle tests were conducted to understand how these new concepts perform and what sort of additional measures and performance tests may be needed. The results of these tests are presented and discussed in the paper. The advent of SEAS structures also presents challenges to characterize and measure their performance. A new rigid override barrier (ORB) concept has been developed and tested for this purpose. This paper also summarizes and discusses the preliminary design and testing of the ORB.

Finite element studies of vehicle-to-barrier

interactions suggest that the axial load cell barriers used prior to 2006 introduced low estimates of force heights on the barrier. In order to understand the error content in previous estimates of force height, several vehicles were crash tested into a high-resolution barrier, which is a 9x16 array of 125x125 mm single-axis load cells, each rated for measuring up to 300kN of compression perpendicular to its face. The results of this crash test program and their implications are discussed in this paper.

INTRODUCTION

In September 2002, NHTSA formed an integrated project team (IPT) to address light vehicle compatibility and in June 2003, the IPT issued its report [NHTSA, 2003]. The proposed initiatives for vehicle strategies were:

Proposed Initiatives:

1. NHTSA will pursue a comprehensive crash test program in an effort to determine whether vehicles of comparable mass, but with considerably differing characteristics (e.g., Average Height of Force – AHOF, initial stiffness, etc.), produce quantifiable injury measurement differences for occupants in the struck vehicle.
2. Using existing fixed rigid barrier crash test data, pairs of vehicles that are comparable in classification (e.g. large SUV), but different in measured characteristics (e.g. high vs. low AHOF) will be identified.
3. Vehicle-to-vehicle crash tests will then be conducted with these vehicle pairs in several configurations to determine whether the vehicle characteristic differences have any influence in the struck vehicle occupant injury outcome.
4. If differences can be quantified, NHTSA will seek to identify countermeasures for potential establishment of compatibility requirements.

Expected Program Outcomes

An expected outcome of this initiative would be to establish a more uniform range of vehicle characteristics within the vehicle fleet. For example, establishing a range (or ranges) for AHOF would lead to improved structural engagement in frontal impacts and would facilitate the design of self protection countermeasures (such as side door beam designs). It may also facilitate improved compatibility with roadside hardware (i.e., guardrails)

Improved energy management between striking and struck vehicles in real world crashes, particularly between passenger cars and LTVs, would be a desired outcome for the longer-range effort. An energy management approach could lead to improved energy sharing in vehicle-to-vehicle crashes. It could also provide the opportunity to improve occupant compartment integrity, there by decreasing intrusion-related fatalities and injuries and improving partner protection.”

In December, 2003, the Alliance signed a voluntary agreement between 15 major carmakers to vertically align 100% of the signatory’s LTV fleet fronts with passenger cars by 2009 [Alliance, 2003 and 2005]. The agreement defined compatibility in terms of mass ratio, difference in frontal stiffness, and difference in height of frontal structures for sharing crush energy, which is a universal concept of the problem. The agreement identified research to be performed on crush energy sharing and identified two options for the carmakers to accomplish this alignment:

- **Option 1** - Equip LTVs with primary load carrying structures (rails) that overlap the Part 581 bumper zone by 50% or more. This zone extends from 16 to 20 inches above the ground and the passenger cars have their primary structures based on this specification.
- **Option 2** - Equip LTVs with primary structures that overlap the Part 581 zone by less than 50%, but fit these vehicles with secondary energy absorbing structures (SEAS) that fully overlap the Part 581 zone to limit override and better engage passenger cars. These LTVs are typically higher off the ground and have higher rails so they need additional low frontal structures to

achieve crash compatibility. A quasi-static test for the Option 2 LTV SEAS structures was also proposed. This was a push test on the SEAS showing that it could resist at least 100 kN of force within the first 400 mm of distance from the front of the rails.

The voluntary agreement was implemented in MY 2004 and, as of November 2006, 62% of applicable LTVs were designed in accordance with the front-front criteria in the agreement [Alliance, 2006]. With this voluntary initiative underway for several years, it is useful to examine the light vehicle compatibility problem to see vehicle structural changes over years from model to model.

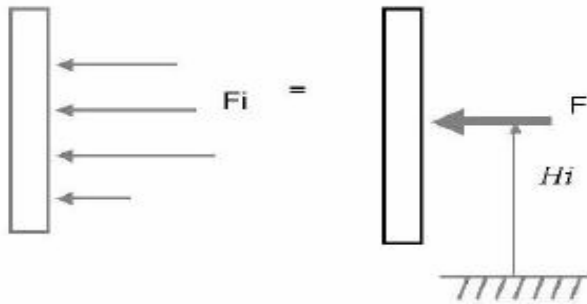
COMPATIBILITY METRICS

In FY 2004, a compatibility crash test program was performed by NHTSA as called for in the IPT report. However, the LTVs tested in that program were chosen and tested in such a way that little in the way of high injury measures were observed. This result provoked a review of the NHTSA approach to measuring compatibility in 2005 and a review of the test procedures for evaluation.

Research on a test procedure for the passenger cars and option 1 LTVs was begun in 2005 with an evaluation of the vehicle compatibility metrics being researched at various sites and their potential for computation from a rigid barrier test, since this was seen as the only option for a near-term test. The objective behind the metrics was to encourage design of a common crush box at the front of each light vehicle that would have similar structural characteristics and thus create a compatible fleet. The common structural characteristics that were selected were average height of force and frontal stiffness. A metric for the crush energy stiffness and the 400 mm depth of the crush box were selected based upon a DaimlerChrysler concept for frontal compatibility [Nusholtz, 2004], and the NHTSA metric for average height of force was redefined to extend only to 400 mm of crush (it previously went to the end of the crush). The two new compatibility metrics selected for study were:

- AHOF400 = average height of force delivered by a vehicle in the first 400 mm of crush,
- Kw400 = stiffness related crush energy absorbed by a vehicle in the first 400 mm of crush (also called the work stiffness).

Computation of AHOF400: When a vehicle hits a rigid load cell barrier in a full frontal impact, the individual forces measured on the array of load cells can be used to calculate the height of force (HOF) as a function of crush (d), as depicted in Figure 1 below. Note that the variables in Figure 1 that are a function of the crush are indicated as such by d in parentheses (e.g. F(d)). Each of the forces that hit the load cells at a given time are multiplied by their respective height from the ground (H_i), those forces are summed, and then divided by the sum of all the forces as illustrated in the equation below. In the equation, “n” represents the number of load cells.



$$HOF(d) = \frac{\sum_{i=1}^n F_i(d) \cdot H_i(d)}{\sum_{i=1}^n F_i(d)}$$

$$AHOF400 = \frac{\sum_{d=25mm}^{400mm} HOF(d) \cdot F(d)}{\sum_{d=25mm}^{400mm} F(d)}$$

Figure 1. Computation of the Height of Force

So, the average height of force (AHOF400) is the weighted average of the HOF values during the first 25 to 400 mm of vehicle crush as illustrated in Figure 1. This crush range is used to eliminate the noise in the data in the first 25 mm of crush when the relatively soft bumper is engaging the wall and is limited to a maximum crush of 400 mm to include the forces exerted on the wall by the rails buckling, but stop before the engine contact exerts significant forces. This approach was thought to focus the metric on the average height of all frontal structures in the compatibility crush box at every step in the crushing process without undue focus on the rails alone.

The data to compute AHOF400 were the net forces on each of the axial load cells in the rigid barrier (F_i in Figure 1). Since the data analysis assumed that these forces were located in the center of each cell, the error in the location of each cell net force could be as much as ½ of the cell dimension. Consequently, a barrier made up of large load cells had a larger error than one made up of smaller load cells. This effect will be examined further in barrier crash tests described below.

Computation of Kw400: The stiffness metric based on crash energy is derived from equating the energy stored in an ideal spring (1/2 K x²) to the work of crushing the vehicle front end (∫Fdx), as shown in the equation below. Again, the integral of the area under the force-deflection curve was evaluated between 25 to 400 mm of vehicle frontal crush to be consistent with the compatibility crush box concept and AHOF400. Here, if there was a lot of area under the force-deflection (F-d) curve, then a lot of work needed to be done to crush the vehicle front. In other words, high F-d area meant high crush work and high stiffness. When a high stiffness vehicle strikes a low stiffness vehicle, most of the crash energy will go into the low stiffness vehicle and its front end will deform the most in absorbing this energy. An example of this is when a high stiffness LTV strikes a soft passenger car, the car is grossly crushed and the occupants severely injured, while the LTV occupants often walk away. This result is a combination of stiffness ratio and mass ratio effects, both of which work against the car occupants.

$$Kw400 = \frac{2 \int_{25mm}^{400mm} Fdx}{(400^2 - 25^2)}$$

Examples of the source data collected in conjunction with the 2005 USNCAP rigid barrier frontal crash testing and how these metrics fit the data are shown in Figures 2 and 3 for a 2005 Chevrolet Trailblazer.

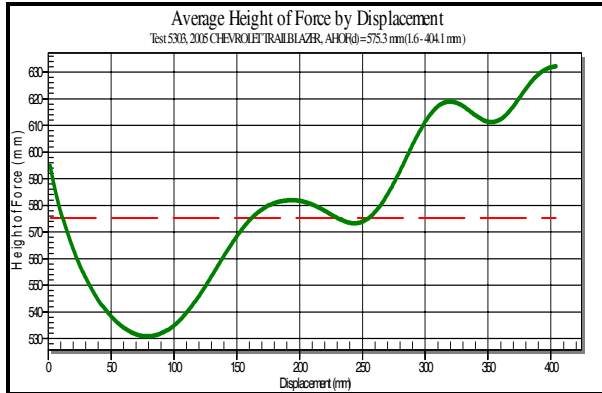


Figure 2. NCAP Test # 5303, Average height of the total force as a function of displacement (crush). The dashed line shows AHOF400

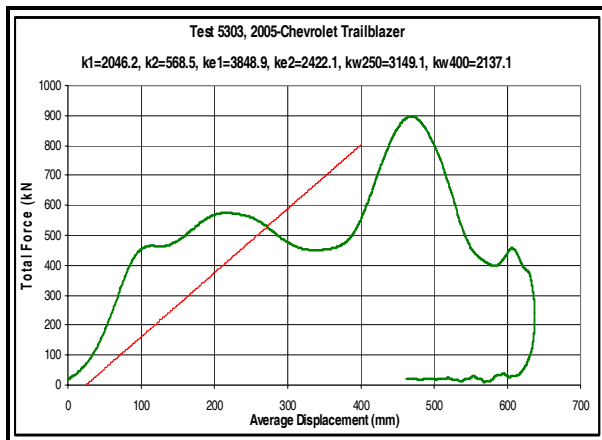


Figure 3. NCAP Test # 5303, Total force as a function of displacement (crush). The straight solid line shows the idealized Kw400 spring stiffness

Figure 2 shows a typical height of force data plot for a modern sport utility vehicle (SUV). Note the value of AHOF400 at about 575 mm, which is indicated by the horizontal dashed line in the figure. This value is a good deal above the typical passenger car (see Figure 4). Another point is that these curves often start very high, at 600-700 mm, and then drop rapidly downward to give an overall average around 550-600 mm. In such cases, the AHOF400 value may be misleading as a predictor of structural

engagement. This is true because, when two vehicles strike each other in a full frontal crash, the first part of the structures that engage will determine the subsequent progress of the engagement. Thus, if the LTV has a high structure in front of the rails and the passenger car has a low, then an override may ensue, regardless of how low is the rearward LTV structure, including the rails. In fact, we observed such a case when we tested a Civic-Silverado crash pair, which will be discussed below. The benefit about height of force data is that it does a good job of capturing all the structural interactions that lead to structural engagement, not just the rails.

Figure 3 shows the force-deflection data for the 2005 Chevrolet Trailblazer. The K values listed in the header are the various stiffness metrics that were investigated and discarded during the year, with the Kw400 value shown at the far right, and as a solid straight line in the plot. There are typically two peaks in these plots – the first is the rails buckling (about 200 mm in Figure 3), and the largest peak is the engine striking the wall (about 460 mm in Figure 3). Because an engine peak adds so much area to the Kw400 computation (through high force to the wall or partner vehicle), this metric can be used to keep the engine back from the front of the vehicle and also ensure that the rail peak does not get too high, which would come from rails that are too stiff.

When Kw400 and AHOF400 are combined with mass ratio, a complete set of compatibility metrics is created to evaluate the benefits of matching frontal structures. This evaluation was begun with an analysis of the dispersion of the metrics in the fleet.

Compatibility Metric Values in the Fleet: The following three figures show the dispersion of the compatibility metrics among vehicles in the fleet. Figure 4 shows a scatter diagram of AHOF400 in model year (MY) 2000-2005 light vehicles tested in the frontal USNCAP program. Figure 5 shows Kw400 for these vehicles. Finally, Figure 6 shows the cumulative distribution of mass ratio in frontal crashes over the last 10 years of the U.S. National Automotive Sampling System (NASS) Crashworthiness Data System (CDS) crash data.

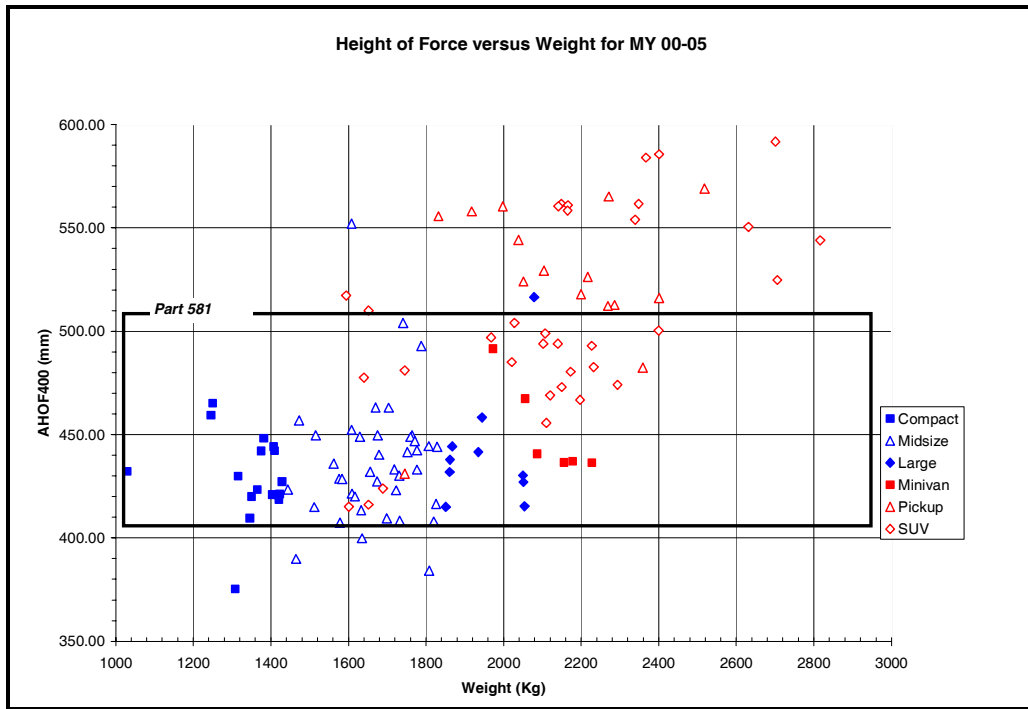


Figure 4. AHOF400 versus vehicle test weight, MY 2000-2005

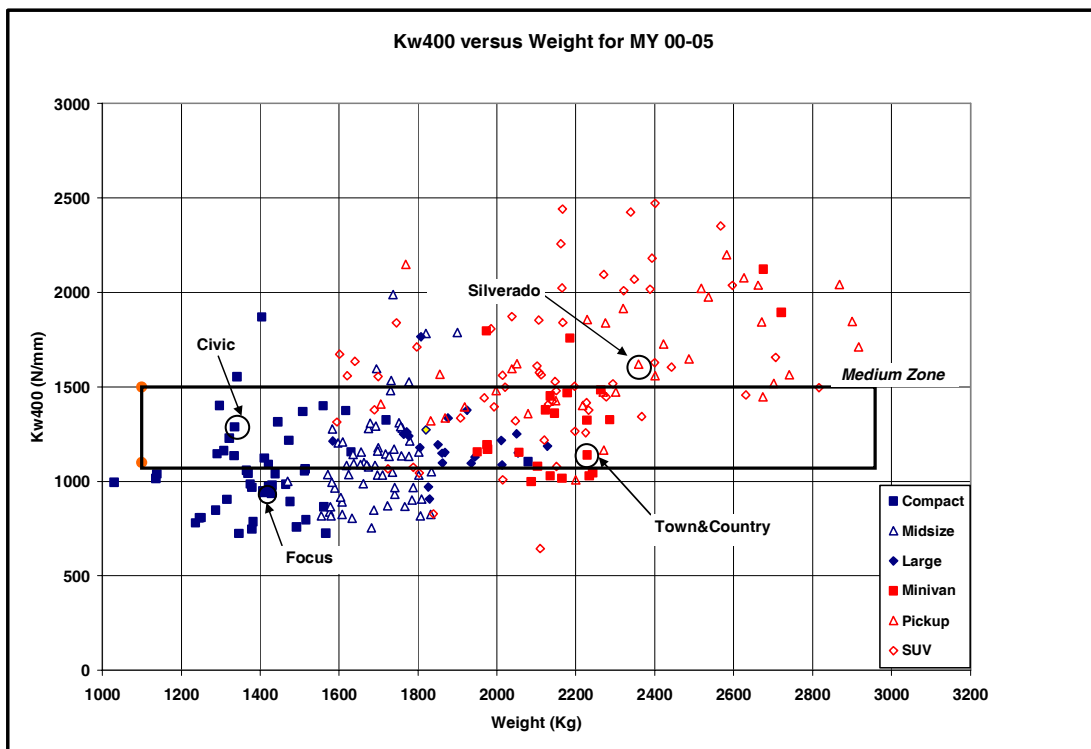


Figure 5. Kw400 versus vehicle test weight, MY 2000 - 2005

The height of the Part 581 bumper zone is shown in Figure 4, along with the modern fleet data for AHOF400, plotted as a function of test weight. The Part 581 bumper zone is 16-20 inches above the ground, or 406-508 mm, as established by NHTSA federal regulation. This zone has been defined by NHTSA as the compliance zone for low speed bumper tests to ensure that light vehicle passenger car bumpers match up and low speed damage is minimized. This zone has also been proposed by the industry as a compliance zone for the height for delivery of forces of LTVs [Alliance, 2003 and 2005]. In order to prepare for problem definition and benefits analysis, the Part 581 zone was defined as the “medium” value of AHOF400. AHOF400 values below this were low, and those above were high. The approach was to evaluate the potential benefits of moving all vehicles into the medium AHOF400 zone by comparing the injury results from vehicle crash pairs with one or more vehicles outside the zone to pairs with both vehicles inside the zone.

In Figure 5, the values of Kw400 are shown for the USNCAP vehicles tested during MY 2000-2005 as a function of weight. Here the medium range, 1100-1500 N/mm, was chosen as a best compromise between values in passenger cars and LTVs, also acknowledging that some of the heavier LTVs should be included so that real world frontal structural designs of medium stiffness at higher weights would be possible. The approach was to evaluate the potential benefit of moving all the vehicles into the medium Kw400 zone by comparing crash performance of vehicles outside the medium zone to those inside the zone. At this time, it is assumed that the most desirable condition is when all Kw400s move into this zone and all vehicles thus are able to more equally share crash energy. However, more research is needed to demonstrate that energy compatibility matching does not have a negative effect on self-protection and if it is the optimal metric to use for energy compatibility.

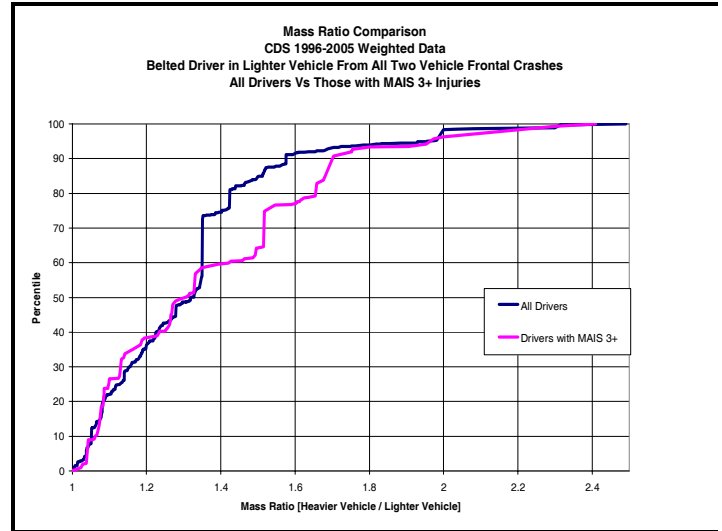


Figure 6. Cumulative distribution of mass ratios in CDS data for light vehicle frontal crashes, MY 1996-2005

In Figure 6, the cumulative distribution of weight ratios in the most recent 10 years of light vehicle frontal crashes in CDS data are shown. These data show that a mass ratio of 1.67 is at about the 93rd percentile for all two vehicle frontal crashes as well as those resulting in MAIS 3+ injuries. At mass ratio of 1.67 (and below) it could reasonably be expected that structural characteristics should be very important for controlling injury outcomes. In fact, the working hypothesis at the outset of FY 2006 was that structural height and stiffness matching could be used to overcome mass ratio effects up to this level and reduce injury outcomes compared to unmatched vehicle pairs.

RIGID BARRIER TEST DATA AND METRICS RELIABILITY ANALYSIS

Nearly all of the rigid barriers that have been used in conjunction with the USNCAP testing have collected axial force data from a matrix of load cells that is 4 rows of 9 columns using 250x250 mm load cells. A few of the barriers had a matrix of 2x3 load cells and fewer still were 9x18. Consequently, a series of crash tests was performed using a high resolution axial barrier (9x18 load cell matrix measuring axial force alone) for comparison to the original data collected during USNCAP from a 4x9 array. This was done to assess how repeatable the metrics were for these aged vehicles and how much AHOF400 might change as a function of barrier resolution in the tests. The results of this research are shown in Table 1 below.

Table 1. Comparison of metrics computed from key tests

NCAP Barrier Data		4x9 Matrix			
	Test No.	Shift (ms)	Kw400 (N/mm)	AHOF400 (mm)	Test Weight(kg)
02 Focus	4216	1.3	934	436	1410
01 Civic 2Dr	3456	-0.1	1265	412	1335
05 Town&Country	4936	1.9	1137	476	2229
03 Odyssey w/o ACE	4463	-2.1	1448	443	2178
03 Silverado	4472	3.1	1619	475	2359
05 Odyssey with ACE	5273	2.0	1456	450	2263
03 Accord	4485	1.3	1027	429 (2x3)	1571
96 Dodge Caravan	2997	0.75	1172	470	2011
High Res Barrier Data		9x18 Matrix			
2006 Test Series	Test No.	Shift (ms)	Kw400 (N/mm)	AHOF400 (mm)	Test Weight(kg)
02 Focus	5712	0.9	947	460	1410
01 Civic 2Dr	5710	0.7	1261	382	1582
05 Town&Country	5713	1.0	1124	463	2354
03 Odyssey w/o ACE	5144	-0.15	1360	467	2146
03 Silverado	5711	1.0	1472	511	2273
05 Odyssey with ACE	5714	1.5	1542	457	2388
2004 Test Series					
04 Accord	5062	1.5	1027	508	1624
96 Dodge Caravan	4990	0.8	1163	475	1976

The first thing to notice about Table 1 is the column labeled “Shift, ms.” The data entered in this column are the amount of time, in milliseconds, that the force data needed to be time-shifted by hand so that the force-deflection curve passed through (0,0). This effect showed up in Figure 3, where the F-d curve did not go through (0, 0). If this time shifting is not done, then the Kw400 could be as much as 10% in error because the area under the F-d curve from 25-400 mm is inaccurate. The need for this shift comes from the test procedure to trigger force data collection, which was done by contact tape on the vehicle bumper. This data collection was triggered separately from the accelerometer data used to compute the displacement. Later, when the data was filtered to smooth out the noise, some rounding in the force-displacement curve took place near (0, 0). For the time being, it was assumed that like causes created like effects (smoothing, etc., would affect all the curves similarly), and, for research purposes, before computing Kw400, initial data were adjusted to start the F-d curve through (0,0).

The second thing to notice about Table 1 is the values for Kw400. Here, the shaded values for Kw400 did not seem to be affected by barrier resolution, the age and use of the vehicles, or test weights. Of particular interest on the latter point are the Honda Civic and the Town & Country. These two vehicles were tested at significantly higher weights in the high resolution barrier tests, yet they showed nearly the same Kw400 values. However, the unshaded Kw400 values tell a different story for the other vehicles. These vehicles do show an increase of Kw400 with weight. The likely explanation of these data is that it depends on where the weight is placed and what it does. If this weight occurs in the crush box and comes from bigger rails, then it will likely also contribute to a higher stiffness of the vehicle. A final point on this is that we have no good estimates of the amount of manufacturing variability for Kw400 of a given vehicle model. Further, this is confounded by age and use of these vehicles. Thus, we should not expect exact agreement between new vehicle tests and tests of used vehicles several years old.

The data for AHOF400 in Table 1 show consistent trends with the variations in test conditions, especially weight. That is, the Focus and the 03 Honda Odyssey were tested at nearly the same weights. In both cases, the AHOF400 changed significantly from the 4x9 to the 9x18 tests, which was expected with the change to a higher resolution barrier and reducing the AHOF400 error as discussed before in Figure 1. Similarly, the Accord AHOF400 showed a great deal of motion upward in moving from a 2x3 barrier to the 9x18 barrier. However, the Civic and Town & Country were tested at higher weights in the 9x18 tests and their AHOF400s moved down, just as expected with the added ballast. The rest of the tests moved up or down depending on the test weight.

FULL FRONTAL VEHICLE-TO-VEHICLE CRASH TEST SERIES

Part I – Option 1 LTVs and Passenger Cars

The vehicle-to-vehicle crash test program in FY 2006 was designed to complete the IPT series for vehicle-to-vehicle crash testing. Specifically, it was designed to complete a set of full frontal car-LTV crash tests to determine injury outcome differences due to different vehicle characteristics. Further, it was desired to investigate the ability of stiffness matching to overcome a fairly high mass ratio for vertically aligned structures. The LTVs in this part

The mass ratio selected for the test was 1.67, which is at the 93rd percentile of all CDS frontal crashes (Figure 6). Ballasting was then employed in the test vehicles as necessary to maintain the weight of the target car at the same value for all crashes, and the weight of the bullet LTV at the same value for all crashes. Thus, frontal height and mass ratio were maintained as close as possible for all tests while varying the frontal stiffness as measured by Kw400.

All vehicles were run with belted Hybrid III 50th percentile male drivers and belted Hybrid III 5th percentile female passengers in the right front seat. All dummies in both bullet and target vehicles except passenger dummy in bullet vehicle were fitted with Thor-Lx legs so lower extremity injury measures could be taken.

Ford Focus-Chevrolet Silverado Test

The first pair tested was a Focus-Silverado

pair, which was chosen because it was thought to be an aggressive pair in terms of stiffness (Figure 5). The target vehicle was a 2002 Ford Focus with a Kw400 of 947 N/mm. The bullet vehicle was a 2003 Chevrolet Silverado with a Kw400 of 1619 N/mm. This pair was used to determine the closing speed for all subsequent testing.

The speed of the test series was desired such that the aggressive LTV/car pair would produce a probability of severe to fatal injury levels in the dummies of the target vehicle. This was done by running tests at three different closing speeds of 70, 75, and 80 mph between the Silverado and Focus. The injury results for this series are shown in Figures 8 and 9 below, overlaid on the probability of injury curves that were used in the preliminary economic analysis for the most recent FMVSS No. 208 upgrade.

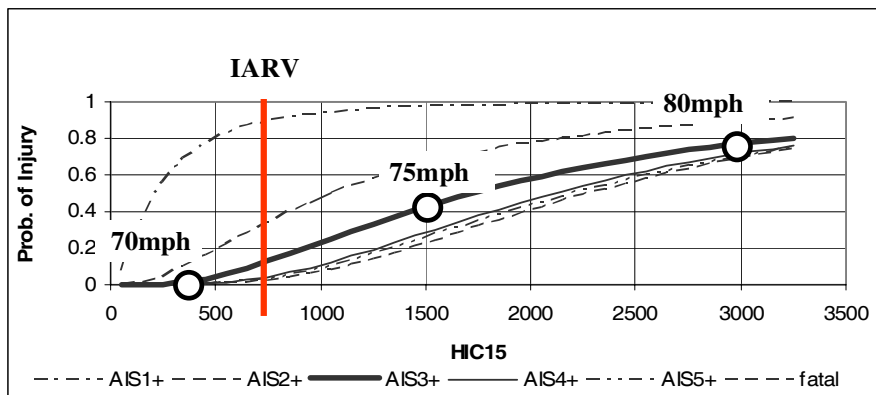


Figure 8. Probability of AIS 3+ head injury for the Focus driver (50th M)

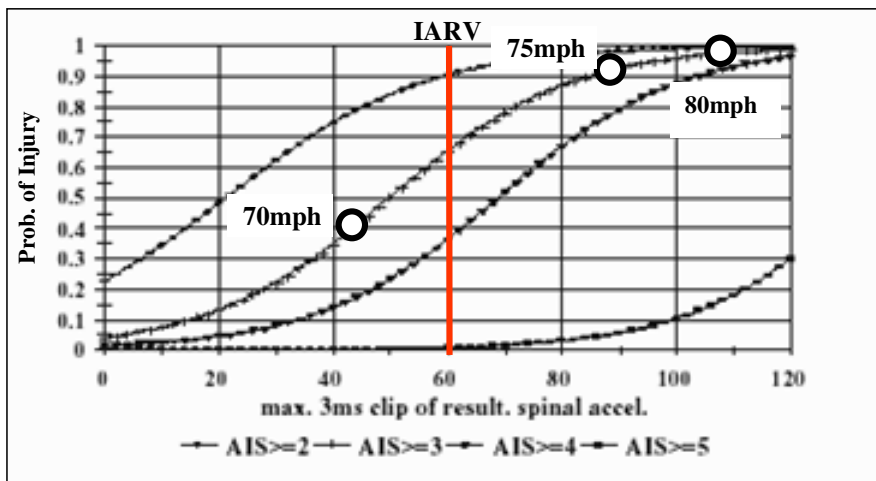


Figure 9. Probability of AIS 3+ chest acceleration injury for the Focus driver (50th M)

Figures 8 and 9 also have overlaid on them the Injury Assessment Reference Values (IARVs), which the agency uses to determine pass/fail in FMVSS No. 208 compliance tests. In addition, the Focus driver injury results are shown as circles on the figures for the three tests conducted. Though many injury measures were taken in these tests, only two showed the most consistent results across all crash conditions. These were the 15 second Head Injury Criteria (HIC15), and the chest acceleration (3 millisecond clip).

Since the Silverado/Focus vehicle pair was chosen as the aggressor pair for this test program, the test speed selected for all the tests needed to be high enough that severe injury measures in the Focus driver dummy could be expected. This requirement was interpreted to mean that the Focus driver injury numbers should be slightly over the IARV values. In this way, if structural matching worked, then the Focus driver injury values for head and chest would move below the IARVs, back into the acceptable zone for injury risk. Thus, Figures 8 and 9 show that 75 mph should be chosen as the closing speed for all vehicle-to-vehicle crash testing in the FY 2006 test series. At this closing speed and these mass ratios, the delta V on the target passenger car was approximately 46 mph (76 kph). Figure 10 shows where this delta V falls with respect to the average annual CDS data for frontal crashes.

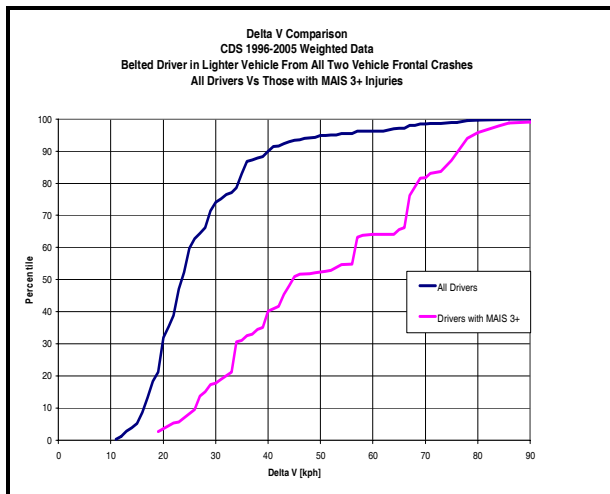


Figure 10. DeltaV distribution for the lighter vehicle in frontal crashes, CDS data 1996-2005

Figure 10 shows that the test condition for a smaller-vehicle delta V of 75 kph was at about the 98th percentile of all two-light-vehicle, belted-drivers, in frontal crashes. Further, when the subset of these

crashes at the higher severity of MAIS 3⁺ is considered, the delta V is at about the 87th percentile. This condition is reasonably extreme and thus meets all the test program design criteria for severity and injury outcome.

Ford Focus-Option 1 LTVs Comparative Test Series

With the test conditions determined, a series of crash tests was performed to compare various LTV frontal stiffness and construction methods. In particular, test data was desired for LTVs constructed with body-on-frame types and a new LTV construction called Advanced Compatibility Engineering (ACE) strategies by Honda. For all of these tests, the 02 Focus was used as the target. The results of this crash test series are shown in Table 2.

Table 2. Probability of Fatality in Belted Focus Driver. 75 mph closing, mass ratio 1.67, aligned structures, HIII 50th M

	Kw400 N/mm	Focus Driver Head (HIC15)	Focus Driver Chest (Chest G)
02 Focus	934		
Bullet Vehicles			
05 Town & Country	1137	17% (1267)	2% (72)
03 Odyssey (no ACE)	1448	30% (1689)	5% (90)
05 Odyssey (ACE)	1456	41% (1951)	5% (90)
03 Silverado	1619	25% (1482)	5% (88)

Table 2 shows a high HIC15 and a high probability of fatality in the Focus for all tests performed in the comparative series - all these LTVs are aggressive crash partners for the soft Focus. According to Honda, ACE construction method adds several significant load paths for crash energy to follow in addition to the usual one through the rails in order to distribute the crash energy more efficiently compared to more typical body-on-frame construction. However, our test results show that this more efficient frontal structure magnified the Kw400 difference to produce a higher injury outcome than the previous version of the 03 Odyssey, which did not have the ACE structure, but did have nearly the same Kw400 value.

Option 1 LTV Stiffness Matching Test

The next crash test was based on finding a matched compatible pair for comparison (Figure 5). A medium compact car was selected to replace the Focus, which was the 01 Civic 2 door, and a medium LTV was selected to replace the Silverado, which was the 05 Town & Country. Again, ballasting was used to maintain the mass ratio, the test was run at the same closing speed, and the matched heights of the structures were checked visually. The crash results for this test are shown in Table 3.

Table 3. Probability of Fatality in Belted Civic Driver. 75 mph closing, mass ratio 1.67, aligned structures, HIII 50th M

	Kw400 N/mm	Civic Driver Head (HIC15)	Civic Driver Chest (Chest G)
01 Civic 2 door	1265		
Bullet Vehicle			
05 Town & Country	1137	4% (802)	1% (66)

Comparison of the results for the crash tests with the 05 Town & Country shown in Tables 2 and 3 demonstrate potential improvement in injury outcomes for the compact car driver when the Kw400 is matched to the striking LTV. A further result in this area stands out when the injuries to the belted LTV driver are also compared, which is done in Table 4.

Table 4. Probability of MAIS 3⁺ injury in belted LTV Driver. 75 mph closing, mass ratio 1.67, aligned structures, HIII 50th M

	LTV Driver Head (HIC15)	LTV Driver Chest (Chest G)
<u>Kw400 Aggressive Pair</u> 02 Focus – 03 Silverado	3% (435)	45% (45)
<u>Kw400 Matched Pair</u> 01 Civic 2Dr – 05 Town & Country	0% (267)	26% (34)

Table 4 shows the surprising result that injuries went down in the LTV when the stiffness was matched to the compact car. Note that these injuries are at the lesser level of MAIS 3⁺ since there was an insignificant probability of LTV driver fatality in any of the compatibility tests conducted in FY 2006. This result came from lowering the stiffness of the LTV from that of the Silverado (1619 N/mm) down to the Town & Country (1137 N/mm), while simultaneously increasing the stiffness of the target car to match. When this was done, the probability of injury in both vehicles went down.

Thus, the goal of the test protocol to overcome the high input crash energy through height and stiffness matching alone was not quite accomplished, but the injury improvement in target and bullet vehicles from unmatched to matched stiffness in terms of head and chest injury metrics was remarkable. Note that all the tests in Table 2 were unmatched pairs, yet making much of the relative ordering of the tests in Table 2 by injury results is premature due to uncertainties in the test procedure and metrics computation as discussed in conjunction with Table 1. Furthermore, the injuries reported in Tables 2 and 3 were due to the full crush event, but the Kw400 metric is only for the first 400 mm of crush. The fact that the matched metric resulted in the lowest injury scores for these severe tests is interesting and adds support to the same result for low speed matched pairs in the CDS analysis discussed elsewhere (Smith, 2006).

Part II – Option 2 LTV Evaluations

NHTSA designed, built and tested a prototype override barrier (ORB) for dynamic testing of LTVs with override protection in FY 2006. Either some sort of override barrier, or a car-like moving deformable barrier (MDB), are the only concepts that can test all presently known types of override-controlling frontal structures. Fixed deformable barriers cannot test the rail extensions that GM is now deploying on the 2007 Silverado, but preliminary results from Europe seem to indicate that they might be able to test the blocker beam structures now being deployed, such as on 2007 Ford F-250 pickups. The ORB can test both. In 2006, NHTSA used finite element models to evaluate ORB test conditions and create data for prototype test design. Vehicle-to-vehicle crash tests were performed on the 2006 Honda Ridgeline and the 2006 Ford F-250 SEAS. In addition, barrier crash tests with these two vehicles were performed with a prototype ORB.

The emergence of SEAS in 2004 on large LTVs caused a great deal of confusion in developing a vehicle dynamic test. There seems to be no clear way forward among researchers, no doubt in part because the various fleet examples of SEAS are so different. One thing is clear however, the performance of all the different types of SEAS frontal structures cannot be evaluated with a full face rigid barrier test, so a new test is needed. The most promising evaluation concepts are either a deformable barrier test of some kind, or a low rigid ORB designed to engage and deform the SEAS to measure its strength in a dynamic test. While other organizations evaluated deformable barrier concepts, NHTSA focused on the ORB in 2006.

The ORB test design objective was to create data that can be used to compute Kw400 for the SEAS structures. This is important in that the industry voluntary test for the SEAS [Alliance, 2005] is a quasi-static push test that requires the SEAS structure to withstand a minimum of 100 kN of force before 400 mm deflection from the front of the primary structure (e.g., the rails on which it is mounted). Such a test may guarantee a minimum strength, but this does not prohibit the structure from being designed too strong for good car compatibility. On the other hand, a Kw400 evaluation could make the SEAS compatible, just as could be done for the full frontal test for option 1 LTVs. In order to understand these frontal structures, a small vehicle-to-vehicle crash program was performed in FY 2006. There are of two main types of SEAS at this time: the so-called “blocker beams” that are cross members mounted below the rails, and rail downward extensions at or near the vehicle front without cross members. A common example of each type was tested.

F-250-Focus Test

For the blocker beam tests, the 2006 Ford F-250 pickup was selected. This vehicle was tested against the 2002 Focus with the closing speed adjusted to create the same delta V on the Focus as the other tests so the injury results in the Focus could be compared to the other tests, even though the F-250 is a much bigger and heavier vehicle compared to the option 1 LTVs tested previously. Thus, the closing speed in these tests was 69 mph, with a Focus delta V of 46 mph as before. The F-250 was tested with its blocker beam in place and with the beam removed to see how much difference this blocker beam makes in injury numbers. The results are shown in Table 5 below.

Table 5. Focus driver probability of fatality and injury values in F-250 tests

	06 F250-02 Focus With Blocker Beam	05 F250-02 Focus Without Blocker Beam
Focus Driver (50th M)	Head 10% (HIC15 = 1023)	Head 25% (HIC15 = 1583)
Probability of Fatality (Injury measure)	Chest 5% (chest G = 86)	Chest 10% (chest G = 99)

Table 5 shows that the blocker beam clearly makes a big difference in injury outcomes for this crash pair. Further, of all the vehicle-to-vehicle crash tests run for compatibility in FY 2006, the probability of Focus driver fatality with the blocker beam is only bested by the match between the Civic and Town & Country (Tables 2 and 3). All other tests had worse outcomes for the Focus driver.

Ridgeline-Focus Test

The other type of SEAS now being deployed by the industry is added structure at the bottom of the rails. For example, the 2006 Ridgeline has downward rail extensions at the front to better engage passenger cars, with unibody construction. The test was run at the same test speed and Ridgeline was ballasted to the same weight as the Silverado in the Focus-Silverado tests so the results could be compared. The results of this test are shown in Table 6 below.

Table 6. Focus driver probability of fatality and injury measures in the Ridgeline test

	02 Focus-06 Ridgeline
Focus Driver (50th M)	Head 90% (HIC15 = 3448)
Probability of Fatality (Injury Measure)	Chest 15% (Chest G = 106)

The injury measures in the Ridgeline test were by far the greatest in all of the FY 2006 compatibility test series. These high injury values suggest that the Ridgeline SEAS structure was stiffer. This result calls for further research to evaluate how such SEAS structures work, and especially to

develop a prototype ORB test to measure their strength.

PROTOTYPE OVERRIDE BARRIER TESTS

The ORB concept allows an Option 2 SEAS equipped LTV to override the low rigid barrier so that the SEAS can be directly engaged and tested. The concept that was developed for preliminary testing is shown in Figure 11 below.

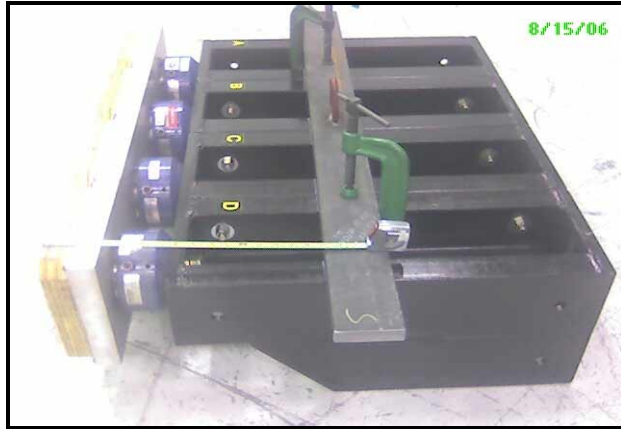


Figure 11. Final assembly of the ORB with a supporting load cell wall behind it

The current ORB prototype is adjustable in height, width, and depth. It has a single row of 250x250 mm load cells mounted on individual plates at the end of the I beams extending 500 mm from a rigid wall to measure the forces exerted on it. The height of the top of the ORB load cells is adjustable from 16-20 inches (406-508 mm) from the ground. The ORB load cells (including the wood facing block) extend 500 mm forward of the back-wall load cells. When the LTV SEAS strikes this barrier, force-deflection data can be generated that can be used to compute Kw400 values for the SEAS

structure. The preliminary determination of test speed was done with finite element modeling.

The F-250 was planned for the initial ORB test since it performed so well in the IPT test series conducted earlier, and since the data from the F-250 ORB test will be used to validate a finite element model of the vehicle. This model was built from a tear-down study performed in conjunction with FHWA, who also want to use it to study roadside safety features.

It would have been best to have the F-250 model to use in simulation of an ORB test and select the test speed. However, the tear-down study to build the model was not complete at the time the model was needed. Further, the data collected from the first ORB tests would be used to validate the F-250 model that was then being built. In other words, the test speed could not be selected using an F-250 model because it was not ready, and it would not be ready until the model could be validated with the data. The approach to this problem was to take the virtual blocker-beam SEAS from the F-250 model and mount it to the rail structure of an existing LTV model. A Ford Econoline model was selected for this virtual test series and ballasted to the F-250 weight. This approach is shown conceptually in Figure 12.

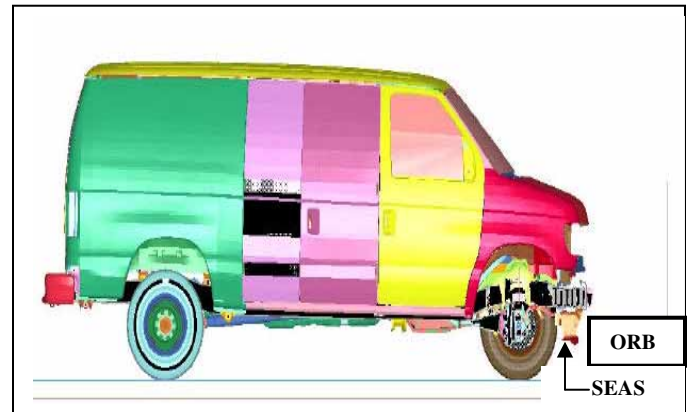


Figure 12. The F-250 SEAS mounted on the Ford Econoline FE model

The rail structure of the Econoline is shown in black in Figure 12 and the SEAS was mounted below it in the same manner as done in the F-250. Clearly, these rails are different from the F-250 rails and this must be considered in the evaluation of the virtual test results. This vehicle model was then impacted into the ORB model in simulated tests at 20 and 30 km/hr, and the results are shown in Figure 13 below. Here, zero displacement was when the ends

of the rails passed over the edge of the ORB. The cross beam was mounted on the rails 100 mm rearward from the end of the rails, which was where the force of deflection began to rise.

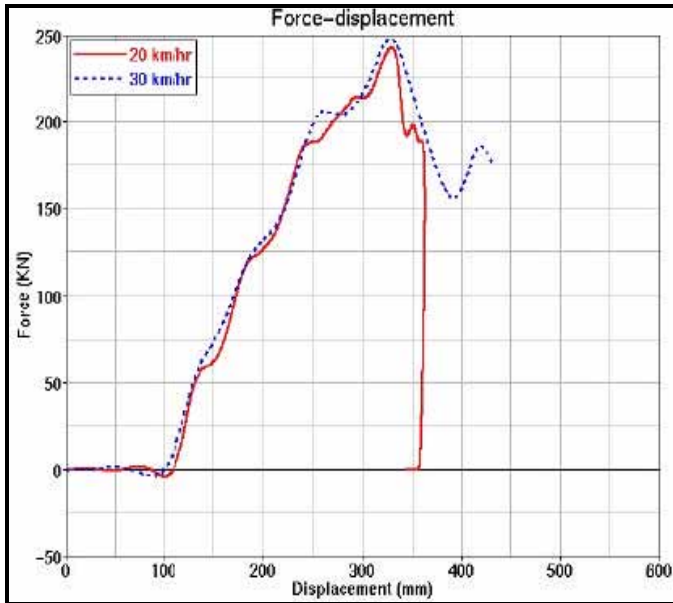


Figure 13. Virtual tests of the F-250 SEAS on the Ford Econoline

Figure 13 shows the two virtual test results that were run for the Econoline with F-250 SEAS to determine test speed. The peak force in these results was nearly the same for both of these tests, but the 20 kph test (12.4 mph) was too slow to create the needed 400 mm of displacement for Kw400 computations. Thus, these results indicate that at least 30 kph (18.6 mph) was needed to achieve 400 mm of crush for this structure. Further, since the F-250 rails are stronger than the Econoline rails, a test speed of 25 mph was selected for the initial F-250 ORB test in the real world.

The strength and performance of the real world prototype ORB was validated by subjecting it to a 25 mph crash using a wrecked car ballasted to the weigh of the F-250 and aligning one of the rails with the end load cell. No damage to the ORB load cells was observed and no load cells were saturated.

The tests of the F-250 and the Ridgeline have been completed, but the results have not been completely analyzed at the time of writing this paper, so they were not included.

CONCLUSIONS

The objective of this test program was to show, in vehicle-to-vehicle crash tests, what improvements might be found through structural matching for compatibility. This structural matching was accomplished using the metrics of AHOF400 and Kw400, the first of these to match height of structures, the second to match energy absorption. These metrics were selected because they could be measured in near-term rigid barrier tests, and they would require no new tests.

For option 1 LTVs and passenger cars, the matched stiffness and alignment crash test pair showed that injury probability fell in both vehicles compared to all unmatched, but comparable, crash tests. However, the test vehicles were chosen close to, or in, the matching zone and very extreme cases have not yet been investigated. Further, more research is needed on how close the stiffness ratio needs to be to one to achieve acceptable injury performance. Also, an injury benefits analysis needs to be completed to understand the real world benefits of the proposed medium compatibility matching zones across the fleet. This work is underway and will be reported elsewhere.

Option 2 LTVs bring in the added SEAS to reduce override of passenger cars. These structures will require a new test, not simply instrumenting a rigid barrier. In 2006, NHTSA researched a rigid override barrier (ORB) as a test concept for option 2 LTVs, with the intent to measure the Kw400 of the SEAS structure so it could be matched to passenger cars just like the Kw400 in a full frontal option 1 LTV test. A prototype ORB was designed, fabricated, and tested. Preliminary testing of this ORB has been completed, but the test results have not yet been analyzed.

REFERENCES

- Alliance of Automotive Manufacturers, "Enhancing Vehicle-to-Vehicle Compatibility – Commitment for Continued Progress by Leading Automakers," December, 2003. (Docket # NHTSA-2003-14623-13)
- Alliance of Automotive Manufacturers, "Enhancing Vehicle-to-Vehicle Compatibility–Commitment for Continued Progress by Leading Automakers." Revised November 2005. (Docket # NHTSA-2003-14623-32)

- Alliance of Automotive Manufacturers, letter to Acting Administrator Glassman, May 10, 2006. (Docket # NHTSA-2003-14623-24)
- Burkle, H., and J. Bakker, "Today's Relevance of Compatibility in Real World Accidents," paper presented at International Technical Automotive Conference, Dresden, Germany, October, 2005.
- Insurance Institute for Highway Safety, "Risk Reduction Estimates, Complying versus Non-Complying SUVs and Pickups," Presentation at EVC-NHTSA Meeting, June, 2006.
- Kiuchi, S., Ishiwata, K., Arai, Y., and K. Mizuno, "Compatibility Analysis Based on Accident Data in Japan," presentation given at International Technical Automotive Conference, Dresden, Germany, October, 2005.
- NHTSA, "Initiatives to Address Vehicle Compatibility," IPT Report, June, 2003. (Docket # NHTSA-2003-14623-1)
- Nusholtz, G.S., Xu, L., Shi, Y., and L.D. Domenico, "Vehicle Mass and Stiffness: Search for a Relationship," SAE Technical Paper No. 2004-01-1168, March, 2004.
- Smith, D.L., "NHTSA Compatibility Research Update," presentation given at SAE Government Industry Meeting, May, 2006.
- Verma, M.K., Lavell, J.P., Tan, S.A., and Robert C. Lange, "Injury Patterns and Effective Countermeasures for Vehicle Collision Compatibility," Enhance Safety of Vehicles Conference, Paper No. 05-0173, June, 2005.

Methodological physical analysis of FWDB and PDB test procedures regarding incompatible physical phenomena observed in real car accident

COULOMBIER Donat

ZEITOUNI Richard
LE BORGNE Gilles
PSA Peugeot Citroën,
France
Paper number 07-0244

ABSTRACT

Many studies have been performed in the field of compatibility between cars. Two test procedures with assessment have been developed to evaluate the compatibility level. The FWDB test is conducted at 56km/h against a 100% overlap rigid wall with deformable elements. The PDB test is a 50% overlap test at 60km/h against a Progressive Deformable Barrier. Assessment criteria are based on the force for FWDB test and on the deformation of the barrier for the PDB test.

If new assessment criteria are often proposed, few outcomes are provided concerning test procedures themselves, even though a lot of open issues still exist.

The aim of this paper is not to review all of them, but to conduct a methodological and physical analysis of both candidate test procedures. "Physical analysis" because it is based on the three incompatibility physical phenomena responsible for real car incompatibility (geometry, energy and stiffness mismatching). And "methodological" because both test procedures are studied using physical tests and virtual testing. Assessment criteria are therefore not considered.

Moreover, as a general agreement exists today that multiple load path with connections could help car front-ends to interact, PSA will present component tests and virtual testing with or without lower load path. Significant outcomes are provided concerning the efficiency of the technical procedures:

- 1) Both procedures can detect a geometry change such as the absence of load path.
- 2) Both procedures can measure a global force. However, its interpretation for the FWDB test is difficult due to the very limited deformation of the front-end undergone in this test.
- 3) Only the PDB test is able to draw up an energy absorption statement which is the only way to evaluate the car crash severity. For the FWDB test, this point represents a major difficulty because energy absorption by deformable elements is significant, about 50kJ.

INTRODUCTION

Compatibility is now studied for many years. Different research programs have therefore developed test procedures and assessment criteria in order to evaluate the compatibility level of cars. For several years, it could be observed that activities in these research programs are mainly addressed to develop assessment criteria, for each test procedures still candidate. During 2004-2006, the compatibility international context has changed for the following reasons.

First of all, the decision taken by the US to implement possible new requirements on compatibility in several steps has lead to a catalyst effect. In concrete terms, a self commitment concerning the height of the longitudinal has been applied has a first step. The following steps would have been based on full rigid width test with dynamical requirements, but the NHTSA has announced in 2006 that it would be very difficult to conclude this program.

Secondly, a new global approach, based on the PDB barrier is supported by the French since 2003 ([1], [2], [3]). This proposal is based on the current ECE R94 regulation. Three main changes are advised: a replacement of the current EEVC barrier by the PDB one, an increase of the test speed from 56 kph to 60 kph and an increase of the overlap from 40% to 50%.

Thirdly, the European VC Compat program has studied both test procedure (FWDB test and PDB test) and possible assessment criteria. The official report of these studies will be available in 2007. So, due to the evolution of the context and due to the progressive consolidation of criteria assessment, it appears necessary to review in a first step the ability of both procedures to measure the main physical aspects that govern compatibility before considering assessment criteria.

PHYSICAL ANALYSIS OF VEHICLE/VEHICLE COLLISION IN REAL CAR ACCIDENTS

Many incompatibility accident cases could be observed in real car accident. Three main physical aspects are involved during such collision: geometry, energy and force. The analysis of all incompatibility cases show that each time, at least one of them could be identified as the best probable reason of the mismatching.

First physical aspect: Geometry or structural interaction

The lack of structural interaction between the front-end of the two cars leads to an overriding phenomenon (see Figure 1).



Figure 1. Overriding phenomenon illustration.

A front-end is made of several load paths such as the longitudinals, the sub frame and sometimes a lower load path. This “geometrical aspect” must therefore allow an interaction between these different load paths of both vehicles, in order to avoid such overriding phenomena.

Second physical aspect: Energy

Among the real car incompatible accidents, it could be regularly observed that the “reference” deformation mode of the front-end is not reproduced during some vehicle/vehicle collision. The “reference” deformation mode corresponds to the optimised front-end behaviour for which the vehicle has been designed for regulation or consumers test procedure (EEVC barrier for example). Figure 2 illustrate, for two different cars, a longitudinal not deformed after a head-on car-to-car collision.

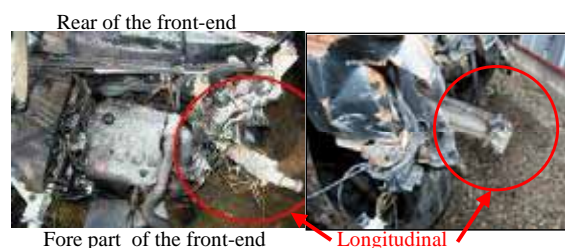


Figure 2. Energy absorption deficit illustration.

The front-end energy absorption ability is therefore under used, this will increase the passenger’s compartment intrusion further in the crash if the collision is severe.

Front-end should be able to absorb a maximum energy to limit deceleration and intrusion for the occupants. This “energy aspect” must therefore insure that each vehicle has the minimum ability to absorb its own kinetic energy.

Third physical aspect: Force

A common well known requirement in order to balance the deformation in both cars involved in the collision consists in defining:

- 1) A passenger’s compartment strength for both vehicles greater than the two front-ends one.
- 2) A passenger’s compartment strength quite equivalent for both vehicles in order to equilibrate intrusion.

Many incompatible accident cases involving two cars with an important mass difference exist (4x4 or SUV against conventional car for example). But incompatibility linked to the force can also appears without mass difference as shown in Figure 3 with a collision case between the same cars, but from different generation (1993 & 1998):



Figure 3. Incompatible passenger’s compartment strength.

The interaction force between both cars is increasing during the crash. When this force reaches the force level of the weaker passenger’s compartment, the remaining crash energy will be absorb by this vehicle. Therefore intrusion is not fairly distributed between cars after crash. This “force aspect” must therefore insure that a vehicle has a sufficient passenger’s compartment strength to limit its intrusion when opposed to another compatible vehicle.

Conclusion on these physical aspects

When considering the real car incompatible accident cases, three main physical aspects (geometry, energy, force) are involved. According to the crash severity and vehicles characteristics, one or several aspects could be observed. They could even be combined (geometry incompatibility, then incompatibility energy and at last force incompatibility). That is the reason why

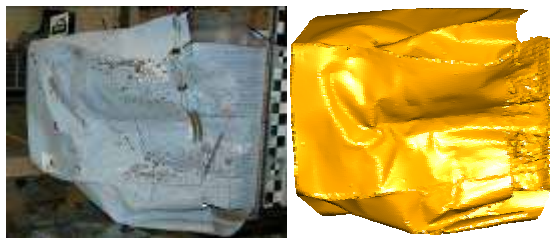
geometrical aspect is widely recognised as the priority to improve compatibility between cars. Without considering any assessment criteria with defined thresholds, a candidate test procedure for compatibility must therefore be able to measure these three aspects.

TECHNICAL REVIEW OF BOTH CANDIDATE TEST PROCEDURES

PDB test procedure

This test procedure is based on a new Progressive Deformable Barrier (PDB barrier) which has been designed to represent the average strength of modern cars. Its 700mm depth allows avoiding bottoming out effect for most vehicles. The test is performed at a speed of 60 km/h with an overlap of 50 % in order to represent an average car to car frontal accident.

The barrier deformation represents the main measure of the PDB test. This deformation is digitalised after the crash. A view of a barrier after crash and its digitalisation is given figure 4.



Note: angle view is different.

Figure 4. View of a real PDB barrier after impact and its digitalisation.

The compatibility level should be evaluated according to deformation characteristics as local perforation, deformation homogeneity, average height of deformation, average depth of deformation, etc. The starting point for developing any assessment criteria is therefore the barrier deformation after crash.

Self protection can also be evaluated with the PDB test procedure, but this aspect will not be developed in this paper [4].

FWDB test procedure

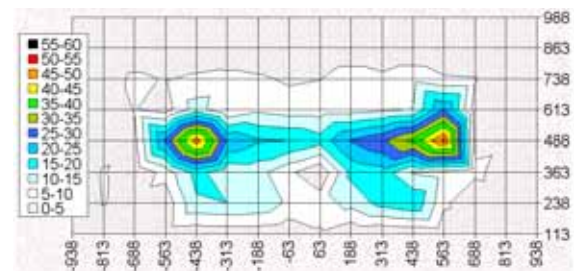
This test procedure is based on the force measured by a wall of 128 load cells. The test is conducted at a speed of 56 km/h with an overlap of 100%. Moreover, a deformable element of 300mm is placed in front of the wall in order to reduce engine load peak without spreading the force on several cells.

The evaluation of the compatibility is based on the force measure, thanks to force cartography measured by the 128 cells.

Figure 5 (a) is an example of force cartography based on the maximum force measured by each cells during the crash. Figure 5 (b) is an illustration of the same force cartography with an interpolation of the force between cells.

0	0	0	0	0	0	0	0	0	0	0	0	0	0	0	0	0	0	0	0
0	0	0	0	1	0	1	0	1	0	0	0	0	0	0	0	0	0	0	0
0	1	6	5	6	7	6	4	5	8	6	8	6	5	2	1				
0	2	5	2	12	5	9	8	8	8	9	10	25	3	2	1				
1	3	3	26	48	24	21	20	17	25	29	36	51	3	4	1				
1	5	1	7	17	11	12	6	0	16	18	9	8	6	3	0				
1	5	3	2	14	15	14	9	8	12	17	20	6	1	3	0				
2	1	1	2	1	1	2	1	4	1	0	1	1	1	1	0				

(a) View of a cartography of force



(b) View of an interpolated force cartography

Figure 5. Two different ways of presenting the results of a FWDB test: (a) Cartography of force (b) Interpolated force cartography.

Different kinds of cartography could be used. For example, at a given time of impact, with the maximum force measured by each cell during the crash, or during a particular crash period.

These cartographies are the main measures on FWDB, from which assessment criteria could be developed to evaluate force homogeneity of the front-end.

Aim of the study

The aim of the study carried out by PSA Peugeot Citroën is to evaluate the ability of each test procedure (PDB and FWDB) to “measure” the three physical compatible aspects: geometry, energy and force. Some tests and virtual testing had therefore been performed (funded by ACEA, by a French consortium or directly by PSA Peugeot Citroën as presented in table 1). The analysis consists in evaluating the sensitivity of each procedure to different loadings (barrier deformation for PDB test and force cartography for FWDB test).

Assessment criteria are not considered in this study.

METHODOLOGY USED

The methodology is mainly based on physical testing and virtual testing conducted on both procedures, PDB and FWDB. In order to have

different kinds of loadings, different types of vehicles have been used (see table 1).

Table 1. List of vehicles tested and their sources of funding.

Vehicle type	Test source
Mini car	PSA Peugeot Citroën
Small family car	PSA Peugeot Citroën
Family car #1	ACEA program
Family car #2	French program (UTAC, Renault and PSA Peugeot Citroën)
Family car #3	French program (UTAC, Renault and PSA Peugeot Citroën)
Component tests #1 on family car with lower load path	PSA Peugeot Citroën
Component tests #2 on family car without lower load path	PSA Peugeot Citroën

City car, small family car and family car tests correspond to non-modified vehicles.

Components tests are based on a family car, which has been “simplified” by removing some components difficult to simulate by virtual testing. Moreover, the influence of the lower load path has been quantified in these component tests.

All the tests performed by PSA Peugeot Citroën have also been analysed by virtual testing according to the following approach:

- 1) The PDB barrier and the deformable element for FWDB test have been validated thanks to several physical component compression tests.
- 2) The vehicle numerical model used has been validated thanks to usual crash configuration such as full-width frontal test and EEVC barrier (ECE 94 or Euro NCAP protocol).
- 3) Analysis of each physical test and improvement of the virtual testing correlation.
- 4) Additional virtual testing to complete the analysis.

As virtual testing could always been discussed, this paper will focus on presenting the physical test results and will present additional results from virtual testing only to complete the information when necessary.

CANDIDATE TEST PROCEDURE ANALYSIS

For each physical aspect (geometry, energy, force), the ability to be detected by PDB and FWDB tests will be analysed.

Capacity to detect structural interaction (Geometry aspect)

For this aspect two notions have been distinguished:

- 1) The ability to detect aggressiveness of a longitudinal as seen in a real-life car accident.
- 2) The ability to detect different front-end geometries in terms of homogeneity.

Ability to detect aggressiveness

The accident data analysis shows that family car #2 is sometimes “aggressive” in real car accidents. Three cases are presented in Figure 6.



(a) Family car #2 versus a family car



(b) Family car #2 versus a mini car



(c) Family car #2 vs. a small family car

Figure 6. Typical deformation of Family car #2 during a real-life car-to-car accident against different cars: (a) versus a family car, (b) versus a mini car (c) versus a small family car.

On the contrary, the longitudinal of the family car #3 never appears as aggressive in real-life car accidents as illustrated in Figure 7 with eight car-to-car collisions.



The deformation of the deformable element for the family car #3 is shown in Figure 11.



(a) Family car #3 after FWDB test



(b) View of the deformable element

0	0	0	0	0	0	0	0	0	0	0	0	0	0	0	0	0	0	0	0
0	0	0	0	0	0	0	0	0	1	0	0	0	0	0	0	0	0	0	0
0	1	2	4	4	6	7	4	4	6	5	6	4	4	4	4	1			
0	1	2	7	7	3	3	5	4	3	6	4	6	2	1	1				
1	1	12	28	26	20	9	6	6	7	24	25	32	20	2	1				
0	1	6	22	22	10	6	3	3	5	8	18	20	8	0	0				
1	1	6	12	14	7	4	2	3	3	7	7	12	3	0	0				
2	2	1	1	1	2	1	1	1	2	1	1	1	1	1	2	0			

(c) Maximum [0-40ms] force cartography

Figure 11. Family car #3 FWDB test results
(a) View of the car after impact, (b) View of the deformable element, (c) View of the maximum [0-40ms] force cartography.

An important bending of the crossbeam due to the stiffness of the deformable element is observed. This test may therefore be interpreted as the crossbeam is too soft whereas real car accidents indicate that the crossbeam is very stiff. In comparison with the results of the family car #2 equipped with a weak crossbeam, FWDB test does not make a significant difference between these two vehicles. The force corresponding to the cells located in front of the crossbeam is about 5 kN for the family car#2 (see figure 10c) to be compared with 7 kN (see figure 11c) for the family car#3. This is opposed to real car accidents observations previously presented.

Ability to detect homogeneity

In the same way, homogeneity will be evaluated by testing the different vehicles (see table 1) against PDB and FWDB and then analysing the response of the barrier deformation or force cartography measured.

PDB tests results

The mini car front-end has been widely deformed. Intrusions in the passenger's compartment are also

observed due to the pushing of the engine on the dashboard and the front left wheel on the sill.



Figure 12. Mini car - PDB test results.
The barrier has been perforated. This result is not surprising due to the weak crossbeam present on this vehicle. Homogeneity of the front-end appears therefore very limited.

The small family car front-end has also been strongly deformed. In this test too, intrusion in the passenger's compartment could be observed due to the engine and front left wheel.



Figure 13. Small family car - PDB test results.

In that test, the barrier deformation does not suffer from local perforation and the homogeneity seems to be very good. Notice that this small family car is equipped with an advanced lower load path.

The result of the PDB test with the family car #1 is shown in Figure 14 has already been presented by ACEA in 2004.



Figure 14. Family car #1 - PDB test results.

The barrier deformation shows a large localised deformation due to the very stiff crossbeam of this vehicle but without local perforation. Homogeneity of the barrier deformation is therefore not quite good. The front-end is also well deformed with a contribution of the engine. Passenger's compartment intrusion could also be noticed.

The component test #1 corresponds to a family car "simplified" with a lower advanced load path.

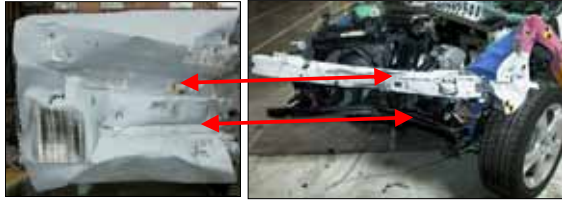


Figure 15. Component test #1 PDB test results.

As shown in Figure 15, the barrier deformation clearly detects the pushing of the stiff upper crossbeam and lower crossbeam. The lower advanced load path is therefore well detected. Barrier deformation homogeneity is judged as relatively good when knowing that no bumper, headlight and bonnet were present during this test.

The component test #2 corresponds to the same test that the previously one, except the removal of the lower advanced load path.

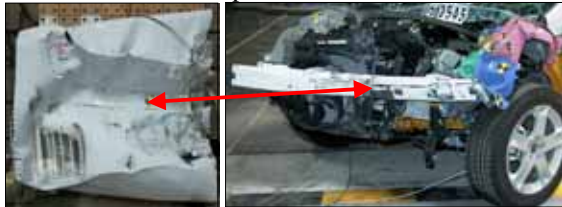


Figure 16. Component test #2 - PDB test results.

The barrier deformation clearly detects the advanced load path removal. The barrier is indeed less deformed at the bottom and the deformation due to the upper crossbeam is deeper than previously. The barrier deformation homogeneity is therefore less good than with the advanced lower load path.

The results of this test series confirm that the PDB barrier is a very good validated tool to check front-end behaviour. Changes in the front-end design are clearly detected by the barrier deformation. For information, a pushing of the engine has also been observed during these component tests #1 and #2.

FWDB tests results

For FWDB tests, as there exist many ways to display force cartographies, tests results will be presented in several manners:

- 1) Two types of cartography display will systematically be shown. The first display will be the maximum force measured by each cells without any force interpolation. The second will be the same measurement but with an interpolation.
- 2) Moreover, as the TRL proposes now to analyse the force only on the first 40ms of the crash, force cartography will first be drawn during the

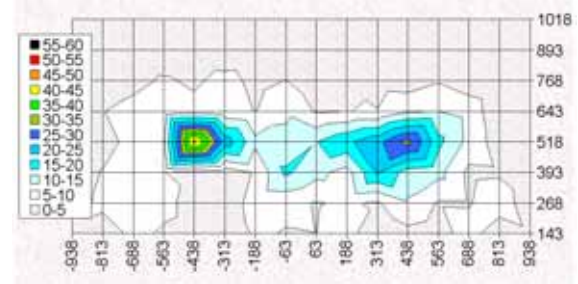
entire crash and secondly during the first 40ms of the crash.

Force cartographies during the entire crash

The mini car cartography is characterised by the pushing of the longitudinals. The maximum forces measured on the left side and on the right side are quite different (see Figure 17).

0	0	0	0	0	0	0	0	0	0	0	0	0	0	0	0	0	0
0	0	0	0	0	0	1	1	1	0	0	0	1	0	0	0	0	0
1	0	3	6	4	7	3	5	2	5	3	2	4	2	0	0	0	0
0	5	8	6	7	6	5	9	4	5	5	9	10	8	1	2	0	0
1	2	7	10	46	23	11	11	15	19	23	31	16	8	2	0	0	0
0	5	5	5	3	2	5	16	12	8	20	13	12	4	4	0	0	0
1	7	6	7	2	3	6	6	5	6	4	9	5	4	9	1	0	0
3	0	7	4	2	1	6	5	5	7	1	4	2	8	0	4	0	0

(a) Mini car maximum force cartography



(b) Maximum force cartography with force interpolation

Figure 17. Mini car FWDB test results (a) Maximum force cartography (b) Maximum force cartography with force interpolation.

The crossbeam seems to be detected on the figure 17(a) in spite of a very low bending stiffness. This is due to the engine pushing that is more visible on the figure 17(b) on the right side.

The homogeneity of the front-end seems therefore quite bad.

For information, as usual in FWDB test, the car front-end post test deformation is very limited. The front wheels didn't even touch the sills, as shown in Figure 18.



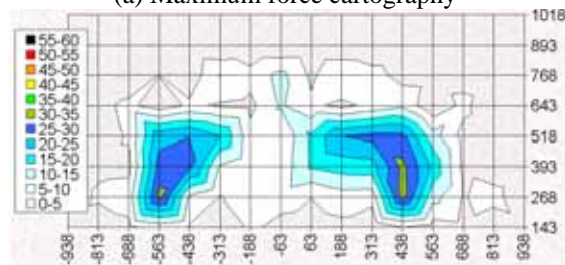
Figure 18. Post impact deformation of the Mini car after FWDB test.

The small family car cartography is characterised by the pushing of the longitudinals and by the vertical connections between the lower advanced load paths and the longitudinals. The upper crossbeam is nevertheless not detected although it presents a good stiffness in bending. The engine

pushing on the right side is also visible (see Figure 19).

0	0	0	0	0	0	0	0	0	0	0	0	0	0	0	0	0	0	0	0
0	0	0	0	1	0	0	0	1	1	0	1	1	1	1	1	0	0	0	0
1	0	1	5	2	10	7	12	4	10	7	3	2	3	2	1	0	0	0	0
1	4	6	2	6	4	4	11	6	4	6	9	0	7	0	2	0	0	0	0
0	2	6	23	25	20	7	5	16	25	27	27	12	3	1	0	0	0	0	0
0	3	4	27	26	9	6	7	16	17	18	31	19	4	1	0	0	0	0	0
0	6	7	31	9	5	7	7	5	8	7	32	12	5	7	0	0	0	0	0
2	0	4	7	5	0	6	3	3	4	0	5	3	4	0	3	0	0	0	0

(a) Maximum force cartography



(b) Maximum force cartography with force interpolation

Figure 19. Small family car test results (a) maximum force cartography, (b) maximum force cartography with force interpolation.

The homogeneity of the front-end appears therefore to be better than the previous mini car one.

For information, as usual in FWDB test, the car front-end post test deformation is very limited. The front wheels didn't even touch the sills as illustrated in Figure 20.

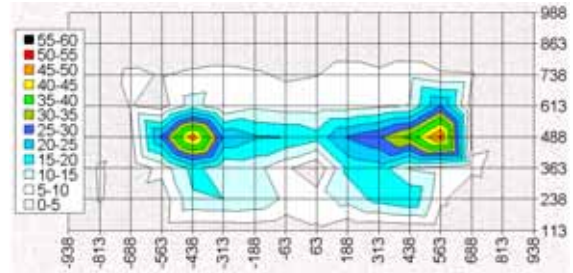


Figure 20. Post impact deformation of the Small family car after FWDB test.

The cartography of the family car #1 FWDB test is characterised by its very stiff crossbeam and by its lower load path which are well detected (see Figure 21).

0	0	0	0	0	0	0	0	0	0	0	0	0	0	0	0	0	0	0	0
0	0	0	0	1	0	1	0	1	0	0	0	0	0	0	0	0	0	0	0
0	1	6	5	6	7	6	4	5	8	6	8	6	5	2	1	0	0	0	0
0	2	5	2	12	5	9	8	8	8	9	10	25	3	2	1	0	0	0	0
1	3	3	26	48	24	21	20	17	25	29	36	51	3	4	1	0	0	0	0
1	5	1	7	17	11	12	6	0	16	18	9	8	6	3	0	0	0	0	0
1	5	3	2	14	15	14	9	8	12	17	20	6	1	3	0	0	0	0	0
2	1	1	2	1	1	2	1	4	1	0	1	1	1	1	0	0	0	0	0

(a) Maximum force cartography



(b) Maximum force cartography with force interpolation

Figure 21. Family car #1 test results (a) maximum force cartography (b) maximum force cartography with interpolation.

The pushing of the engine is not quite visible. The homogeneity of the front-end seems therefore better than the mini car one, but worse than the small family car one.



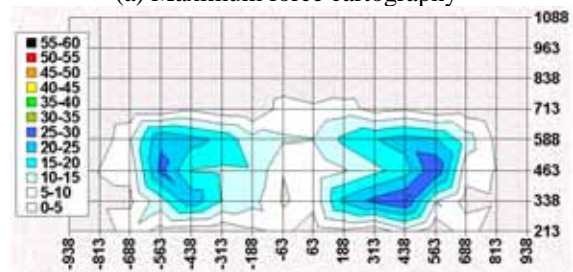
Figure 22. Post impact deformation of the Family car #1 after FWDB test.

Here again, as usual in FWDB test, the car front-end post test deformation is very limited. The front wheels didn't even touch the sills (see Figure 22).

The component test #1 with an advanced lower load path shows the longitudinals and the lower load path on the cartography. The engine, the rigid upper and lower crossbeams are however not clearly visible (see Figure 23).

0	0	0	0	0	0	0	0	0	0	0	0	0	0	0	0	0	0	0	0
0	0	0	0	0	0	0	0	0	0	0	0	0	0	0	0	0	0	0	0
0	0	0	0	0	1	0	2	1	0	0	0	0	0	0	0	0	0	0	0
0	0	1	1	4	1	0	7	6	7	3	4	1	2	0	0	0	0	0	0
0	1	10	24	22	19	11	11	10	16	20	22	21	13	4	1	0	0	0	0
0	5	6	26	15	14	14	5	6	9	14	17	29	7	5	1	0	0	0	0
0	4	4	13	23	15	12	5	6	21	26	30	10	3	4	1	0	0	0	0
2	1	9	3	1	1	4	6	2	4	1	8	1	8	1	4	0	0	0	0

(a) Maximum force cartography



(b) Maximum force cartography with force interpolation

Figure 23. Component test #1 FWDB test results (a) maximum force cartography, (b) maximum force cartography with interpolation.

The homogeneity of the front-end appears therefore to be close to the small family car one. As usual, the front-end deformation is very limited without contact between the front wheels and the sills as shown in Figure 24.

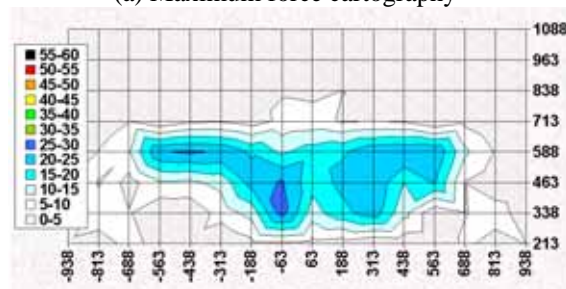


Figure 24. Post impact deformation of the Component test #1 after FWDB test.

The component test #2 is very interesting (see Figure 25). Firstly, the removal of the lower load path is well detected compared with the previous component test. Secondly, the crossbeam seems to be weaker than previously even though it has not been changed. This can be explained one time more by the engine. Indeed, as the absorption energy of the front-end has decreased due to the removal of the lower load path, the deformation of the front-end is quite higher, thus leading to a higher pushing of the engine on the crossbeam and therefore on the wall.

0	0	0	0	0	0	0	0	0	0	0	0	0	0	0	0	0	0	0	0
0	0	1	0	0	0	1	1	0	0	2	0	0	1	0	0	0	0	0	0
0	0	0	1	0	2	3	5	4	5	2	1	0	1	1	0	0	0	0	0
1	1	5	1	4	4	2	6	7	4	5	5	0	3	0	1	0	0	0	1
0	5	10	25	26	24	19	14	18	19	24	25	25	11	5	1	0	0	0	0
1	10	3	9	9	11	22	26	17	22	24	15	20	5	1	0	0	0	0	0
1	8	5	1	1	7	12	27	13	18	23	12	1	5	8	2	0	0	0	0
4	3	6	3	3	0	3	4	3	2	0	1	1	6	3	5	0	0	0	0

(a) Maximum force cartography



(b) Maximum force cartography with force interpolation

Figure 25. Component test #2 FWDB test results (a) maximum force cartography, (b) maximum force cartography with interpolation.

As usual, the front-end deformation remains limited without contact between the front wheels and the sills as shown in Figure 26.



Figure 26. Post impact deformation of the Component test #2 after FWDB test.

At last, the homogeneity of the component test #2 front-end appears good. Compared the component test #1 equipped with lower load path, the component test #2 homogeneity could even be judged as better. This is opposite to the common understanding of most of the stakeholders involved in Compatibility research groups. According to them, multiple load paths with vertical and horizontal connections should indeed improve the ability of a front-end to interact with others.

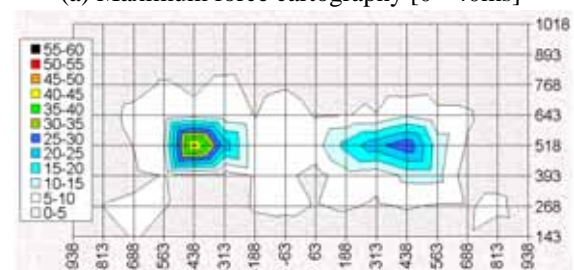
Force cartographies during the first 40ms

This is the new orientation given by TRL in March 2006 during EEVC WG15 / VC Compat meeting.

The mini car cartography is not really affected by this evolution. The engine pushing is less visible, but still exists (see Figure 27).

0	0	0	0	0	0	0	0	0	0	0	0	0	0	0	0	0	0	0	0	0
0	0	0	0	0	0	0	0	1	0	0	0	0	0	0	0	0	0	0	0	0
0	0	2	6	4	7	3	4	1	5	2	2	3	2	0	0	0	0	0	0	0
0	2	7	6	7	6	5	9	4	5	5	9	6	6	0	1	0	0	0	0	1
0	1	5	10	46	23	6	5	8	17	23	29	12	4	1	0	0	0	0	0	0
0	2	4	5	3	2	5	6	3	8	6	11	12	2	2	0	0	0	0	0	0
0	5	6	5	2	2	6	6	5	6	4	5	5	4	7	0	0	0	0	0	0
2	0	6	2	1	0	2	2	2	2	0	2	1	5	0	2	0	0	0	0	2

(a) Maximum force cartography [0 - 40ms]



(b) Maximum force cartography [0 - 40ms] with force interpolation

Figure 27. Mini car FWDB test results limited to [0 - 40ms] (a) maximum force cartography, (b) maximum force cartography with force interpolation.

It is exactly the same for the small family car (see Figure 28).

Multiple load paths are clearly penalized in this case.

Conclusion

Without limitation of time regarding the force analysis, the results of this test series show that FWDB test is able to detect several changes in the front-end design such as the presence or not of a lower load path or vertical connection between it. Nevertheless, these results also show that the engine behaviour is not comparable in all tests. For mini and small family cars, a pushing of the engine is visible, which may give a false conclusion in the homogeneity of the front-end. It is not the case for larger cars. Moreover, when removing a lower load path, homogeneity is detected as to be better. This is due to an increase of the engine pushing, permitted by the decreasing of the front-end absorption energy.

The limitation of the analysis to the first 40ms of crash enables to limit the influence of the engine pushing. It was particularly important for both component tests with and without lower advanced load path, since the engine pushing is not visible even when the lower load path is removed. Nevertheless, this time limitation also leads to a main drawback. It limits one more time the front-end deformation corresponding to the force analysis. Indeed, virtual testing reveals that 40ms correspond to a very limited deformation of the longitudinal as illustrated in Figures 32 to 35.



Figure 32. 120 mm longitudinal deformation for the Mini car at 40ms.

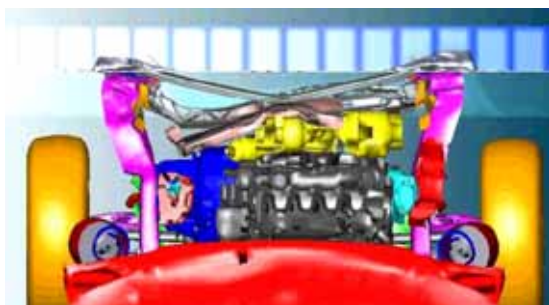


Figure 33. 90 mm longitudinal deformation for the small family car at 40ms.

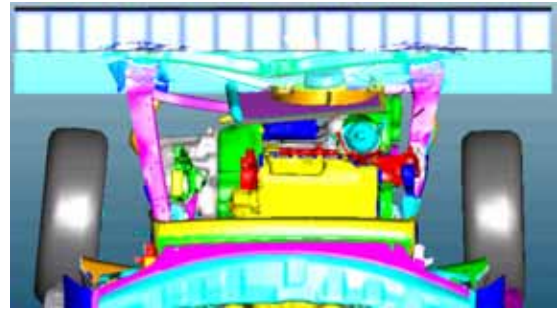


Figure 34. 140 mm longitudinal deformation for the test component #1 (with advanced lower load path) at 40ms.

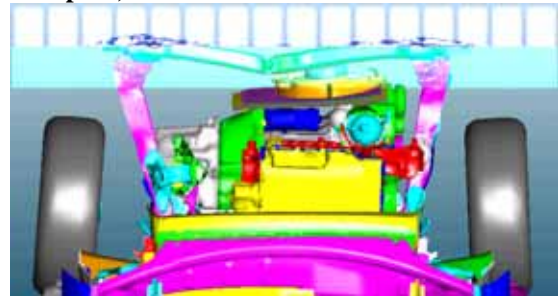


Figure 35. 150 mm longitudinal deformation for the test component #2 (without advanced lower load path) at 40ms.

Moreover, this limitation raises a problem for cars not equipped with advanced lower load path (like the Family car #1 one), because these kind of multiple load path disappears in the cartography and would be therefore penalised in terms of homogeneity.

The problem seems difficult to solve. The aim is to avoid engine pushing. The 40ms limitation goes in the right direction even if engine pushing still exist for mini and small car, but it leads to a very limited front-end deformation, about 90 and 150 mm. Is it sufficient to evaluate geometry interaction in a usual car-to-car accident which highlights incompatible problems?

Such difficulties do not exist in PDB test, since the front-end is deformed significantly for all kind of cars.

The PDB test appears therefore to be more able to detect various type of front-end design than the FWDB test. On top of that, homogeneity changes are fully in line with the common understandings of the main stakeholders involved in Compatibility research programmes.

Capacity to detect energy absorption (energy aspect)

One target of this aspect is to evaluate the ability for a front-end to absorb energy and to detect energy incompatible phenomenon. The better example is given by a longitudinal which could be underused in a car-to-car accident (see figure 2 and 6).

PDB test

The principle is to evaluate the energy level absorbed by the barrier, thus enables to estimate the energy level absorbed by the vehicle.

This evaluation is made from the barrier digitalisation. A theoretical compression barrier law is needed for the different barrier strength zones. The result obtained remains therefore an estimation. However, this method reveals significant changes of the energy level absorbed by the barrier. Results obtained for the two component tests are given in figure 36.

The barrier energy absorbed for the component test #1 with advanced lower load path represents 32.1% of the kinetic crash energy.

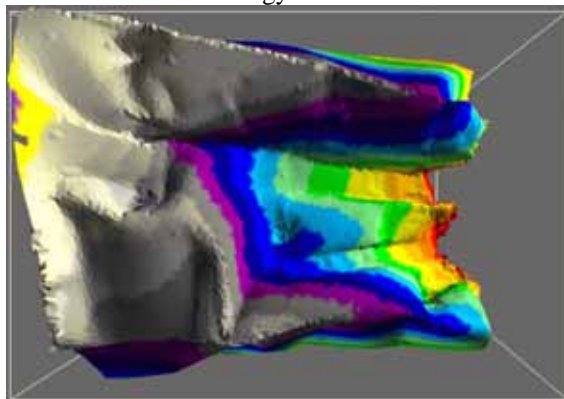


Figure 36. Component test #1 barrier deformation.

For the component test #2 without lower load path, the barrier energy absorption corresponds to 38.4% of the kinetic crash energy (see Figure 37).

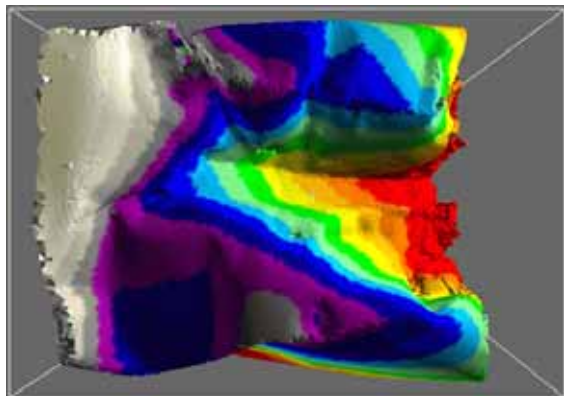


Figure 37. Component test #2 barrier deformation.

Without lower load path, the barrier deformation is deeper.

This results show that with an indicator of this type, PDB test procedure is able to evaluate the level of energy absorbed by the vehicle, and therefore able

to check if this level is sufficient to absorb its own kinetic energy in a vehicle/vehicle frontal collision.

FWDB test

As the deformable element is not covered by an aluminium plate, a standard easy digitalisation is impossible.

The estimation of the energy absorption will first require a covering of all the different pieces of the barrier, but will stay even though difficult, because the second honeycomb layer blocks have been observed as unstable during the different tests carried out up to now.

However, in order to have a deformable element energy absorption order of size, ACEA has manually digitalized the barriers of three FWDB test carried out on the family car #1 model.

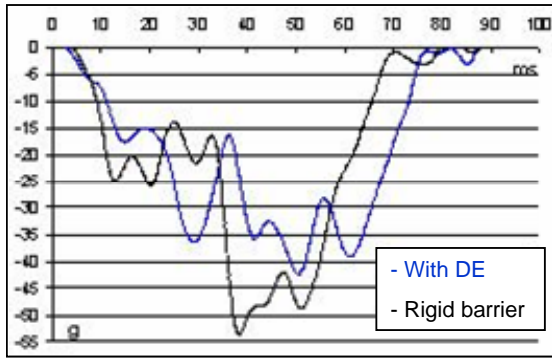
Table 2. Barrier energy absorption for the Family car #1 tests.

Crossbeam	Energy in the barrier	Kinetic energy	% Ek in the barrier
Weak	57 kJ	197 kJ	29%
Serial	59 kJ	195 kJ	30%
Serial test 2	59 kJ	196 kJ	30%
Stiff	60 kJ	196 kJ	31%

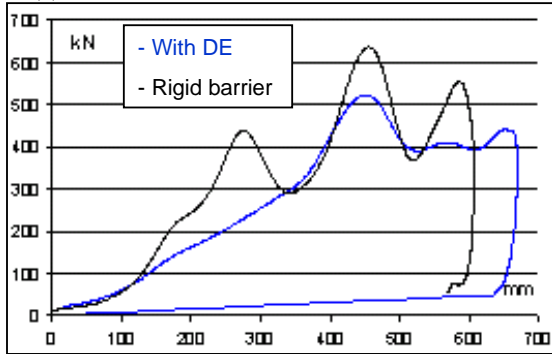
The result reveals that the energy absorbed by deformable element is far from being neglected. This is confirmed by virtual testing.

For instance, the energy absorbed by the deformable element for the small family car corresponds to “47.8”kJ.

For information, virtual testing performed with and without deformable element show that the severity of the FWDB test is decreasing when deformable element is present as seen on figure 38 and Table 3.



(a) Deformable Element effect on deceleration



(b) Deformable Element effect on global force

Figure 38. Effect of the deformable element on (a) deceleration, (b) global force.

Table 3. Influence of the deformable element.

Barrier	Max accel.	Max Disp.
With DE	42,5 g	690 mm
Rigid	55,5 g	600 mm
Variation w/wo DE	+ 23 %	+ 15 %

Without any deformable element, the maximum deceleration is 23% higher and the maximum vehicle deformation is 15% increased.

Deformable element could therefore not be considered as non influent on the crash severity. This point must be highlighted when considering the evaluation of occupant restraint system with this test.

Capacity to detect force (force aspect)

PDB test

If the global force during the whole crash is needed for a particular reason, a dynamometrical wall behind the PDB barrier could be implemented. On a physical point of view, this maximum global force does not correspond to the maximum force that the passenger's compartment is able to support. The severity of the PDB test is indeed sufficient to deform totally the vehicle front-end and to begin loading the passenger's compartment. But this severity does not allow checking the maximum force of the passenger's compartment.

FWDB test

The measure of the global force during the crash is obviously possible with this procedure. Nevertheless, the question raised is to know how to interpret it, since the vehicle front-end is so little deformed. The maximum force could therefore not be considered as the maximum force that the front-end could support. And moreover, no information can be obtained with this test concerning the passenger's compartment force. This global force does therefore not be interpreted as a real characteristic of the front-end or passenger's compartment force. This information does not seem to be relevant.

DISCUSSION ON ADVANTAGES AND DRAWBACKS OF BOTH PROCEDURES

Synthesis of the previous analysis

Following the results of this study, the main results or observations could be resumed for each test procedure.

PDB test

The PDB barrier is confirmed to be a very relevant tool to evaluate structural interaction. Indeed, the real car accident aggressiveness observations concerning the behaviour of a crossbeam or a longitudinal are well reproduced during the PDB test. Moreover, PDB deformation is also able to detect different kind of front-end design, with or without lower load path for instance. It should be highlighted that as the PDB test completely deforms the front-end of the vehicle tested, the lower load path is detected even if it is located far from the beginning of the front-end. The energy absorbed by the barrier after the test can also be estimated from a theoretical compression barrier law. This is an important aspect since this is the only way to evaluate the front-end energy absorption ability of the vehicle. As the deformation mode of the front-end during PDB test is very close to real car accident, this evaluation is all the more relevant.

Finally, the maximum force during the crash could be measured by a dynamometrical wall to be located behind the barrier. For most of the cars, this force corresponds to an average force between the front-end deformation force and the maximum force that the passenger's compartment is able to support.

The three physical aspects involved in incompatibility phenomena could therefore be measured with the PDB test in consistence with the analysis of the real-life car accidents.

FWDB test

The comparison of the front-end deformation mode between the real car accident and FWDB test for same car shows several differences. An important point is the crossbeam behaviour, since a rigid crossbeam detected as such in the real car accident is detected as too soft in the FWDB test (case of the family car #3). Another difficulty concerns the contribution of the engine. According to the size of the car, the engine pushing is different. For instance, the engine pushing is not visible for a large car contrary to what happens for a small car. A good example is the crossbeam of the mini car (see figure 17) which is not detected as weak thanks to the engine pushing. It is even so the case and this is also confirmed by the PDB test result (see figure 12). The engine has therefore an influence not comparable on the force cartography, depending on the car size. This could sometimes lead to wrong conclusions.

The analysis limited to the first 40ms for the force measurement goes in the right direction since the effect of the engine is limited. But in that case, lower load paths located far from the front-end (such as the family car #1 one) are not detected and will therefore be penalized. Moreover, front-end deformation corresponding to 40ms is very limited. The longitudinal deformation is about 120mm. The front wheels do not move back. Is it a sufficient deformation to evaluate the structural interaction that could occur in a car-to-car accident?

To conclude, FWDB is therefore able to detect some changes in the front-end design but could lead to wrong conclusion for some cases (engine effect and lower load path are not always detected). Energy absorption is not measurable and not relevant for assessment in the FWDB test since the front-end is not totally deformed. The maximum force of the FWDB is available. But as for the energy, its interpretation is difficult due to the low deformation of the front-end. As far as the virtual testing are concerned, the instability of the second layer observed in physical tests is very difficult to correlate.

Possible actions to improve both test procedure

Geometry

No major problem has been detected for the PDB test. Several additional reproducibility tests may be realized to confirm the stability of the results already observed during 2004 with the family car #1 tests carried out within ACEA.

Concerning the FWDB test, it appears difficult to avoid the engine pushing for all vehicles. In order to have a comparable influence of the engine for all, a possible improvement could be to increase the

front-end deformation. This could be obtained by a modification of the procedure in terms of deformable element stiffness, depth or/and impact speed. An improvement of the deformable element appears also necessary to detect correctly a rigid crossbeam in consistence with the real car accident.

Energy

The level of energy absorbed by the PDB barrier is measurable. This requires to define a theoretical barrier compression law from PDB characteristics and dynamical PDB compression tests. Another aspect could be to improve the digitalisation barrier procedure. It seems indeed important to decide for instance if the edges of the barrier should be taken into account or not.

The FWDB procedure is not able to evaluate this aspect. Covering the deformable element by an aluminium plate could be helpful, but it could also affect the force measurement. Moreover, even if this measure was available, the interpretation is not relevant since the front-end is not totally deformed. Due to the lack of energy measurement, another point to highlight is the possibility to limit intentionally the energy capability of the front-end in order to increase the engine pushing and therefore improve the homogeneity as it is measured in the FWDB test. Such an evolution would be counterproductive in the real car accident where the energy aspect could not be neglected.

Force

The maximum PDB force corresponds to an average force located between the front-end deformation force and the maximum force that the passenger's compartment is able to support. This observation is a general trend.

For FWDB test, the maximum force does not help to evaluate the compatibility regarding the force since this measured force only corresponds to the beginning front-end deformation.

CONCLUSION

The aim of this paper was to conduct a methodological and physical analysis of both candidate test procedures in order to evaluate their ability to measure the three incompatibility physical phenomenon involved in real world incompatibility (geometry, energy and stiffness mismatching).

This study, based on physical and virtual testing, with or without lower load path, enables to draw significant outcomes:

- 1) Both procedures can detect a geometry change such as the absence of load path. However, for the FWDB test, a rigid crossbeam for a large car should not be detected as enough rigid contrary to real world accident observation. This is due to the high stiffness of the second

layer of the deformable element. On the contrary, a weak crossbeam for a mini car would not be detected so weak due to the engine pushing which is systematically taken in account in the force analysis for small cars.

Moreover, the limitation of the force analysis at 40ms will penalise cars not equipped with advanced lower load path as the family car #1.

This point is directly link to the procedure itself.

- 2) Both procedures can measure a global force. However, its interpretation for the FWDB test is difficult due to the very limited deformation of the front-end sustained in this test.
- 3) Only the PDB test is able to draw up an energy absorption statement which is the only way to evaluate the car crash severity and the front-end absorption capability. For the FWDB test, this point represents a major difficulty because energy absorption by deformable elements is significant, about 50kJ, thus decreasing the severity of the test.

No inconsistencies have been found for the PDB test when comparing the physical and virtual testing with the real word accident. This means that the PDB barrier seems to be a good tool to evaluate compatibility. The next step could therefore consist in confirming its reproducibility.

Several difficulties appear concerning the FWDB test. Improvements are needed on the procedure. The deformable elements are mainly concerned. Firstly because inconsistencies have been observed with the real-life car accident and secondly because the instability of the second layer honeycomb blocks makes virtual testing very difficult to carried out. They could therefore be changed in terms of stiffness or/and depth. Another point is also to solve the difficulties linked to the relevancy of the force measured, for instance in the case of rigid plate trolley test. As this point is well known and often discussed, it has not been highlighted in this paper but this problem still exists.

When considering all the results obtained, the PDB test appears therefore to be the best test procedure to evaluate a maximum of physical aspects with only one test.

A general rule to keep in mind is that developing assessment criteria appears completely useless until all test procedure problem have not been solved.

The results of this paper show that assessment criteria could therefore now be studied concerning the PDB test. For FWDB test, further improvements are still needed on the procedure itself before being able to work on assessment criteria.

ACKNOWLEDGMENTS

The authors wish to thank all the labs and researchers that where involved in this study.

REFERENCES

[1] Delannoy P., Martin T., Castaing P., « Comparative Evaluation of Frontal Offset Tests to Control Self and Partner Protection », Enhanced Safety of Vehicles Conference, Paper No. 05-0010, June 2005.

[2] Delannoy P., Faure J., Coulombier D., Zeitouni R., “New Barrier Test and Assessment Protocol to Control Compatibility, SAE paper no. 2004-01-1171

[3] PDB test protocol - EEVC WG15 website, www.eevc.org.

[4] Coulombier D., Zeitouni R., « Consequences on self-protection for a car designed with PDB », Compatibility in road traffic conference, Dresden October 2005

SECOND REPORT OF RESEARCH ON STIFFNESS MATCHING BETWEEN VEHICLES FOR FRONTAL IMPACT COMPATIBILITY

Shigeru Hirayama

Taisuke Watanabe

Kazuhiro Obayashi

Tomosaburo Okabe

Nissan Motor Co., Ltd.

Japan

Paper Number 07-0261

ABSTRACT

Through the global research of the past decade, it can be said that fundamental issues of frontal impact compatibility have been almost fully understood. The first step is to enhance the structural interaction between the front-end structures of colliding vehicles and the next step is to help match the stiffnesses between vehicles. In the previous ESV conference, the authors reported the results of a study in which stiffness matching in SUV-to-car frontal impact was accomplished by increasing the car's stiffness only[9]. In this paper, the stiffness matching in SUV-to-car frontal impact will be accomplished by only reducing the SUV's stiffness using FE (finite element) vehicle models. These two studies would contribute to furthering the research for more practical compatibility countermeasures.

INTRODUCTION

Automobile manufacturers' continuous efforts to improve vehicle safety performance in cooperation with the introduction of various vehicle safety standards and the new car assessment programs have led to significant improvement of vehicle self-protection performance over the past years. As a consequence, the improvement of impact compatibility for partner-protection is recognized as an indispensable approach to further help enhance vehicle safety performance.

Many studies in the past several years have indicated that the fundamental issues of frontal impact compatibility were to enhance structural interaction between the front-end structures of colliding vehicles as the first step, and to help match stiffnesses

between vehicles as the subsequent necessary step. On the basis of this philosophy, various approaches to improve frontal impact compatibility have been proposed and discussed around the world [2]-[8].

The authors have been focusing their attention on the stiffness matching issue in the case where good structural interaction was ideally achieved and reported the results of a study in which stiffness matching in SUV-to-car frontal impact was tried only by increasing the car's stiffness[9]. The results were reported in the previous ESV conference. The conclusion of that study was that achieving good stiffness matching between a SUV and a car only by increasing car's stiffness was unrealistic due to substantial weight increase by the necessary reinforcement of the body structure.

On the other hand, NHTSA(National Highway Traffic Safety Administration) is now studying the effect of reducing the SUV's stiffness on stiffness matching by the introduction of new metrics called KW400[10]. In this paper, stiffness matching in SUV-to-car frontal impact (see Table 1) was performed only by reducing the SUV's stiffness to a certain level of KW400. In order to focus on stiffness matching, it was assumed that structural interaction between the vehicles is ideal. The study was done using FE vehicle models(see Figure 1). The FE vehicle models were respectively correlated with fixed-barrier physical impact tests.

Table 1.
SUV-to-car impact conditions

Vehicle type	SUV	Car (Middle-sized sedan)
Curb mass	2500kg	1400kg
Overlap ratio	Full overlap	



Figure 1. FE vehicle models.

INFLUENCE OF KW400 ON VEHICLES

NHTSA's report shows that KW400 is calculated as shown in Figure 2 using a vehicle force-deformation curve obtained in a 56km/h full overlap frontal impact test. Although the appropriate upper limit of KW400 for SUVs has not been decided yet, NHTSA indicates that the occupant injury probability in impacts between vehicles whose KW400 is between 1300N/mm and 1700N/mm is lower than that in impacts between other vehicles[11]. Therefore in this study, it was assumed that the SUV's KW400 shall not exceed 1700N/mm.

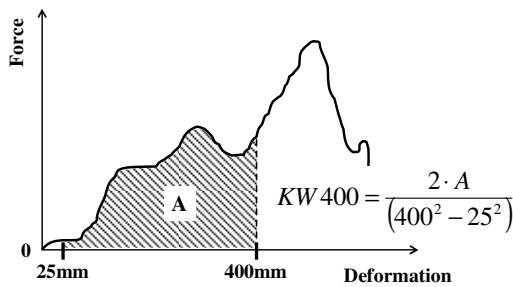


Figure 2. Dification of KW400.

Figure 3 represents the force-deformation curve of the SUV shown in Table 1, which is obtained from the result of FE simulation for a 56km/h full overlap impact test. The SUV's KW400 is approximately 2400N/mm and larger than the assumed upper limit of 1700N/mm. The measure that was considered was to decrease the KW400 below the upper limit.

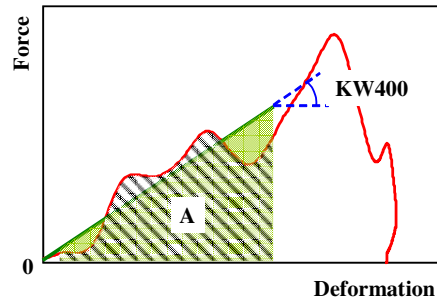


Figure 3. Force-deformation curve of SUV in 56km/h full overlap impact.

According to the KW400 definition, it is expected that reducing the front longitudinal stiffness where vehicle deformation ranges from 0mm to 400mm will lead to the achievement of preferable KW400 values. However this causes the reduction of energy absorption in the engine compartment. As a result, it is believed that passenger compartment intrusion increases and occupant injury indexes increase. The increase in occupant injury results from a combination of delay in occupant restraint and changes in allowable relative occupant displacement due to deformation and intrusion.

Therefore reducing the front longitudinal stiffness to decrease the KW400 has to be combined with some of the following measures to improve vehicle safety performance.

- To prevent increased passenger compartment intrusion
 - Prevent the energy absorption in engine compartment from decreasing by means of extending vehicle front overhang.
 - Increase vehicle stiffness where vehicle's deformation is over 400mm.
- To prevent increased relative displacement of occupant to vehicle
 - Improve the restraint system performance.

At the same time, automotive manufacturers generally take into consideration the following viewpoints when deciding on which measures should be adopted.

- Minimizing vehicle front overhang in order to maintain vehicle exterior design flexibility and good handling performance among other factors.
- Keeping cabin strength below a certain level to

avoid the increase of relative displacement of occupant to vehicle.

- Technical limitations associated with improving restraint system performance.

Based on the above-mentioned factors, a set of measures to decrease the SUV's KW400 below 1700N/mm without an increase of occupant injury indexes in a 56km/h full overlap impact was determined using FE simulation. The result is shown in Table 2 and Figure 4.

Table 2.

A set of measures to decrease the SUV's KW400

Front overhang	Increased
Restraint system	Improved
Vehicle force-deformation curve	See Figure 4

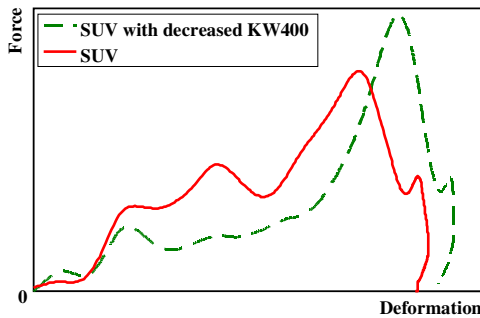


Figure 4. Force-deformation curve in 56km/h full overlap impact of SUV with decreased KW400.

EFFECT OF KW400 ON STIFFNESS MATCHING IN SUV-TO-CAR IMPACTS

In the previous chapter, a set of measures to achieve the preferable SUV's KW400 from a compatibility viewpoint without an increase of occupant injury indexes in a 56km/h full overlap impact was shown. As a next step, we compared whether the car's deformation decreased or not in a SUV-to-car frontal impact with an SUV that had preferable KW400 values.

At the beginning, the following basic study was conducted.

When an SUV with a mass m_1 impacts a car with a mass m_2 at a relative speed of V , the deformation energy of both vehicles E , is given by:

$$E = \frac{1}{2} \cdot \frac{m_1 \cdot m_2}{m_1 + m_2} \cdot V^2 \quad (1).$$

In the above equation, it is assumed that the impact is perfectly inelastic. When the force-deformation curves of both vehicles are known, the deformation of each vehicle in this impact can be derived from the relationship identified in the hatched area of Figure 5 is equal to E .

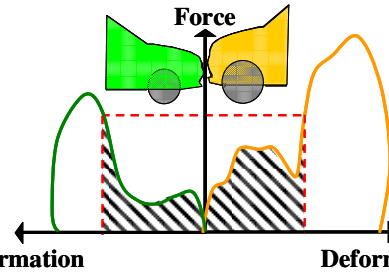


Figure 5. Prediction method of vehicle deformation.

Using the above-mentioned method, the deformation of each vehicle was predicted. Additionally, prediction of two impact scenarios using different impact speeds was performed. The detailed impact conditions are shown in Table 3. The prediction of Case 1 was done using force-deformation curves obtained in 56km/h full overlap impact FE simulations. In contrast, in the prediction of Case 2, a force-deformation curve of a car was obtained in a 70km/h full overlap impact FE simulation because it was expected that the car's deformation in Case 2, SUV-to-car impact, was larger than that in a 56km/h full overlap impact.

Table 3. SUV-to-car impact conditions

Case	1		2	
	SUV	Car (Middle-sized sedan)	SUV	Car (Middle-sized sedan)
Curb mass	2500kg	1400kg	2500kg	1400kg
Impact speed	32km/h each vehicle		56km/h each vehicle	
Overlap ratio	Full overlap		Full overlap	

Figure 6 shows the prediction result. In both Cases 1 and 2, the car's deformations were larger than SUV's deformations. These results are not considered compatible.

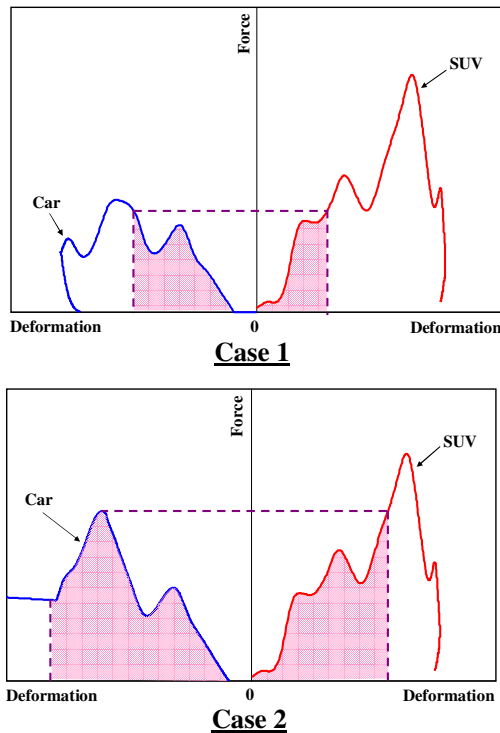


Figure 6. Deformation prediction of SUV and car.

Next, the deformation of each vehicle when a SUV with decreased KW400 was modeled (by installing the measures shown in the previous chapter), and the impacts on a car were predicted. Also, prediction of two impact scenarios using different impact speeds was performed.. The detailed impact conditions are shown in Table 4.

Table 4. SUV-to-car impact conditions

Case	3		4	
Vehicle type	SUV with decreased KW400	Car (Middle-sized sedan)	SUV with decreased KW400	Car (Middle-sized sedan)
Curb mass	2500kg	1400kg	2500kg	1400kg
Impact speed	32km/h each vehicle		56km/h each vehicle	
Overlap ratio	Full overlap		Full overlap	

The prediction result is shown in Figure 7. The car's deformation in Case 3 decreases in comparison with that in Case 1 and compatibility is improved. However the car's deformation in Case 4 increases in comparison with that in Case 2 and compatibility is deteriorated. The reason of this deterioration is that the energy absorbed by the SUV at this

comparatively high impact speed has decreased due to measures meant to achieve the preferable SUV's KW400.

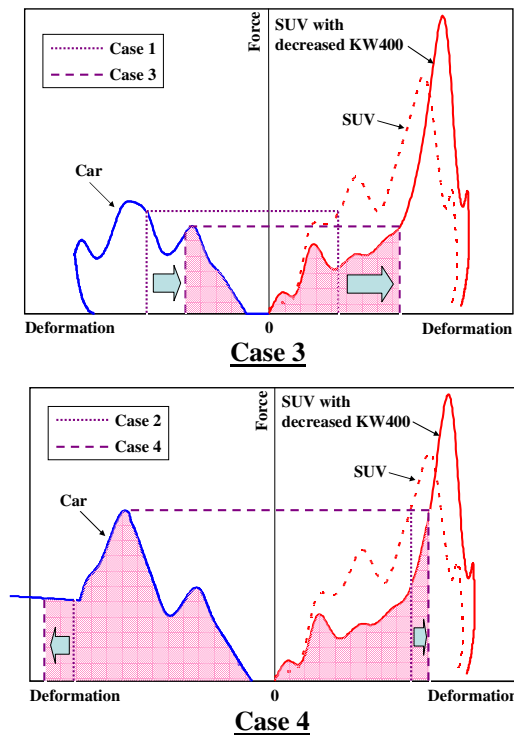


Figure 7. Deformation prediction of SUV with decreased KW400.

From these results, it is expected that there is a critical impact speed at which the effect of decreasing the SUV's KW400 below the assumed upper limit on the car's deformation changes from reduction to increase. The method described above indicates that the critical impact speed is approximately 52km/h(see Figure 8).

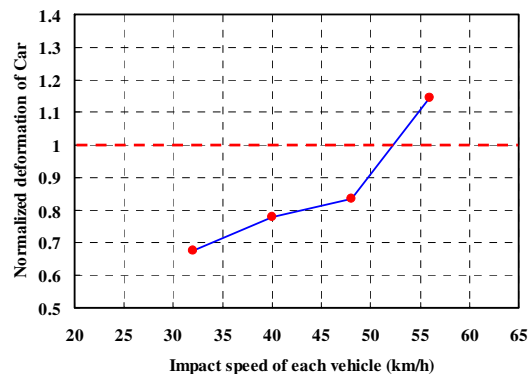


Figure 8. Relation between variation of car's deformation and impact speed.

The result obtained by the above basic study suggests

that, depending on how to decrease the SUV's KW400, compatibility in SUV-to-car frontal impact under a critical impact speed is improved while compatibility in SUV-to-car frontal impact over the critical impact speed could be deteriorated.

In the above-mentioned basic study, it was assumed that impact is perfectly inelastic, but an actual impact is not. In addition, vehicle force-deformation curves in SUV-to-car impacts may not correspond to those in full overlap impacts, especially at a late impact stage due to static/dynamic ratios and other factors. Therefore in order to verify the result more accurately, SUV-to-car frontal impact FE simulations were conducted (see Figure 9) for all four cases shown in Table 3 and 4. In these FE simulations, a plane perpendicular to a vehicle's longitudinal direction was set at the junction between both vehicles to assume that structural interaction between both vehicles is ideal. The plane can move only in a vehicle's longitudinal direction.

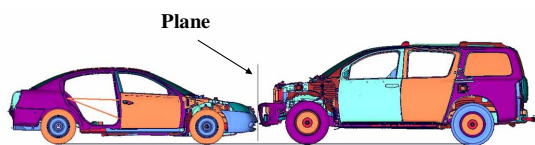


Figure 9. SUV-to-car frontal impact FE simulation model.

Figure 10 shows the result. In the cases that impact speed of each vehicle is 32km/h, the car's deformation in Case 3 decreases in comparison with that in Case 1. However, in the case where the impact speed of each vehicle is 56km/h, which slightly exceeds the critical impact speed obtained from the basic study, the car's deformation in Case 4 does not decrease but rather slightly increases in comparison with that in Case 2. The FE simulations correspond well to the basic study.

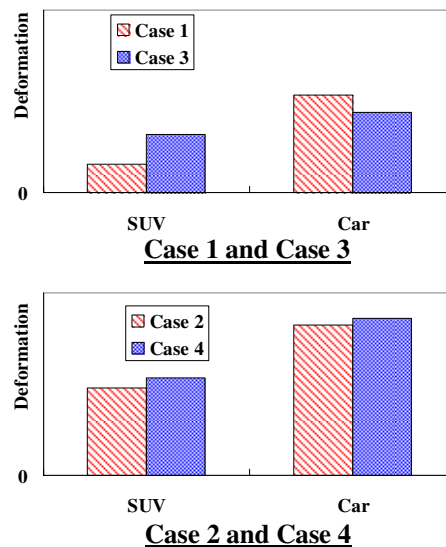


Figure 10. Calculation result of vehicle deformation.

DISCUSSION

The purpose of this study is to validate the effectiveness of the SUV's KW400 reduction as a countermeasure for compatibility improvement in SUV-to-car frontal impact. For that purpose, at the beginning a set of realistic measures to decrease the SUV's KW400 below the assumed upper limit without the increase of occupant injury indexes in 56km/h full overlap impact was determined. The measures are an example of solutions with a practical balance between safety performance and other requirements in actual vehicle design and contain not only vehicle stiffness reduction but also vehicle front overhang extension, restraint system improvements and so on.

However, as a result of subsequent SUV-to-car frontal impact FE simulations using the SUV model installed with the above measures, it turned out that such design changes, which were originally intended to improve compatibility between two vehicles, can be effective in a certain impact speed range, but at the same time could not be effective and worsen the situation over the entire speed range.

In the latter case, it is apparent that the reason why the SUV's stiffness reduction based on KW400 metrics results in an increase of the opponent car's deformation is the deficiency of the SUV's energy absorption capability in the engine compartment per the design change. Such deficiency of energy

absorption has often been considered as a result of poor structural interaction.

Perhaps a promising approach to enhance stiffness matching without the problem described above is to establish guidelines for the amount of minimum necessary energy absorption by a certain force level for both vehicles(see Figure 11). However, a wide range of studies about how to decide appropriate energy amounts and force levels and a cautious feasibility assessment from a viewpoint of actual vehicle design are necessary to translate the approach into reality.

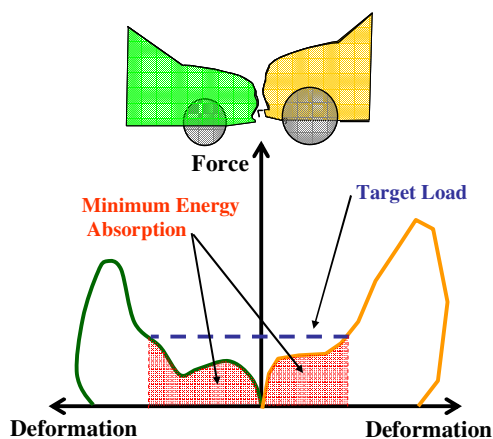


Figure 11. Overview of target load and minimum energy absorption.

CONCLUSIONS

Stiffness matching in SUV-to-car frontal impact by only reducing the SUV's stiffness was studied using FE models of actual existing vehicles in the market. The following conclusions were made.

- In order to decrease the SUV's KW400 below the assumed upper limit, 1700N/mm, without an increase of occupant injury indexes in 56km/h full overlap impact, vehicle front overhang extension, restraint system improvements and other alterations in addition to vehicle stiffness reduction are needed.
- The results of SUV-to-car frontal impact FE simulations using the SUV model installed with the above design changes for KW400 reduction indicates that the design changes can reduce the opponent car's deformation under a certain impact speed, but could increase and worsen the situation at higher impact speeds.

REFERENCES

- [1] Edwards, M., et al., "Development of Test Procedures and Performance Criteria to Improve Compatibility in Car Frontal Collisions." Vehicle Safety 2002.
- [2] Delannoy, P., et al., "Proposal to Improve Compatibility in Head on Collisions." 16th International Conference on the Enhanced Safety of Vehicles, Paper No. 98, Windsor, Canada, 1998.
- [3] Summers, S., et al., "Design Consideration for a Compatibility Test Procedure." Society of Automotive Engineers, Paper No. 2002-01-1022, 2002.
- [4] Delannoy, P., et al., "New Barrier Test and Assessment Protocol to Control Compatibility." Society of Automotive Engineers, Paper No. 2004-01-1171.
- [5] Takizawa, S., et al., "Experiment Evaluation of Test Procedure for Frontal Collision Compatibility." Society of Automotive Engineers, Paper No. 2004-01-1162.
- [6] Haenchen, D., et al., " Feasible Steps towards Improved Crash Compatibility." Society of Automotive Engineers, Paper No. 2004-01-1167.
- [7] Verma, M.K., et al., "Significant Factors in Height of Force Measurements for Vehicle Collision Compatibility." Society of Automotive Engineers, Paper No. 2004-01-1165.
- [8] Hirayama, S. et al., "Compatibility for Frontal Impact Collisions Between Heavy and Light Cars." 18TH International Conference on the Enhanced Safety of Vehicles, Paper No. 454, Nagoya, Japan, May 2003.
- [9] Watanabe, T. et al., "Research on Stiffness Matching between Vehicles for Frontal Impact Compatibility." 19TH International Conference on the Enhanced Safety of Vehicles, Paper No. 05-0302, Washington, USA, May 2005.

[10]Smith, D., “NHTSA’s Approach to Addressing the Vehicle Compatibility Problem.” Compatibility in Road Traffic Workshop, Dresden, Germany, October 2005.

[11]Smith, D., “The U.S. Crash Compatibility Problem.” Compatibility in Road Traffic Workshop, Dresden, Germany, October 2005.

PDB BARRIER FACE EVALUATION BY DSCR AND NHTSA'S JOINT RESEARCH PROGRAM

Pascal Delannoy

Teuchos, SAFRAN Group - UTAC Passive Safety Dpt

Tiphaine Martin

UTAC

France

Susan Meyerson, Lori Summers, Christopher Wiacek

NHTSA

USA

Paper number: 07-0303

ABSTRACT

Vehicle compatibility combines aspects of both self and partner protection. Self protection involves a vehicle's compartment strength and occupant protection systems. Partner protection involves vehicle design attributes that work towards providing occupant crash protection of a vehicle's collision partner. Research has suggested that crush force matching (or good engagement of the front structures) and high compartment strength are essential components for improving compatibility between passenger cars and other vehicles [1]. However, recent trends have shown that incompatible force distributions and greater relative front end stiffness are prevalent in the fleet. To research this issue, the Progressive Deformable Barrier (PDB) face was evaluated for its ability to assess the compatibility between the front end force of heavier vehicles with the compartment strength of lighter ones.

The paper investigates the feasibility of a high energy absorption PDB in full frontal and offset frontal crash test configurations. A joint research program was carried out at the Union Technique de l'Automobile du Motocycle et du Cycle (UTAC) in conjunction with the Directorate for Road Traffic and Safety (DSCR) in France and the National Highway Traffic Safety Administration (NHTSA) of the United States (U.S.) to investigate whether barrier deformation using the PDB could differentiate compatibility performances between two different U.S. light trucks and vans (LTVs).

INTRODUCTION

Safety researchers around the world, including the U.S. and France, have been concerned with vehicle compatibility in crashes for many years. NHTSA has conducted studies on vehicle aggressiveness (injury risk vehicles pose to drivers of other vehicles with which they collide) and methods for measuring it for over 25 years [2]. Examination of U.S. crash statistics shows a disparity in fatality risk for

passenger car occupants in vehicle-to-vehicle collisions with LTVs. Past studies have shown that LTVs, as a class, were found to be twice as aggressive toward their collision partners as passenger cars [2]. This mismatch in crash performance has considerable consequences for the traffic safety environment, as approximately half of all passenger vehicles sold in the U.S. are LTVs.

While LTVs are not nearly as prevalent in Europe, vehicle compatibility has been a growing concern for its countries as well. Researchers have observed that European vehicles have been generally produced with greater mass, stiffer front ends and higher compartment strengths to provide occupant crash protection in fixed offset barrier crash tests [1]. However, as vehicles get heavier and stiffer, the deformable barriers used for the evaluation of frontal offset crash protection begin bottoming out. As a consequence, the test becomes more severe for the stiffer, heavier vehicles, and they become more incompatible with smaller collision partners.

In 1996, European Enhanced Vehicle-Safety Committee Working Group 15 on vehicle compatibility was established in order to explore methodologies to assess vehicle compatibility, and develop test procedures to address it. In March 2002, vehicle compatibility was included as an area of focus for the exchange of information in the program of work adopted under the World Forum for the Harmonization of Vehicle Regulations (WP.29) 1998 Global Agreement. Both the U.S. and France are signatories to that agreement, and have been concurrently active participants in international research collaborations, such as the International Harmonized Research Activities on vehicle compatibility [3].

In 2004, NHTSA and the DSCR signed a bilateral agreement to enhance cooperation and increase the efficient use of resources. One form of this cooperation includes conducting joint analyses to promote the development of improved vehicle safety

programs and related regulations. The two parties decided that one area of focus would relate to issues of vehicle compatibility. A joint research program was initiated to investigate the use of a PDB in discerning levels of partner and self protection of heavy passenger vehicles in full width and offset test configurations. Based on its own research program on vehicle compatibility, NHTSA identified two sets of LTVs with differing levels of aggressiveness for the PDB study [4]. UTAC was selected as the site location for conducting the tests.

DSCR has been researching the PDB test procedure approach for over 8 years as a means to address vehicle compatibility [1]. The PDB progressively increases in stiffness in depth and upper and lower load levels, which contributes to its name, PDB, as a Progressive Deformable Barrier. Its characteristics were designed to represent an actual vehicle structure with sufficient force level and energy absorption capacity to mitigate any occurrences of bottoming out. In doing so, the PDB may be able to better harmonize test severity among vehicles of different masses. The approach aims to encourage lighter vehicles to be stronger without increasing the force levels of large vehicles [1]. By its design, the PDB is also able to detect all frontal structures involved in a crash (i.e. cross members, subframes, blocker beams, and longitudinal frame rails). By detecting the impact deformations, the test procedure can encourage vehicle designs to incorporate structures that distribute homogeneous force levels over large surfaces.

METHOD OF TEST EVALUATION

Test Severity

One approach toward evaluating both self protection and partner protection is to normalize the test severity for all vehicles, large and small by using the PDB. The test velocity alone is not a good indication of the severity of the event because, unlike a rigid barrier test, a portion of the test energy is absorbed by the deformable element of the barrier. The energy absorbed by the barrier is a factor of the vehicle's mass, design and stiffness. Therefore, the parameter used to equate the test severity for different vehicles at a common speed using the PDB is the Energy Equivalent Speed (EES).

$$EES(km/h) = 3.6 \times \sqrt{\frac{2 \times Eabs}{M}}$$

Eabs = energy absorbed by the vehicle (J)

Eabs = Kinetic energy – Energy in the barrier

M = mass of the vehicle (kg)

$$E_{barrier} = \int_{x_{min}}^{x_{max}} F dx \quad F = P * S$$

P = barrier stiffness (MPa) S = crushed surface (m²)

Self protection

The concept of self protection is the ability to protect the occupants within the striking vehicle in a vehicle-to-vehicle crash. Many of the crashworthiness regulations around the world are directed toward evaluating a vehicle's "self protection," or how the vehicle protects its own occupants. To achieve good self protection, front end design must limit intrusion and acceleration levels in the passenger compartment as well as limit occupant injury criteria. The following parameters were measured to evaluate the level of self protection the vehicles offered:

- Compartment intrusion
- Dummy injury criteria
- Vehicle acceleration

Partner protection

The concept of partner protection involves vehicle design attributes that function to maximize protection of the occupants within the collision partner (struck) vehicle. In order to take advantage of the potential energy absorption of a vehicle front end in a vehicle-to-vehicle crash, good engagement of the vehicle structures must occur. To achieve this result, the deformation of the front end must be distributed over a large surface. In this study, barrier digitization is used to examine the different barrier engagement patterns. The study also compares the following parameters that have been identified in previous research as influential in the evaluation of partner protection [5]:

- Average Height of Deformation (AHOD): height at which the median deformation occurs, (evaluates the frontal geometry of a vehicle)
- Average Depth of Deformation (ADOD): average deformation over the barrier, (evaluates the frontal stiffness of a vehicle)
- Maximum Deformation (Dmax)

Calculation method:

- Average Height of Deformation (AHOD):

For a given rectangular investigation region, the "depth profile" is computed as a function of height.

$$\rho(z) = k \int_{y_{min}}^{y_{max}} X(y, z) dy$$

Where k is a normalization constant ensuring that:

$$\int \rho(z) dz = 1$$

The AHOD is then obtained as a mean value:

$$AHOD = \int z \rho(z) dz$$

- Average Depth of Deformation (ADOD):

For a given investigation region with an area S :

$$ADOD = \frac{1}{S} \int X(y, z) dy dz$$

TEST CONFIGURATION

PDB+ Offset Test configuration

	PDB+ Offset	
	Barrier	PDB + 50%
	Speed	60km/h
	Overlap	50%
	Dummies	H3 50% male H3 5% female + Leg Lx

Figure 1: Vehicle in front of the offset PDB

This test procedure is based on the current PDB test protocol (Figure 2) [6]. The only difference is in the barrier construction itself. In order to avoid bottoming out the barrier with large and heavy LTVs, a layer of 90 mm honeycomb at 1.71 MPa was added to the back of the barrier (Figure 2). The stiffness of other barrier parts were similar to the current PDB. For the purposes of this study, this modified barrier, with a rear layer, is called “PDB+.”

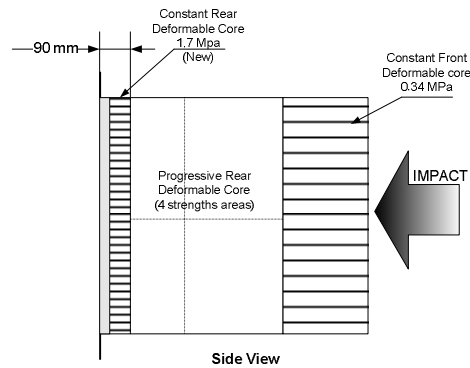
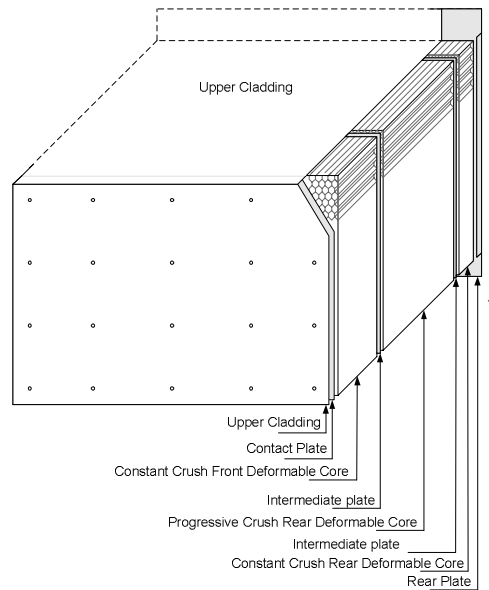


Figure 2 : PDB + barrier specification.

PDB+ Full Width test configuration

	PDB+ Full Width	
	Barrier	PDB + 100%
	Speed	60km/h
	Overlap	100%
	Dummies	H3 50% male H3 5% female + Leg Lx

Figure 3: Vehicle in front of the full width PDB

The “full width” test configuration used a full width PDB+ (Figure 4). This barrier was built as a standard PDB, considering stiffness and layers, but it is 2 meters wide instead of 1 meter. This barrier was also built with a rear layer of 90 mm of honeycomb at 1.71 MPa. The test speed was fixed at 60 km/h to ensure that the test would be sufficiently severe for LTVs and the results could be compared with previous offset PDB tests [1] and full width rigid wall tests.



Figure 4: Full width PDB+

A belted Hybrid III 50th percentile male dummy was in the driver position and a belted Hybrid III 5th percentile female dummy was seated in the right front passenger position. Both dummies were instrumented with lower leg instrumentation.

VEHICLE SELECTION

To evaluate the performance of the PDB+, the 2003 Chevrolet Silverado pickup truck (Figure 5 and Figure 6) and the 2005 Chrysler Town & Country minivan (Figure 7 and Figure 8) were selected for this study based upon their design, construction geometry, test weight, frontal stiffness and force matching height, collected as part of the United States New Car Assessment Program (USNCAP). In this test program, vehicles equipped with belted 50th percentile male dummies are impacted into a rigid barrier at 56 km/h, and load cell data is collected from the test.

The intent of the vehicle selection was to identify those that had similar force matching heights during impact, but also had a difference in frontal structural stiffness, which could represent two incompatible vehicles. The Silverado and Town & Country vehicles also represent two distinct vehicle design approaches. The Silverado used a separate body on frame construction whereas the Town & Country was built with a unibody structure. From USNCAP test data, it was determined that the average height of the force when impacting an instrumented rigid barrier was similar for both the Silverado and the Town & Country. However, the Silverado’s front structure was estimated to be over 40 percent stiffer. Since the vehicles had similar force matching heights, they were identified as good candidates to evaluate how the PDB discriminates not only different front structural stiffness, but also differing frame construction. Figure 6 and Figure 8 provide details on the mass, width, and structure.



Figure 5: Silverado

Silverado	
Test Mass	2293 kg
Width	1994 mm
Structure	Body on frame

Figure 6: Silverado Specifications



Figure 7: Town & Country

Town & Country	
Test Mass	1950 kg
Width	1920 mm
Structure	Unibody

Figure 8: Town & Country Specifications

TEST RESULTS

Four tests were performed according to the matrix below (Figure 9). The following sections describe the test results based on test severity, self protection and partner protection.

Test Matrix		
	50% Offset PDB+	Full Width PDB+
Silverado	√	√
Town & Country	√	√

Figure 9: Test Matrix

PDB+ Offset test

Town & Country

Test severity

The amount of energy absorbed in the offset PDB+ was 73 kJ for the Town & Country test. The calculated EES for this test is 51 km/h, which is 9 km/h less than the test speed.

Self protection

In terms of self protection, the Town & Country maintained its occupant compartment integrity (Figure 10). The front end crushed uniformly without any undeformed load paths.



Figure 10: Town & Country PDB+ offset

The injury measures for the 50th percentile male driver and 5th percentile female passenger are reported in Figure 11.

	Driver	Pass.
HIC36	450	295
HIC15	265	217
Chest Def (mm)	36	29
Chest Gs	47	42
Left Femur (kN)	1.98	1.57
Right Femur (kN)	1.56	0.17
UL Tibia Index	0.559	0.112
UR Tibia Index	0.337	0.390
LL Tibia Index	0.237	0.250
LR Tibia Index	0.296	---

Figure 11: Town & Country PDB+ offset – Dummy Injury Measures

None of the occupant injury measures were elevated in this test. Intrusion measures in this test (Figure 12) were low, except for the footwell area on the driver’s side. However, the dummy lower leg injury measures were not significantly affected.

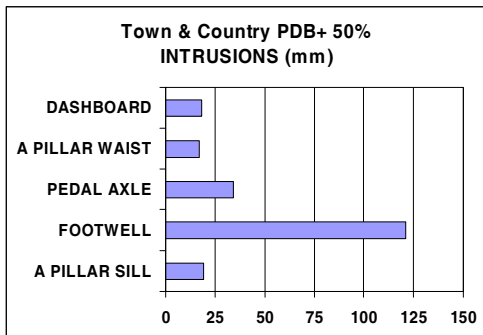


Figure 12: Town & Country PDB+ Offset – Driver side intrusions

The maximum acceleration measured was 31 g at 93 ms, corresponding to 1.023 m of displacement (Figure 13). The average acceleration was 17.6 g.

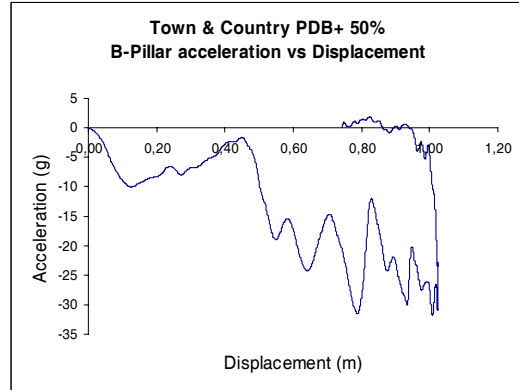


Figure 13: T&C PDB+ offset – Acceleration pulse

Partner protection

In the PDB+ offset test, the forces generated by the longitudinal and lower load paths of the Town & Country are distributed, resulting in homogeneous deformation (Figure 14 and Figure 15). There was good engagement between the front of the vehicle and the barrier. No bottoming out of the barrier was observed.



Figure 14: Town & Country PDB+ offset – front end deformation



Figure 15: Town & Country PDB+ offset – barrier deformation

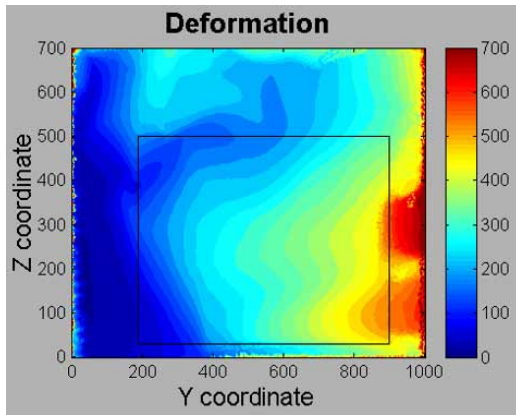


Figure 16: Town & Country PDB+ offset – barrier digitization

In Figure 16, the barrier was able to detect the lower load path of the vehicle. The calculated parameters based on barrier digitization analysis are presented in Figure 17. The energy absorbed in the barrier is 73 kJ which represent 27% of the total kinetic energy.

Partner protection	
ADOD (X)	275 mm
AHOD (Z)	404 mm
Dmax	570 mm

Figure 17: Partner Protection Parameters for the Town & Country PDB+ offset test

Silverado

Test severity

The amount of energy absorbed in the offset PDB+ was 85 kJ for the Silverado test. The calculated EES for this test is 51 km/h, which is 9 km/h less than the test speed.

Self protection

In terms of self protection, the Silverado resulted in significant deformation of the roof and sill between the A- and B-Pillar in the PDB+ offset test. The rear door of the extended cab even exhibited structural deformation (Figure 18).



Figure 18: Silverado PDB+ offset

The injury measures for the 50th percentile male driver and 5th percentile female passenger are reported in Figure 19. The head and chest injury measures of the dummies were relatively low; however, some of the driver leg injury measures were elevated.

	Driver	Pass.
HIC36	505	358
HIC15	285	201
Chest Def (mm)	28	15
Chest Gs	40	35
Left Femur (kN)	5.54	3.20
Right Femur (kN)	6.12	2.62
UL Tibia Index	0.987	0.419
UR Tibia Index	0.929	0.446
LL Tibia Index	0.668	0.475
LR Tibia Index	0.671	0.237

Figure 19: Silverado PDB+ offset Dummy Injury Measures

This is consistent with the high intrusion levels exhibited in the footwell area (Figure 20).

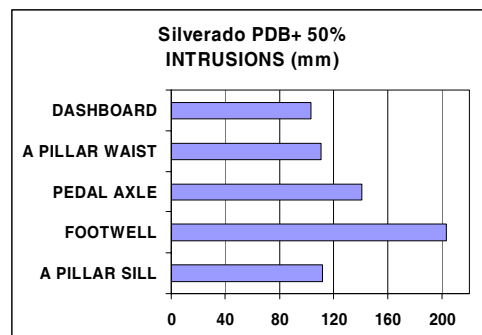


Figure 20: Silverado PDB+ Offset – Driver side intrusions

The maximum acceleration measured is 36 g at 88 ms, corresponding to 1.150 m of displacement (Figure 21). The average acceleration is 14.4 g.

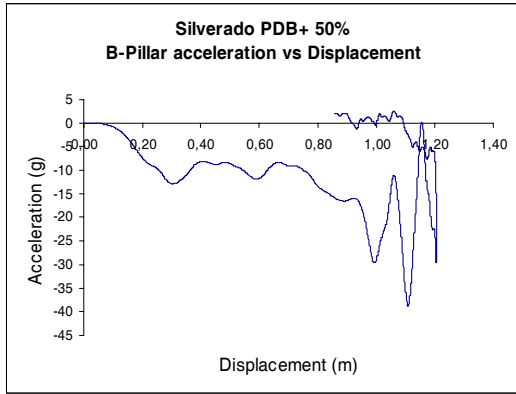


Figure 21: Silverado PDB+ offset – Acceleration

Partner protection

There was good integrity and no bottoming out of the PDB+ after the Silverado test. However, the deformation was largely inhomogeneous since the deformation was localized in front of the longitudinal and connecting beam (Figure 22). The PDB+ was able to detect the unique load path of this vehicle (Figure 23).



Figure 22: Silverado PDB+ 50% - front end deformation



Figure 23: Silverado PDB+ 50% - barrier deformation

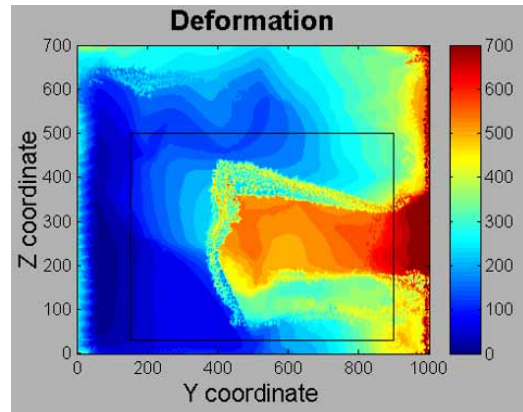


Figure 24: Silverado PDB+ 50% – barrier digitization

The calculated parameters based on barrier digitization analysis (Figure 24) are presented below (Figure 25). The energy absorbed in the barrier was 85 kJ which represents 27% of the total kinetic energy.

Partner protection	
ADOD (X)	289 mm
AHOD (Z)	414 mm
Dmax	654 mm

Figure 25: Partner Protection Parameters for the Silverado PDB+ offset test

PDB+ Full Width test

Town & Country

Test severity

In the PDB+ full width test of the Town & Country, the amount of energy absorbed in the barrier was 33 kJ. The calculated EES for this test was 56 km/h which is 4 km/h less than the test speed, but comparable with the severity of a full frontal rigid barrier test at 56 km/h.

Self protection

The Town & Country minivan exhibited good structural integrity after the full width PDB+ test (Figure 26).



Figure 26: T&C PDB+ Full Width

The injury measures for the 50th percentile male driver and 5th percentile female passenger dummies are reported in Figure 27. Head injury measures for both dummies were low; however, the chest acceleration measurement for the passenger dummy was high.

	Driver	Pass.
HIC36	437	419
HIC15	229	281
Chest Def (mm)	51	30
Chest Gs	49	57
Left Femur (kN)	1.68	3.94
Right Femur (kN)	1.67	1.49
UL Tibia Index	0.452	0.526
UR Tibia Index	0.477	0.500
LL Tibia Index	0.371	0.532
LR Tibia Index	0.516	0.338

Figure 27: Town & Country PDB+ full width – Dummy Injury Measures

Intrusions were relatively low, except in the footwell area, where there was more than 125 mm of intrusion (Figure 28).

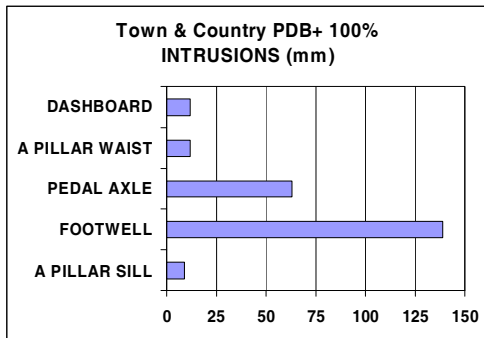


Figure 28: Town & Country PDB+ Full Width – Driver side intrusions

The maximum acceleration measured in the test was 44 g at 60 ms, corresponding to 0.775 m of displacement (Figure 29). The average acceleration was 21.6 g.

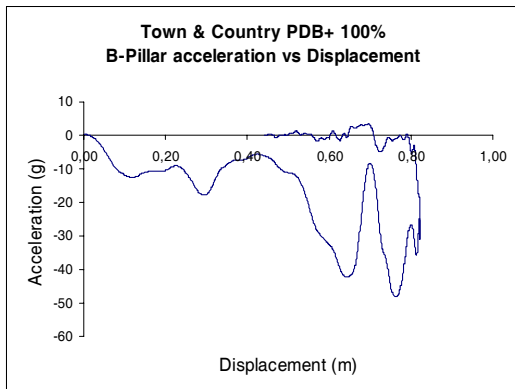


Figure 29: Town & Country PDB+ offset – Acceleration

Partner protection

In the Town & Country full width PDB+ test, there was very good integrity of the barrier and good engagement with the barrier; no bottoming out was observed. The deformation was large and homogeneous. The front end of the vehicle fitted with two levels of load paths, was able to distribute the loads (Figure 30 and Figure 31).



Figure 30: Town & Country PDB+ Full Width – front end deformation

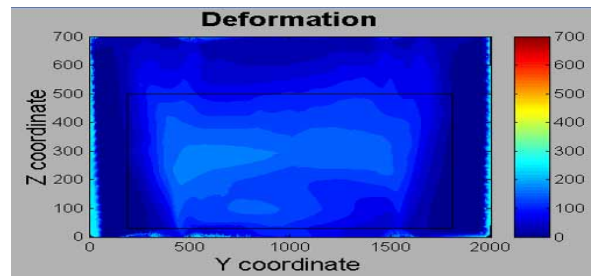
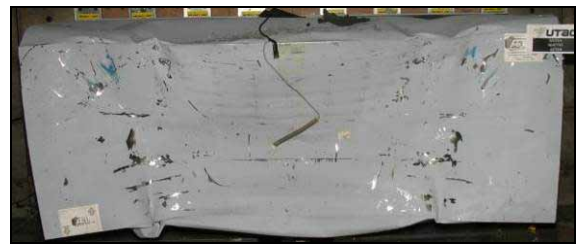


Figure 31: Town & Country PDB+ Full Width – barrier deformation and digitization

The calculated parameters based on barrier digitization analysis (Figure 31) are presented in Figure 32 below. The energy absorbed in the barrier was 33 kJ which represents 12% of the total kinetic energy.

Partner protection	
ADOD (X)	105 mm
AHOD (Z)	425 mm
Dmax	174 mm

Figure 32: Partner Protection Parameters for the Town & Country PDB+ Full Width

Silverado

Test severity

In the PDB+ full width test of the Silverado, the amount of energy absorbed in the barrier was 68 kJ. The calculated EES for this test was 53 km/h which is 7 km/h lower than the test speed and lower than the severity of a full frontal rigid barrier test at 56 km/h.

Self protection

There was good structural integrity of the Silverado after the full width PDB+ test (Figure 33).



Figure 33: Silverado PDB+ Full Width

The injury measures for the 50th percentile male driver and 5th percentile female passenger are reported in Figure 34.

	Driver	Pass.
HIC36	727	988
HIC15	410	787
Chest Def (mm)	35	23
Chest Gs	43	42
Left Femur (kN)	5.24	3.38
Right Femur (kN)	6.99	5.08
UL Tibia Index	0.605	0.498
UR Tibia Index	0.534	0.463
LL Tibia Index	0.391	0.311
LR Tibia Index	0.454	0.312

Figure 34: Silverado PDB+ Full Width – Dummy Injury Measures

The driver dummy had relatively low injury measures; however, the passenger dummy had high head injury measures. There were low levels of intrusion in the driver compartment, except in the footwell area where there was nearly 80 mm of deformation (Figure 35).

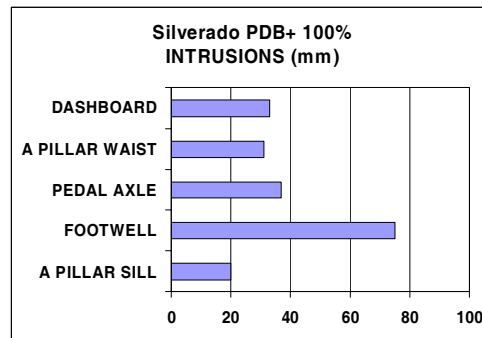


Figure 35: Silverado PDB+ Full Width – Driver side intrusions

The maximum acceleration measured was 33 g at 74 ms, corresponding to 0.887 mm of displacement (Figure 36). The average acceleration was 16.5 g.

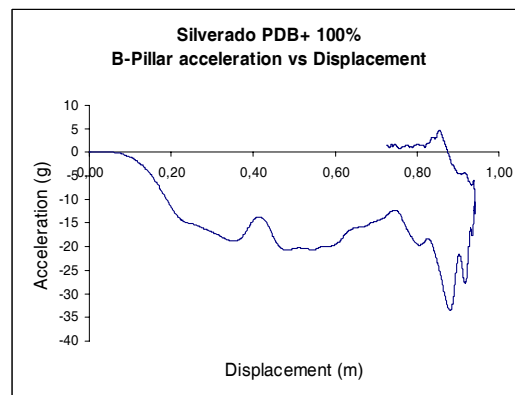


Figure 36: Silverado PDB+ Full Width – Acceleration

Partner protection

There was good integrity and no bottoming out of the full width barrier in the Silverado full width test. However, the deformation was inhomogeneous and localized in front of the longitudinal (Figure 37).



Figure 37: Silverado PDB+ Full Width - Front end deformation

The imprint of the connecting beam was not well detected, as it was positioned back from the front of the longitudinal and the deformation was not enough to detect this device (Figure 38).

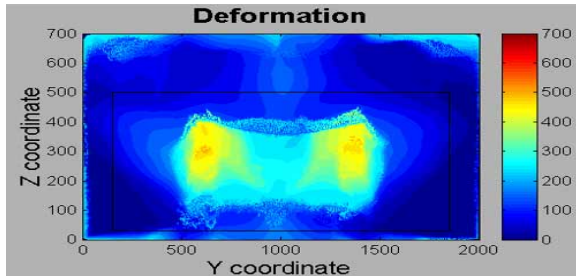


Figure 38: Silverado PDB+ Full Width - barrier deformation and digitization

The calculated parameters based on barrier digitization analysis are presented in Figure 39 below. The energy absorbed in the barrier was 68 kJ which represents 21% of the total kinetic energy.

Partner protection	
ADOD (X)	163 mm
AHOD (Z)	423 mm
Dmax	516 mm

Figure 39: Partner Protection Parameters for the Silverado PDB+ full width

DISCUSSION

Test severity

The test severity in the offset test configuration is similar for the Town and Country and Silverado; even with 350 kg differences in car mass, the evaluation of the EES is 51 km/h for both cars. Considering full width configuration, EES for the Silverado is slightly lower than for the Town and Country (53 km/h vs. 56 km/h).

The PDB barrier shows good capability for absorbing different amounts of energy. Thus it seems possible to normalize test severity with the use of a deformable element, which will allow for controlling other parameters, such as partner protection. Test severity harmonization could encourage heavier vehicles to be less stiff and result in less disparity between heavy and light vehicles because of the test set-up. Thus it has the potential of reducing the front end force difference.

Self protection

In the offset PDB+ tests, both vehicles demonstrated good performance in protecting the head and chest of the dummy. The injury numbers were not elevated in these tests. Similarly, most of the head and chest injury performance measures were relatively low in the full width PDB+ tests. However, there were a few notable exceptions. In the Town & Country full width PDB+ test, the passenger dummy resulted in a high chest acceleration measure, and in the Silverado test, the 5th percentile passenger dummy resulted in a high head injury reading.

It is interesting to note that when compared to the injury measures from the USNCAP full width rigid barrier tests of the same vehicle models (Figure 40 and Figure 41), it was found that the elevated passenger head injury criteria in the Silverado test was consistent with elevated passenger head injury criteria in the USNCAP program (in spite of it using a different dummy size). However, the elevated passenger chest acceleration in the Town & Country test was not found in the USNCAP test. Most other injury measures were comparable between the two test procedures.

	Town & Country Driver		Silverado Driver	
	Full PDB+	US NCAP	Full PDB+	US NCAP
Dummy	50 th	50 th	50 th	50 th
HIC36	437	482	727	738
HIC15	229	284	410	523
Chest Def (mm)	51	39	35	29
Chest Gs	49	44	43	45
L Femur (kN)	1.68	3.21	5.24	4.09
R Femur (kN)	1.67	2.09	6.99	4.35

	Town & Country Passenger		Silverado Passenger	
	Full PDB+	US NCAP	Full PDB+	US NCAP
Dummy	5 th	50 th	5 th	50 th
HIC36	419	385	988	990
HIC15	281	204	787	629
Chest Def (mm)	30	31	23	32
Chest Gs	57	46	42	49
L Femur (kN)	3.94	3.55	3.38	4.64
R Femur (kN)	1.49	3.45	5.08	4.36

Figure 40 and Figure 41: Comparison of PDB+ and USNCAP Dummy Injury Measures

Based upon this limited data, the measured self-protection of the vehicles in the full width PDB test was nearly equivalent to a full frontal rigid barrier crash test.

In terms of intrusions, the Town & Country produced relatively low levels in both the full width and offset configurations (Figure 42). Footwell intrusions were the exception to this. The values were 122 mm and 140 mm for the offset and full width tests, respectively. Though, in spite of the noted footwell intrusions, none of the dummy lower leg injury readings were elevated in these tests.

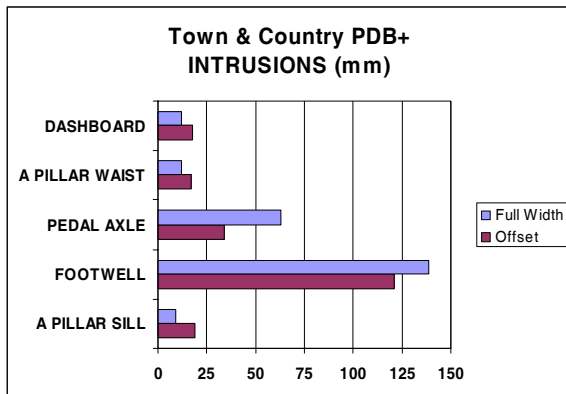


Figure 42: Comparison of driver side intrusions – Town & Country

All of the intrusion levels in the Silverado were higher in the offset test than the full width test (Figure 43). This is not unexpected, given the nature of the test configuration. The driver footwell intrusion in the Silverado offset test was over 200 mm. This was consistent with the elevated lower leg injury measures for the driver dummy in this test. The tibia indexes were 0.987 and 0.929 for the left and right legs, respectively.

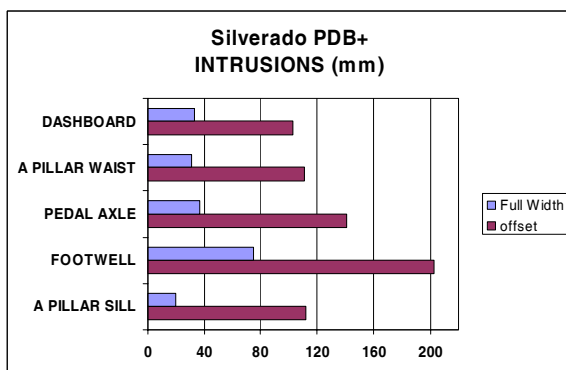


Figure 43: Comparison of driver side intrusions – Silverado

Aside from the footwell and pedal axle intrusions, the structural intrusions in the Silverado were generally greater than the Town & Country.

Partner protection

The test results showed that structural differences between the two vehicles are detected by the PDB+ in the offset test configuration (Figure 44). The Silverado barrier deformation is localized in front of the lower rail. The vehicle’s crossbeam is also detected. In contrast, the deformation of the Town & Country barrier is large and homogenous.

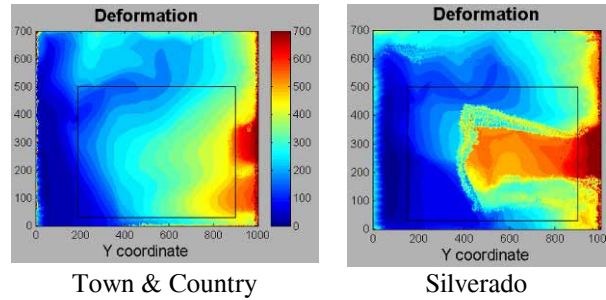


Figure 44: Comparison of barrier deformation – Offset

Figure 45 summarizes the parameters calculated for this test configuration. As expected from the vehicle selection, the AHOD values for the Town & Country and Silverado were within 2 percent of each other. This is consistent with USNCAP tests that similarly found the average height of force (AHOF400) values to be 476 mm, and 475 mm for the Town & Country and Silverado, respectively [7]. The ADOD and Dmax were slightly higher in the Silverado, as expected from the digitization.

PDB+ Offset			
	T&C	Silverado	Δ %
ADOD (X) (mm)	275	289	5
AHOD (Z) (mm)	404	414	2
Dmax (mm)	570	654	13

Figure 45: Comparison of Partner protection Parameters in the Offset Tests

Similarly, in the full frontal barrier tests, the deformation patterns were very different between the two tested vehicles. The Silverado, fitted with a stiff single load path, created an inhomogeneous deformation, localized in front of the lower rail. On the other hand, the Town and Country resulted in a more homogeneous deformation pattern due to the front cross beam and lower load paths. The forces were distributed over a large area (Figure 46).

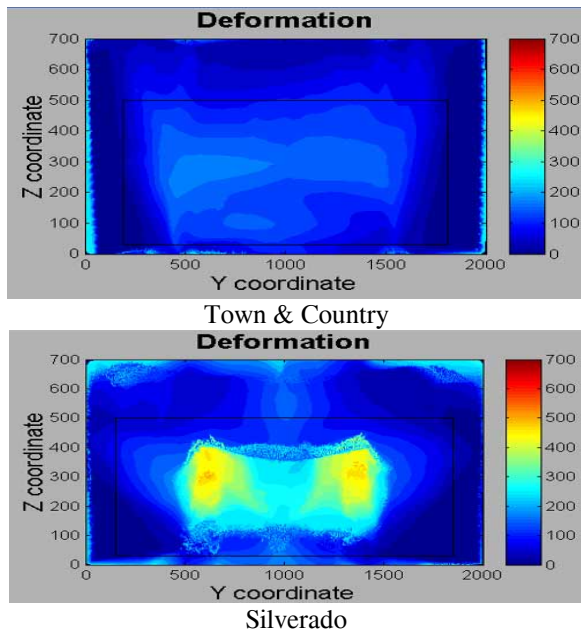


Figure 46: Comparison of barrier deformation – Full Width

Figure 47 summarizes the parameters calculated in the full width test configuration. Again, the AHOD values for the Town & Country and Silverado were very close in magnitude (within 1 percent) and consistent with USNCAP findings. On the other hand, the Dmax values were considerably different for the two vehicles in the full width PDB+ tests. The Town & Country resulted in only 174 mm of deformation, whereas the Silverado resulted in 516 mm.

PDB+ Full Width			
	T&C	Silverado	$\Delta\%$
ADOD (X) (mm)	105	163	35
AHOD (Z) (mm)	425	423	1
Dmax (mm)	174	516	66

Figure 47: Comparison of Partner protection Parameters in the Full Width Tests

NHTSA is also evaluating the merits of a stiffness metric, KW400, in its compatibility research program [4]. As part of this research, NHTSA conducted two full frontal vehicle-to-vehicle crash tests using both the Town and Country and Silverado. Each vehicle was impacted by a standard collision partner, the 2002 Ford Focus. The results showed that the Silverado imparted higher head and chest injury measures to the driver dummy of Ford Focus than did the Town & Country. Head and chest injury measures were increased 15 and 18 percent, respectively. The crash test results are directionally consistent with the partner protection findings in this study.

Future considerations of the PDB+ test procedure

The PDB+ test configuration was able to discriminate between the Silverado’s body on frame vehicle

structure and the unibody construction of the Town & Country. Future research could include evaluating the PDB+’s ability to identify secondary energy absorbing structures, or other novel designs, and assess their partner protection performance for crash compatibility. Research can also be expanded to appraise how the PDB+ performs with vehicles that have similar frontal stiffness and force matching to identify additional design factors that may play a roll in crash compatibility. Finally, additional full width PDB+ testing could be conducted to verify if there is a correlation with the self-protection measurements of a rigid barrier.

The DSCR is developing a parameter to assess the homogeneity of the vehicle crush pattern using the barrier digitization analysis. It will be based on the shape of the deformation, discriminating between localized deformation and homogeneous deformation. This parameter has the potential to be very useful in differentiating the crash characteristics of the two vehicles.

In this testing, a load cell wall was installed behind the PDB+ to measure the global front end force. The PDB+ procedure is able to measure this force with a high level of accuracy. Although the global force is reported for informational purposes in this paper, with further research it could be used for evaluating self and partner protection. (See test results in the Appendix).

CONCLUSIONS

- Different frontal designs, in terms of force and geometry were well detected by both the full width and offset PDB+ test configurations.
- The deformable element of the PDB+ absorbs different amounts of energy, so that the concept of force matching appears to be obtainable.
- In the four tests, no bottoming out or instability of the PDB+ was observed. The size and stiffness seemed to be appropriate for these heavier vehicles.
- In this test series, the Silverado demonstrated crash protection concerns that were well identified by the PDB+ test procedure both in terms of self and partner protection. The barrier forces were transmitted through the stiff Silverado front to a relatively soft occupant compartment, which led to higher compartment intrusion particularly in the footwell area.
- The full width and offset test configurations were also able to evaluate the self protection of a vehicle in addition to its partner protection.
- The testing showed that the measured self-protection in the full width PDB+ test was reasonably equivalent to that achieved in a full frontal rigid barrier for the two vehicles evaluated.

- The results from these PDB tests are consistent with vehicle-to-vehicle crash tests.
- Under the bilateral agreement between NHTSA and DSCR, resources were leveraged to carry out a joint research program on vehicle compatibility. Results and knowledge gained from this test procedure evaluation proved to be useful to both countries.

ACKNOWLEDGEMENTS

The authors would like to acknowledge: AFL, the barrier supplier, for developing the PDB+ (50 and 100%) and the Université de Provence (Aix Marseille 1) for the PDB software analysis.

REFERENCES

1. Delannoy, P., Martin, T., Castaing, P., “Comparative Evaluation of Frontal Offset Tests to Control Self and Partner Protection,” Enhanced Safety of Vehicles Conference, Paper No. 05-0010, June 2005.
2. National Highway Traffic Safety Administration, “Initiatives to Address Vehicle Compatibility,” June 2003, NHTSA Docket No. NHTSA-2003-14623-1.
3. International Harmonized Research Activity, established at the 15th International Conference on the Enhanced Safety of Vehicles, Melbourne Australia, May 1996.
4. Patel, S., Smith, D., and Prasad, A., “NHTSA’s Recent Vehicle Crash Test Program on Compatibility in Front-To-Front Impacts,” 20th International Conference on the Enhanced Safety of Vehicles, Paper No. 07-02311, June 2007.
5. Delannoy, P., Castaing, P., “Offset Test Approach Proposal,” IHRA Meeting, Washington DC, May 14, 2004.
6. PDB test protocol - EEVC WG15 website, www.eevc.org.
7. The 2003 Silverado and 2005 Town and Country, NHTSA database test numbers are 4472 and 4936, respectively. See www.nhtsa.dot.gov.

APPENDIX

Global force

PDB+ Offset test - Town & Country

The maximum global force is 436 kN at 1 meter displacement of the B-Pillar (Figure 48).

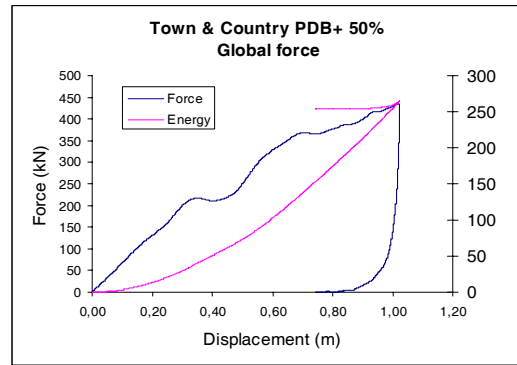


Figure 48: Town & Country PDB+ offset – Global force

PDB+ Offset test - Silverado

The maximum force was 495 kN at 1.150 m displacement of B-Pillar (Figure 49).

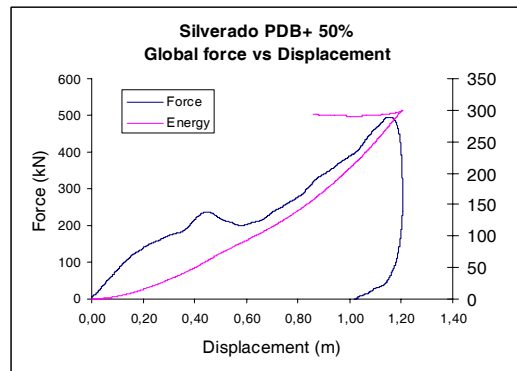


Figure 49: Silverado PDB+ offset – Global force

PDB+ Full Width test - Town & Country

The measured global force (Figure 50) could not be validated. The calculated energy was 10% higher than the kinetic energy. An investigation was conducted, but no explanation was found. Therefore, for this test, the force measurement can not be interpreted, as it is probably overestimated.

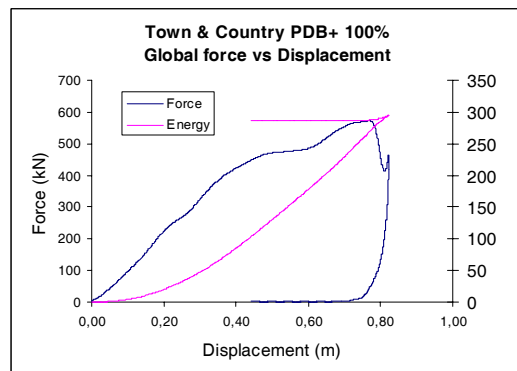


Figure 50: Town & Country PDB+ Full Width – Global force

PDB+ Full Width test - Silverado

The maximum force was 541 kN at 0.801 m displacement of the B-Pillar (Figure 51).

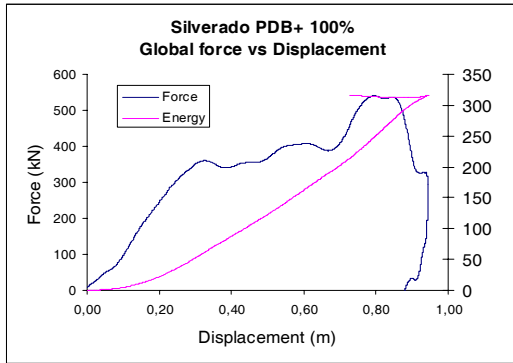


Figure 51: Silverado PDB+ Full Width – Global force

VEHICLE COMPATIBILITY ASSESSMENT USING TEST DATA OF FULL FRONTAL VEHICLE-TO-VEHICLE AND VEHICLE-TO-FULL WIDTH DEFORMABLE BARRIER IMPACTS

Saeed Barbat

Xiaowei Li

Steve Reagan

Priya Prasad

Passive Safety Research and Advanced Engineering

Ford Motor Company

United States

Paper Number 07-0348

ABSTRACT

This paper provides an update of Ford's research activity in vehicle compatibility. Vehicle manufacturers extrapolate compatibility performance in real-world accidents using data from controlled crash test environments. Several test procedures and various compatibility measures which use data obtained from rigid or deformable barrier tests to quantify expected compatibility with smaller vehicles have been previously proposed. The purpose of this research is to examine potential compatibility measures obtained from vehicle-to-barrier impact as well as to evaluate the effectiveness of the "BlockerBeam[®]" in vehicle-to-vehicle impact. The BlockerBeam[®] is one method of designing a Secondary Energy Absorbing Structure (SEAS). The BlockerBeam[®] is attached to the front end of the rail/frame of an SUV or full size pick-up below the bumper. It can enhance structural interaction and reduce override during frontal impact with a passenger car.

The current research presents data analyses obtained from vehicle-to-barrier and vehicle-to-vehicle crash tests to develop assessment methodologies intended to evaluate vehicle compatibility. Full size heavy-duty pick-ups with and without a BlockerBeam[®] were instrumented and tested in 57 km/h frontal impacts against a full width deformable barrier. The barrier consisted of 128 high resolution, 125 mm by 125 mm load cells arranged in a 16 row by 8 column array. Identical full size pick-ups with and without a BlockerBeam[®] were also tested in vehicle-to-vehicle full frontal impact. In these tests, the impact speed of the bullet vehicle (full size heavy-duty pick-up) was set to a value intended to induce a 56 kph velocity change in the stationary target vehicle (small size 4-door sedan). The bullet

and target vehicles were equipped with instrumented 50th% dummies in the mid-position for the drivers and 5th% dummies in the full forward position for the passengers.

Test data collected from load cells in the barrier tests was reviewed and analyzed to evaluate potential compatibility measures for use in assessing vehicle-to-vehicle crashes. Correlation between barrier test results and vehicle-to-vehicle test results for assessment of compatibility measures and test procedures is discussed.

1. INTRODUCTION

On February 11-12, 2003, the Alliance of Automobile Manufacturers (AAM) and the Insurance Institute for Highway Safety (IIHS) cosponsored an international meeting in Washington D.C. on enhancing vehicle-to-vehicle crash compatibility. It was decided during the meeting to pursue a concerted industry-wide effort to develop performance criteria to further enhance vehicle compatibility. The participants agreed to set up two technical working groups of experts to develop initiatives and actions. One working group was established to address ways to improve compatibility in front-to-side crashes, the other to address front-to-front crashes [1].

The first year's research of the TWG resulted in development and implementation of the Phase I requirements that were announced on December 3, 2003 [2] as a first step towards improving geometrical compatibility. These requirements state that participating manufacturers will begin designing light trucks in accordance with one of the following two geometric alignment alternatives, with the light truck at unloaded vehicle weight (as defined in 49 CFR 571.3):

OPTION 1: The light truck's primary frontal energy-absorbing structure shall overlap at least 50 percent of the Part 581 zone AND at least 50 percent of the light truck's primary frontal energy-absorbing structure shall overlap the Part 581 zone (if the primary frontal energy-absorbing structure of the light truck is greater than 8 inches tall, engagement with the entire Part 581 zone is required), OR,

OPTION 2: If a light truck does not meet the criteria of Option 1, there must be a secondary energy-absorbing structure (SEAS), connected to the primary structure, whose lower edge shall be no higher than the bottom of the Part 581 bumper zone.

Phase II research of the TWG focused on the development of specification and criteria for SEAS. This secondary structure shall withstand a load of at least 100 KN exerted by a loading device, as described in reference [1], Appendix A, before this loading device travels 400 mm as measured from a vertical plane at the forward-most point of the significant structure of the vehicle.

Beginning September 1, 2009, 100 percent of each participating manufacturer's new light truck up to 10,000 pounds Gross Vehicle Weight Rating (GVWR), with limited exceptions, intended for sale in the United States and Canada will be designed in accordance with either geometric alignment Option 1 or Option 2.

Ford Motor Company had already introduced a "BlockerBeam[®]" concept in their 2000 year model full sized SUV (as a means to improve vehicle compatibility through structural interaction during frontal impacts with passenger cars). The BlockerBeam[®] is a Secondary Energy Absorbing Structure (SEAS) attached to the front end of the rail/frame of an SUV or full size pick-up below the bumper. It has the potential to reduce override. Ford had migrated and implemented the BlockerBeam[®] concept in their 2001 production heavy-duty pick-ups. This particular design among others bring Ford's full size SUV and heavy-duty pick-ups into compliance with the Alliance Phase I option II requirements.

Phase III research for the TWG has been focused on the development of test assessment methodologies and metrics to evaluate vehicle compatibility. Previous research focusing on the development of test procedures for evaluating vehicle compatibility was reported by Barbat, et. al. [3, 4] and Edwards, et. al. [5]. Test and simulation results obtained from frontal impacts with various Load Cell Walls (LCW)

and from vehicle-to-vehicle impacts to support phase III research were previously analyzed by TWG members and presented during the 19th ESV conference held in Washington D.C. in 2005 [1]. The Average Height of Force (AHOF) introduced by Digges et. al. [6] and NHTSA [7, 8] as a compatibility metric was the focus of the TWG investigation. Initial finding was that AHOF alone was an insufficient metric and did not correlate with the Aggressivity Metric (AM) defined by NHTSA [1]. Other metrics obtained from LCW such as force homogeneity within a defined corridor and enforcing force limits in certain load cell rows were studied. Currently alternative metrics and test procedures are under investigation by the TWG [9].

The purpose of the current Ford's research falls into two folds: First is to evaluate the real-world effectiveness of the BlockerBeam[®] in vehicle-to-vehicle frontal and side crashes. Secondly, to evaluate various metrics from vehicle-to-barrier tests, Edwards [10], and vehicle-to-vehicle crash tests that could explain the accident data.

Full size, heavy-duty pick-ups with and without a BlockerBeam[®] were instrumented and tested in a 57 kph frontal impact against a full width deformable barrier at PMG by Transport Canada (TC). The barrier consisted of 128 high resolution, 125 mm by 125 mm load cells arranged in a 16 row by 8 column array. Identical full size heavy-duty pick-ups with and without a BlockerBeam[®] were selected to be the bullet vehicles in vehicle-to-vehicle full frontal impacts conducted at Ford.

The struck target vehicle was selected to be a small size 4-door sedan. The bullet and target vehicles were equipped with instrumented 50th% dummies in the mid-position for the drivers and 5th% dummies in full forward position for the passengers. Details of test procedures, data analyses obtained from Load Cell Wall barrier and full frontal collinear vehicle-to-vehicle impact to assess compatibility metrics will be discussed in the following sections.

2. REAL-WORLD EFFECTIVENESS OF FORD'S BlockerBeam[®] IN IMPROVING VEHICLE COMPATIBILITY

The effect of adding secondary energy absorbing structures, SEAS (one of the recommendations of TWG) to Light Truck Vehicle (LTVs) was evaluated by comparing the collision performance of LTVs with and without Ford's BlockerBeam[®] SEAS in 1999-2003 FARS data for collisions involving:

- One light passenger vehicle with at least one non-ejected fatal occupant and “motor vehicle” coded as ‘most harmful event’, and
- One collision partner from models and the model years of interest: Ford F250 and Ford F350 pick-ups from model years 1999-2000 (without BlockerBeam®) and 2001-03 (with BlockerBeam®).

The cases selected as ‘frontal impact’ are identified by principal impact direction (or initial impact direction, if principal impact direction was unknown) coded as 11, 12, or 1 o’clock. The registered vehicle years (RVY) for collision partner are calculated from R. L. Polk National Vehicle Population Profile.

Table 1: Effect of BlockerBeam®; Front-to-Front Crashes

Collision Partner	Crashes		Rate per 10k RVY		P-value Ha: p1>p2
	MY99-00	MY01-03	MY99-00	MY01-03	
F-250	95	38	0.55	0.43	0.11
F-350	35	12	0.64	0.38	0.06
Control Group	36	48	0.53	0.54	0.52

In Table 1, a significant reduction in fatality rates is observed for vehicles with the added BlockerBeam®, although this data by itself is not sufficient to identify a single factor as the cause for this reduction. The data for a control group consisting of a pick-up truck similar to the F-series trucks above is also shown. This truck does not conform to the EVC recommendations and did not have any significant change in its structural height in the years under study. The data shows that for the control group, no statistically significant changes in its crash rates occurred.

Similar data is shown in Table 2 for the cases where the fronts of LTVs impacted the near side of other vehicles. Again, the effect of adding a BlockerBeam® to the LTV is seen to provide a significant reduction in the fatality rate in the struck vehicle.

Table 2: Effect of BlockerBeam®; Front-to-Near Side Impacts with Near-Side Fatalities

Collision Partner	Crashes		Rate per 10k RVY		P-value Ha: p1>p2
	MY99-00	MY01-03	MY99-00	MY01-03	
F-250	98	34	0.56	0.39	0.03

3. VEHICLE-TO-BARRIER CRASH TESTS SETUP AND PROCEDURES

Table 3 provides the significant test information regarding the mass, impact velocity, and ride heights of the two heavy-duty pick-ups considered in this test sequence. The test setup is illustrated in Figures 1A through 1C. A deformable face honeycomb material is attached to a rigid, load cell equipped barrier. The specifications of the deformable face, which consists of two 150 mm thick layers of aluminum honeycomb, are the same as those developed by Transport Research Laboratory in the U.K. (TRL). The stiffness of the layers is 0.34 MPa and 1.71 MPa for the front and rear layers, respectively. The second layer of the baseline barrier is segmented along each load cell row and column, meaning this deformable layer will not transfer load to adjacent cells.

Table 3: Test Conditions for Full-Frontal Vehicle-to-Barrier Impact Test.

		Heavy Duty Pickup with SEAS	Heavy Duty Pickup without SEAS
Vehicle Configuration	Mass (kg)	3185.6	3184.6
	Impact velocity (kph)	57.47	57.39
	Ride Height (mm) (Left / Right)	Front 995 / 995 Rear 1018 / 1020	Front 994 / 999 Rear 1017 / 1025
Height of the first row of Load Cell Wall		330 mm	330 mm



Figure 1A. Test setup for heavy-duty pick-up-to-barrier test: Top View.

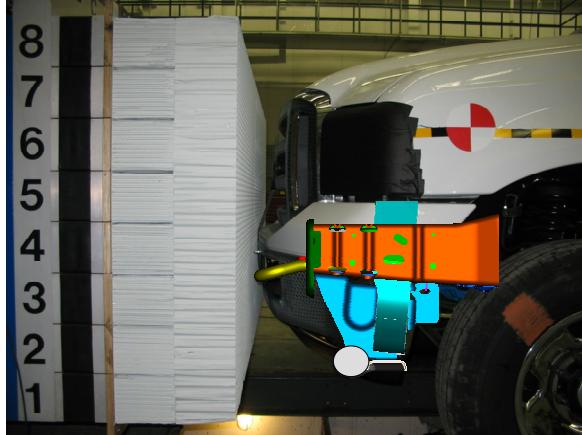


Figure 1B. Driver's side view of heavy-duty pick-up with SEAS showing key front structure and barrier.



Figure 1C. Driver's side view of heavy-duty pick-up w/o SEAS showing key front structure and barrier.

The lower edge of the lowest row of load cells was 330 mm above the ground for the test. The impacting heavy-duty pick-ups with and without SEAS were aligned so that the vehicle centerline was aligned with the horizontal center of the barrier face (see Figure 1A). Figures 1B and 1C show the vertical height of front structure components and the lower radiator support structure. The primary energy absorbing structure (PEAS) is considered the front rails. The BlockerBeam[®] with attachment brackets as the secondary energy absorbing structure (SEAS) are also seen in the figures. The SEAS is directly attached to the front rails via these brackets as seen in Figure 1B.

Figure 2 shows a simplified CAD representation of the passenger side front rail and secondary energy absorbing structure along with the associated attachment bracket. The driver's side is similar. The SEAS and associated attachment bracket (Figure 2) were removed in the second test.

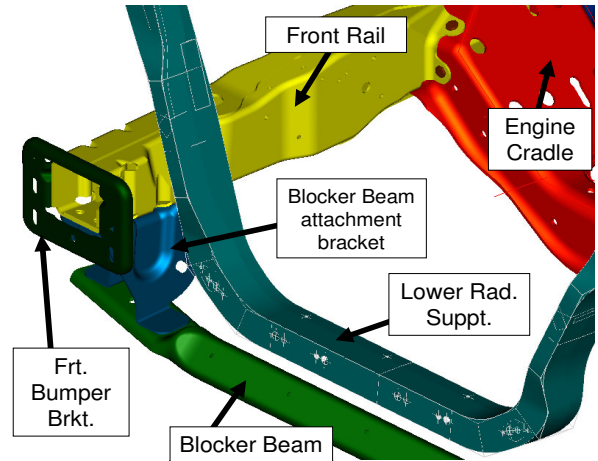


Figure 2. Front structure components in the heavy-duty pick-up.

Two full frontal NCAP tests against the LCW with deformable face at 57 kph were conducted with heavy-duty pick-ups. All vehicle parameters and test conditions (make, model, year model, body style, mass, impact speed, impact point etc.) were identical. The only difference in the two tests was the presence ("with SEAS") or absence ("without SEAS") of the secondary energy absorbing structures.

4. VEHICLE-TO-BARRIER: TEST RESULTS AND DISCUSSION

An objective of the current research is to evaluate the ability of the LCW with deformable face to detect the presence of SEAS such as the "BlockerBeam[®]" and to evaluate new or existing compatibility metrics. Figures 3 and 4 show the load-time history of each cell obtained from 57 kph impacts of heavy-duty pick-ups respectively. On the same figures it is also plotted the part 581 zone and locations of the PEAS and SEAS. Bigger percentage of the rail cross section (PEAS) falls in row 5 and some percentage in row 6.

The calculated AHOF values from both tests, with and without SEAS, are indicated on these figures. These values of the AHOF do not clearly discriminate the presence of SEAS. Figures 5 and 6 show the post impact deformation of the heavy-duty pick-ups with and without SEAS along with their corresponding barrier deformable faces respectively.

The major energy absorbing structure in smaller passenger cars falls mostly in rows 3 and 4 and therefore development of compatibility metrics should focus within these rows. Higher forces within rows 5 and 6 are generally evident as seen in Figures 3 and 4. Load cells near the PEAS record higher

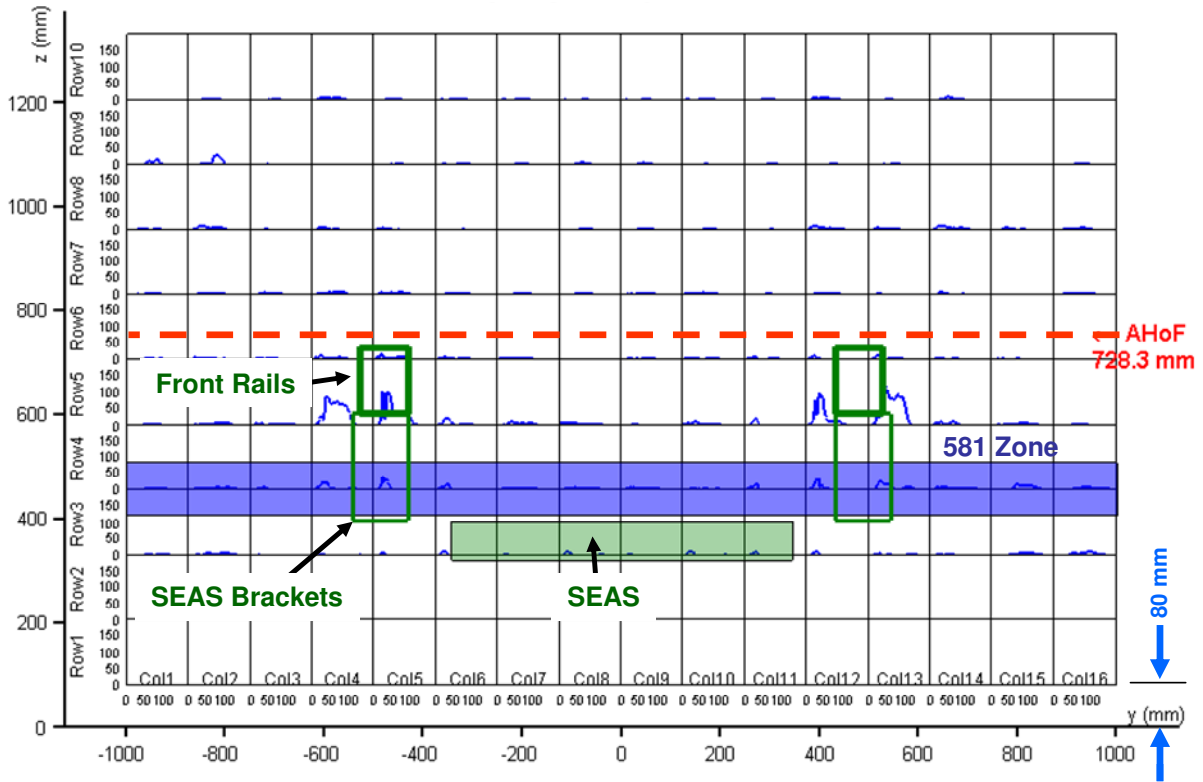


Figure 3. LCW force-time histories for heavy-duty pick-up with SEAS.

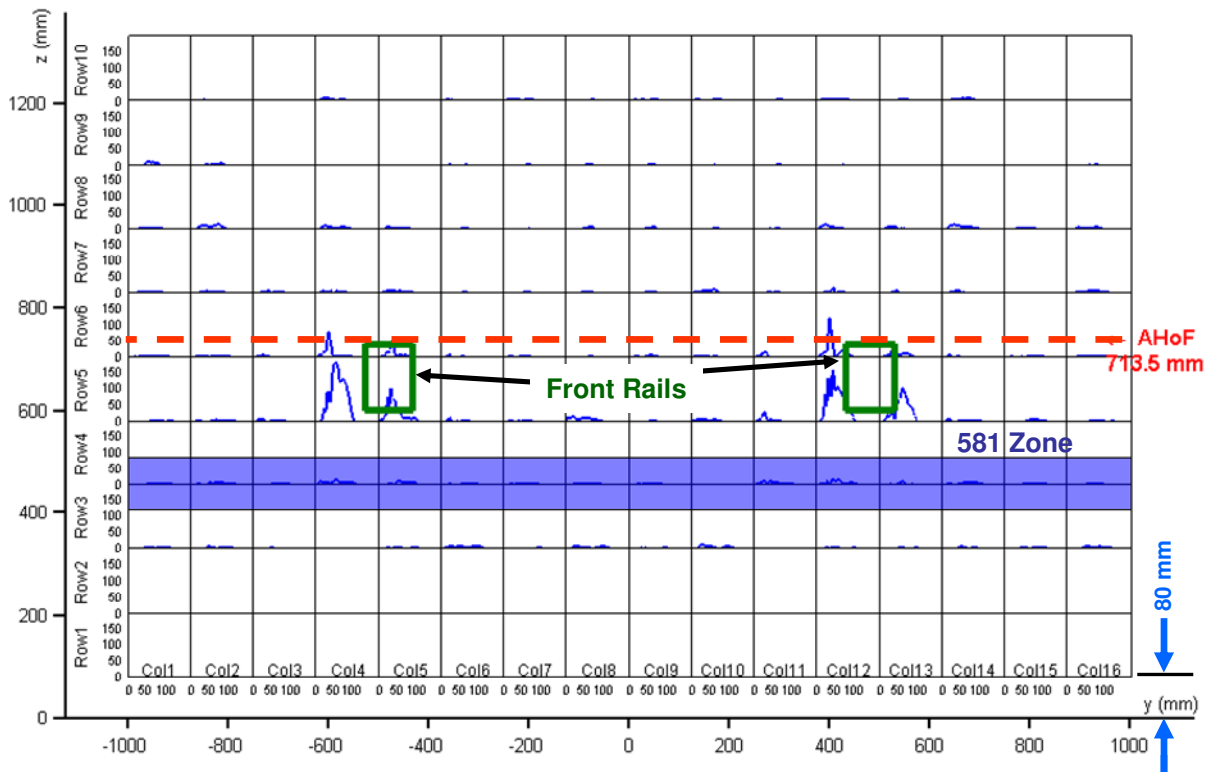


Figure 4. LCW force-time histories for heavy-duty pick-up without SEAS.

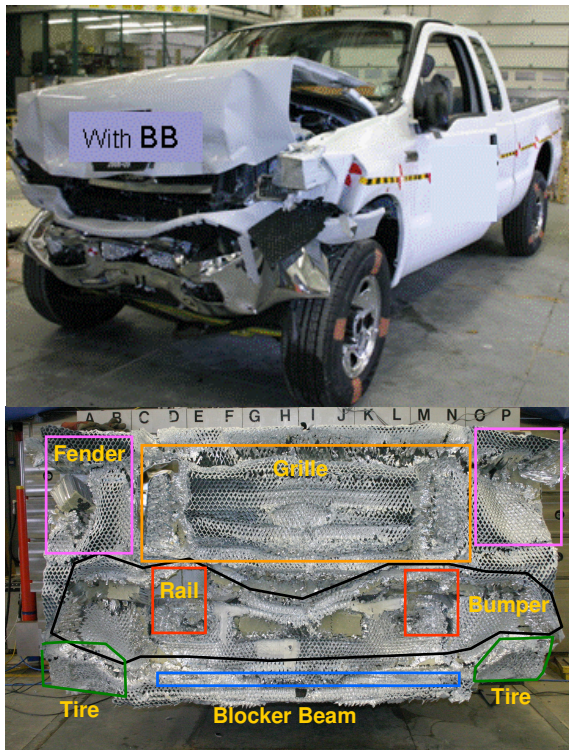


Figure 5. Post-impact pictures of the heavy-duty pick-up with SEAS and the corresponding barrier.

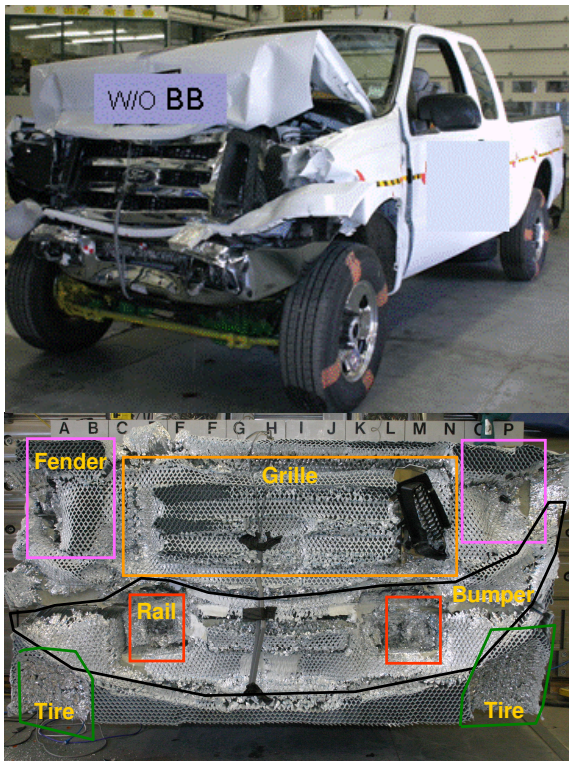


Figure 6. Post-impact pictures of the heavy-duty pick-up without SEAS and the corresponding barrier.

levels of forces than the surrounding cells. Additionally, the forces in PEAS associated cells for the heavy-duty pick-up with SEAS are lower than similar cells of the LCW when impacted by the heavy-duty pick-up without SEAS.

This is true because ideally the total LCW force should be the same due to impacts with the heavy-duty pick-ups with or without SEAS. However, LCW force profile seems to be slightly different indicating different collapse mechanisms of structure (see Figure 7). In cases where SEAS are present, wall cells around those structures will record more load as compared to cases where impact occurred without SEAS.

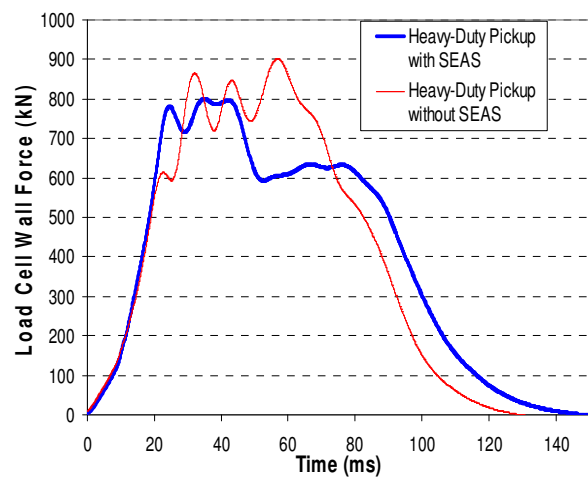


Figure 7. Time-history plots for the total barrier force of heavy-duty pick-ups with and without SEAS

Examination of the deformed vehicle and barriers faces (Figures 3-6) shows that the SEAS applied more load on rows 3 and 4 and resulted in less penetration into the deformable face with more load distribution. This is also evident from the observation of the deformed honeycomb faces in the tire, grille and bumper zones.

Figure 8 below gives the distribution of forces in rows 3 and 4 with respect to time for the heavy-duty pick-up with SEAS impact. For each row, all cells forces in that row are added with respect to time to form a row total force-time history in which the row's peak magnitude can be identified at a certain time. This differs from adding the peak force in each cell in a row, irrespective of the occurrence times, to find the row peak force magnitude. Figure 9 shows similar force-time history plots in rows 3 and 4 for the heavy-duty pick-up without SEAS impact.

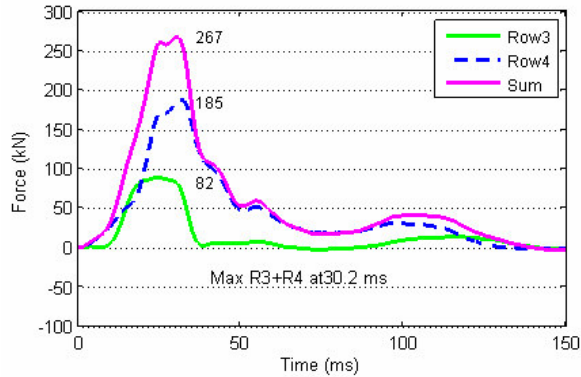


Figure 8. Force-time histories for rows 3 and 4 for the heavy-duty pick-up with SEAS.

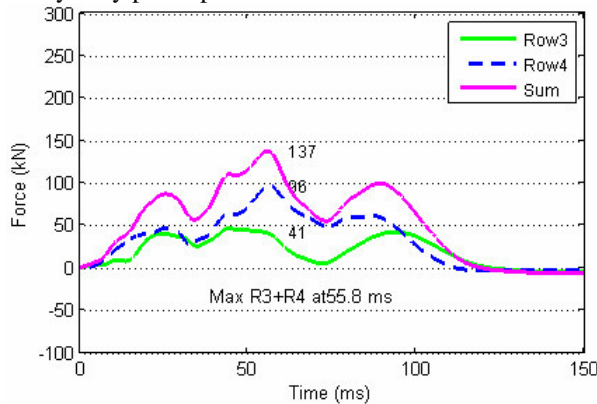


Figure 9. Force-time histories for rows 3 and 4 for the heavy-duty pick-up without SEAS.

A comparison between Figures 8 and 9 shows that rows 3 and 4 carry a significantly higher proportion of the load when the SEAS structure is present. It is also significant to note that the maximum force level of rows 3 and 4 combined occurs much later (at 55.8 ms as compared to 30.2 ms) without SEAS than with SEAS, respectively. This suggests that for developing a compatibility metric associated with peak row force magnitudes, it is suggested to restrict the window to one where the force peaks due to early interaction of the energy absorbing structures rather than due to engine engagement, which occurs later in the event. Therefore, a window of 0 to 40ms is recommended by this study as suggested by Edwards [10].

Figures 8 and 9 show that when the heavy-duty pick-up with SEAS impacts the LCW the SEAS structure transferred more of the dynamic force to lower portions (rows 3 and 4) of the LCW than when no SEAS. These figures also show that the difference in total load supported by rows 3 and 4 has a maximum magnitude of 130 KN. This is believed to be the force provided by the SEAS structure.

Figures 10 and 11 graphically show the dispersion of load horizontally across rows 3 and 4 for both pick-ups with and without SEAS respectively. The load dispersion in these rows is plotted at 30.2 ms and 55.8 ms for the case with and without SEAS respectively. These times correspond to the time the sum of the total forces in rows 3 and 4 is a maximum. The outer two load cells represented by columns 1, 2, 15, and 16 are omitted since very little load was recorded there. Figures 10 and 11 indicate the mean load levels in rows 3 and 4 were higher by nearly a factor of 2 when the pick-up impacting the LCW had SEAS than when it did not.

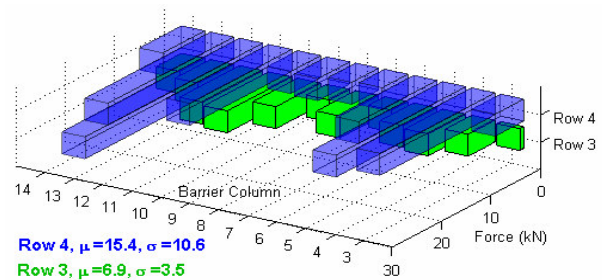


Figure 10. Horizontal load dispersion for the heavy-duty pick-up with SEAS at 30.2 ms.

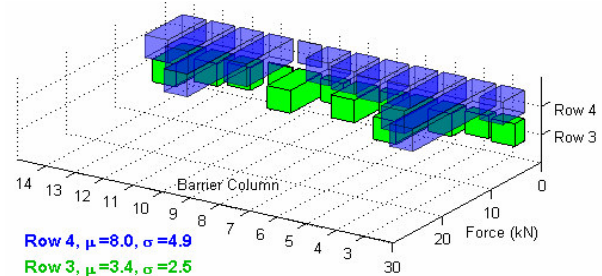


Figure 11. Horizontal load dispersion for the heavy-duty pick-up without SEAS at 55.8 ms.

Another approach for examining the horizontal force variation (similar to that seen in Figures 10 and 11) would be to find the peak force recorded in each load cell within a particular row independent of when it occurred. The results are shown in Figures 12 and 13 for rows 3 and 4 for the pick-ups with and without SEAS, respectively. Similarly, as with Figures 10 and 11, the average load levels seen in rows 3 and 4 are about twice as large when SEAS are present as when it is not.

In summary, the total maximum force appearing in a certain row, e.g. Row_i, can be characterized using two different methods. The force is denoted as the “Peak Load for Row_i” if the force time-histories from

all load cells within Row_i are combined to form a Row_i total force-time history, whose maximum value for a given time period is taken. If instead, the peak loads in each load cell within Row_i are first found irrespective of the precise time they occur and then summed, this force is denoted as “Sum of Peak Cell Loads for Row_i”. In each method described, the values denoted by either “Peak Load for Row_i” or “Sum of Peak Cell Loads for Row_i” can be determined within a 40 ms time window. This leads to four different measures for a Row_i force.

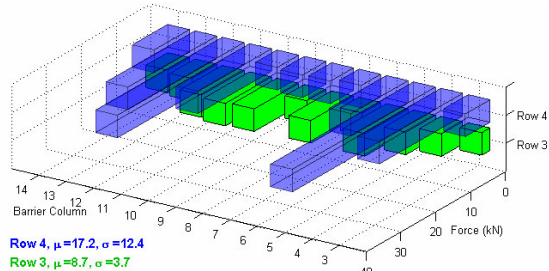


Figure 12. Peak load cell forces for the heavy-duty pick-up with SEAS (independent of time).

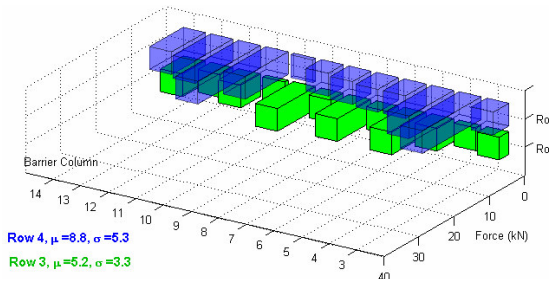


Figure 13. Peak load cell forces for the heavy-duty pick-up without SEAS (independent of time).

Figure 14 indicates that, for the heavy-duty pick-up with SEAS, the loads seen in rows 3-6 gradually increases and then decreases in approximately a 100-200-450-100 KN pattern. For the heavy-duty pick-up without SEAS, as seen in Figure 15, the loads in rows 3-6 build up gradually and in approximately a 50-50-400-300 KN pattern.

A shifting of load from rows 3 and 4 occurs when SEAS are absent since the total barrier load in both cases must remain the same (the impacting vehicle mass and velocity are the same). A noticeable increase occurs in row 5 due to the pick-up's frame or PEAS impact at this location. Additionally, there is more variability across the four measurement methods for row 5 when SEAS are not present (quantified in Figure 15). It should be noted that this load increase pattern is the same regardless of the

method of calculation (Sum of Peak Loads vs. Peak Row), the only difference being the higher variability when SEAS is not present.

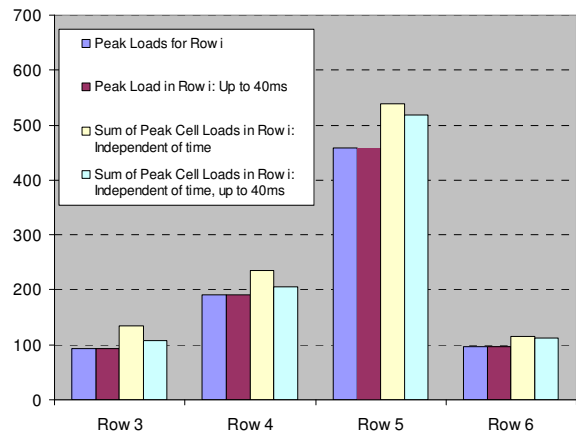


Figure 14. Peak loads in rows 3-6 for the heavy-duty pick-up with SEAS.

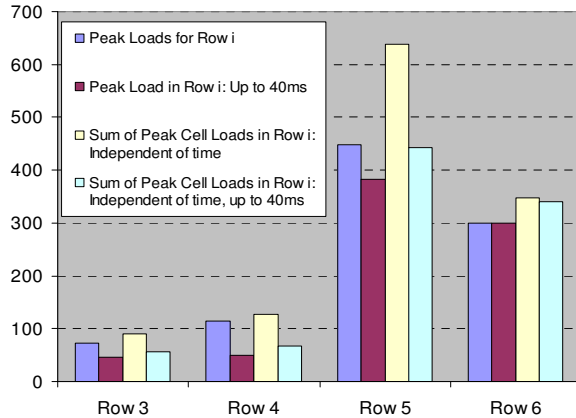


Figure 15. Peak loads for rows 3-6 for the heavy-duty pick-up without SEAS.

Edwards [10] has proposed row load based metrics VNT (Vertical Negative Deviation) and VSI (Vehicle Structure Interaction) as compatibility metrics. The aim of the vertical component is to ensure that there is sufficient vehicle structure in alignment with the common interaction area, rows 3 and 4. It sets a target row load of 100 KN minimum and calculates the load below the target row. The VNT is essentially characterized by the sum of peak force method and the VSI are generally characterized by the same sum of peak values up to 40 ms.

In the current research the authors attempt to evaluate the VNT and VSI metrics using the LCW discussed results (Figures 3-15) and results obtained from heavy-duty pick-ups with and without SEAS in full frontal impacts against a small passenger car.

Since the sequence of structural component collapse is important and depends on time, the current authors suggest and prefer to use the time-dependent “Peak Load for Row_i” instead of non-time dependent “Sum of Peak cell Loads for Row_i” to calculate the VNT and VSI. It is preferred that if lower bounds for force level are intended for row load targets, conservative or minimum values should be used. The sum of peak values will always be greater than or equal to the peak row loads for any given row (e.g. the peak row load is a lower bound for the sum of peak cell loads for any row). Since in vehicle-to-vehicle impact compatibility focuses on front-end structural interactions and not those from the engine, a window of 40ms is recommended here.

Figures 8, 9, 14, and 15 clearly show that the peak row loads using a 40ms window limit can distinguish the presence of SEAS. The force levels seen in rows 3 through 6 indicate that the SEAS shifted a good percentage of the total barrier load into rows 3 and 4. A target load of 100KN on rows 3 and 4 has a potential to discriminate presence of SEAS. Table 4 below contains the calculated compatibility measures.

Table 4: Summary of Vertical and Horizontal Negative Deviation Measures

		Heavy Duty Pickup with SEAS	Heavy Duty Pickup without SEAS	
Vehicle Metrics	AHOF	728.3	713.5	
	AHOF400	694.6	743.6	
	Approx. VNT	Σ peak cell loads in Row 3, all time	134.5	90.5 < 100
		Σ peak cell loads in Row 4, all time	235.5	127.5
	Approx. VSI	Σ peak cell loads in Row 3, t < 40 ms	108.0	56.2 < 100
		Σ peak cell loads in Row 4, t < 40 ms	205.5	66.5 < 100

5. VEHICLE-TO-VEHICLE TEST SETUP AND PROCEDURES

The test configuration of full frontal collinear vehicle-to-vehicle impact is shown in Figure 16. Figure 17 shows a close-up view of the geometrical alignments and differences between structural front-end components of the impacted vehicles. Two tests were conducted with the target vehicles chosen to be the same (small size passenger cars) while the bullet vehicles were selected to be heavy-duty pick-ups with and without SEAS. The bullet pick-ups were identical to those used in LCW tests and had identical characteristics and specifications. All vehicles were fully instrumented. Dimensional analyses points and sections were specified on all vehicles for pre- and post-crash deformation analyses. The target vehicle was initially at rest in both tests. The bullet vehicle's

velocity was selected based on the relative masses involved, i.e., the bullet vehicle impact velocity was mass adjusted to 82 kph in order to induce a 56 kph barrier-equivalent velocity (BEV) in the target vehicle. The 56 kph BEV was selected to model the test conditions of NCAP.

In all the Pick-up-to-Car tests, both the bullet and target vehicles used a Hybrid III 50th percentile, male dummy in the driver mid position and a Hybrid III 5th percentile, female dummy in the passenger full forward position. All the dummies were belted and the airbags were active. A summary of test conditions for the two vehicle-to-vehicle tests is given in Table 5. Figure 16 shows top and side views of the test setup prior to impact.

Table 5: Vehicle-to-Vehicle Test Conditions

	Test 1		Test 2	
	Heavy-Duty Pickup with SEAS	Small Passenger Car	Heavy-Duty Pickup without SEAS	Small Passenger Car
Model Year	2007	2005	2007	2005
Vehicle Weight	3191 kg	1531 kg	3186 kg	1538 kg
Vehicle Ride Height (mm, RH / LH)	1010 / 1000	647 / 641	1002 / 994	658 / 654
Impact Velocity	82.55 kph	0.0	83.05 kph	0.0
Velocity Change	26.71 kph	55.84 kph	27.04 kph	56.02 kph



Figure 16. Top and side views of the vehicle-to-vehicle test set-up.

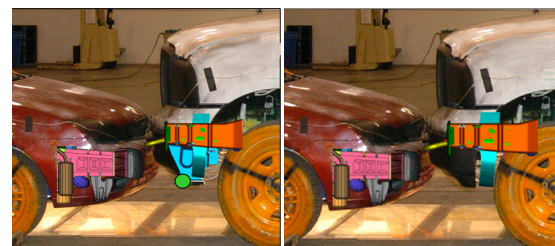


Figure 17. Views of PEAS and SEAS geometrical differences between target and bullet vehicles.

6. VEHICLE-TO-VEHICLE TEST RESULTS AND DISCUSSION

Evaluation of proposed compatibility metrics (VNT and VSI) obtained from LCW tests and their correlation with target vehicle's occupant responses and intrusions obtained from vehicle-to-vehicle impact was the primary objective of this study. Unfortunately, most of the driver dummy's and some of the passenger dummy's channel recordings were lost in the test of the heavy-duty pick-up with SEAS against a passenger car due to a high voltage anomaly. Therefore, only vehicle decelerations, displacements, and intrusions will be used for the correlation and conclusions. The authors' plan is to repeat the test and successfully collect all dummy responses for use in correlation of the compatibility metrics with occupant responses. The results will be reported in future publications.

6.1 Vehicle Deceleration Pulse Comparisons

Figures 18 and 19 show the comparison of the deceleration pulses of the target and bullet vehicles resulting from the 82 kph full frontal impacts by heavy-duty pick-ups with and without SEAS respectively.

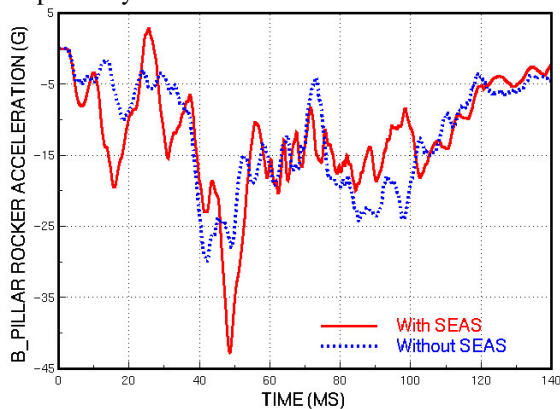


Figure 18. A comparison of target vehicle pulses.

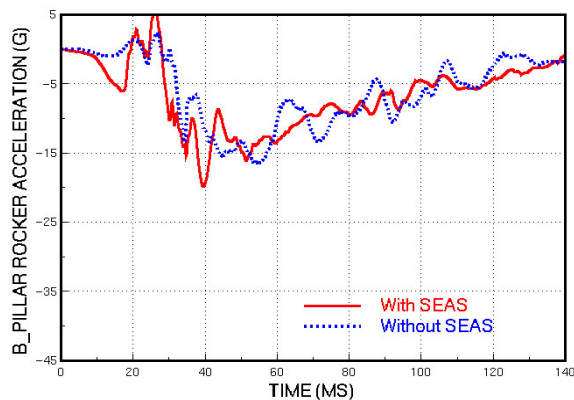


Figure 19. A comparison of bullet vehicle pulses.

The effect of the presence of SEAS is quite obvious from Figures 18 and 19. The SEAS on the striking heavy-duty pick-up engages the front end PEAS of the passenger car and transmit a larger force to the target vehicle early in the impact event, less than 20 ms, as seen in these figures. SEAS cause the 20 G deceleration at approximately 20 ms experienced by the target vehicle.

From Newton's law, by considering the mass times the deceleration, approximately 304 KN of force is acting on the vehicles at this particular time. Such force level was observed in the interaction zone (rows 3 and 4) in the LCW test impacted by the heavy-duty pick-up with SEAS (see Table 4). The target vehicle experienced a much lower deceleration level when impacted by the heavy-duty pick-up without SEAS, Figure 18. This means that within 20-25 ms of initial impact, the pick-up missed engagement with the passenger car PEAS and contacted the passenger car's engine at approximately 30 ms. This is evident from the sudden jump of the crash pulses in both the target and bullet vehicles as seen in Figures 18 and 19, respectively.

6.2. Correlation Between LCW and Vehicle-to-Vehicle Results for Proposed Metrics Evaluation

In the LCW deformable barrier tests it was shown in Table 4 that the heavy-duty pick-up with SEAS delivered forces in rows 3 and 4 around 100 KN and 200KN respectively. The force in the interaction zone between two impacted vehicles characterized by rows 3 and 4 can total to about 300 KN. This force is acting on the PEAS of the target vehicle and reacted on the SEAS of the bullet vehicle during approximately the first 40 ms of impact.

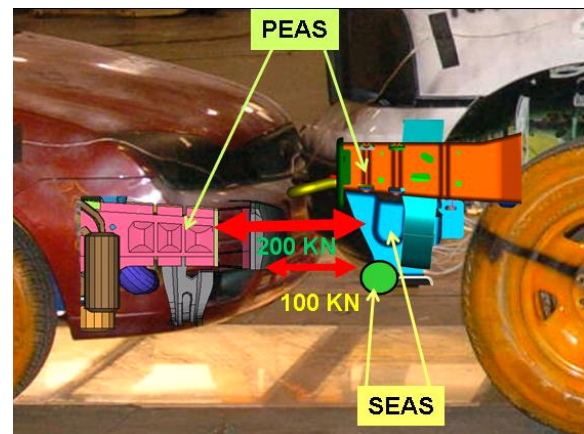


Figure 20. Forces in the interaction zone between the target and bullet vehicles.

This force level acting on the target vehicle is both sufficient to crush the front part of its PEAS and to deform the SEAS of the bullet vehicle, represented by the BlockerBeam® and its attachment brackets. It is always recommended to have both vehicles involved in the crash absorb some energy. Figure 20 shows a graphical representation of the force acting on both vehicles.

6.3. Comparison of Overall Deformation of Target and Bullet Vehicles

Figures 21 and 22 show the overall deformations of the bullet and target vehicles with and without SEAS in the bullet vehicle. Examining the bullet vehicles it is shown that the vehicle with SEAS experienced more deformation in the bumper and grille areas compared to that without SEAS. This is due to more structural interaction between the front-ends of the impacting vehicles in the case of the impact with SEAS compare to that without SEAS.

The target vehicle impacted by the bullet with SEAS has less overall deformation compared to that impacted by bullet without SEAS (Figures 21 and 22). This is very clear in the deformation zone around the A-pillar/roof rail and B-pillar roof rail joints. This is due to a greater override of the bullet vehicle onto the target when the SEAS is removed.



Figure 21. Post impact pictures of the bullet and target vehicles with SEAS on the bullet vehicle.



Figure 22. Post impact pictures of the bullet and target vehicles with no SEAS on the bullet vehicle.

Figure 23 is a CAD representation of the undeformed shape of the front-end and engine of the target vehicle. Figures 24 and 25 show the specific collapse modes of the PEAS of the target passenger vehicle impacted by the bullet vehicle with and without SEAS. Axial collapse is first observed in the target vehicle's fore-rail followed by a bending collapse near the engine mount due to the presence of SEAS and better structural interactions (see Figure 24). In the second test with the SEAS removed, the bullet vehicle's PEAS missed the front portion of the target vehicle's rail causing more override that resulted in excessive rotation and bending of aft rail of the target vehicle as shown in Figure 25.

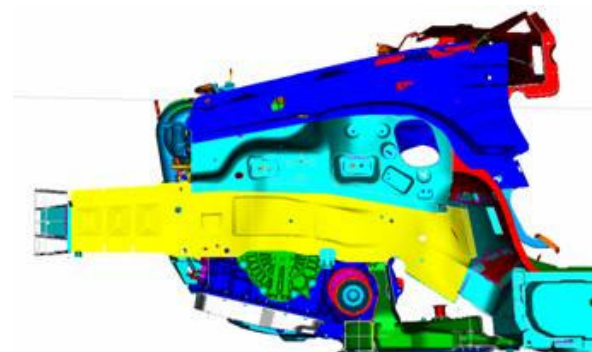


Figure 23. The undeformed shape of the front-end and engine of the target vehicle.

Comparing Figures 24 and 25, it is evident that the presence of SEAS resulted in less rotation of the spring box and engine. This is due to less override and more structural interaction that led to less structural intrusions in general.

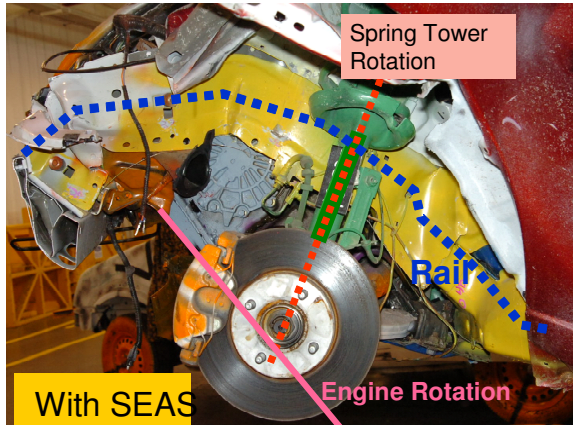


Figure 24. The post crash deformation of the front-end structure and engine rotation in the target vehicle impacted by bullet vehicle with SEAS

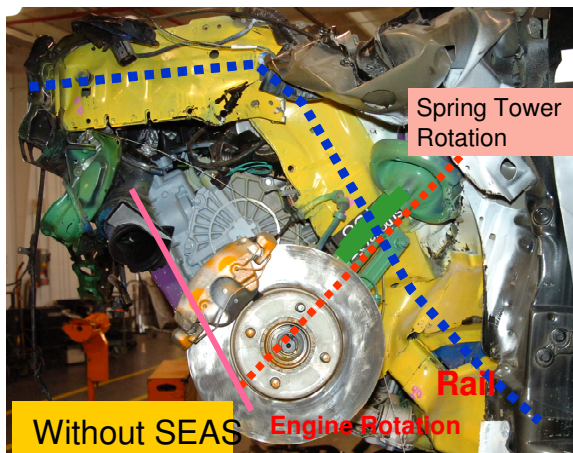


Figure 25. The post crash deformation of the front-end structure and engine rotation in the target vehicle impacted by bullet vehicle without SEAS.

6.4. Comparison of Vehicles Displacement During Impact

The crash pulses of both target and bullet vehicles shown in Figures 18 and 19 were double integrated to obtain their corresponding displacements. Figure 26 shows displacement of the target and bullet vehicles for the case of the heavy-duty pick-up with SEAS impacting a small size passenger car. Similarly, Figure 27 shows the displacements resulting from the

heavy-duty pick-up without SEAS impacting a similar small size passenger car.

In Figures 26 and 27, the difference between the two curves represents relative displacement between points on the B-pillar/rocker on the bullet and target vehicles involved in the crash. This difference includes deformation and override. The maximum relative displacement happened at the rebound time when the two vehicles began to separate.

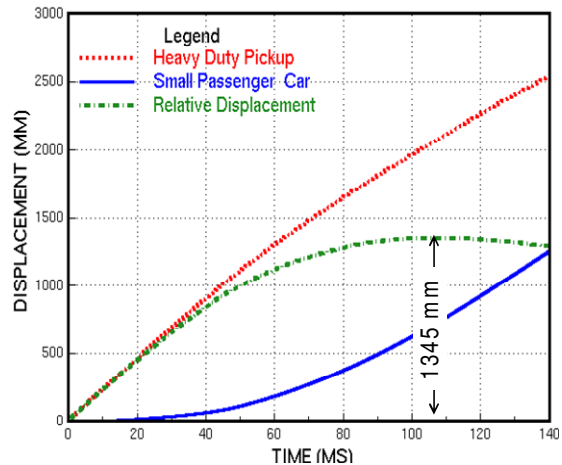


Figure 26. Displacement time-histories obtained from bullet vehicle with SEAS-to-target vehicle impact.

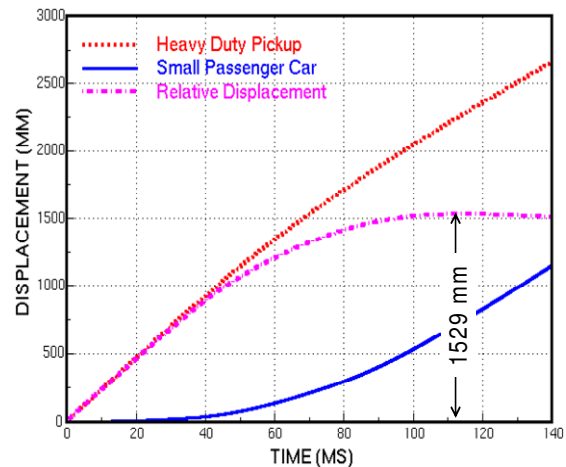


Figure 27. Displacement time-histories obtained from bullet vehicle without SEAS-to-target vehicle impact.

Comparing Figures 26 and 27 it is evident that the maximum relative displacement in the absence of SEAS is 184 mm more than that with SEAS (1529 mm vs. 1345 mm). This indicates that there is more override over the target vehicle and more intrusion resulted in the case of no SEAS compared to that with SEAS.

6.5. Dimensional Analyses

Pre-and post-crash dimensional analyses on target vehicles impacted by bullet vehicles with and without SEAS were carried out to obtain intrusion profiles shown in Figures 28 and 29 respectively. Intrusion profiles represented by sections from the cowl top to the floor panel at the driver centerline, vehicle centerline and passenger centerline are shown in Figures 30-32.

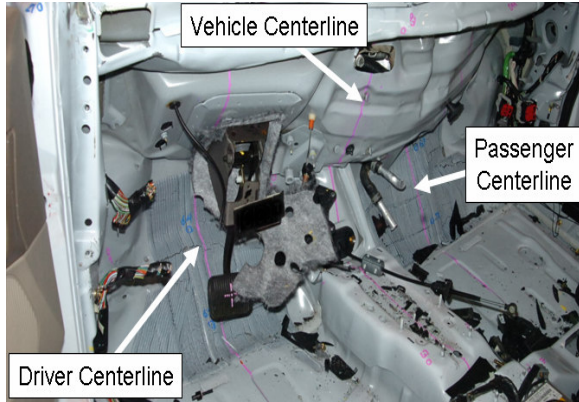


Figure 28. Post-crash sections on target vehicle impacted by the bullet vehicle with SEAS.

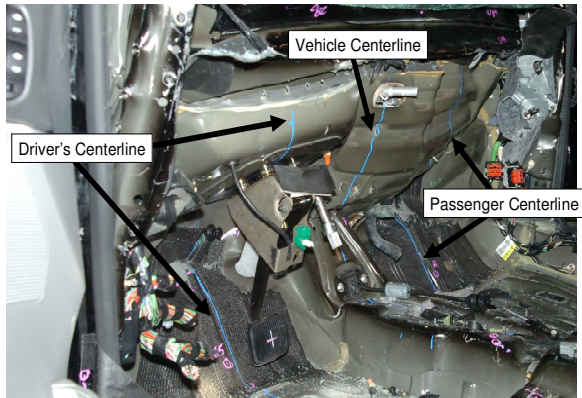


Figure 29. Post-crash sections on target vehicle impacted by the bullet vehicle without SEAS.

In Figure 30 it is evident that having the SEAS on the bullet vehicle has significantly reduced cabin intrusions at the driver centerline, specifically at the instrument panel area due to improved structural interactions and reduced override. Higher engine rotation in the target vehicle when impacted by the bullet vehicle without SEAS caused larger upper dash intrusions. Figure 31 shows a small difference between the dash intrusion profiles on the target

vehicle caused by the bullet vehicles with and without SEAS at the vehicle centerline.

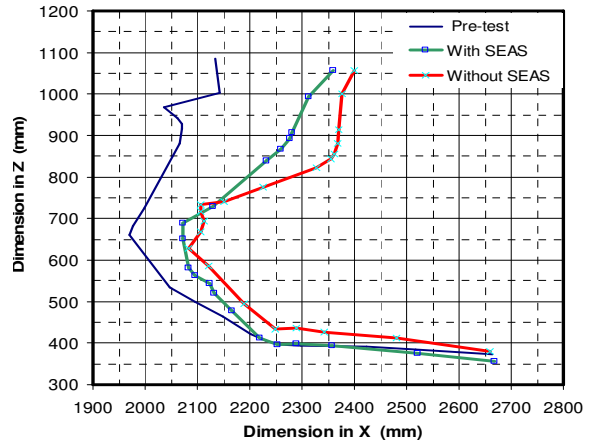


Figure 30. Dash intrusion for the target vehicle at the driver's centerline.

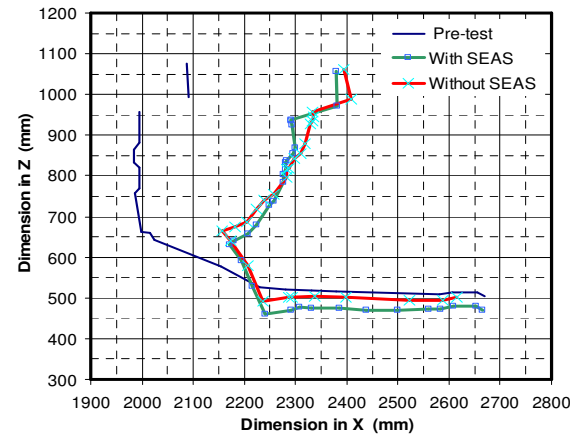


Figure 31. Dash intrusion for the target vehicle at the vehicle centerline.

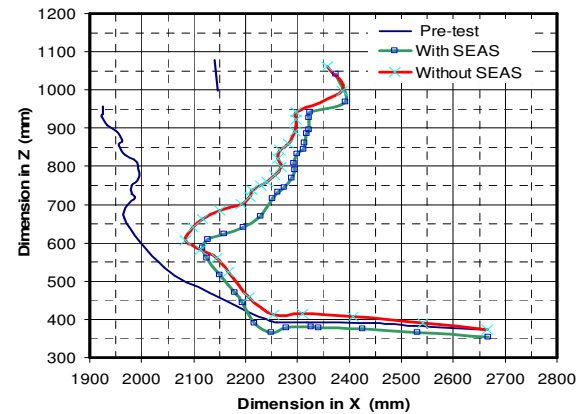


Figure 32. Dash intrusion for the target vehicle at the passenger centerline.

For the passenger centerline intrusions, Figure 32 shows mixed results. Intrusions are improved in the

lower part of the cabin at the foot pedal and foot rest areas with the presence of SEAS. Intrusions at the upper part get worse near instrument panel area. Very careful examination of the post-crashed target vehicles was conducted to better understand this observation. The engine is transversely mounted and is pivoted at a point approximately one-third of its transverse dimension towards the driver side and two-third towards the passenger side. In the case of the pick-up with SEAS impact, higher forces were transmitted to the engine in the interaction zone compared to that without SEAS. This caused more rotation of the intruded engine towards the passenger side.

Post-crash deformation of significant points in the target vehicle, such as points on fore rail, mid rail, bumper mounting, and spring tower, impacted by bullet vehicles with and without SEAS are presented in Figure 33. Having the SEAS provided significant improvement in reducing the intrusions at these points.

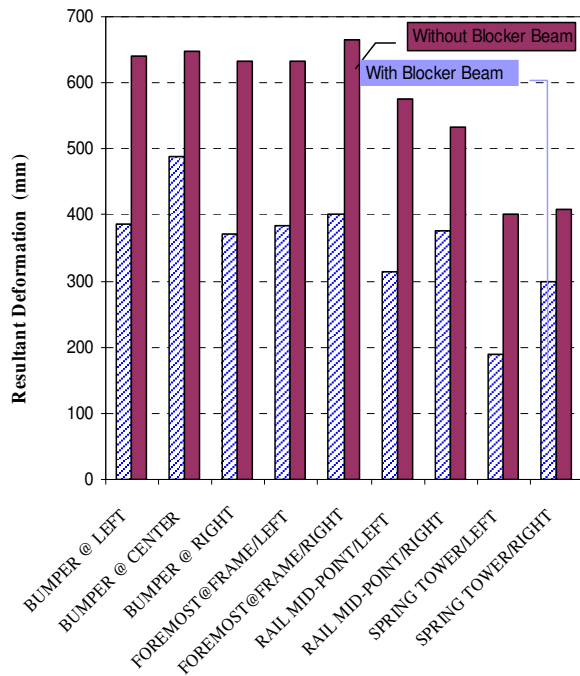


Figure 33. Resultant deformation of points on the target vehicle's primary structure.

Figures 34 and 35 present the dimensional analyses of the pre- and post-crash of the target vehicle's passenger compartment resulting from impact with bullet vehicles with and without SEAS. In Figure 34, A represents a point at the A-pillar/roof joint, B represents a point at the B-pillar/roof joint, C

represents a point at B-pillar/beltline, D represents a point at the B-pillar/rocker joint, E represents a point at the A-pillar/rocker joint, and F represents a point at the A-pillar/beltline. It is indicated from this figure that the presence of SEAS provided significant improvement in reducing the override which led to less overall deformation and intrusions in the passenger compartment of the target vehicle.

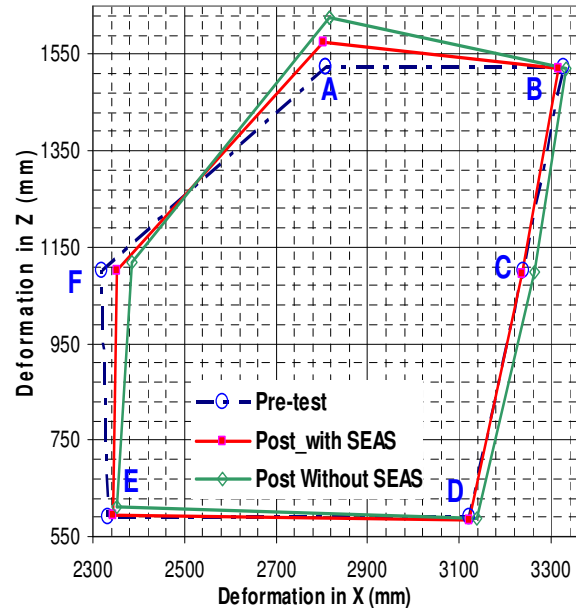


Figure 34. Passenger compartment deformation of the target vehicle impacted by bullet vehicle with and without SEAS.

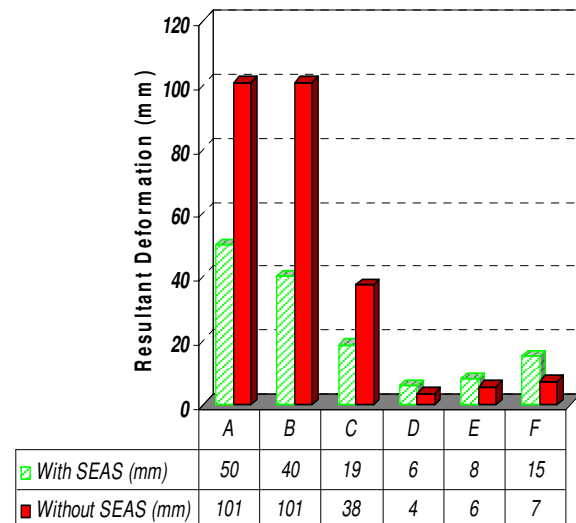


Figure 35. Resultant deformation of points at joints on the target vehicle's cabin impacted by bullet vehicles with and without SEAS.

7. CONCLUSIONS

- Real-world accident data analyses had been conducted to evaluate the effectiveness of Ford's BlockerBeam® (a Secondary Energy Absorbing Structures, SEAS, one of the recommendations of TWG) in vehicle-to-vehicle frontal and side crashes. A comparison of the collision performance between LTVs with and without Ford's BlockerBeam® showed a significant reduction in fatality rates for vehicles with the added BlockerBeam® in frontal impact. This data by itself is not sufficient to identify a single factor as the cause for this reduction. Results also showed significant reduction in the fatality rate in the struck vehicle when the striking LTVs has Ford's BlockerBeam® in near side impact.
- Vehicle-to-barrier and vehicle-to-vehicle crash tests were conducted to develop assessment procedures and metrics that can be used to predict compatibility performance.
- Heavy-duty pick-ups with and without SEAS were tested in the NCAP configuration against high resolution LCW with a deformable face to detect the presence of SEAS (BlockerBeam®) and to evaluate potential compatibility metrics.
- LCW results showed that the heavy-duty pick-up with SEAS helped in transferring dynamic force to lower portions (rows 3 and 4) of the LCW. Results obtained from pick-up impacts with and without SEAS identified a difference in total load supported by rows 3 and 4 of 130 KN. This force may be attributed to the SEAS structure.
- In calculating metrics such as VNT, VSI or other potential force-based metrics, it is suggested to use the time-dependent peak load instead of non-time dependent sum of the peak cell loads.
- The peak row loads using a 40ms time limit can distinguish the presence of SEAS. A target load of 100KN on rows 3 and 4 has a potential to discriminate presence of SEAS.
- 82 kph full frontal collinear impacts of bullet vehicles (heavy-duty pick-ups with and without SEAS) against a stationary target vehicle (small size passenger car) were also conducted. Barrier test results and associated metrics were correlated to results obtained from vehicle-to-vehicle tests for assessment of compatibility measures and test procedures.
- During the first 40 ms in vehicle-to-vehicle impact when the bullet vehicle has SEAS, approximately 304KN of force acts on the vehicles in the interaction zone. This force level is correlated to that observed in the interaction zone (rows 3 and 4)

in the LCW test impacted by the heavy-duty pick-up with SEAS.

- The presence of the SEAS on the bullet vehicle provided good interaction with the PEAS of the target vehicle. This led to reduction in override of the target vehicle that resulted in significant reduction of the overall deformations and intrusions in the target vehicle's passenger compartment.
- Finally, the LCW with deformable face investigated in this study has a potential to be used to assess vehicle compatibility.

8. ACKNOWLEDMENT

The authors would like to acknowledge Kay Sullivan and Scott Henry from the Automotive Safety Office at Ford for their contribution to the accident data analyses to evaluate the effectiveness of Ford's BlockerBeam®. The authors wish to thank Ms. Suzanne Tylko of Transport Canada and Mr. Alain Bussières of PMG for conducting the vehicle-to-barrier tests.

9. REFERENCES

- [1] Barbat, S. 2005. "Status of Enhanced Front-To-Front Vehicle Compatibility Technical Working Group Research and Commitments", 19th ESV Conference, Washington, D.C., Paper No. 05-463.
- [2] Auto Alliance, 2003. "Enhanced Vehicle-to-Vehicle Crash Compatibility: Commitment for Continued Progress by Leading Automakers".
- [3] Barbat, S., Li, X., and Prasad, P. 2001. "Evaluation of Vehicle Compatibility in Various Frontal Impact Configurations." 17th ESV, Amsterdam, Netherlands. Paper No. 01-S7-O-09.
- [4] Barbat, S., Li, X., and Prasad, P. 2001. "A Comparative Analysis of Vehicle-to-Vehicle and Vehicle-to-Rigid Fixed Barrier Frontal Impact." 17th ESV, Amsterdam, Netherlands. Paper No. 01-S7-O-01.
- [5] Edwards, M., Davies, H., and Hobbs, A. 2003. "Development of Test Procedures and Performance Criterion to Improve Compatibility in Car Frontal Collisions", 18th ESV Conference, Nagoya, Japan, Paper No. 86.
- [6] Diggs, K., Eigen, A., and Harrison, J., 1999. "Application of Load Cell Barrier Data to Assess Vehicle Crash Performance and Compatibility", SAE, Warrendale, PA, 1999-01-0770.

[7] Summers, S., Prasad, A., and Hollowell, W.T. 2001. "NHTSA's Compatibility Research Program Update", SAE, Warrendale, PA, 2001-01-1167.

[8] Summers, S., Hollowell, W.T. and Prasad, A. 2002. "Design Considerations for a Compatibility Test Procedure", SAE, Warrendale, PA, 2002-01-1022.

[9] Verma, M. 2007. "Enhanced Vehicle Collision Compatibility – Progress Report of US Technical Workgroup for Front-to-Front Compatibility", 20th ESV Conference, Lyon, France. Paper No. 07-0291.

[10] Edwards, M., Cuerden, R., and Davies, H. 2007. "Current Status of the Full Width Deformable Barrier Test", 20th ESV Conference, Lyon, France. Paper No. 07-0088